Dr n. przyr. Wanda Gordon-Krajcer

Zmiany w ekspresji:
białka beta amyloidu (βA), prekursora amyloidowego białka beta (ß-APP)
oraz w strukturze i ufosforylowaniu białka tau,
wywołane czynnikami zaburzającymi homeostazę komórki
w mózgu osób chorych na chorobę Alzheimera,
oraz w doświadczeniach *in vivo* i *in vitro*.

Rozprawa habilitacyjna

Pracownia Farmakoneurochemii
Zakład Neurochemii
Instytut Medycyny Doświadczalnej i Klinicznej
im. M. Mossakowskiego
Polskiej Akademii Nauk

Warszawa 2005

Rozprawa obejmuje cykl publikacji:

1. Gordon-Krajcer W., Gajkowska B.: Excitotoxicity-induced expression of amyloid precursor protein (β-APP) in the hippocampus and cortex of rat brain. An electron-microscopy and biochemical study. Folia Neuropathol., 39 (3): 163-173, 2001.
   IF = 0.501 ilość cytowań = 1

2. Gordon-Krajcer W., Salińska E., Łazarewicz W.: N-methyl-d-aspartate receptor-mediated processing of β-amyloid precursor protein in rat hippocampal slices: in vitro –superfusion study. Folia Neuropathol., 40 (1), 13-17, 2002.
   IF = 0.501 ilość cytowań = 3

3. Gordon-Krajcer W., Yang L.-S., Ksiezak-Reding H.: Conformation of paired helical filaments blocks dephosphorylation of epitopes shared with fetal tau except Ser 199/202 and Ser 202/Thr 205. Brain Research, 856: 163-175, 2000.
   IF = 2.389 ilość cytowań = 14

4. Yang L.-S., Gordon-Krajcer W., Ksiezak-Reding H.: Tau released from paired helical filaments with formic acid or guanidine is susceptible to calpain-mediated proteolysis. J. Neurochem. 69: 1548-1558, 1997.
   IF = 4.824 ilość cytowań = 7

5. Ksiezak-Reding H., He D., Gordon-Krajcer W, Kress Y., Lee S., Dickson D.W.: Induction of Alzheimer-specific tau epitope AT100 apoptotic in human fetal astrocytes. Cell Motility and the Cytoskeleton, 47: 236-252, 2000.
   IF = 3,068 ilość cytowań = 14

6. Grieb P., Gordon-Krajcer W., Frontczak-Baniewicz M., Walski M., Ryba M.S., Kryczka T., Fiedorowicz M., Kulinowski P., Sułek Z., Majcher K., Jasiński A.: 2-Deoxyglucose-induces β-APP overexpression, tau hyperphosphorylation and expansion of trans – Golgi. Acta Neurobiol. Exp.,64: 491-502, 2004.
   IF = 1,075 ilość cytowań = 1

Sumaryczny IF – współczynnik przebicia wg listy filadelfijskiej na rok 2004 dla wyżej wymienionych prac od 1-6, IF = 12.358

Podziękowania

Pomimo rozczarowań
Nie potrafimy wyrzec się marzeń
I podążamy za głosem powołania
Ku Wielkiej Niewiadomej –
w Nieograniczoną Przestrzeń Nauki

/W. Gordon-Krajcer/

Dziękuję z głębi serca
Wszystkim, którzy poświęcili
swój czas na urzeczywistnienie
moich marzeń naukowych

Wszystkim Współautorom publikacji –
które stanowią istotę niniejszej pracy habilitacyjnej –
serdecznie dziękuję za współpracę
oraz ciekawe dyskusje naukowe.

Panu Profesorowi dr hab. Jerzemu Łazarewiczowi
serdecznie dziękuję za życzliwość, wyrozumiałość i pomoc
w czasie długoletniej mojej pracy wZakładzie Neurochemii
kierowanym przez Pana Profesora .

Koleżankom i Kolegom
z Zakładu Neurochemii IMDiK PAN
bardzo dziękuję za życzliwą atmosferę

Panu Profesorowi dr hab. Pawłowi Griebowi
bardzo dziękuję za inspirujące dyskusje naukowe oraz życzliwość.

Pani Docent dr Hannie Księżak – Reding
Serdecznie dziękuję za cenne wskazówki w przygotowaniu publikacji,
dyskusje oraz miłą atmosferę podczas mojego pobytu w USA

Pani Halinie Nowińskiej
dziękuję za wspaniałą pomoc techniczną w czasie prowadzenia
eksperymentów, przyjaźń, serdeczność i wsparcie duchowe.

KOMENTARZ

do rozprawy habilitacyjnej:

Zmiany w ekspresji:
białka beta amyloidu (βA), prekursora amyloidowego białka beta (ß-APP)
oraz w strukturze i ufosforylowaniu białka tau,
wywołane czynnikami zaburzającymi homeostazę komórki
w mózgu osób chorych na chorobę Alzheimera,
oraz w doświadczeniach *in vivo* i *in vitro*.

STOSOWANE SKRÓTY

AD	-	choroba Alzheimera (ang. Alzheimer's disease)
Aß	-	peptyd beta amyloidu
ßAPP	-	prekursor amyloidowego białka ß
Akt = PKB	-	kinaza białkowa B (ang. phosphoinositide 3 kinase)
Apo E2 / Apo E3	-	apolipoproteina E2 / apolipoproteina E3
AMPA	-	kwas alfa-amino-3-hydroksy-5-metylizoksazol-4-propionowy
CaM	-	kalmodulina
CaM-K II	-	wielofunkcyjna kinaza białkowa II zależna od Ca^{2+} i kalmoduliny
Cdk 5	-	cyklinozależna kinaza (ang. cyklin – dependent kinase 5)
DNA	-	kwas dezoksyrybonukleinowy
ERK 2	-	kinaza 2 z rodziny MAP kinaz (ang. Extracellular signal – regulated kinase 2)
GSK 3ß	-	kinaza syntezy glikogenu (ang. glycogen synthase kinase 3ß)
IP3	-	1,4,5, trisfosforan inozytolu (ang. inositol 1,4,5-trisphosphate)
KA	-	kwas kainowy
MAP-2	-	białko zasocjowane z mikrotubulami (ang. microtubul associated protein)
MARCK	-	białka substratowe PKC (ang. myristoylated alanine-rich C kinase substrate)
mRNA	-	informacyjny RNA
MK 801	-	dizocylpina, 5metylo-10,22dwuhydro5H-dibenzo cyklohepten-5,10,iminomaleinian (antagonista receptorów NMDA)

NMDA - kwas N-metylo-D-asparaginowy
(ang. N-methyl-D-aspartic acid)

OA - kwas okadaikowy

PCP - fencyklidyna

PKC - kinaza białkowa C (ang. protein kinase C)
a PKC – grupa atypowych PKC
c PKC – grupa klasycznych (konwencjonalnych) PKC
n PKC – grupa nowych PKC

PHF - parzyste helikalne włókna białka tau/sploty neurofibrylarne
(ang. paired helical filaments)

p 25 - jednostka regulatorowa Cdk5, podjednostka p 35

p 35 - jednostka regulatorowa Cdk5

PP2A - fosfataza 2A

ROS - rodniki tlenowe / reaktywne formy tlenu
(ang. reactive oxygen species)

SOD - dysmutaza ponadtlenkowa

WSTĘP

Badania neuropatologiczne ostatnich dwudziestu lat wykazały, iż w krajach rozwiniętych najczęstszą i jedną z najgroźniejszych chorób otępiennych jest choroba, pierwszy raz opisana przez Alojza Alzheimera w 1907 roku, i nazwana jego nazwiskiem. Choroba Alzheimera (AD - ang. Alzheimer's disease) cechuje się stopniowym zanikiem pamięci i innych funkcji poznawczych oraz zmianami neurozwyrodnieniowymi w mózgu, które są najczęstszą przyczyną otępienia. W obrazie neuropatologicznym tej choroby stwierdza się naczyniowe i śródtkankowe złogi amyloidu ß w postaci kongofilnej angiopatii naczyniowej, oraz występowanie płytek/blaszek starczych – których centrum stanowi odkładany pozakomórkowo, nierozpuszczalny amyloid ß. Blaszki starcze występują w mózgu nierównomiernie, najwięcej powstaje ich w korze potyliczno – skroniowej, najmniej w hipokampie. Równocześnie z występowaniem płytek starczych w obrazie neuropatologicznym obserwujemy zwyrodnienie włókienkowe komórek nerwowych, widoczne w postaci splotów neurofibrylarnych. Stwierdza się także ubytek komórek nerwowych i zakończeń synaptycznych (Selkoe, 1996, Tanzi i wsp. 1996). Choroba pozostaje w stadium przedklinicznym przez wiele lat, postępując stopniowo niszczy ośrodki układu limbicznego (Holmes C., Wilkinson D., 2000). Czynnikami patogenetycznymi prowadzącymi do rozwoju choroby Alzheimera są zmiany genetyczne lub czynniki środowiskowe. Czynniki związane ze środowiskiem mogą prowadzić do zmian patologicznych: w mitochondriach, zmian w obrębie struktur błonowych – peroksydacji lipidów, nadmiernej glikacji, powstawania wolnych rodników tlenowych, zaburzeń w metabolizmie Ca^{2+} i Fe^{2+}, zaburzeń glikolizy, zaburzeń w procesie proteolizy, degradacji DNA, apoptozy. W chorobie Alzheimera podłoże genetyczne stwierdza się w 10–40 % przypadków, chociaż niektórzy autorzy uważają, że występuje ono prawie u wszystkich chorych (Selkoe D., 1999). Szacuje się, że tylko u 2% - 3% wszystkich przypadków osób z chorobą Alzheimera to wczesna, rodzinna postać tej choroby – powstała w wyniku dziedziczenia autosomalnego dominującego (Tanzi R.E., 2001). Zmiany genetyczne dotyczą głównie mutacji w genach: **białka ß-APP; białka tau; presenilin – PS1 i PS2** (*białka biorące udział w proteolizie ßAPP, identyfikowane jako kofaktor γ-sekretazy lub γ-sekretaza*) (Thinakaran G., 2001); **apolipoprotein – głównie apolipoproteiny E (Apo E)** (Beffert i wsp. 1998, Gomez – Ramos i wsp. 2001) (*białka biorące udział w metabolizmie i redystrybucji lipidów*

w mózgu, w tym cholesterolu [Beffert U.1998]. Ekspresja mRNA apolipoprotein ma miejsce głównie w mózgu. Apolipoproteiny są syntetyzowane głównie przez astrocyty, nie stwierdzono ich syntezy w neuronach. Apo E znajduje się pozakomórkowo, wiąże się do włókien cytoszkieletu, indukując powstawanie splotów neurofibrylarnych [HuangY.i wsp. 2001]. Spadek poziomu ApoE powoduje wzrost odkładania się ßA i przyspiesza tworzenie blaszek starczych [Cho H.S. i wsp. 2001, Terai K. i wsp. 2001]. Stosując techniki immunoenzymateczne znaleziono fragmenty ApoE w mózgach osób z chorobą Alzheimera. Apo E jest kodowana przez gen na chromosomie 19. Znamy trzy izoformy ApoE – ε 2 ε 3 ε 4; a zatem trzy homozygotyczne i trzy heterozygotyczne genotypy. Występowanie allelu ε 4 wiąże się z wystąpieniem objawów choroby Alzheimera w młodszym wieku. Jego obecność jest czynnikiem ryzyka, zwłaszcza w przypadkach występowania rodzinnej choroby Alzheimera. Allel ε 4 ma prawdopodobnie wpływ na ekspresję i odkładanie się amyloidogennego peptydu Aß42 [Camicioli R.i wsp. 1999]; **białka pasma 3** *(główne białko transportowe anionów, poziom tego białka w erytrocytach odzwierciedla jego zmiany w mózgu)* (Kay M.M.B., Goodman J., 1997); **białka α-2-makroglobuliny** (Barcikowska M., 1998); **białka p97** (melanotransferyna) (Yamada i wsp. 1999a); **cystatyny C** *(inhibitor proteazy cysteinowej. Hamuje aktywnośc lizosomalnych katepsyn: B, H L, S. Zaburzenia w polimorfiźmie jej genu są wiązane z późnym wystąpieniem choroby Alzheimera)* (Beyer K.i wsp. 2001); **metaloproteinazy błony komórkowej** *(biorą udział w proteolizie, pełnią rolę adhezyjną przy wiązaniu integryn. Aktywność metaloproteinaz jest podwyższona u osób z zwyrodnieniem włókienkowym neuronów)* (Gerst i wsp. 2000); **proteoglikanów i glikozaminoglikanów** *(wiążą się do peptydów ßA, hamują proteolizę włókien amyloidowych)* (Mc Laurin J. i wsp. 1999); **α/ ß /γ- synukleiny** *(zaburzenia w proporcji poszczególnych synuklein wiążą się z chorobami neurodegeneracyjnymi. Poziom ß-synukleiny jest znacznie obniżony u osób z chorobą Alzheimera. Synukleiny gromadzą się w splotach neurofibrylarnych, tworząc tzw. skupiska filamentowe)* (Marui i wsp. 2000, Masliah E., i wsp. 2001)**, AD7c-NTP** *(należy do rodziny genów kodujących białka włókienek neuronalnych, w odniesieniu do odpowiedniej wiekowo kontroli występuje w wysokim stężeniu w płynie mózgowo–rdzeniowym oraz w osoczu u osób z chorobą Alzheimera,. Jego nadekspresja powoduje odkładanie się hiperufosforylowanego białka tau)* (De la Monte S.M., i wsp., 1999)**, konwertazy angiotensyny** *(enzym in vitro zapobiega nagromadzaniu się amyloidu, poprzez opóźnianie tworzenia włókien amyloidowych i agregacji form ßA, rozkłada peptydy ßA i inhibuje ich cytotoksyczność* (Crawford F. i wsp.,2000; Hu J. i wsp., 2001); **katepsyny D** *(wewnątrzkomórkowa kwaśna proteza istotny czynnik ryzyka w AD)* (Papassotiropoulos A. i

wsp., 2000); a także – **ubikwityny, α-antychymotrypsyny, butyrylocholinoesterazy K** (Haines J.L. i wsp. 2001).

Na uwagę zasługuje fakt, że płytki starcze i sploty neurofibrylarne pojawiają się w hipokampie i innych obszarach mózgu istotnych dla funkcji poznawczych u osób już w wieku około lat pięćdziesięciu, co nie stanowi jeszcze o procesie chorobowym, rozróżnienie bowiem pomiędzy normalnym starzeniem się a chorobą Alzheimera jest przede wszystkim ilościowe, chociaż, w porównaniu z normalnie starzejącym się mózgiem w płytkach starczych występuje znacznie więcej rozpuszczalnego i nierozpuszczalnego Aß42 z większą ilością różnego typu modyfikacji w C-końcowych aminokwasach Aß42 i Aß40 takich jak: racemizacja i oligomeryzacja (Funato H. i wsp. 1998). Odkładanie się płytek amyloidowych obserwujemy: w chorobie Downa (Glenner i wsp., 1984b), w neuronalnej ceroido-lipofuscynozie (Wiśniewski i wsp., 1993), w chorobie Parkinsona (Boller i wsp. 1980) w chorobie Huntingtona, holenderskiej wrodzonej amyloidozie z krwotokami mózgowymi, w chorobach wywołanych prionami, w stwardnieniu zanikowym bocznym rdzenia kręgowego, encefalopatii pourazowej oraz w niedokrwieniu mózgu (Abe i wsp., 1991, Kalaria i wsp., 1993). Zmiany morfologiczne typu zwyrodnienia nerwowo – włókienkowego również nie są patognomiczne tylko dla choroby Alzheimera, występują one w wielu innych zespołach chorobowych takich jak: zespole GSS, zespole stwardnienia zanikowego bocznego, chorobie Picka, otępienia z Guam, encefalopatii bokserskiej i wielu innych (Wiśniewski K.E. i wsp. 1985, Księżak – Reding i wsp., 1994, Suzuki i wsp., 1995, Fanny i Dickson 1996). Amyloid jaki odkłada się śródtkankowo w postaci tzw. płytek starczych u osób z chorobą Alzheimera obserwowany jest w mniejszej liczbie zespołów chorobowych aniżeli zwyrodnienie neurofibrylarne. Dotychczas nie do końca wyjaśniono na skutek jakich mechanizmów dochodzi u osób z chorobę Alzheimera do wzmożonego nagromadzania się w mózgu włókien amyloidowych, których głównym składnikiem jest peptyd nazwany β-amyloidem (Glenner i Wong., 1984b, Masters i wsp., 1985b), oraz splotów neurofibrylarnych, powstałych w skutek wysokiego ufosforylowania białka tau, które tworzy parzyste włókna heliakalne (PHF – paired helikal filaments). W patogenezie choroby Alzheimera odkładanie się amyloidu w postaci płytek starczych jest wcześniejsze, niż powstawanie splotów neurofibrylarnych (Wang D.S. i wsp. 2001).

Struktura i funkcja białka beta amyloidu (βA) oraz jego prekursora (β-APP)

W 1987 roku wykazano, że βA stanowi część znacznie większego białka prekursorowego β-APP. Białko to jest glikoproteiną typu I o znacznej zawartości konformacji ß (fałdowych) II-rzędowej struktury białek i ciężarze około 110-140 kDa. Gen ß-APP składający się z 19 eksonów zlokalizowany jest na chromosomie 21 (21q 21), (Goldgaber i wsp.,1987, Kang i wsp., 1987, Robakis i wsp., 1987, Tanzi i wsp., 1987, DeSauvage, Octave, 1989, Lemaire i wsp., 1989). W wyniku naprzemiennego splicingu może powstawać przynajmniej osiem transkryptów tego genu a w konsekwencji białek β-APP o różnej długości łańcucha, zawierających od 365 do 770 aminokwasów. Najczęstszymi izoformami β-APP są APP695, APP751 oraz APP770 (Tanaka i wsp., 1988). Obie dłuższe formy β-APP posiadają w części N-końcowej 56 aminokwasową wstawkę wykazującą znaczny stopień homologii z inhibitorami protez serynowych typu Kunitza (APP-KPI) (Kitaguchi i wsp., 1988, 1990, Ponte i wsp., 1988, Tanzi i wsp., 1988). Główną izoformą występującą u człowieka w ośrodkowym układzie nerwowym jest APP 695 (Tanaka i wsp., 1988, Clark i wsp., 1989, Golde i wsp., 1990, Yoshikai i wsp., 1990).

β-APP jest białkiem transbłonowym, o długim N-końcowym fragmencie pozakomórkowym, krótkim odcinku wewnątrzbłonowym oraz C-końcowym fragmencie wewnątrzkomórkowym. N-końcowy fragment cząsteczki APP-KPI uwalniany w wyniku proteolizy do przestrzeni pozakomórkowej odpowiada proteazie neksyny-II (Oltersdorff i wsp., 1989, Van Nostrand i wsp., 1989, Ramabhadran i wsp., 1993). Proces dojrzewania i posttranslacyjnych modyfikacji β-APP zachodzi w aparacie Golgiego i po odcięciu sekwencji sygnałowej, obejmuje glikozylację i sulfatację w N-końcowym fragmencie cząsteczki β-APP.

Cząsteczka βA stanowi 39-43 aminokwasowy fragment N-końcowego, wewnątrzbłonowego odcinka β-APP. 28 aminokwasów N-końcowych cząsteczki βA położonych jest pozakomórkowo, natomiast 11-14 aminokwasów C-końcowych występuje w błonie komórkowej. Cząsteczka βA stanowiąca produkt białkowy eksonu 16 i 17, tworzona jest w wyniku proteolizy cząsteczki β-APP. Dokładne mechanizmy powstawania βA oraz enzymy zaangażowane w ten proces nie zostały jeszcze dokładnie scharakteryzowane. Uważa się, że istnieją dwa główne szlaki metaboliczne β-APP: (i) szlak sekrecyjny oraz (ii) szlak endosomalno-lizosomalny. Enzymy włączone w proces proteolitycznego rozpadu cząsteczki ß-APP i tworzenia βA nazwano sekretazami: α, β i γ. Podczas fizjologicznego metabolizmu

Dwie drogi obróbki prekursora amyloidowego białka beta (ß-APP)

Nie-amyloidogenna

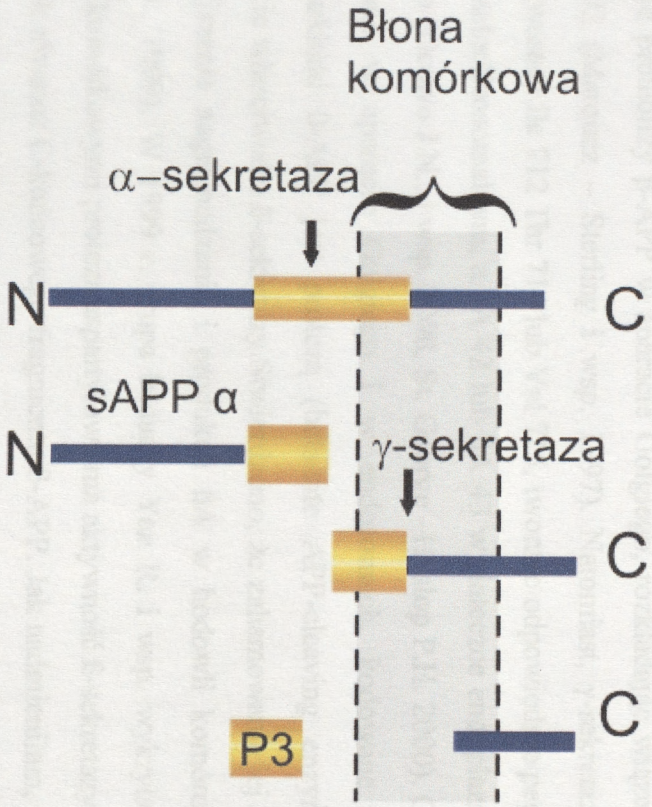

Amyloidogenna

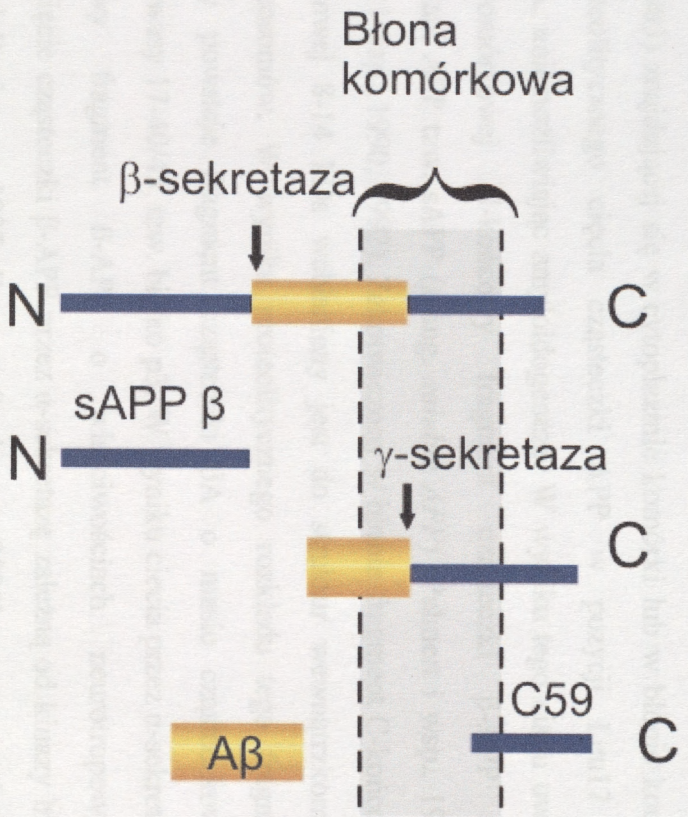

sAPPα i sAPPβ mają działanie neuroprotekcyjne.
Cięcie przez α-sekretazę zapobiega tworzeniu się amyloidu (Aβ)

cząsteczka β-APP ulega proteolizie przez α-, ß-, i γ-sekretazy w trzech miejscach między resztami 671-672 (N-koniec), 687-688 (16-17 ßA), 713-714 (C-koniec).

Około 10-30% β-APP ulega przemianom na szlaku sekrecyjnym (Weidemann i wsp., 1989, Caporaso i wsp., 1992). Ten fizjologiczny proces zachodzi przy udziale α-sekretazy, (metaloproteazy przynależnej do rodziny adamalizin - ADAM 9, ADAM 10, ADAM17), (Allinson i wsp. 2003) znajdującej się w cytoplazmie komórki lub w błonie komórkowej i prowadzi do proteolitycznego cięcia cząsteczki APP w pozycji Leu17 sekwencji aminokwasowej βA, uniemożliwiając amyloidogenezę. W wyniku tego ciągu uwalniany do przestrzeni pozakomórkowej N-końcowy fragment cząsteczki β-APP odpowiada rozpuszczalnej postaci APP tzw. sAPP (z ang. *soluble APP*) (Palmert i wsp., 1989, Esch i wsp., 1990, Sisodia i wsp., 1990, 1992). Zakotwiczony w błonie fragment C-końcowy ß-APP o masie cząsteczkowej 8-14 kDa wchłaniany jest do struktur wewnątrzkomórkowych, przypuszczalnie lizosomów. W wyniku proteolitycznego rozkładu tego fragmentu przy udziale γ-sekretazy powstaje fragment cząsteczki βA o masie cząsteczkowej 3-kDa obejmujący aminokwasy 17-40/43, tzw. białko p3. W wyniku ciecia przez α-sekretazę zostaje odcięty C-końcowy fragment ß-APP o właściwościach neurotropowych oraz cytotoksycznych. Cięcie cząsteczki β-APP przez α-sekretazę zależną od kinazy białkowej C (PKC), (Marambaud P., i wsp. 1997, Rossner S., i wsp. 2001) nazwano także szlakiem nieamyloidogennym. Za szlak amyloidogenny uznaje się szlak endosomalno-lizosomalny i rozkład proteolityczny β-APP przy udziale sekretaz β i γ **(Ryc. 1)**. Patologiczny metabolizm β-APP rozpoczyna się od wewnątrzbłonowego proteolitycznego działania ß-, i γ-sekretaz. ß-sekretaza dokonuje proteolizy β-APP w aparacie Golgiego, rozkładając wiązanie między Met 671 a ASP 672 (Marquez – Sterling i wsp. 1997). Natomiast, γ-sekretaza rozkłada wiązania po aminokwasach Ile 712 Thr 714 lub Val 715, tworząc odpowiednie peptydy ßA40 w układzie endosomalnolizosomalnym, a ßA 42 lub ßA 43 w siateczce endoplazmatycznej i w aparacie Golgiego (Octavo J.N., i wsp. 2000, St. George –Hyslop P.H. 2000). Okazało się, że białko znalezione w aparacie Golgiego i w endosomach, kodowane przez gen proteolitycznego rozkładu ß-APP jest protezą (beta-site APP-cleaving enzyme-BACE), wykazującą wszystkie właściwości ß-sekretazy.Stwierdzono, że zahamowanie jej aktywności powodowało zmniejszenie nagromadzania i produkcji ßA w hodowli komórek HK 293 (McLaurin J. i wsp., 1999). W 1999 r. grupa badaczy Yan R. i wsp. wykryła, że nowa, związana z błonami komórkowymi proteza aspartylowa ma aktywność ß-sekretazy, zmniejsza ona produkcję ßA jak również C-końcowego fragmentu ß-APP. Jak nadmieniłam, γ-sekretazy biorą udział w ostatnim etapie obróbki ß-APP i generacji ßA. Istnieje szereg dowodów

wskazujących, że preseniliny (PS) a szczególnie PS1 mogą być kofaktorem γ-sekretazy, albo γ-sekretazą (Selkoe D.J., 2001a, Thinakaran G., 1999). Ustalono, że heterodimery presenilin stanowią część katalityczną γ-sekretazy (Wolfe M.S., 2001). Preseniliny PS1 i PS2 są białkami o wysokiej homologii (Thinakaran G., 2001), które mogą pełnić funkcje receptorów błonowych lub kanałów wapniowych. Występują one głównie w komórkach nerwowych, szczególnie widoczna jest ich ekspresja w komórkach hipokampa, nie występują natomiast w astrocytach i oligodendrocytach (Fraser P.E. i wsp. 2000). Preseniliny PS1 i PS2 są kodowane przez geny (odpowiednio) na chromosomie 14 i 2. Okazało się, że preseniliny są związane i odpowiedzialne głównie za występowanie wczesnej rodzinnej choroby Alzheimera (Selkoe D.J., 2001b). Choroba związana z mutacją w genach PS1 pojawia się w wieku 30-50 lat a mutacje w genach preseniliny PS2 powodują pojawienie się symptomów choroby w wieku ok. 60 lat (Ezqurrra M. i wsp., 2000). Preseniliny regulują homeostazę wapniową w siateczce endoplazmatycznej, oraz indukują wzrost podatności na apoptozę (Kuźnicki J., Puzianowska-Kuźnicka M., 1998, St. George-Hyslop P.H., 2000, Thinakaran G., 1999). Mutacje w PS1 naruszają strukturę II rzędową białka ß-APP - wpływając na stopień jego pofałdowania (Katayama T. i wsp., 1999). W 2001 roku A. Fergani i wsp. opublikowali pracę, w której scharakteryzowali białko nazwane nikastryną, które reaguje z presenilinami i z białkiem ß-APP, wpływając także na produkcję ßA. W badaniach na myszach transgenicznych wykazano, że wzrost ekspresji PS1 – zmutowanej lub normalnej nie ma wpływu na ilość Aß40 natomiast w sposób istotny zwiększa ilość Aß42 (Sołtysiak Z., 2000). Zaobserwowano, że u ludzi z mutacjami PS1 występuje we krwi wzrost stężenia Aß42, zarówno przed jak i w czasie wystąpienia ostrej fazy choroby Alzheimera (Selkoe D., 1999). Na obecnym etapie badań należy uznać, że każda ze zidentyfikowanych mutacji w presenilinach wyzwala kaskadę procesów prowadzących do utraty neuronów i otępienia, poprzez zmiany we włóknach neurofibrylarnych, oraz powstanie ß-amyloidozy.

Białko β-APP jest białkiem o krótkim okresie półtrwania ok. 45-60 min. (Selkoe D.J. 2001). Jego obecność stwierdzono u wszystkich przebadanych pod tym względem ssaków (Brzyska M., Elbaum D., 2000). β-APP jest białkiem obecnym we wszystkich komórkach organizmu. Funkcje biologiczne β-APP nie zostały dotychczas dokładnie poznane. Budowa cząsteczki β-APP sugeruje, że białko to może pełnić rolę receptora błonowego (Kang i wsp., 1987) i poprzez oddziaływanie z układem białek G brać udział w błonowym przekazywaniu sygnałów (Nishimoto i wsp., 1993). β-APP bierze udział w dojrzewaniu i podziałach komórek (Saitoh, 1989), w odczynach immunologicznych (Schubert i wsp., 1993), w procesach

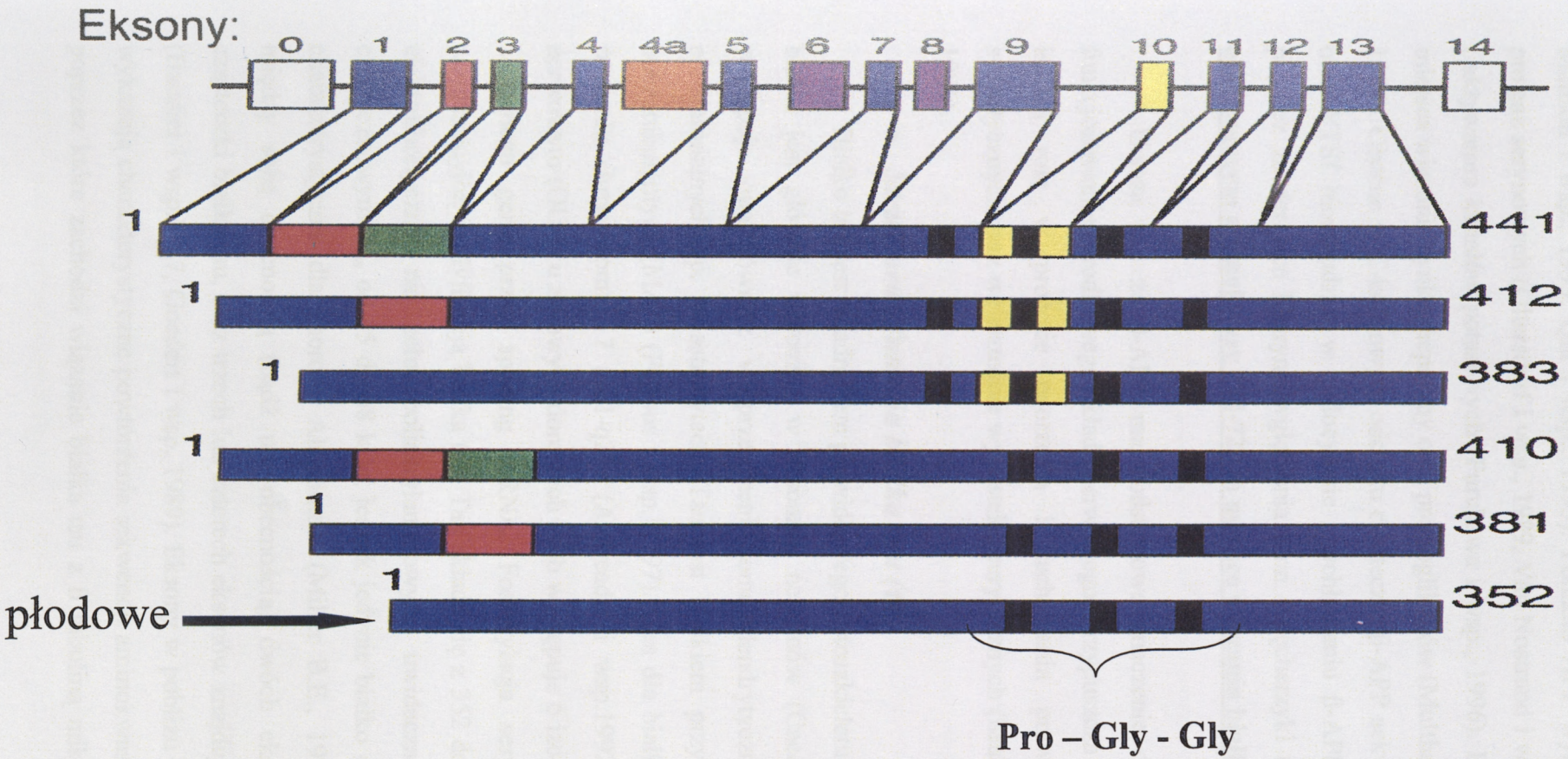

Schemat genu Tau i jego izoform u ludzi.
Eksony: E0 i E14 nie są kodowane, Eksony: E2, E3, E10 są odpowiedzialne za powstanie 6 izoform białka Tau. Ekson E4a jest ekspresjonowany w obwodowym układzie nerwowym.

regeneracji tkanek (Smith RP et al., 1990, Van Nostrand i wsp., 1990, Milward i wsp., 1992, Mattson i wsp., 1993, Qiu i wsp., 1995). Ponadto APP wykazuje właściwości inhibitora proteaz serynowych (Oltersdorf i wsp., 1989, Van Nostrand i wsp., 1989, Sinha i wsp., 1990) i aktywatora kanałów potasowych (Furukawa i wsp., 1996). Fragment N-końcowy zawiera miejsca wiązania cynku, heparyny oraz proteoglikanów (Multhaup i wsp., 1995, Small i wsp., 1996). Obecne w C-końcowym odcinku cząsteczki β-APP sekwencje aminokwasowe NPTY oraz YTSI biorą udział w endocytozie i wchłanianiu β-APP z błony cytoplazmatycznej poprzez zawierające klatrynę wgłębienia błon i pęcherzyki (Lai i wsp., 1995). **Odcinek obejmującym aminokwasy 714-723 to miejsce wiązania białka tau (Smith i wsp., 1995).**

Uważa się, że β-APP ma podstawowe znaczenie dla prawidłowego rozwoju i funkcjonowania ośrodkowego układu nerwowego. Przypuszcza się, że β-APP może odgrywać istotną rolę w procesie tworzenia i zachowania prawidłowej struktury połączeń synaptycznych oraz we wzroście wypustek neurytycznych (Mucke i wsp.,1996, Small i wsp., 1996).

- ***Struktura i funkcja białka tau (τ)***

Białko tau jest składnikiem prawidłowego cytoszkieletu neuronalnego. Ekspresja tego białka jest głównie widoczna w aksonach neuronów (Caceres i Kosik 1990), chociaż występuje ono również w przestrzeni somatodendrytycznej a także w komórkach nieneuronalnych np. w astrocytach. Tau jest białkiem przynależnym do rodziny białek mikrotubularnych (MAP) (Fellous i wsp. 1997). Gen dla białka tau znajduje się na długim ramieniu chromosomu 17 (q21-q22) (Andreadis i wsp.1992). W ośrodkowym układzie nerwowym (OUN) u zdrowych dorosłych osób występuje 6 izoform białka tau, powstających z jednego genu przez splicing mRNA. Fosforylacja seryny i treoniny jest jedyną potranslacyjną modyfikacją białka tau. Tau składa się z 352 do 441 aminokwasów. Rozkład elektroforetyczny na żelu poliakrylamidowym uwidacznia 6 pasków o ciężarze cząsteczkowym M_w od 45 do 68 kDa, jednak jedynie białko o M_w 68 kDa wydaje się być charakterystyczne dla choroby Alzheimera (Miller B.E., 1999) Izoformy tau różnią się między sobą obecnością (bądź nie obecnością) dwóch eksonów w obszarze N-końca cząsteczki białka tau, oraz trzech lub czterech eksonów znajdujących się w pobliżu C-końca (Baudier i wsp.1987, Goedert i wsp. 1989). Eksony w pobliżu C-końca cząsteczki białka tau wykazują charakterystyczne powtórzenia sekwencji aminokwasowych **Pro-Gly-Gly (Ryc. 2)** poprzez które zachodzi wiązanie białka tau z ß tubuliną mikrotubul (Iqbal, Grudke-Iqbal,

1996). Większa ilość eksonów w odcinku C-końcowym białka tau, zwiększa jego wiązanie do mikrotubul. Tau poprzez wiązanie z β tubuliną bierze udział w procesie tworzenia, polimeryzacji i stabilizacji mikrotubul (Drechsler i wsp. 1992), w wyznaczaniu polarności aksonu. Zmniejszanie ekspresji tau prowadzi do zahamowania wzrostu aksonów (Caceres i Kosik,1990). Nadmierne ufosforylowanie białka tau prowadzi do jego polimeryzacji w proste włókna, które następnie po reakcji glikozylacji (Ledesma i wsp., 1995) łączą się i skręcają, tworząc parzyście skręcone włókna neurofibrylarne, zwane również splotami neurofibrylarnymi (PHF – paired helical filaments), które zawierają 6 - izoform tau. W następnym etapie PHF łączą się w struktury o wyglądzie kłębków (Brion i wsp. 2001), które nazwano kłębkami neurofibrylarnymi (NFT – neurofibrillary tangles). Obecność hiperufosforylowanych epitopów tau pojawia się w komórkach nerwowych wcześniej, aniżeli tau w postaci PHF (Bancher i wsp., 1989). Jak wykazano, nadmierna fosforylacja tau zmniejsza jego powinowactwo wiązania do mikrotubul cytoszkieletu. W konsekwencji nadmierna fosforylacja białka tau może doprowadzić do uszkodzenia cytoszkieletu, zaburzeń w procesie transportu aksonalnego, podziału komórki a w konsekwencji do śmierci komórki (Busciglio i wsp.1995). Na uwagę zasługuje fakt, iż tau tworzące PHF jest fosforylowane w tych samych pozycjach aminokwasowych co płodowe białko tau (Goedert, 1996) oraz dodatkowo na innych epitopach w zależności od stopnia fosforylacji. Ufosforylowanie białka tau w mózgu dorosłego zdrowego człowieka wynosi 2-3 mole fosforu / mol białka, w mózgu płodu ludzkiego 6 moli fosforu / mol białka (po urodzeniu gwałtownie spada), zaś w mózgu osób z chorobą Alzheimera 5-9 moli fosforu / mol białka (Köpke E i wsp. 1993, Morishima – Kawashima M.i wsp. 1995a).W białku tau tworzącym sploty neurofibrylarne – PHF określono ponad 20 miejsc fosforylacji (Morishima – Kawashima M i wsp. 1995b, Hanger D.P.i wsp 1998) .

Nasilenie objawów choroby Alzheimera bardzo dobrze koreluje ze wzrostem ilości splotów neurofibrylarnych (Buee L. i wsp., 2000), co jest koronnym argumentem zwolenników teorii o dominującej roli białka tau w patogenezie choroby Alzheimera. Dopełnieniem tej teorii jest fakt, iż mutacje w genie obecnym w chromosomie 17 i odpowiedzialnym za tworzenie się nieprawidłowo ufosforylowanego białka tau stwierdzono w wielu innych patologiach miedzy innymi w otępieniu czołowo–skroniowym z towarzyszącym parkinsonizmem, - w obrazie neuropatologicznym tej choroby występuje zwyrodnienie włókienkowe, ale nie obserwuje się złogów ß amyloidu. Zatem, w tej chorobie zmiany w strukturze i funkcji tau, bez koniecznej obecności ß amyloidu , prowadzą do utraty neuronów i postępującego otępienia.

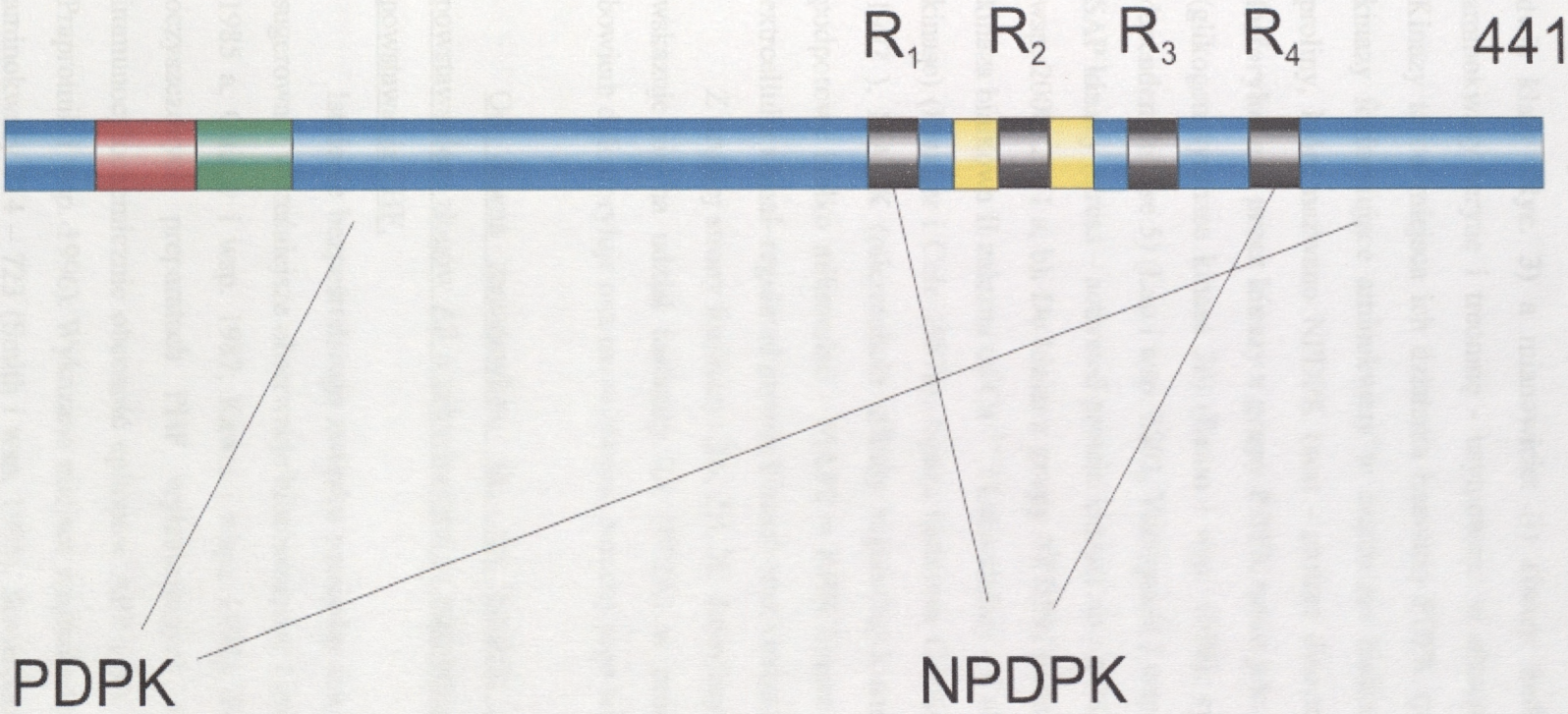

Schemat białka tau (izoformy 1-441) i obszar działania kinaz z grupy PDPK i NPDPK

- ***Fosforylacja / Defosforylacja białka tau***

Stopień ufosforylowania białka tau jest konsekwencją i wypadkową działania kinaz i fosfataz. Dotychczas zidentyfikowane kinazy, które fosforylują tau zostały zgrupowane w dwie klasy **(Ryc. 3)** a mianowicie: (i) kinazy fosforyzujące w cząsteczce białka tau aminokwasy serynę i treoninę - usytuowane w obszarze (pobliżu) występowania proliny. Kinazy te od miejsca ich działania nazwano PDPK (proline directed protein kinases), (ii) kinazy fosforylujące aminokwasy w cząsteczce białka tau nie usytuowane w sąsiedztwie proliny, które nazwano NPDPK (non - proline directed protein kinases). **Białko tau jest fosforylowane przez kinazy z grupy PDPK takie jak:** kinaza syntezy glikogenu - **GSK–3ß** (glikogen synthase kinase 3ß) (Baum i wsp. 1996); cyklinozależna kinaza **Cdk5** (cyklin–dependent kinase 5) (Lau i wsp. 2002, Yamaguchi i wsp. 1996), kinazy aktywowane stresem- **SAP kinazy** (stress – activated protein kinase) np.**: p 38, p 49** (Goedert i wsp. 1997, Zhu X. i wsp. 2000, 2001 a, b**). Do kinaz z grupy NPDPK fosforylujących białko tau należą m.in.:** kinaza białkowa II zalezna od Ca^{2+} i kalmoduliny - **CaMPKII** (Ca^{2+}/calmodulin dependent kinase) (Baudier i Cole 1987a); kinaza białkowa C-**PKC** (protein kinase C) (Correas i wsp. 1992), **MARK** (microtubule affinity regulating kinase) (Trinczek i wsp., 1995) a także podporowe białko mikrotubul - **MAP2 = ERK** kinaza (microtubule associated protein 2 = extrcellular signal–regulated protein kinase) oraz kinaza białkowa A-**PKA** (protein kinase A).

Z drugiej strony fosfatazy: 2A, 2B, 2C defosforylują tau (Iqbal i wsp. 1997). Głównie wskazuje się na udział fosfatazy 2A (PP2A) w procesie regulacji ufosforylowania tau, bowiem defosforyluje ona tau w obrębie domeny jego wiązania z tubuliną (Lu i wsp. 1999).

Od dawna zastanawiano się, czy istnieje związek patogenetyczny pomiędzy powstawaniem złogów Aβ a zaburzeniami w metabolizmie MAP – tau, które prowadzą do powstawania PHF.

Istnienie bezpośredniego związku pomiędzy tau, β-APP i βA w chorobie Alzheimera sugerowały wcześniejsze obserwacje biochemiczne i immunocytochemiczne. (Masters i wsp. 1985 a, Guiroy i wsp. 1987, Kawai i wsp., 1992). Wykazano obecność sekwencji βA w oczyszczonych preparatach PHF wyizolowanych z mózgów chorych na AD, zaś immunocytochemicznie obecność epitopów APP i βA w PHF wykazali (Perry i wsp.1993, Praprotnik i wsp. 1996). Wykazano miejsce wiązania tau do β APP w odcinku obejmującym aminokwasy 714 – 723 (Smith i wsp. 1995). Stwierdzono, również że ß - amyloid indukuje fosforylację tau (Busciglio i wsp. 1995).

Nie wiadomo dotychczas, jakiego rodzaju proces patologiczny ostatecznie prowadzi do odkładania się włókienek amyloidu w neuropilu. Nie wiemy również, jaki czynnik inicjuje powstanie splotów neurofibrylarnych (PHF).

Przeszkodą w ustaleniu sekwencji procesów prowadzących do: uwalniania białka ß amyloidu z cząsteczki prekursora tego białka, powstawania PHF, jest niewątpliwie brak wygodnego zwierzęcego układu modelowego choroby Alzheimera.

Badanie tego procesu na dobrze poznanym modelu zwierzęcym być może pozwoliłoby lepiej zrozumieć i przyczyniłoby się do poznania sekwencji zdarzeń doprowadzających do odkładania się włókien amyloidowych i splotów neurofibrylarnych. W ostatnich 10 – 15 latach badania dotyczące obróbki β- APP i βA były prowadzone na dość dobrze już poznanym i opracowanym modelu niedokrwienia (ischemii) mózgu. Podjęcie takich badań na modelu niedokrwienia mózgu wydaje się być słuszne w zestawieniu z wynikami mówiącymi, że na skutek głębokich zranień głowy (Gentlemant i wsp. 1993) lub na skutek powtarzalnych urazów głowy, co ma miejsce np. u bokserów, powstaje syndrom zwany dementia pugilistica, następuje proces przyspieszonego nagromadzania się w mózgu białka beta amyloidu w wyniku wadliwej obróbki jego prekursora a także nadmiernej fosforylacji białka tau i tworzenia splotów neurofibrylarnych.

Na podstawie badań własnych stwierdziłam, że niedokrwienie pewnego obszaru mózgu powstałe na skutek sprowokowanego wylewu podpajęczynówkowego (SAH) u szczura - powodowało znaczny, statystycznie znamienny wzrost immunoreakcji (w stosunku do immunoreakcji obserwowanej u szczura poddanego pozorowanej operacji) z przeciwciałami przeciwko epitopom: C-końcowej, M-wewnątrzbłonowej (reakcja z przeciwciałem 6E10, skierowanym przeciwko fragmentowi 597 – 613 aa) i N-końcowej domeny białka β-APP. Badania prowadzone były na homogenatach z kory mózgowej oraz z hipokampa. Wyniki zostały przedstawione w pracy (M. Ryba i wsp., 1999).

Inni badacze (Kalaria i wsp., 1993, Robinson i wsp., 1993, Pluta i wsp. 1994) również wykazali, iż na skutek niedokrwienia (ischemii) w mózgu następuje nagromadzanie różnych fragmentów β-APP. Godnym odnotowania jest fakt opisany przez Abe i wsp., 1991, o zwiększonej selektywnej indukcji mRNA fragmentu β-APP zawierającego domenę inhibitora proteinazy serynowej typu białka Kunitza (KPI) w procesie ischemii.

Z prac dotyczących ischemii wynika, że wapń jest jednym z głównych czynników neurotoksycznych w tym procesie, a jego przemieszczenie przez błonę komórkową do wnętrza komórki odbywa się w wyniku pobudzenia przez endogenny kwas glutaminowy

receptorów pobudzających aminokwasów wrażliwych na kwas N-metylo-D-Asparaginowy (NMDA) a także przypuszczalnie receptorów dla kwasu kainowego (KA) i 2-amino-3-hydroxy-5-methyloisoxazolo - 4–propionianu (AMPA).

Z drugiej strony wiemy, że wapń w OUN jest jednym z najważniejszych wewnątrzkomórkowych przekaźników. Odgrywa podstawową rolę w rozwoju neuronów, transmisji synaptycznej oraz w regulacji wielu dróg metabolicznych. Wiemy również, że stężenie wapnia w tkance mózgowej pacjentów z chorobą Alzheimera jest podwyższone, przy czym największe w neuronach znajdujących się w NFT.

Hipotetycznie zakładamy, że zaburzenie homeostazy wapnia w komórce będące elementem cytotoksycznego działania aminokwasów pobudzających w kaskadzie procesów biochemicznych powoduje w pierwszym etapie proteolizę β-APP, a dalej poprzez jego indukcję nagromadzenie w mózgu zarówno prekursora, jak i neurotoksycznego białka-beta (βA). Indukcja białka-beta uruchamia z kolei szereg procesów (które schematycznie uwidoczniłam na **Ryc. 4.)**, powodując m.in. zaburzenie homeostazy wapnia w komórce.

Zmiana homeostazy wapnia oraz powstawanie reaktywnych rodników tlenowych może być wynikiem zmian w endogennym układzie transportu jonów białek receptorowych błon komórkowych. (Kourie J.I. 2001).

Wiadomo, że wzrost wewnątrzkomórkowego stężenia jonów wapnia wpływa .na aktywność Ca^{2+}-zależnych kinaz/fosfataz, proteaz, a te wpływają na fosforylację/defosforylację i proteolizę różnych białek, także białka tau.

Kalcyneuryna (zwana także fosfatazą 2B) jest głównym białkiem wiążącym kalmodulinę w mózgu oraz jedyną fosfatazą seryna/treonina, będącą pod kontrolą układu Ca^{2+}/ kalmodulina. Uważa się, że jedna z trzech izoform kalcyneuryny może zapobiegać fosforylacji i nagromadzaniu się białka tau we wczesnym okresie choroby Alzheimera. (Hata R., i wsp.,2001). Wiele danych wskazuje na ważną rolę rodników tlenowych (ROS – ang. reactive oxygen species) i szoku oksydacyjnego w patogenezie AD.

Cytotoksyczne dzialanie peptydów Aß polega m.in.na zaburzeniu homeostazy Ca^{2+} i wytwarzaniu reaktywnych rodników tlenowych. Indukcja ROS powoduje peroksydację fosfolipidów błonowych, a co się z tym wiąże modyfikuje wewnątrzkomórkowy transport jonów, powoduje spadek cytoplazmatycznego ph oraz spadek poziomu ATP, wpływając na inhibicję fosforylacji (Kourie J.I. 2001). W tym procesie jony metali, zwłaszcza Fe^{3+}, Cu^{2+} i Zn^{2+}, a także Al^{3+} w zależności od równowagi pomiędzy ich komórkowymi związkami mogą pełnić rolę pro lub antyoksydantów (Papassotiropoulos A., i wsp., 2000; Sayre L.M. i wsp., 2000).

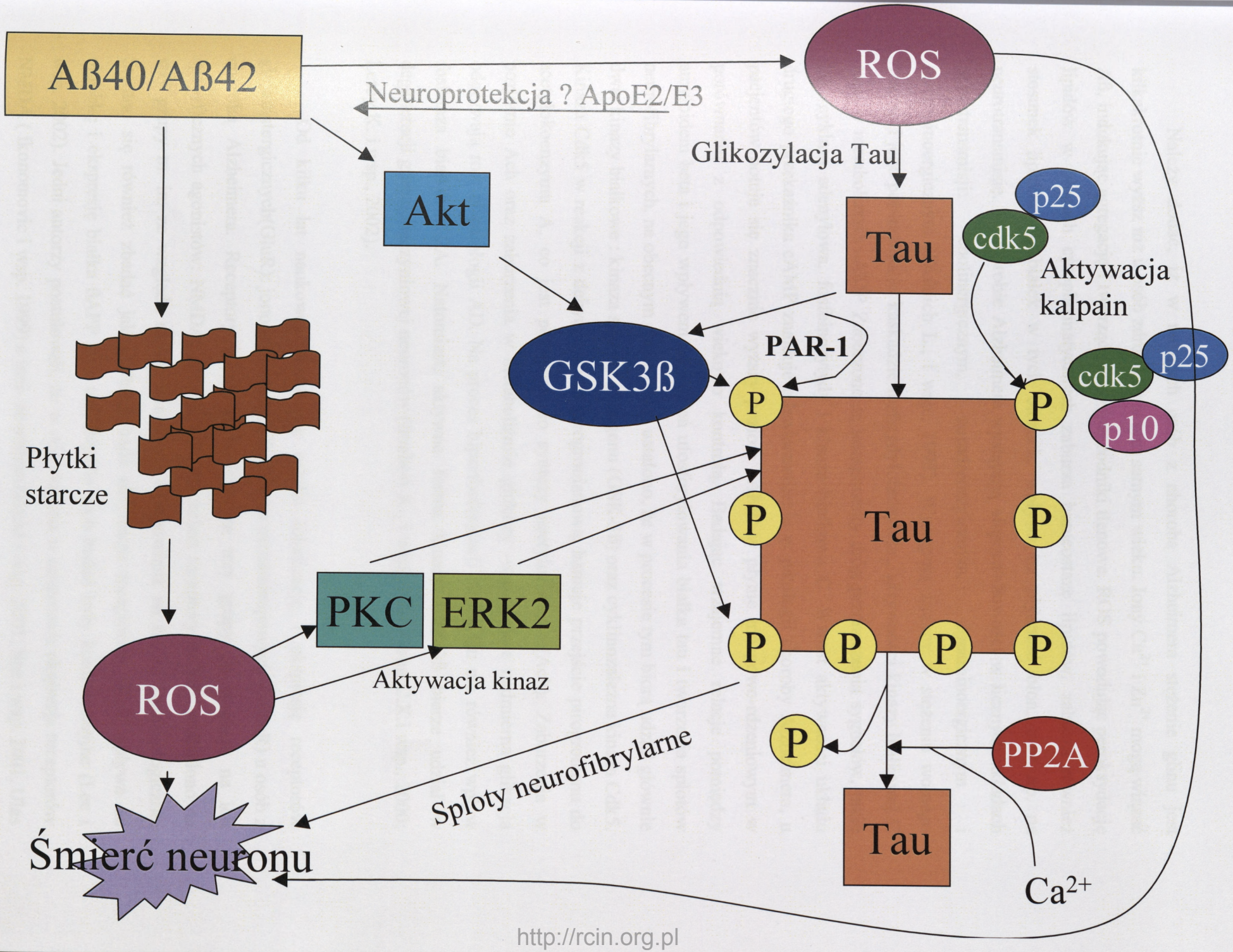

Należy dodać, iż w mózgach osób z chorobą Alzheimera stężenie glinu jest kilkakrotnie wyższ niż u osób zdrowych w tym samym wieku. Jony Cu^{2+} i Zn^{2+} mogą wiązać Aß, indukując agregację i tworząc reaktywne rodniki tlenowe. ROS powodując peroksydację lipidów w błonach cytoplazmatycznych zaburza homeostazę lipidów, zaburza również stosunek lipidów do białek w tych błonach, wpływa na płynność błon, oraz np. na neurotransmisję. W chorobie Alzheimera występują nieprawidłowości w licznych układach neurotransmisji: cholinergicznym, noradrenergicznym, dopaminoergicznym i serotoninoergicznym (Frohlich L., i wsp., 1998). Występują zmiany w stężeniu wolnego wapnia i jego pobieraniu, w kaskadzie fosfatydyloinozytolu., aktywności kinazy białkowej C oraz w metabolizmie cAMP Zaburzone są komponenty dróg przenoszenia sygnałów, takie jak: cyklaza adenylowa, fosfoinozytydy i kinaza białkowa C. Wzrost aktywności układu drugiego przekaźnika cAMP znajduje odzwierciedlenie w patologii choroby Alzheimera, u pacjentów notuje się znacznie wyższy poziom cAMP w płynie mózgowo-rdzeniowym w porównaniu z odpowiednią wiekowo kontrolą. Badając wzajemne relacje pomiędzy amyloidem beta i jego wpływem na stopień ufosforylowania białka tau i tworzenia splotów neurofibrylarnych, na obecnym etapie badań ustalono, że w procesie tym biorą udział głównie dwie kinazy białkowe : kinaza syntezy glikogenu (GSK-3ß) oraz cyklinozależna kinaza Cdk5. Kinaza Cdk5 w reakcji z dehydrogenazą pirogronianową, hamuje przejście pirogronianu do acetylokoenzymu A, co jest potrzebne do syntezy acetylocholiny (Ach). Zaburzenia w poziomie Ach oraz zaburzenia w metaboliźmie glukozy –szczególnie nadmierna glikacja odgrywają rolę w patologii AD. Na proces hiperfosforylacji białka tau ma również wpływ fosfataza białkowa 2A. Natomiast, aktywna forma kinazy GSK-3ß bierze udział w degeneracji granulonaczyniowej neuronów (Imahori K., i wsp., 1997 Gong C.X.i wsp., 2000; Leroy K. i wsp., 2002).

Od kilku lat naukowcy starali się ustalić lokalizację i ekspresję receptorów glutamatergicznych(GluR): jonotropowych (iGluR) oraz metabotropowych (mGluR) u osób z chorobą Alzheimera. Receptory iGluR podzielono na trzy grupy ze względu na ich specyficznych agonistów: NMDA, AMPA, KA, natomiast receptory mGluR podzielono na trzy grupy m. in. ze względu na ich homologię i odpowiedź na środki farmakologiczne. Starano się również zbadać jak inhibicja bądź aktywacja receptorów GluR wpływa na obróbkę i ekspresję białka ßAPP oraz tau. Wyniki tych badań były kontrowersyjne (Lee i wsp. 2002). Jedni autorzy postulowali, że w AD wzrasta w neuronach ekspresja receptorów NMDA (Ikonomovic i wsp. 1999) a inni- że maleje (Hynd i wsp. 2001, Sze i wsp. 2001, Ulas

i Cotman 1997), jeszcze inni badacze twierdzili, że nie ma różnicy pomiędzy AD a odpowiednią wiekowo kontrolą (Bi i Sze 2002; Panegyres i wsp. 2002; Thorns i wsp. 1997; Wakabayashi i wsp. 1999).

Zagadnienie jest istotne, ze względu na rolę receptorów NMDA w konsolidacji / rekonsolidacji pamięci (Clayton i wsp. 2002; Nakazawa i wsp. 2002). W 1986 r. Geddes i Cotman stwierdzili korelację pomiędzy dystrybucją receptorów NMDA a występowaniem płytek starczych i splotów nurofibrylarnych. Nie stwierdzono jednak, jaka jest rola receptorów NMDA w procesie powstawania PHF i płytek amyloidu.

Wyniki badań odnośnie roli receptorów AMPA i KA w patologii AD były również kontrowersyjne. Jedni autorzy postulowali ich udział i w tym schorzeniu (Page i wsp. 1991; Weiss i wsp. 1994) inni (Armstrong i wsp. 1994; Ikonomovic i wsp. 1995) twierdzili odwrotnie - argumentując, że ilość receptorów AMPA w obszarach mózgu istotnych i dotkniętych zmianami chorobowymi była znikoma, natomiast obserwowano w tym rejonie znaczną ilość PHF. Takie kontrowersje między autorami publikacji, skłoniły mnie do podjęcia badań w tym kierunku.

Obecnie coraz większą uwagę zwraca się na rolę wtórnych przekaźników w procesie metabolizmu β-APP. Jest prawdopodobne, że w tej kaskadzie następujących po sobie zdarzeń będziemy mogli poprzez ingerencję w pewne etapy przemian metabolicznych, zahamować proces nagromadzania się beta-amyloidu i powstawania zwyrodnienia włókienkowego **(Ryc. 4).** Aby tak się stało, konieczne jest dokładne poznanie sekwencji zdarzeń w tym cyklu. Mając powyższe na uwadze w poszczególnych pracach składających się na kompendium pracy habilitacyjnej dążyłam do pogłębienia wiedzy na ten temat.

Omawiana praca nr.1.

Tytuł pracy: „Excitotoxicity – induced expression of amyloid precursor protein (β-APP) in the hippocampus and cortex of rat brain. An electron-microscopy and biochemical study", Folia Neuropathologica 39, 2001.

Cel pracy: Postanowiliśmy zbadać jak pobudzenie ekscytotoksyczne, wywołane domózgowym podaniem (metodą mikroinjekcji) do CA I hipokampa szczura aminokwasów pobudzających: kwasu glutaminowego, AMPA lub NMDA wpływa na obróbkę i ekspresję białka β-APP oraz jaki jest wpływ ekscytotoksycznego pobudzenia na ultrastrukturę komórki i komórkową lokalizację Ca^{2+}.

W homogenatach otrzymanych z CA I hipokampa oraz z kory mózgowej, po mikroinjekcji NMDA, obserwowaliśmy wzrost immunoreakcji z przeciwciałami przeciwko różnym domenom białka β-APP. Immunoreakcja z przeciwciałami skierowanymi przeciwko epitopom N-końcowym białka β-APP była widoczna dopiero po upływie 12 godz. od mikroinjekcji, wzrastała ona 4,5 krotnie, po upływie 24 godz. od podania, zaś po trzech dniach obserwowaliśmy spadek immunoreakcji do wartości kontrolnej. Podobną immunoreaktywność obserwowano z przeciwciałami skierowanymi przeciwko domenie C-końcowej i śródbłonowej (M) białka β - APP.

Podanie dootrzewnowo, 30 min przed właściwym eksperymentem MK–801–antagonistę receptorów NMDA hamowało ekspresję i obróbkę białka β-APP, co wyrażało się znacznym spadkiem immunoreakcji z przeciwciałami - skierowanymi przeciwko epitopom N M i C – końcowym. Iniekcja NMDA do CAI hipokampa powodowała znaczne zmiany w ultrastrukturze: neuronów, synaps, gleju i naczyń krwionośnych. W trzy i siedem dni po mikroinjekcji NMDA w wielu neuronach zaobserwowano zmiany w aparacie Golgiego i znaczne zmiany w cytoszkielecie. Stwierdzono również znaczny napływ Ca^{2+} do mitochondrii.

Iniekcja 50 mM AMPA do CAI hipokampa spowodowała znamienny wzrost immunoreakcji z przeciwciałami skierowanymi przeciwko domenie N, M i C - końcowej prekursora białka β-APP. Nie obserwowano zmian w immunoreakcji (w stosunku do kontroli) z przeciwciałem 4G8 (613-620 aa) skierowanym przeciwko błonowej domenie amyloidowego białka β. Immunoreakcja odpowiednich przeciwciał skierowanych przeciwko różnym domenom β-APP była widoczna już po 2 godz., zaś maksymalna po trzech dniach od iniekcji

AMPA. Podanie MK-801 niwelowało tę reakcję. Po mikroinjekcji AMPA do CAI hipokampa, nie obserwowano zmian w ultrastrukturze nerwów i synaps, natomiast zaobserwowano dramatyczne zmiany w mielinie aksonów, po upływie 24 godz. od podania. Uzyskane wyniki bezsprzecznie wskazują na udział receptorów dla aminokwasów pobudzających na obróbkę i nagromadzanie różnych fragmentów białka ß-APP, poprzez aktywację α i γ sekretazy. Nagromadzanie fragmentów C- końcowych białka ß-APP, (które są cytotoksyczne) wyrażone znacznym wzrostem immunoreakcji z przeciwciałami świadczy o znacznej aktywacji γ- sekretazy, której obszar działania umiejscowiony jest w retikulum endoplazmatycznym. Jest zatem prawdopodobne, że napływ Ca^{2+} do neuronów powoduje uwalnianie Ca^{2+} z magazynów wewnątrzkomórkowych w retikulum endoplazmatycznym (ER), (na skutek aktywacji receptorów wrażliwych, na trójfosforan inozytolu (IP_3R) oraz wrażliwych na Ca^{2+} receptorów rianodynowych (RyR) znajdujących się na błonie endoplazmatycznej) i powoduje aktywację γ- sekretazy. Proces uwalniania Ca^{2+} z reticulum endoplazmatycznego znany jest jako „zależne od wapnia uwalnianie wapnia wewnątrzkomórkowego (ang. calcium induced calcium release–CICR) (Verkhratsky 2002). Udział receptorów NMDA w patogenezie AD potwierdziły badania: Danysz W. i Parson G.G. 2003; Parsons C.G. i wsp. 1999; Reisberg B., i wsp. 2003, którzy wykazali, że terapeutyczne dawki Memantyny – antagonisty receptorów NMDA, poprawiają proces uczenia się /plastyczność neuronalną, w warunkach tonicznej aktywacji receptorów NMDA. Jak podają autorzy, na podstawie badań przedklinicznych można sugerować działanie nauroprotekcyjne Memantyny w chorobie Alzheimera.

Omawiana praca nr.2.

Tytuł pracy: „N-methyl-d-aspartate receptor - mediated processing of β-amyloid precursor protein in rat hippocampal slices: in vitro – superfusion study", Folia Neuropathologica 40, 2002.

Celem pracy było: Zbadanie udziału receptorów dla aminokwasów pobudzających typu NMDA na metabolizm β-APP oraz βA w hipokampie mózgu szczura w doświadczeniach in vitro – stosując metodę superfuzji skrawków hipokampa.

Postanowiliśmy zbadać jaki jest wpływ aktywacji receptorów NMDA na proces degradacji (obróbki) białka β-APP. Zastosowaliśmy metodę superfuzji skrawków hipokampa i badaliśmy uwalnianie fragmentów białka β-APP do superfuzatu. Doświadczenie prowadzono w aparacie do superfuzji typu „Brandel". Skrawki hipokampa mózgu szczura po preinkubacji i wstępnej superfuzji poddawano właściwemu doświadczeniu. Po 20–minutowej superfuzji w medium kontrolnym, podawano przez następne 20 minut media o różnym składzie, a następnie powracano do medium kontrolnego. Doświadczenie prowadzono w medium bezmagnezowym.

Media doświadczalne miały skład:

(1) 100 μM NMDA w buforze K-R zawierającym 1,2 mM Ca Cl_2; (2) 250 μM NMDA w buforze K-R zawierającym 1,2 mM $CaCl_2$; (3) 250 μM NMDA w buforze K-R, bez wapniowym; (4) 250 μM NMDA w buforze K-R zawierającym 1,2 mM $CaCl_2$ i 1 μM MK-801; (5) 250 μM NMDA w buforze K-R zawierającym 1,2 mM $CaCl_2$ i 100 μM CPP.

Media kontrolne były o składzie odpowiadającym mediom doświadczalnym, nie zawierały jednak NMDA.

Skład mediów doświadczalnych umożliwiał zbadanie uwalniania fragmentów białka β-APP w zależności od stężenia NMDA.

W doświadczeniach prowadzonych w obecności wapnia stwierdzono wzmożone uwalnianie fragmentów N- M- i C-końcowych prekursora białka β-APP w czasie i po podaniu NMDA. Efekt ten ulegał zahamowaniu w mediach bez wapniowych oraz w obecności MK–801 (dibenzocykloheksimina) i PCP (fencyklidyna)-antagonistów receptorów NMDA.

Omawiana praca nr.3.

Tytuł pracy: „Conformation of paired helical filaments blocks dephosphorylation of epitopes shared with fetal tau except Ser 199/202 and Ser 202/Thr 205", Brain Reseach 856, 2000.

Celem pracy było: Zbadanie, czy wysokie ufosforylowanie białka tau jest rezultatem nieefektywnego działania endogennych fosfataz, czy zależnej od struktury tego białka – PHF, zmniejszonej dostępności dla fosfataz miejsc ufosforylowania tego białka.

Badano działanie egzogennej alkalicznej fosfatazy na białko tau, występujące w postaci splotów neurofibrylarnych - PHF, które wyizolowano z mózgu osoby zmarłej na chorobę Alzheimera: natywne, oraz poddane uprzednio działaniu kwasu mrówkowego (w celu rozwinięcia splotów i zwiększenia dostępności ufosforylowanych miejsc białka tau). Równolegle badano działanie egzogennej alkalicznej fosfatazy na wysoko ufosforylowane białko tau wyizolowane z mózgu płodu ludzkiego. Próbki inkubowano z 20 IU/ml egzogennej alkalicznej fosfatazy przez 30 min., 1, 2, 5, 24 godziny. Po rozdziale elektroforetycznym i transferze na błony nitrocelulozowe, przeprowadzano reakcje immunologiczne z przeciwciałami na odpowiednie epitopy białka tau.

Stwierdzono, że:

- **PHF ulegają defosforylacji przez egzogenną alkaliczną fosfatazę tylko w N-końcowych epitopach Ser 199/202 i Ser 202/Tr 205,**
- PHF po inkubacji z kwasem mrówkowym ulegają defosforylacji przez alkaliczną fosfatazę we wszystkich epitopach, a szczególnie szybko w C-końcowych epitopach,
- białko tau wyizolowane z płodów ludzkich ulega defosforylacji przez alkaliczną fosfatazę we wszystkich epitopach. Stopień defosforylacji tego białka jest zbliżony do defosforylacji PHF po inkubacji z kwasem mrówkowym,
- **hiperfosforylacja C-końca białka tau wpływa na jego konformację, która z kolei ogranicza dostęp alkalicznej fosfatazy,**
- przebieg i stopień defosforylacji PHF w epitopach Ser 199/202 i Ser 202/Thr 205 jest równy stopniu defosforylacji w białku tau wyizolowanym z płodów ludzkich.

Okazało się, że istotnie podwyższony poziom białka tau fosforylowanego na Ser 199 skorelowany z całkowitym tau w płynie mózgowo-rdzeniowym może być nowym biomarkerem w diagnozie AD. Wykrywalność wynosi 0,2 fmol/ml, czułość 85,2%,

specyficzność 85% (Itoh N. i wsp., 2001). Podwyższony poziom fosforylacji białka tau na prolinie – Pro181 jest markerem różnicującym pomiędzy chorobą Alzheimera a otępieniem z ciałami Lewy'ego. Natomiast fosforylacja tau na treoninie Tr231 pozwala na różnicowanie AD od innych chorób otępiennych (Molina L. i wsp., 1999; Sjogren M., i wsp., 2001; Venmechelch E., i wsp., 2001)

Omawiana praca nr.4.

Tytuł pracy: „Tau released from Paired Helical Filaments with formic acid or quanidine is susceptible to calpain – mediated proteolysis" J. Neurochem. 69, N° 4, 1997.

Celem pracy było: Zbadanie w doświadczeniach „in vitro" działania kalpain na frakcję PHF wyizolowaną z mózgu osób chorych na chorobę Alzheimera oraz na białko tau wyizolowane z mózgu płodów ludzkich.

Za przeprowadzeniem tego typu doświadczeń przemawiał fakt, iż u osób z chorobą Alzheimera stwierdzono wzrost aktywności kapalin. Od kilkunastu lat wiadomo o roli wapniowo – zależnych proteaz obojętnych - kalpain w procesach neurodegeneracji.

Kalpainy w warunkach zwiększonego napływu jonów wapnia do neuronów (jak to ma miejsce np. w ischemii) ulegają autolitycznej aktywacji, tworząc formę aktywną (76 kDa), zdolną do proteolizy specyficznych białek substratowych. Jednym z najwcześniejszych efektów niedokrwienia jest zależne od czasu jego trwania, przemieszczenie kalpain do frakcji błon plazmatycznych, widoczne we wczesnej fazie patologii niedokrwiennej. Przemieszczenie takie jest zgodne z ogólnie akceptowaną hipotezą aktywacji kalpain na błonach plazmatycznych. Równocześnie obserwuje się znaczący przyrost poziomów produktów proteolitycznego rozpadu kinazy białkowej C i fodryny – specyficznych substratów kalpainy. (Domańska – Janik K., Zalewska T., 1992). Nadmierna proteoliza przy udziale kalpain może prowadzić do uszkodzenia cytoszkieletu komórki, do zmiany struktury i funkcji błon plazmatycznych.

Poddanie wyizolownej frakcji PHF działaniu kwasu mrówkowego lub guanidyny zmieniało konformację splotów neurofibrylarnych - PHF, ale nie zmieniało jej aktywności immunologicznej. Obie procedury znacznie zwiększały czułość PHF na proteolityczne działanie kalpain. Wykazano, iż proteolityczne działanie kalapin jest uzależnione bardziej od konformacji białka tau niż od stopnia jego ufosforylowania.

Omawiana praca nr.5.

Tytuł pracy: „Induction of Alzheimer – specific tau epitope AT 100 in apoptotic human fetal astrocytes". Cell Motility and the Cytoskeleton 47, 2000.

Celem pracy było: Zbadanie, jak kwas okadaikowy (ang. okadaic acid) (OC) – induktor apoptozy, inhibitor fosfatazy białkowej 1 i 2A wpływa na ekspresję i stopień ufosforylowania białka tau w doświadczeniach „in vitro".

Doświadczenia prowadzono na hodowli astrocytów, wyizolowanych z 19-24 tygodniowych płodów ludzkich. Hodowla była prowadzona przez 3-4 miesiące. Czystość hodowli sprawdzano stosując całą gamę przeciwciał skierowanych przeciwko m.in.: glejowemu kwaśnemu białku włókienkowemu – GFAP, ß–tubulinie, vimentynie, MAP 2. W celu określenia żywotności oraz obecności lub braku cech apoptozy zastosowano Hoechst 33258. Hodowlę poddano działaniu kwasu okadaikowego o stężeniu 50 nM i 250 nM przez okres 1 godz., 5 godz. i 24 godz.

Przeciwciało AT 100 rozpoznaje miejsce podwójnej fosforylacji Thr 212/Ser 214 białka tau. Immunoreakcja z tym przeciwciałem występuje jednak tylko wtedy, jeżeli zmieniona jest konformacja białka tau, a mianowicie wówczas, gdy występuje ono w postaci splotów neurofibrylarnych – PHF, jak to ma miejsce w chorobie Alzheimera.

Prowadzono hodowlę astrocytów, które wyizolowano z mózgów płodów ludzkich, (śmierć płodów była spowodowana śmiercią matek na skutek wypadków samochodowych). Białka astrocytów poddawano elektroforetycznemu rozdziałowi, przeprowadzano transfer na błony nitrocelulozowe metodą Western blot i przeprowadzano immunoreakcje z odpowiednimi przeciwciałami. Trzy polipeptydy o masie cząsteczkowej 52, 64 i 70 kDa, wykazywały immunoreakcję z przeciwciałami przeciwko nieufosforylowanym epitopom białka tau. Trzy wyżej wymienione polipeptydy wykazywały immunoreakcję z przeciwciałem PHF-I, ale nie z przeciwciałami: Tau 1, 12E8, AT8 i AT 100. Potraktowanie hodowli astrocytów kwasem okadaikowym - OA, który jest inhibitorem fosfataz: 1 oraz 2A, spowodowało 3-5 krotny wzrost ilości białka tau i wzrost jego ufosforylowania, co obserwowano poprzez znaczny wzrost immunoreakcji z przeciwciałami rozpoznającymi ufosforylowane epitopy, także z przeciwciałem AT100. Wzrost ufosforylowania domeny białka tau reagującej z przeciwciałem AT100 zachodzi prawdopodobnie poprzez inhibicję przez OA fosfatazy 2A i aktywację kinazy białkowej B (Akt) oraz kinazy Cdc2.

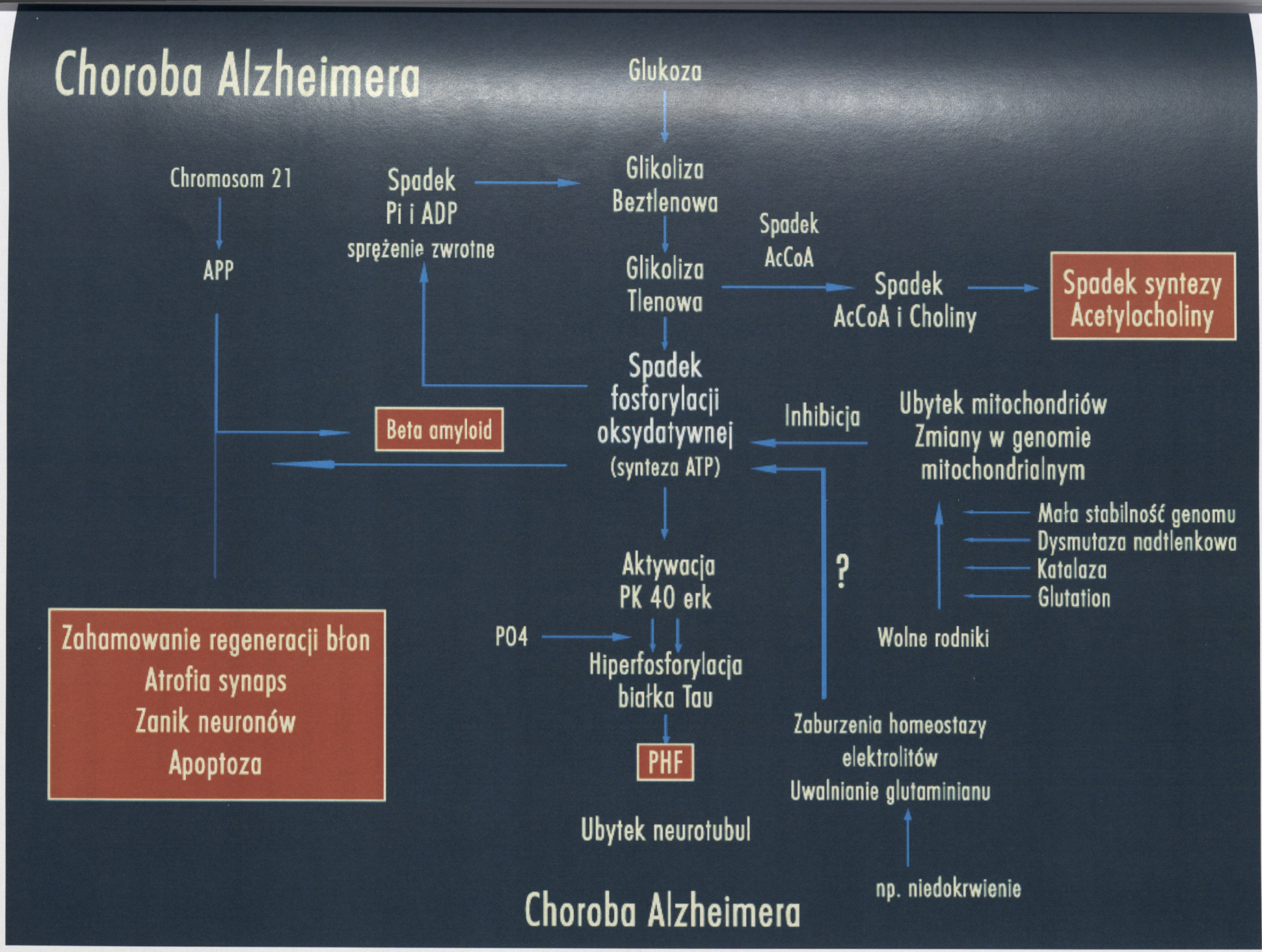

Potraktowanie hodowli astrocytów kwasem okadaikowym powodowało apoptozę komórek, co wyrażało się kondensacją chromatyny jądrowej, fragmentaryzacją jądra komórkowego, przerwami w błonie cytoplazmatycznej.

Omawiana praca nr.6.

Tytuł pracy: „2-Deoxyglucose–induces β-APP overexpression, tau hiperphosphorylation and expansion of the *trans*- part of Golgi complex in rat cerebral cortex ". Acta Neurobiol. Exp. 64, 2000.

Celem pracy było: ustalenie czy podanie szczurom dootrzewnowo pojedynczej dawki 2-deoksyglukozy spowoduje zmiany fosforylazji białka tau oraz zmiany w ekspresji i obróbce białka β-APP w korze mózgowej.

W chorobie Alzheimera spustoszeniu morfologicznemu towarzyszą poważne zaburzenia biochemiczne. Zarówno w korze mózgowej jak i w hipokampie drastycznie o ok. 70% maleje poziom acetylotransferazy cholinowej, spada metabolizm glukozy. Meier-Rouge i współpracownicy w latach 1984 – 1997, sformułowali hipotezę o centralnej roli jaką odgrywa uszkodzenie metabolizmu glukozy w patogenezie AD. Rolę inicjującą odgrywać mają mutacje genomu mitochondrialnego spowodowane przez reaktywne rodniki tlenowe (ROS) i prowadzące do zaburzeń metabolizmu glukozy i syntezy ATP. Jeśli na tle uszkodzonego metabolizmu glukozy i względnego niedoboru ATP dojdzie w tkankach mózgowych (np. wskutek ischemii bądź urazu mózgu) do zwiększenia syntezy prekurosora białka amyloidu beta (β-APP), uruchomiona zostanie kaskada procesów patologicznych złożona z:

- zahamowania syntezy acetylocholiny, której prekursorem jest acetylokoenzym A,
- hiporfosforylacji białka tau spowodowanej aktywacją kinazy białkowej 40 ERK,
- nieprawidłowej obróbki posttranslacyjnej β-APP, co w konsekwencji może prowadzić do nagromadzania się w beta amyloidu, który z kolei hamuje aktywność fosfofruktokinazy, inicjując dodatnie sprzężenie zwrotne wiodące do pogłębiających się zaburzeń metabolizmu glukozy i rozwoju AD.

Kaskadę zdarzeń mających wpływ na ww. procesy oraz wzajemne korelacje przedstawia **(Ryc. 5).**

Badacze uznają zaburzenia metabolizmu glukozy za jeden z głównych czynników w etiopatogenezie AD. Hipoteza glukozowa jest nadto zgodna z zaobserwowanym zmniejszeniem gęstości białek transportujących glukozę w mózgu chorych na AD.

Uważaliśmy, że jeśli hiperfosforylacja białka tau i nieprawidłowa posttranslacyjna obróbka β-APP rzeczywiście są skutkiem zaburzeń metabolizmu glukozy to glukodeprywacja wywoływana podawaniem farmakologicznych dawek 2-deoksyglukozy (2-DG) jest odpowiednim modelem dla doświadczalnej weryfikacji hipotezy o zasadniczej roli zaburzeń metabolizmu glukozy w patogenezie AD. 2-Deoksyglukoza (2-DG) jest analogiem glukozy pobieranym przez komórki, podlegającym fosforylacji podobnie do glukozy z tą różnicą, że 6-fosforan DG nie jest substratem dla izomerazy 1,6-dwufosfoglukozy. Dzięki tej właściwości znakowana radioaktywnie 2-DG i jej pochodna fluorowa (2-F-2-DG) znalazły zastosowanie w pomiarach tempa metabolizmu glukozy w mózgu metodami autoradiografii *in vitro* ([^{14}C]- N 2-DG) i *in vivo* ([^{11}C]-2-DG, [^{18}F]-2-F-2-DG w metodach PET – pozytronowa tomografia emisyjna). Podanie 2-DG w ilościach farmakologicznych (u szczura w dawce 200-500 mg/kg) prowadzi do restrykcji mózgowego metabolizmu glukozy i jest modelem glukodeprywacji mózgowej.

Zaburzenia metaboliczne wywołane w mózgu podaniem farmakologicznych dawek 2-DG są dość słabo zbadane. Stwierdzono jednak, że następuje wzrost mózgowego przepływu krwi, co autorzy wiążą z akumulacją produktów katabolizmu AMP (adenozyny, inozyny i hipoksantyny) w tkankach, podczas gdy w podwzgórzu następuje uwalnianie acetylocholiny (ACh) do przestrzeni pozakomórkowych oraz spadek stężenia ACh i wzrost stężenia choliny w komórkach. W literaturze nie znaleźliśmy żadnych danych dotyczących wpływu farmakologicznych dawek 2-DG na metabolizm β-APP i białka tau w mózgu.

Po dootrzewnowym podaniu szczurom niemetabolizowanej pochodnej glukozy, tj. 2 – deoksyglukozy (2DG), w jednorazowej dawce 500mg/kg, stwierdzono:

- szybki wzrost immunoreakcji z przeciwciałami przeciwko środkowej (śródbłonowej) i C-końcowej domenie białka β-APP,
- obniżenie po upływie dwóch godzin od podania immunoreakcji z przeciwciałami skierowanymi przeciwko epitopom N-końcowym białka β-APP a następnie stopniowy wzrost immunoreakcji, która po upływie 24 godzin była trzykrotnie wyższa niż w kontroli,
- znaczny wzrost ufosforylowania środkowej i C-końcowej domeny białka tau,
- zmiany w komórkach nerwowych na poziomie ultrastrukturalnym, które dotyczyły zarówno jądra jak i innych organelli. Stwierdzono dezorganizację chromatyny jądrowej i szkieletu jądra komórkowego. Obserwowano znaczną

rozbudowę gładkiej siateczki śródplazmatycznej. Zmiany ultrastrukturalne aparatu Golgiego dotyczyły zarówno jego wielkości jak i budowy, szczególną uwagę zwracała bardzo rozbudowana strefa – trans i znacznie poszerzony układ cystern. Nie obserwowano występowania pęcherzyków w przestrzeni pomiędzy siateczką śródplazmatyczną i strefą cis – aparatu Golgiego. Mitochondria nie wykazywały cech obrzęku, chociaż miały znacznie zmienioną architekturę. Uwagę zwracała fragmentacja filamentów pośrednich i neurotubul, w wypustkach aksonalnych.

Uzyskane wyniki są zgodne z hipotezą, że zaburzenia metabolizmu glukozy w mózgu mogą prowadzić do nadekspresji i akumulacji β-APP, hiperfosforylacji białka tau, oraz zmian w ultrastrukturze komórek nerwowych. Z drugiej strony z pracy Dodarta i wsp. 1999 r. wiadomo, że u transgenicznych myszy z nadekspresją ßAPP jeszcze przed powstaniem złogów ßA w mózgu, odnotowano znaczny spadek metabolizmu glukozy. Natomiast autorzy Xie i wsp.2002, wykazali, że ßA jest inhibitorem kompetycyjnym receptora insulinowego.

Podsumowanie

Eksperymenty opisane w publikacjach zamieszczonych w kompendium niniejszej pracy habilitacyjnej, pozwoliły nam poznać niektóre z czynników i mechanizmów mających wpływ na:

- generację i obróbkę białka β-APP,
- na konformację białka tau - poprzez indukcję zmian w procesie jego fosforylacji / defosforylacji,
- równolegle zaistniałe zmiany w ultrastrukturze komórek.

wykazano że:

- pobudzenie ekscytotoksyczne i receptory dla aminokwasów pobudzających: glutaminianu, NMDA i AMPA ma wpływ na obróbkę i nagromadzanie białka ß APP, a szczególnie na indukcję cytotoksycznego epitopu C-końcowego ß-APP. Antagoniści receptorów NMDA hamują ten proces.
- podanie ekscytotoksyn powoduje zmiany w ultrastrukturze komórek.
- egzogenna alkaliczna fosfataza defosforyluje PHF tylko w N-końcowych epitopach Ser 199/202 i Ser 202/Tr 205,
- hiperfosforylacja C-końca białka tau wpływa na jego konformację (tworzenie PHF), która z kolei **ogranicza dostęp alkalicznej fosfatazy**,
- przebieg i stopień defosforylacji PHF w epitopach Ser 199/202 i Ser 202/Thr 205 jest równy stopniu defosforylacji w białku tau wyizolowanym z płodów ludzkich,
- wykazano, iż proteolityczne działanie kalapin jest uzależnione bardziej od konformacji białka tau, niż od stopnia jego ufosforylowania,
- inhibicja PP2A - kwasem okadaikowym, zwiększa ufosforylowanie białka tau, a szczególnie domeny C-końcowej tego białka,
- inhibicja PP2A powoduje zmianę konformacji białka tau, prowadzącą do wytworzenia skręconych parzycie włókien tego białka i splotów neurofibrylarnych,
- zaburzenia metabolizmu glukozy w mózgu mogą prowadzić do nadekspresji i akumulacji β-APP, hiperfosforylacji białka tau, oraz zmian w ultrastrukturze komórek nerwowych.

W dalszym ciągu jednak wiele mechanizmów mających wpływ na. proces nieprawidłowej obróbki ß-APP oraz fosforylacji / defosforylacji białka tau, jak również mechanizmów wpływających na wzajemne zależności tych procesów pozostaje do wyjaśnienia.

PIŚMIENNICTWO

1. Abe K, Tanzi R.E., Kogure K.: Selective induction of Kunitz-type protease inhibitor domain-containing amyloid precursor protein mRNA after persistent focal ischemia in rat cerebral. Neuroscience Letters **1991**, 125, 172-174.
2. Allinson T.M., Parkin E.T., Turner A.J., Hooper N.M.: ADAMs famili members as amyloid precursor protein alpha – secretases. J Neurosci. Res. **2003**, 74, 342-352.
3. Almkvist O., Winblad B.: Early diagnosis of Alzheimer dementia based on clinical and biochemical factors. Eur. Arch. Psych. Clin Neurosci. **1999**, 249, 3-9.
4. Alvarez G., Muńoz-Montańo J.R., Satrústegui J., Avila J., Bogonez E., Diaz-Nido J.: Lithium protects cultured neurons against beta-amyloid-induced neurodegeneration. FEBS Lett **1999**, 453, 260-264.
5. Anderton B.H., Betts J., Blackstock W.P., Brion J.P., Chapman S., Connell J., Dayanandan R., Gallo J.M., Gibb G., Hanger D.P., Hutton M., Kardalinou E., Leroy K., Lovestone S., Mack T., Reynolds C.H., Van Slegtenhorst M.: Sites of phosphorylation in tau and factors affecting their regulation. Biochem. Soc. Symp. **2001**, 67, 73-80.
6. Andreadis A.,Brown W.M., Kosik K.S.: Structure and novel exons of the human tau gene. Biochemistry **1992**,31, 10626-10633.
7. Armstrong D.M., Ikonomovic M.D., Sheffield R., Wenthold R.J.: AMPA-selective glutamate receptor subtype immunoreactivity in the entorhinal cortex of non-demented elderly and patients with Alzheimer's disease. Brain. Res. **1994**, 639, 207-216.
8. Bancher C., Brunner C., Lassmann H., Budka H., Jellinger K., Wiche G., Seitelberger F., Grundke-Iqbal I., Iqbal K., Wiśniewski H.M.: Accumulation of abnormally phosphorylated tau precedes the formation of neurofibrillary tangles in Alzheimer's disease. Brain Res. **1989**, 477, 90-99.
9. Barcikowska M.: Choroba Alzheimera jako przykład schorzenia neurodegeneracyjnego. Post. Biol. Kom. **1998**, Suppl.11, 5-14.
10. Barcikowska M.: New therapeutic approaches in Alzheimer's disease. Folia Neuropathol. **2004**, 42, 251-255.
11. Baudier J., Cole R.D.: Phosphorylationof tau protein to a state like that in Alzheimer's brain is catalyzed by a calcium / calmodulin – dependent kinase and modulated by phospholipids. J. Biol Chem.**1987a**, 262, 17577-17583.
12. Baudier J., Lee S.H., Cole R.D.: Separation of the different microtubule associated tau protein species from bovine brain and their modeII phosphorylation by Ca^{2+}/phospholipid – dependent protein kinase C. J. Biol. Chem. **1987b**, 262, 17584-17590.
13. Baum L. HansenL., Masliah E., Saitoh T.: Glycogen synthetase kinase 3 alteration in Alzheimer disease is related to neurofibrillary tangle formation. Mol. Chem. Neuropathol. **1996**, 29, 253-261.
14. Beffert U., Danik M., Krzywkowski P., Ramassamy C., Berra da F., Poirier J.: The neurobiology of apolipoproteins and their receptors in the CNS and Alzheimer's disease. Brain Res. Rev.**1998,** 27,119-142.
15. Beyer K., Lao J.I., Gomez M., Riutort N., Latorre P., Mate J.L., Ariza A.: Alzheimer's disease and the cystatin C gene polymorphism: an association study. Neurosci. Lett. **2001**, 315, 17-20.
16. Bi H., Sze C.I.: N-methyl-D-aspartate receptor subunit NR2A and NR2B messenger RNA levels are altered in the hippocampus and entorhinal cortex in Alzheimer's disease. J. Neurol. Sci. **2002**, 200, 11-18.

17. Boller F., Mizutani T., RoessmannU., Gambetti P.: Parkinson's disease, dementia, and Alzheimer's disease: clinicopathologic correlations. Ann. Neurol. **1980**, 7, 329-335.
18. Brion J.P., Anderton B.H., Authelet M, Dayanandan R., Leroy K., Lovestone S., Octave J.N., Pradier L., Touchet N., Tremp G.: Neurofibrillary tangles and tau pathology. Boichem. Soc. Symp. **2001**, 67, 81-88.
19. Brzyska M., Elbaum D.: Choroba Alzheimera. w Mózg a zachowanie .WN PWN (red.: Górska T., Grabowska A., Zagrodzka J.) **2000,** 338-358.
20. Buee L., Bussiere T., Buee-Scherrer V., Delacourte A., Hof P.R.: Tau protein izoforms, phosphorylation and role in neurodegenerative disorders. Brain Res. Rev. **2000,** 33, 95-130.
21. Busciglio J., Gabuzda D., Yankner B.A.: Inhibition of bata amyloid production by activation of protein kinase C. Society for Neuroscience, Abstracts, **1993**, 19, 1276.
22. Busciglio J., Gabuzda D.H., Matsudaira P., Yankner B.A.: Generation of ß- amyloid in the secretory pathway in neuronal and nonneuronal cells: Proc. Natl. Acad Sci. USA **1993**, 90, 2092-2096.
23. Busciglio J., Lorenzo A., Yeh J., Yankner B.A.: ß- amyloid fibrils induce tau phosphorylation and loss of microtubule binding. Neuron **1995**, 14, 879-888.
24. Caceres A., Kosik K.S.: Inhibition of neurite polarity by tau antisense oligonucleotides in primary cerebellar neurons. Nature **1990**, 343, 461-463.
25. Camicioli R., Kaye J., Payami H., BallM.J., Murdoch G.: apolipoprotein E epsilon 4 is associated with neuronal loss in the substantia nigra in Alzheimer's disease. Dement. Geriatr. Cogn. Disordr. **1999,**10,437-441.
26. Caporaso G.L., Gandy S.E., Buxbaum J.D., Greengard P.: Chloroquine inhibits intracellular degradation but not secretion of Alzheimer βA4 amyloid precursor protein. Proc. Natl. Acad. Sci. USA. **1992**, 89, 2252-2256.
27. Clark A.W., Krekoski C.A., Parhad I.M., Liston D., Julien J.P., Hoar D.I.: Altered expression of neuronal messenger RNA in Alzheimer cortex. Prog.Clin.Biol.Res. **1989**, 317, 511-515.
28. Clayton D.A., Mesches M.H., Alvarez E., Bickford P.C., Browning M.D.: A hippocampal NR2B deficit can mimic age-related changes in long-term potentiation and spatial learning in the Fischer 344 rat. J. Neurosci. **2002**, 22, 3628-3637.
29. Cho H.S., Hyman B.T., Greenberg S.M., Rebeck G.W.: Quantitation of apoE domains in Alzheimer disease brain suggests a role for apoE in Aß aggregation. J. Neuropathol. Exp. Neurol. **2001,** 60,342-349.
30. Colman S.L., Halfter W., Cole G.J.: Agrin binds to ß-amyloid (Aß), accelerates Aß fibril formation, and is localized to Aß deposits in Alzheimer's disease brain. Mol. Cel. Neurosci. **2000,** 15, 183-198.
31. Correas I., Diaz–Nido J., Avila J.: Microtubule – associated protein tau is phosphorylated by protein kinase C on its tubulin binding domain. J. Biol Chem. **1992**, 267, 15721-15728.
32. Crawford F., Abdullah I., Schinka J., Suo Z.M., Gold M., Duara R., Mullan M.: Gender specific association of the angiotensin converting enzyme gene with Alzheimer's disease. Neurosci. Lett. **2000**, 280, 215-219.
33. Danysz W., Parsons C.G.: An NMDA receptor antagonist memantine as a symptomatological and neuroprotective treatment for Alzheimer's disease preclinical evidence. International J. Geriatric Psych. **2003**,18, S23-S32.
34. De la Monte S.M., Ghanbari H., Ghanbari K., Averback P., Wands J.R.: AD7c-NTP biomarker for Alzheimer's disease. Alzheimer's Report **1999**,2, 327-332.
35. DeSauvage F., Octave J.N.: A novel mRNA of the A4 amyloid precursor gene coding for a possibly secreted protein. Science **1989**,245,651-653

36. De Strooper B., Umans L., Van Leuven F., Van Den Berghe H.: Study of the synthesis and secretion of normal and artificial mutants of murine amyloid precursor protein (APP): Clavage of APP-occurs in a late compartment of the default secretion pathway. J. Cell Biol. **1993**, 121, 295-304.
37. Dodart J.C., Mathis ch., bales K.R., Paul S.M., Ungerer A.: Early regional glucose hypometabolism in transgenic mice overexpressing the V717F ß-amyloid precursor protein Neurosci. Lett. **1999**, 277, 49-52.
38. Domańska – Janik K., Zalewska T.: Effect of brain ischemia on protein kinase C. J. Neurochem. **1992**, 58, 1432-1439.
39. Drechsler D.N., Hyman A.A., Cobb M.H., Kirschner M.W.: Modulation of the dynamic instability of tubulin assembly by the microtubule-associated protein tau. Mol. Biol. Cell **1992**, 3, 1141-1154.
40. Dumanchin-Njock C., Alves da Costa C., Mercken L., Pradier L., Checler F.: The caspase-derived C-terminal fragment of ßAPP induced caspase-independent toxicity and triggers selective increase of Aß42 in mammalian cells. J. Neurochem. **2001**, 78, 1153-1161.
41. El-Agnaf O.M.A., Bodles A.M., Guthrie D.J.S., Harriot P., Irvine G.B.: The N-terminal region of non-Aß component of Alzheimer's disease amyloid is responsible for its tendency to assume ß-sheet and aggregate to form fibrilis. J. Bioch. **1998**, 258, 157-163.
42. Esch F.S., Keim P.S., Beattie E.C., Blacker R.W., Culwell A.K., Oltersdorf T., McClure D., Ward P.J.: Cleavage of amyloid β peptide during constitutive processing of its precursor. Science **1990**, 248, 1122-1124.
43. Ezqurra M., Carnero C., Blesa R., Oliva R.:A novel presenilin 1 mutation (Leu166arg) associated with early-onset Alzheimr's disease. Arch. Neurol. **2000**,57,485-488.
44. Fanny M.B., Dickson D.W.: Neurodegenerative disorders with extensive tau pathology. A comparative study and review. Ann. Neurol. **1996**, 40, 139-148.
45. Fellous A., Francon J., Lennon A.M., Nunez J.: Microtubule assembly in vitro. Purification of assembly – promoting factors. Eur. J. Biochem. **1977**, 78, 167-174.
46. Fergani A., Yu G., St. George-Hyslop P., Checler F.: Wild – type and mutated nicastrins do not display aminopeptidase M-and B-like activities. Bioch. Bioph. Res. Com. **2001**, 289,678-680.
47. Frackowiak J., Mazur-Kolecka B., Kaczmarski W., Dickson D.: Deposition of Alzheimer's vascular amyloid-ß is associated with decreased expression of brain L-3-hydroxy-acyl-coenzyme A dehydrogenase (ERAB). Brain. Res. **2001**, 907, 44-53.
48. Fraser P.E., Yang D.S., Yu G., Levesgue L., Nishimura M., Arawaka S., Serpell L.C., Rogaeva E., St. George-Hyslop P.: Presenilin structure, function and role in Alzheimer disease. Bioch.Bioph. Acta. **2000.** 1502, 1-15.
49. Frohlich L., Blum-Degen D., Bernstein H.-G., Engelsberger S., Humrich J., Laufer S., Muschner D., Thalheimer A., Turk A., Hoyer S., Zochling R., Boissl K.W., Jellinger K., Riederer P.: Brain insulin and insulin receptor in aging and sporadic Alzheimer's disease. J. Neurol. Transm. **1998**, 105, 423-438.
50. Funato H., Yoshimura M., Kusui K., Tamaoka A., Ishikawa K., Ohkoshi N., Namekata K., Okeda R., Ihara Y.: Quantitation of amyloid ß-protein (Aß)in the cortex during aging and in Alzheimer's disease. Am.J. Pathol. **1998,** 152, 1633-1640.
51. Furukawa K., Barger S.W., Blalock E.M., Mattson M.P.: Activation of K+ channels and suppression of neuronal activity by secreted β-amyloid precursor protein. Nature **1996,** 379, 74-78.

52. Gandy S., Bhasin R., Ramabhadran T.V., Koo E.H., Price D., Goldgaber D., Greengard P.: Alzheimer β / A4 amyloid precursor protein: evidence for putative amyloidogenic fragment. J. Naurochem. **1992**, 58, 383-386.
53. Geddes J.W., Cotman C.W.: Plasticity in hippocampal excitatory amino acid receptors in Alzheimer's disease. Neurosci. Res. **1986**, 3, 672-678.
54. Gentlemant S.M., Graham D.J., Roberts G.W.: Molecular pathology of head trauma: altered ß-APP metabolism and the artiology of Alzheimer's disease. Progress in Brain Research **1993,** 96, 237-246.
55. Gerst J.L., Raina A.K., Pirim I., McShea A., Harris P.L.R., Siedlak S.L., Takeda A., PetersenR.B., Smith M.A.: Altered cell-matrix associated ADAM proteins in Alzheimer's disease. J. Neurosci. Res. **2000**, 59,680-684.
56. Ghiso J., Wiśniewski T., Frangione B.: Unifying features of systemic and cerebral amyloidosis. Mol. Neurobiol.**1994,** 8, 49-64.
57. Glenner G.G., Wong C.W.: Alzheimer's disease: initial report of the purification and characterization of a novel cerebrovascular amyloid protein. Biochem. Biophys. Res. Commun. **1984 a,** 120, 885-890.
58. Glenner G.G., Wong C.W.: Alzheimer's disease and Down syndrome: Sharing of a unique cerebrovascular amyloid fibril protein. Biochem. Biophys. Res. Commun. **1984b**, 122, 1131-1135.
59. Goedert M., Wischik C.M., Crowther R.A., Walker J.E., Klug A.: Cloning and sequencing of the cDNA encoding a core protein of the paired helical filament of Alzheimer disease: identification as the microtubule – associated protein tau. Proc. Natl. Acad. Sci. USA **1988,** 85, 4051-4055.
60. Goedert M., Spillantini M.G., Jakes R., Rutherford D., Crowther R.A.: Multiple isoforms of human microtubule – associated protein tau: sequences and localization in neurofibrillary tangles of Alzheimer's disease. Neuron **1989**, 3, 519-526.
61. Goedert M.: Tau protein and the neurofibrillary pathology of Alzheimer's disease. Ann. N Y Acad. Sci. **1996**, 777, 121-131.
62. Goedert M., Hasegawa M., Jakes R., Lawler S., Cuenda A., Cohen P.: Phosphorylation of microtubule – associated protein tau by stress – activated protein kinases. FEBS Lett. **1997**, 409, 57-62.
63. Golde T., Estus S., Usiak M., Younkin L.H., Younkin S.G.: Expression of β amyloid protein precursor mRNAs: recognition of a novel alternatively spliced from and quantitation in Alzheimer's disease using PCR. Neuron **1990**, 4, 253-267.
64. Goldgaber D., Lerman M.I., McBride O.W., Saffiotti U., Gajdusek D.C.: Characterization and chromosomal localization of a cDNA encoding brain of Alzheimer's disease. Science **1987**, 235, 877-880.
65. Gomez – Ramos P., Mufson E.J., Moran A.: Apolipoprotein E immunoreactivity in neurons and neurofibrillary degeneration of aged non-demented and Alzheimer's disease patients. Microsc. Res. Techn. **2001,** 55, 48-58.
66. Gomez-Ramos A., Diaz-Nido J., Smith M.A., Perry G., Avila J.: Effect of the lipid peroxidation product acrolein on tau phosphorylation in neural cells. J. Neurosci. Res. **2003**, 71, 863-870.
67. Gong C.X., Lidsky T., Wegiel J., Zuck L., Grundke-Iqbal I., Iqbal K.: Phosphorylation of microtubule-associated protein tau is regulated by protein phosphatase 2A in mammalian brain. Implication for neurofibrillary degeneration. J. Biol. Chem. **2000**, 275, 5535-5544.
68. Gsell W., Conrad R., Hickethier M., Sofic E., Frolich L., Wichart I., Jellinger K., Moll G., Ransmayr G., Beckmann H. and et al. Decreased catalase activity but

unchanged superoxide dismutase activity in brains of patients with dementia of Alzheimer type. J. Neurochem. **1995**, 64, 1216-1223.
69. Guiroy D.C., Miyazaki M., Multhaup G., Fischer P., Garruto R.M., Beyreuther K., Masters C.L., Simms G., Gibbs C.J., Gajdusek C.: Amyloid of neurofibrillary tangles of Guaminian Parkinsonism-dementia and Alzheimer disease share identical amino acid sequence. Proc. Natl. Acad. Sci. **1987**, 84, 2073-2977.
70. Haines J.L., Bailey L.R., Grubber J.M., Hedges D., Hall J.L., West S., Santoro L., Kremmerer B., Saunders A.M., Roses A.D.: A genomic search for Alzheimer's disease genes. In Alzheimer's Disease: Advances in Etiology, Pathogenesis and Therapeutics. Eds.: Iqbal K., Sisodia S.S., Winblad B., John Wiley Sons Ltd. **2001**, 33-43.
71. Hanger D.P., Betts J.C., Loviny T.L.F., et al. New phosphorylation sites identified in hyperphosphorylated tau (paired helical filament-tau) from Alzheimer's disease brain using nanoelectrospray mass spectrometry. J. Neurochem **1998**, 71, 2465-2476.
72. Hata R., Masumura M., Akatsu H., Li F., Fujita H., Nagai Y., Yamamoto T., Okada H., Kosaka H., Sakanaka M., Sawada T.: Up-regulation of calcineurin Aß mRNA in the Alzheimer's disease brain: assessment by cDNA microarray. Bioch. Bioph. Res. Com. **2001**, 284, 310-316.
73. Heal J.R., Roberts G.W., Christie G., Miler A.D.: Inhibition of ß-amyloid aggregation and neurotoxicity by complementary (antisense) peptides. Chembiochem. **2002**, 3 86-92.
74. Hensley K., Floyd R.A., Zheng N.Y., Nael R., Robinson K.A., Nguyen X., Pye Q.N., Stewart C.A., Geddes J., Markesbery W.R., Patel E., Johnson G.V.W., Bing G.Y.: p38 kinase is activated in the Alzheimer's disease brain. J. Neurochem. **1999**, 72, 2053-2058.
75. Holmes C., Wilkinson D.: Molecular biology of Alzheimer's disease. Adv. Psych. Treatment. **2000**, 6, 193-200.
76. Hoyer S.: Is sporadic Alzheimer disease the brain type of non-insulin dependent diabetes mellitus ? A challenging hypothesis. J. Neural. Transm. 1998, 105, 415-422.
77. Hu J., Igarashi A., Kamata M., Nakagawa H.: Angiotensin-converting enzyme degrades Alzheimer amyloid ß-peptide (Aß); retards Aßaggregation, deposition, fibril formation; and inhibits cytotixicity. J.Biol. Chem. **2001**, 276, 47863-47868.
78. Huang Y., Liu X.Q., Wyss-Coray T., Brecht W.J., Sanan D.A., Mahley R.W.: Apolipoprotein E fragments present in Alzheimer's disease brains induce neurofibrillary tangle-like intracellular inclusions in neurons. Proc. Natl. Acad. Sci. **2001**, 98, 8838-8843.
79. Husseman J.W., Hallows J.L., Bregman D.B., Leverenz J.B., Nochlin D., Jin L.-W., Vincent I.: Hyperphosphorylation of RNA polymerase II and reduced neuronal RNA levels precede neurofibrillary tangles in Alzheimer's disease. J. Neuropathol. Exp. Neurol. **2001**, 60, 1219-1232.
80. Hynd M.R., Scott H.L., Dodd P.R.: Glutamate (NMDA) receptor NR1 subunit m RNA expression in Alzheimer's disease. J. Neurochem. **2001**, 78, 175-182.
81. Ikeda S., Yanagisawa N., Glenner G.G., Allsop D.: Gerstmann–Straussler–Scheinker disease showing ß–protein deposits in the peripheral regions of PrP – immunoreactive amyloid plaques. Neurodegeneration **1992,** 1, 281-288.
82. Ikonomovic M.D., Sheffield R., Armstrong D.M.: AMPA-selective glutamate receptor subtype iimmunoreactivity in the hippocampal formation of patients with Alzheimer's disease. Hippocampus **1995**, 5, 469-486.
83. Ikonomovic M.D., Mizukami K., Warde D., Sheffield R., Hamilton R., Wenthold R.J., Armstrong D.M.: Distribution of glutamate receptor subunit NMDAR1 in the

hippocampus of normal elderly and patients with Alzheimer's disease. Exp. Neurol. **1999**, 160, 194-204.
84. Iqbal K., Grundke-Iqbal I.: Molecular mechanisms of Alzheimer's neurofibrillary degeneration and therapeutic intervention. Ann N. Y. Acad. Sci. **1996**, 77, 132-138.
85. Imahori K., Uchida T.: Physiology and pathology of tau protein ki-nases in relation to Alzheimer's disease. J. Biochem. **1997**, 121, 179-188.
86. Itoh N., Hiroyuki A., Urakami K., Ishiguro K., Ohno H., Hampel H., Buerger K., Wiltfang J., Otto M., Kretzschmar H. et al.: Large-scale, multicenter study of cerebrospinal fluid tau protein phosphorylated at serine 199 for the ante mortem diagnosis of Alzheimer's disease. Ann. Neurol. **2001**, 50, 150-156.
87. Iqbal K., Alonso A.D., Gong C.X., Khatoon S., Pei J.J., Wang J.Z., Grundke–Iqbal I.: Tau phosphatases. In: Brain Microtubule – associated Protein (Eds. J. Avila, R. Brandt and K.S. Kosik), Harwood Academic Publ, Switzerland. **1997**, 95-111.
88. Kalaria R.N., Bhatti S.U., Platinsky E.A., Pennington D.H., Shelton E.R., Chan H.W., Perry G., Lust W.D.: Accumulation of the – amyloid precursor protein at sites of ischemic injury in rat brains. NeuroReport **1993**, 4, 211-214.
89. Kang J., Lemaire H.G., Unterbeck A., Salbaum J.M., Masters C.J., Grzeschik K.H., Multhaup G., Beyreuther K., Muller-Hill B.: The precursor of Alzheimer's disease A4 protein resembles a cell-surface receptor. Nature **1987**, 325, 733-736.
90. Katayama T., Imaizumi K., Sato N., Miyoshi K., Kudo T., hitomi J., Morihara t., Yoneda T., Gomi F., Mori Y., Nakano Y., Takeda J., Tsuda T., Itoyama Y., Murayama O., Takashima A., St.George-Hyslop. P., Takeda M., Tohyama M.: Presenilin-1 mutations down regulate the signaling pathway of the unfolded-protein response. Nature Cell Biol. **1999,** 1, 479-485.
91. Kawai M., Cars P., Richey P., Tabaton M., Lowery D.E., Gonzalez-DeWhitt P.A., Greenberg B.D., Gambetti P., Perry G.: Subcellular localization of amyloid precursor protein in senile plaques of Alzheimer's disease. Am. J. Pathol. **1992**, 140, 947-958.
92. Kay M.M.B., Goodman J.: Brain and erythrocyte anion transporter protein, band 3, as a marker for Alzheimer's disease: structural changes detected by electron microscopy, phosphoryllation, and antybodies. Gerontology **1997**, 43, 44-66.
93. King M.E., Ahuja V., Binder L.I., Kuret J.: Ligand dependent tau filament: Implications for Alzheimer's disease progression. Biochemistry **1999**, 38, 14851-14859
94. Kitaguchi N., Takahashi Y., Tokushima S., Ito H.: Novel precursor of Alzheimer's disease amyloid protein shows protease inhibitory activity. Nature **1988**, 331, 530-532.
95. Kitaguchi N., Takahashi Y., Oishi K., Shiojiri S., Tokushima Y., Utsunomiya T., Ito H.: Enzyme specificity of proteinase inhibitor region in amyloid precursor protein of Alzheimer's disease: different properties compared with protease nexin. Biochim. Biophys. Acta **1990,** 1038, 105-113.
96. Kosik K.S., Orecchio L.D., Bakalis S., Neve R.L.: Developmentally regulated expression of specific tau sequences. Neuron **1989,** 2, 1389-1397.
97. Kourie J.I.: Mechanisms of amyloid ß protein –induced in ion transport systems: implications for neurodegenerative diseases. Cell mol. Neurobiol. **2001**, 173-213.
98. Köpke E., Tung Y.C., Shaikh S., Alonso A. del C., Iqbal, K., Grundke-Iqbal I. Microbutule associated protein tau: abnormal phosphorylation of a non-paired helical filament pool in Alzheimer disease. J. Biol. Chem. **1993**, 268, 24374-24384.
99. Ksiezak-Reding H., Morgan K., Mattiace L.A., Davies P., Liu W-K., Yen S-H., Weldenhein K., Dickson D.W.: Ultrastructure and biochemical composition of paired helical filaments in corticobasal degeneration. Am. J. Pathol. **1994**, 145, 1-13.

100. Kuentzel S.L., Gonzalez-DeWhitt P.A., Lowery D.E., Altman R.A., Leone J.W., Heinrikson R.L., Greenberg B.D., Raub T.J.: Overexpression of a COOH-terminal fragment of β-amyloid precursor protein in HeLa cells results in accumulation in a pre-Golgi compartment and generation of an Aβ-like fragment. Amyloid: Int. J. Exp. Clin. Invest. **1996**, 3, 86-99.
101. Kurochkin I.V., Goto S.: Alzheimer's ß-amyloid peptide specifically interacts with and is degraded dy insulin degrading enzyme. FEBS Lett. **1994**, 345, 33-37.
102. Kuźnicki J., Puzianowska-Kuźnicka M.: Jony wapnia a apoptoza. Post. Biol. Komórki **1998,** 25, 29-42.
103. Lai A. Sisodia S.S., Trowbridge I.S.: Characterization of sorting signals in the ß-amyloid prekursor protein cytoplasmic domain. J. Biol. Chem. **1995**, 270, 3565-3573.
104. Lau L.F., Schachter J.B., Seymour P.A., Sanner M.A.: Tau protein phosphorylation as a therapeutic target in Alzheimer's disease. Curr. Top. Med. Chem. **2002,** 2, 395-415.
105. Layfield R., Alban A., Mayer R.J., Lowe J.: The ubiquitin protein catabolic disorders. Neuropath. Appl. Neurobiol. **2001**, 27, 171-179.
106. Lee H.G., Zhu X., Ghanbari H.A., Ogawa O., Raina A.K., O'Neill M.J., Perry G., Smith M.A.: Differential regulation of glutamate receptors in Alzheimer's disease. Neurosignals **2002**, 11, 282-292.
107. Lemaire H.G., Salbaum J.M., Multhaup G., Kang J., Banyey R.M., Unterbeck A., Beyreuther K., Müller-Hill B.: The Pre A4 695 precursor protein of Alzheimer's disease A4 amyloid is encoded by 16 exons. Nucleic Acids Res. **1989**, 17, 517-522.
108. Leroy K., Boutajangout A., Authelet M., Woodgett J.R., Anderton B.H., Brion J.P.: The active form of glycogen synthase kinase-3ß is associated with granulovascular degeneration in neurons in Alzheimer's disease. Acta Neuropathol. **2002**, 103, 91-99.
109. Liu W.K., Williams R.T., Hall F.I., Dickson D.W., Yen S.H.: Detection of a cdc2 – related kinase associated with Alzheimer paired helical filaments. Am.J. Pathol. **1995,** 146, 228-238.
110. Lovell M.A., Xie C., Markesbery W.R.: Acrolein is increased in Alzheimer's disease brain and is toxic to primary hippocampal cultures. Neurobiol. Aging **2001**, 22, 187-194.
111. Lu P.J., Wulf G., Zhou X.Z., Davies P., Lu K.P.: The prolyl isomerase Pin 1 restores the function of Alzheimer – associated phosphorylated tau protein. Nature **1999**, 399, 784-788.
112. Mandybur T.I.: The distribution of Alzheimer's neurofibrillary tangles and gliosis in chronic subacute sclerosing panencephalitis. Acta. Neuropathol. (Berl) **1990**, 80, 307-310.
113. Mandelkow E.M., Drewes G., Biernat J., Gustke N., Van L.J., Vandenheede J.R., Mandelkow E.: Glycogen synthase kinase-3 and the Alzheimer–like state of microtubule–associated protein tau. FEBS Lett. **1992**, 314, 315-321.
114. Marambaud P., Lopez-Perez E., Wilk S., Checler F.: Constitutive and protein kinaseC-regulated secretory cleavage of Alzheimer's ß-amyloid precursor protein: different control of early and late events by the proteasome. J. Neurochem. **1997**, 69, 2500-2505.
115. Martinez M., Fernandez E., Frank A., Guaza C., de la Fuente M., Hernanz A.: Increased cerebrospinal fluid c-AMP levels in Alzheimer's disease. Brain Res. **1999**, 846, 265-267.
116. Martinez-Senac M.D., Villalain J., Gomez-Fernandez J.C.: Structure of the Alzheimer ß-amyloid peptide (25-35) and its interaction with negatively charged phospholipids vesicles. Eur. J. Bioch. **1999**, 265, 744-753.

117. Marquez–Sterling N.R., Lo A.C., Sisodia S.S., Koo E.H.: Trafficking of cell–surface beta–amyloid precursor protein: evidence that a sorting intermediate participates in synaptic vesicle recycling. J. Neurosci. **1997**, 17, 140-151.
118. Marui W., Iseki E., Ueda K., Kosaka K.: Occurrence of human α-synuclein immunoreactive neuronswith neurofibrillary tangle formation in the limbic areas of patients with Alzheimer's disease. J. Neurol. Sci. **2000**, 174,81-84.
119. Masliah E., Rockenstein E., Veinbergs I., Sagara Y., Mallory M., Hashimoto M., Mucke L.: ß-Amyloid peptides enhance α-synuclein accumulation and neuronal deficits in a transgenic mouse model linking Alzheimer's disease and Parkinson's disease. Proc. Natl. Acad. Sci. **2001,** 98, 12245-12250.
120. Masters C.L., Multhaup G., Simms G., Pottgiesser J., Martins R.N., Beyreuther K.: Neuronal origin of a cerebral amyloid: neurofibrillary tangles of Alzheimer's disease contain the same protein as the amyloid of plaque cores and blood vessels. EMBO J. **1985 a**, 4, 2757-2763.
121. Masters C.L., Simms G., Weinman N.A., Multhaup G., McDonald B.L., Beyreuther K.: Amyloid plaque core protein in Alzheimer disease and Down syndrome. Proc. Natl. Acad. Sci. USA **1985 b**, 82, 4245-4249.
122. Mattson M.P., Cheng B., Culwell A.R., Esch F.S., Lieberburg I., Rydel R.E.: Evidence for excitoprotective and intraneuronal calcium-regulating roles for secreted forms of the *ß*–amyloid precursor protein. Neuron **1993**, 10, 243-254.
123. Mattson M.P., Fu W.M., Waeg G., Uchida K.: 4-hydroxynonenal, a product of lipid peroxidation, inhibits dephosphorylation of the microtubule-associated protein tau. Neuroreport **1997**, 8, 2275-2281.
124. McLaurin J., Franklin T., Kuhns W.J., Fraser P.E.: A sulfated proteoglycan aggregation factor mediates amyloid–ß fibril formation and neurotoxicity. Amyloid-Int. J. Exp.Clin. Invest. **1999**, 6, 233-243.
125. Mehta P.D., Pirttila T., Patrick B.A., Barshatzky M., Mehta S.P.: Amyloid ß protein 1-40 and 1-42 levels in matched cerebrospinal fluid and plasma from patients with Alzheimer disease. Neurosci. Lett. **2001**, 304, 102-106.
126. Meier-Ruge W., Iwangoff P., Reichlmeier K.: Neurochemical enzyme changes in Alzheimer's and Pick's disease. Arch. Gerontol. Geriatr. **1984**, 3, 161-165.
127. Meier-Ruge W., Bertoni-Freddari C., Iwangoff P.: Changes in brain glucose metabolism as a key to the pathogenesis of Alzheimer's disease. Gerontology **1994**, 40, 246-252.
128. Meier-Ruge W., Iwangoff P., Bertoni-Freddari C.: What is primary and what is secondary for amyloid deposition in Alzheimer's disease? Ann. NY Acad. Sci. **1994**, 719, 230-237.
129. Meier-Ruge W., Bertoni-Freddari C.: The significance of glucose turnover in the brain in the patogenetic mechanisms of Alzheimer's disease. Rev. Neurosci. **1996,** 7, 1-19.
130. Meier-Ruge W., Bertoni-Freddari C.: Pathogenesis of decreased glucose turnover and oxidative phosphorylation in ischemia and trauma-induced dementia of the Alzheimer type. Ann. N Y Acad. Sci. **1997**, 826, 229-241.
131. Miller B.E.: Comparison of A68 levels in Alzheimer diseased and non-Alzheimer's diseased brain by two ALZ50 based methods. Life Sci. **1999**,65,2215-2222.
132. Milward E.A., Papadoupoulos R., Fuller S.J., Moir R.D., Small D., Beyreuther K., Masters C.L.: The amyloid protein precursor of Alzheimer's disease is a mediator of the effects of nerve growth factor on neurite outgrowth. Neuron **1992**, 9, 129-137.
133. Molina L., Touchon J., Herpe M., Lefranc D., Duplan L., Cristol J.P., Sabatier R., Vermersch P., Pau B., Mourton-Gilles C.: Tau and apo E in CSF:

potential aid for discriminating Alzheimer's disease from other dementias. NeuroReport **1999**, 10, 3491-3495.
134. Morishima–Kawashima M., Hasegawa M.,Takio T, et al.:Hyperphosphorylation of tau in PHF. Neurobiol. Aging **1995a**, 16, 365-380
135. Morishima–Kawashima M., Hasegawa M., Takio K., Suzuki M., Yoshida H., Titani K., Ihara Y.: Proline–directed and non–proline–directed phosphorylation of PHF–tau. J. Biol. Chem. **1995b**, 270, 823-829.
136. Mönning U., König G., Banati R.B., Mechler H., Czech C., Gehrmann J., Schreiter-Gasser U., Masters C.L., Beyreuther K.: Alzheimer ß/A4-amyloid protein precursor in immunocompetent cells. J. Biol. Chem. **1992**, 267, 23950-23956.
137. Mucke L., Abraham C.R., Masliah E.: Neurotrophic and neuroprotective effects of hAPP in transgenic mice. Ann. N Y Acad. Sci. **1996**, 777, 82-86.
138. Multhaup G., Mechler H., Masters C.L.: Characterization of the high affinity binding site of the Alzheimer's disease ß/A4 amyloid precursor protein (APP) and its enhancement by zinc (II). J. Mol. Recognit. **1995**, 8, 247-257.
139. Nakai M., Tanimukai S., Yagi K., Saito N., Taniguchi T., Terashima A., Kawamata T., Yamamoto H., Fukunaga K., Miyamoto E., Tanaka C.: Amyloid ß protein activates PKD-d and induces translocation of mirystoylated alanine – rich C kinase substrate (MARCKS) in microglia. Neurochem. Intern. **2001**, 38,593-600.
140. Nakazawa K., Quirk M.C., Chitwood R.A., Watanabe M., Yeckel M.F., Sun L.D., Kato A., Carr C.A., Johnston D., Wilson M.A., Tonegawa S.: Requirement for hippocampal CA3 NMDA receptors in associative memory recall. Science **2002**, 297, 211-218.
141. Nishimoto I., Okamoto T., Matsuura Y., Takahashi S., Murayama Y., Ogata E.: Alzheimer amyloid protein precursor complexes with brain GTP-binding protein G. Nature **1993**, 362, 75-79.
142. Nordstedt C., Gandy S.E., Alafuzoff I., Caporaso G.L., Iverfeldt K., Grebb J.A., Winbland B., Greengard P.: Alzheimer ß/A4 amyloid precursor protein in human brain: Aging-associated in holoprotein and in a proteolytic fragment. Proc. Natl. Acad. Sci. USA **1991**, 88, 8910-8914.
143. Octavo J.-N., Essalmani R., Tasiaux B., Menager J., Czech C., Mercken L.: The role of presenilin 1 in the γ-secretase cleavage of the amyloid precursor protein of Alzheimer's disease. J. Biol. Chem. **2000,** 275, 1525-1528.
144. Oltersdorf T., Fritz L.C., Schenk D.B., Lieberburg I., Johnson-Wood K.L., Beattie E.C., Ward P.J., Blacher R.W., Dovey H.F., Sinha S.: The secreted form of the Alzheimer's amyloid precursor protein with the Kunitz domain is protease nexin-II. Nature **1989**, 341, 144-147.
145. Page K.J., Everitt B.J., Robbins T.W., Marston H.M. Wilkinson L.S.: Dissociable effects on spatial maze and passive avoidance acquisition and retention following AMPA-and ibotenic acid-induced excitotoxic lesions of the basal forebrain in rats: differential dependence on cholinergic neuronal loss. Neuroscience **1991**, 43, 457-472.
146. Palmert M., Podlisny M., Witker D., Oltersdorf T., Younkin L., Selkoe D., Younkin S.: The ß amyloid precursor of Alzheimer's disease has soluble derivatives found in human brain and spinal fluid. J. Neuropathol. Exp. Neurol. **1989**, 48, 378.
147. Panegyres P.K., Zafiris-Toufexis K., Kakulas B.A.: The mRNA of the NR1 subtype of glutamate receptor in Alzheimer's disease. J. Neural. Transm. **2002**, 109, 77-89.
148. Parsons C.G., Danysz W., Quack G.: Memantine is a clinically well tolerated N-methyl-D-aspartate (NMDA) receptor antagonist – a review of preclinical data. Neuropharmacology **1999**, 38, 735-767.

149. Papassotiropoulos A., Bagli M., Kurz A., Kornhuber J., Forstl H., Maier W., Pauls J., Lautenschlager N., Heun R.: A genetic variation of cathepsin D is a major risk factor for Alzheimer's disease. Ann. Neurol. **2000**, 47,399-403.
150. Perez M., Hernandez F., Gomez-Ramos a., Smith M., Perry G., Avila J.: Formation of aberrant phosphotau fibrillar polymers in neural cultured cells. Eur.J. Biochem. **2002**, 269, 1484-1489.
151. Perry G., Richey P.L., Siedlak S.L., Smith M.A., Maulvihill P., DeWitt D.A., Barnett J., Greenberg B.D., Kalaria R.N.: Immunocytochemical evidence that the ß-protein precursor is an integral component of neurofibrillary tangles of Alzheimer's disease. Am. J. Pathol. **1993**, 143, 1586-1593.
152. Pluta R., Kida E., Lossinsky A.S., Golabek A.A., Mossakowski M.J., Wisniewski H.M.: Complete cerebral ischemia with short–term survival in rats induced by cardiac arrest. I. Extracellular accumulation of Alzheimer's ß-amyloid protein precursor in the brain. Brain Res. **1994,** 649, 323-328.
153. Ponte P., Gonzales-DeWhitt P., Schilling J., Miller J., Hsu D., Greenburg B., Davis K., Wallace W., Leiberburg I., Fuller F., Cordell B.: A new A4 amyloid mRNA contains a domain homologous to serine protease inhibitors. Nature **1988,** 331, 525-527.
154. Praprotnik D., Smith M.A., Richey P.L., Vinters H.V., Perry G.: Filament heterogeneity within the dystrophic neurites of senile plaques blockage of fast axonal transport in Alzheimer's disease. Acta Neuropathol. **1996**, 91, 226-235.
155. Qiu W.Q., Ferreira A., Miller C., Koo E.H., Selkoe D.J.: Cell-surface ß-amyloid precursor stimulates neurite outgrowth of hippocampal neurons in an isoform-dependent manner. J Neurosci **1995**, 15, 2157-2167.
156. Reisberg B., Doody R., Stöffler A., Schmitt F., Ferris S., and Möbius H.J.: Memantine in moderate–to–severe Alzheimer's disease. N Engl. Med. **2003**, 348, 1333-1341.
157. Ramabhadran T.V., Gandy S.E., Ghiso J., Czernik A.J., Ferris D., Bhasin R., Goldgaber D., Frangione B., Greengard P.: Proteolytic processing of human amyloid ß-protein precursor in insect cells. Major carboxyl-terminal fragment is identical to its human counterpart. J. Biol. Chem. **1993**, 268, 2009-2012.
158. Reisberg B., Doody R., Stoffler A., Schmitt F., Ferris S., Mobius H.J.: Memantine in moderate-to-severe Alzheimer's disease. N. Engl. J. Med. **2003**, 348, 1333-1341.
159. Robakis N.K., Ramakrishna N., Wolfe G., Wiśniewski H.M.: Molecular cloning and characterization of a cDNA encoding the neuritic plaque amyloid peptides. Proc. Natl. Acad. Sci. USA **1987**, 84, 4190-4194.
160. Robison P.M., Clemens J.A., Smalstig E.B., Stephenson D. and May P.C.: Decrease in amyloid precursor protein precedes hippocampal degeneration in rat brain following transient global ischemia. Brain Research **1993,** 608, 334-337.
161. Rossner S., Mendela K., Schliebs R., Bigl V., Protein kinase Cά and ß1 isoforms are regulators of α -secretory proteolytic processing of amyloid precursor protein in vivo Eur. J. Neurosci. **2001**, 13, 1644-1648.
162. Russell r.l., Siedlak S.L., Raina A.K., Bautiska A.K., Smith M.A., Perry G.: Increased neuronal glucose-6-phosphate dehydrogenase and sulfhydryl levels indicate reductive compensation to oxidative stress in Alzheimer's disease. Arch Bioch Bioph. **1999,** 370, 236-239.
163. Ryba M.S., Gordon-Krajcer W., Walski M., Chalimoniuk M., Chrapusta S.J.: Hydroxylamine attenuates the effects simulated subarachnoid hemorrhage in the rat brain and improves neurological outcome. Brain Research **1999**, 850, 225-233.
164. Sagara Y., Dargusch R., Klier F.G., Schubert D., Behl C.: Increased antioxidant enzyme activity in amyloid beta protein-resistant cells. J. Neurosci. **1996**, 16, 497-505.

165. Saitoh T., Sundsmo M., Roch J-M., Kimura N., Cole G., Schubert D., Oltersdorf T., Schenk D.B.: Secreted form of amyloid ß protein precursor is involved in the growth regulation of fibroblasts. Cell **1989,** 58, 615-622.
166. Sayre L.M., Zelasko D.A., Harris P.L.R., Perry G., Salomon R.G., Smith M.A.: 4-hydroxynonenal-derived advanced lipid peroxidation end products are increased in Alzheimer's disease. J. Neurochem. **1997**, 68, 2092-2097.
167. Sayre L.M., Perry G., Harris P.L.R., Liu Y.H., Schubert K.A., Smith M.A.: *In situ* oxidative catalysis by neurofibrillary tangles and senile plaques in Alzheimer's disease:A central role for bound transition metals. J. Neurochem. **2000,** 74, 270-279.
168. Schubert W., Masters C.L., Beyreuther K.: APP+T lymphocytes selectively sorted to endomysial tubes in polymyositis displace NCAM-expressing musclefibers. Eur. J. Cell Biol. **1993**, 62, 333-342.
169. Selkoe D.J.: Amyloid ß-protein and the genetics of Alzheimer's disease. Biol. Chem. **1996**, 271, 18295-18298.
170. Selkoe D.J.: Translating cell biology into therapeutic advances in Alzheimer's disease. Nature **1999**, 399, A23.
171. Selkoe D.J.: Presenilin, Notch, and the genesis and treatment of Alzheimer's disease. Proc. Natl. Acad. Sci. **2001a,** 98, 11039-11041.
172. Selkoe D.J.: Alzheimer's disease: genes, proteins, and therapy. Physiol. Rev. **2001b,**81,741-766.
173. Sinha S., Dovey H.F., Seubert P., Ward P.J., Blacher R.W., Blaber M., Bradshaw R.A., Arici M., Mobley W.C., Lieberburg I.: The protease inhibitory properties of the Alzheimer's ß-amyloid precursor protein. J. Biol. Chem. **1990**, 265, 8983-8985.
174. Sisodia S.S., Koo E.H., Beyreuther K., Unterbeck A., Price D.L.: Evidence that ß-amyloid protein in Alzheimer's disease is not derived by normal processing. Science **1990**, 248, 492-495.
175. Sisodia S.S.: ß amyloid precursor protein cleavage by a membrane-bound protease. Proc. Natl. Acad. Sci. USA **1992**, 89, 6075-6079.
176. Sjögren M., Davidsson P., Tullberg M., Minthon L., Wallin A., Wikkelso C., Granerus A.-K., Vanderstichele H., Vanmrchelen E.I., Blennow K.: Both total and phosphorylared tau are increased in Alzheimer's disease. J. Neurol. Neurosurg. Psych.**2001**, 70, 624-630.
177. Small D.H., Williamson T., Reed G., Clarris H., Beyreuther K., Masters C.L., Nurcombe V.: The role of heparan sulfate proteoglycans in the pathogenesis of Alzheimer's disease. Ann. N Y Acad. Sci. **1996,** 777, 316-321.
178. Smith M.A., Siedlak S.L., Richey P.L., Mulvihill P., Ghiso J., Frangione B., Tagliavini F, Giaccone G., Bugiani O., Praprotnik D., Kalaria R.N., Perry G.: Tau protein directly interacts with the amyloid ß-protein precursor: implications for Alzheimer's disease. Nature Med. **1995**, 1, 365-369.
179. Smith R.P., Higushi D.A., Broze G.J.: Platelets coagulation factor IIa-inhibitor, a form of Alzheimer amyloid precursor protein. Science **1990,** 248, 1126-1128.
180. Sols A., Crane R.K.: Substrate specificity of brain hexokinase. J. Biol. Chem. **1954**, 210, 581-595.
181. Sołtysiak Z.: Badania porównawcze nad amyloidozą-B i zwyrodnieniem neurowłókienkowym (ZNW) w ośrodkowym układzie nerwowym (OUN) różnych gatunków starych zwierząt I ludzi z chorobą Alzheimera. Zesz. Nauk. AR we Wrocławiu. **2000,** 372, 15-1492.
182. Spillantini M.G., Crowther R.A., Goedert M.: Comparison of the neurofobrillary pathology in Alzheimer's disease and familial presenile dementia with tangles. Acta Neutopathol. **1991**, 92, 42-48.

183. St. George-Hyslop P.H.: Molecular genetics of Alzheimer's disease. Biol. Psychiatry **2000**, 47, 183-199.
184. Suzuki K., Parker C.C., Pentcher D.K., Ghetti B., D'Agostino A.N., Carstea E.D.: Neurofibrilary tangles in Niemann-Pick disease type C. Acta Neuropathol. (Berl) **1995**, 89, 227-238.
185. Sze C., Bi H., Kleinschmidt-DeMasters B.K., Filley C.M., Martin L.J.: N-Methyl-D-aspartate receptor subunit proteins and their phosphorylation status are altered selectively in Alzheimer's disease. J. Neurol. Sci. **2001**, 182, 151-159.
186. Takeda A., Smith M.A., Avila J., Nunomura A., Siedlak S.L., Zhu X., Perry G., Sayre L.M.: In Alzheimer's disease, home oxygenase is coincident with alz50, an epitope of tau induced by 4-hydroxy-2-nonenal modification. J. Neurochem. **2000**, 75, 1234-1241.
187. Takahashi M., Dore S., Ferris C.D., Tomita T., Sawa A., Wolosker H., Borchelt D.R., Iwatsubo T., Kim S.H., Thinakaran G., Sisodia S.S., Snyder S.H.: Amyloid precursor proteins inhibit heme oxygenase activity and augment neurotoxicity in Alzheimer's disease. Neuron **2000**, 28, 461-473.
188. Tanaka S., Nakamura S., Ueda K., Kameyama M., Shiojiri S., Takahashi Y., Kitaguchi N., Ito H.: Three types of amyloid protein precursor mRNA in human: their differential expression in Alzheimer's disease. Biochem. Biophys. Res. Commun. **1988**, 157, 472-479.
189. Tanzi R.E., Gusella J.F., Watkins P.C., Bruns GAP, St. George-Hyslop P., Van Keuren M.L., Patterson D., Pagan S., Kurnit D.M., Neve R.L.: Amyloid ß-protein gene: cDNA, mRNA distribution and genetic linkage near the Alzheimer locus. Science **1987**, 235, 880-884.
190. Tanzi R.E., McClatchy A.I., Lamperti E.D., Villa-Kornaroff L., Gusella J.F., Neve R.L.: Protease inhibitor domain encoded by an amyloid precursor mRNA associated with Alzheimer's disease. Nature **1988**, 331, 528-530.
191. Tanzi R.E., Koacs D.M., Kim T.W., Moir R., Guenette S.Y., and Wasco W.: The gene defects responsible for familial Alzheimer' s disease. Neurobiol. Dis. **1996,** 3, 159-168.
192. Tanzi R.S.: Alzheimer's disease-from genes to drugs. IBC 9th Annual Conference on Alzheimer's Gene Discovery to Therapeutic Applications. Atlanta, CA, Feb.8-9, **2001**
193. Terai K., Iwai A., Kawabata S., Sasamata M., Miyata K., Yamaguchi T.: Apolipoprotein E deposition and astrogliosis are associated with maturation of ß-amyloid plaques in ßAPPs transgenic mouse. Implications for the pathogenesis of Alzheimer's disease. Brain Res. **2001,** 900, 48-56.
194. Thinakaran G.: The role of presenilins in Alzheimer's disease. J. Clin. Invest. **1999**, 104, 1321-1327.
195. Thinakaran G.: Metabolism of presenilins. J. Molec. Neurosci. **2001**, 900, 48-56.
196. Thorns V., Mallory M., Hansen L., Masliah E.: Alterations in glutamate receptor 2/3 subunits and amyloid precursor protein expression during the course of Alzheimer's disease and Lewy body variant. Acta Neuropathol (Berl) **1997**, 94, 539-548.
197. Triniczek B., Biernat J., Baumann K., Mandelkow E.M., Mandelkow E.: Domains of tau protein, differential phosphorylation, and dynamic instability of microtubules. Mol. Biol Cell.**1995**, 6, 1887-1902.
198. Ulas J., Cotman C.W.: Decreased expression of N-methyl-D-aspartrte receptor 1 messenger RNA in select regions of Alzheimer brain. Neuroscience **1997**, 79, 973-982.
199. Vanderklish P.W., Bahr B.A.: The pathogenic activation of calpain: a marker and mediator of cellular toxicity and disease states. Int. J. Exp. Path. **2000**, 81,323-339.

200. Vanmechelen E., Van Kerschaver-Blennow K., De Deyn P.P., Galasko D., Parnetti L., Sindic C.J.M., AraiH., Riemenschneider M., Hampel H.et al.: CSF-phospho-tau (181P) as a promising marker for discriminating, Alzheimer's disease from dementia with Lewy bodies. Alzheimer's Disease: Advances in Etiology, Pathogenesis and Therapeutics. Ed. Iqbal K., Sisodia S.S., Winblad B., John Wiley Sons, Ltd.**2001.**
201. Van Nostrand W.E., Wagner S.L., Suzuki M., Choi B.H., Farrow J.S., Geddes J.W., Cotman C.W., Cunningham D.D.: Protease nexin-II, a potent antichymotrypsin, shows identity to amyloid ß-protein precursor. Nature **1989**, 341, 546-549.
202. Van Nostrand W.E., Schmaier A.H., Farrow J.S., Cunningham D.D.: Protease nexin-II (amyloid ß-protein precursor): a platelet alpha granule protein. Science **1990**, 248, 745-748.
203. Verkhratsky A.: The endoplasmic reticulum and neuronal calcium signaling. Cell Calcium **2002,** 32, 393-404.
204. Wakabayashi K., Narisawa-Saito M., Iwakura Y., Arai T., Ikeda K., Takahashi H., Nawa H.: Phenotypic down-regulation of glutamate receptor subunit GluR1 in Alzheimer's disease. Neurobiol. Aging. **1999**, 20, 287-295.
205. Wang D.S., Cochran E., Bennett D., Mufson E., Eckman C., Dickson D.W: Amyloid, PHF-tau, ubiquitin and synaptic markers in the progression of Alzheimer's disease: immunochemical analyses of frontal cortex from prospectively studied elderly humans.Alzheimer's Disease: Advances in Etiology, Pathogenesis and Therapeutics. Eds.: Iqbql K., Sisodia S.s., Winblad B., John Wiley Sons Ltd.**2001,** 165-180.
206. Weidemann A., König G., Bunke D., Fischer P., Salbaum J.M., Masters C.L., Beyreuther K.: Identification, biogenesis and localization of precursors of Alzheimer's disease A4 amyloid protein. Cell **1989**, 57, 115-126.
207. Weiss J.H., Yin H.Z., Choi.: Basal forebrain cholinergic neurons are selectively vulnerable to AMPA/kainite receptor-mediated neurotoxicity. Neuroscience **1994**, 60, 659-664.
208. Wiśniewski K.E., Jervis G.A., Moretz R.C., Wiśniewski H.M.: Alzheimer neurofibrillary tangles in diseases other than senile and presenile dementia. Ann. Neurol. **1979**, 5, 288-294.
209. Wiśniewski K.E., Dalton A.J., Crapper MacLachlan D.R., Wen G.Y., Wiśniewski H.M.: Alzheimer's disease in Down syndrome: clinicopathologic studies Neurology **1985**, 35, 957-961.
210. Wiśniewski K.E., Gordon-Krajcer W., and Kida E.: Abnormal processing of carboxy-terminal fragment of beta precursor protein (ß-APP) in Neuronal Ceroid Lipofuscinosis (NCL) cases. J. Inher. Metab. Dis. **1993**, 16, 312-316.
211. Wolfe M.S.: γ-Secretase inhibitors as molecular probes of presenilin function. J. Mol. Neurosci. **2001,** 17, 199-204.
212. Xie L., Helmerhorst E., Taddei K., Plewright B., Van Bronswijk W., Martins R.: Alzheimer's beta-amyloid peptides compete for insulin binding to the insulin receptor. J. Neurosci. **2002**, 250, 279-282.
213. Yamaguchi H., Ishiguro K., Shoji M., Yamazaki T., Nakazato Y., Ihara Y., Hiral S.: Amyloid ß/A4 protein precursor is bound to neurofibrillary tangles in Alzheimer-type dementia. Brain Res. **1990a**, 537, 318-322.
214. Yamada T., Tsujioka Y., Taguchi J., Takahashi M., Tsuboi Y., Moreo I., Yang J., Jefferies W.A.: Melanotransferrin is produced by sinile plaque-associated reactive mocroglia in Alzheimer's disease. Brain Res. **1999a**, 845, 1-5.
215. Yamada M., Sodeyama N., Itoh Y., Suematsu N., Otomo E., Matsushita M., Mizusawa H.: A deletion polymorphism of α (2)–macroglobulin gene and cerebral amyloid angiopathy. Stroke **1999**, 30, 2277-2279.

216. Yamaguchi H., Ishiguro K., Uchida T., Takashima A., Lemere C.A., Imahori K.: Preferential labeling of Alzheimer neurofibrillary tangles with antisera for tau protein kinase (TPK) I glycogen synthetase kinase-3 beta and cyclin-dependent kinase 5, a component of TPK II. Acta Neuropathol. (Berl.) **1996**, 92, 232-241.
217. Yan R., Bienkowski M.J., Shuck M.E., Miao H., Tory M.C., Pauley A.M., Brashler A.E., Stratman N.C., Mathews W.R., Buhl A.E., Carter D.B., Tomasseli A.G., Parodi L.A., Heinrikson R.L., Gurney M.E.: Membrane–anchored aspartyl protease with Alzheimer's disease-secretase activity. Nature **1999,** 402, 533-537.
218. Yip C.M., McLaurin J.: Amyloid-ß peptide assembly: A critical step in fibrillogenesis and membrane disruption. Bioph. J. **2001**, 80, 1359-1371.
219. Yoshikai S., Sasaki H., Doh-ura K., Furuya H., Sakaki Y.: Genomic organization of the human amyloid ß-protein precursor gene. Gene **1990,** 87, 257-263.
220. Zhu G., Wang D., Lin Y.-Huei McMahon T., Koo E.H., Messing R.O.: Protein kinase C ε suppresses Aß production and promotes activation of α-secretase. Bioch. Bioph. Res. Com. **2001**, 285, 997-1006.
221. Zhu X., Rottkamp C.A., Boux H., Takeda A., Perry G., Smith M.A.: Activation of p38 kinase links tau phosphorylation, oxidative stress, and cell cycle-related events in Alzheimer disease. J. Neuropathol. Exp. Neurol. **2000**, 59, 880-888.
222. Zhu X., Raina A.K., Rottkamp C.A., Aliev G., Perry G., Boux H., Smith M.A.: Activation and redistribution of c-jun N-terminal kinase/stressactivated protein kinase in degenerating neurons in Alzheimer's disease. J. Neurochem. **2001a**, 76, 435-441.
223. Zhu X., Castellani R.J., Takeda A., Nunomura A., Atwood C.S., Perry G., Smith M.A.: Differential activation of neuronal ERK, JNK/SAPK and p38 in Alzheimer disease: the 'two hit' hypothesis. Mech. Ageing Dev. **2001b**, 123, 39-46.

Publikacja 1

VIA MEDICA

ORIGINAL ARTICLE

Folia Neuropathol.
Vol. 39, No. 3, pp. 163–173

ISSN 1641–4640

Excitotoxicity-induced expression of amyloid precursor protein (β-APP) in the hippocampus and cortex of rat brain. An electron-microscopy and biochemical study

Wanda Gordon-Krajcer[1], Barbara Gajkowska[2]

[1]Department of Neurochemistry, Medical Research Centre, Polish Academy of Sciences, Warszawa,
[2]Laboratory of Cell Ultrastructure, Medical Research Centre, Polish Academy of Sciences, Warszawa

After stereotaxic microinjection of N-methyl-D-aspartate (NMDA) or alpha-amino-3-hydroxy-5-methyl isoxazole-4-propionic acid (AMPA) to CA1 of rat hippocampus, the animals were sacrificed: 0 h, 2 h, 12 h, 24 h and 3 days after the insult. Other groups of animals before microinjection of the excitotoxins received intraperitoneal injection of dizocilpine (MK-801). Expression of β-APP was assessed by immunohistochemical and immunobiochemical methods, and the results were correlated with changes in tissue ultrastructure observed in the electron microscopy. The results of the immunochemical analyses study demonstrated that application of NMDA and AMPA resulted in the increase of the expression of β-APP in the CA1 of hippocampus and to a less extent in the cortex. Pretreatment with MK-801 strongly suppressed this effect. β-amyloid release was not detected. Morphological and cytochemical study revealed that NMDA injection induced massive damage of hippocampal and cortical neurones, associated with mitochondrial calcium sequestration and unusual accumulation of neurofilaments. Ultrastructural changes after AMPA application were limited to the brain cortex.

These data indicate that although excitotoxic insult induces hyperexpression of β-APP, there is no relation between this effect and neurodegeneration, and excitotoxicity does not induce amyloidogenic processing of β-APP.

key words: β-amyloid precursor protein, NMDA receptor, AMPA receptor, excitotoxicity

INTRODUCTION

Repeated head trauma, as experienced by boxers, has been linked to the development of the clinicopathological entry known as *dementia pugilistica* (DP). Symptoms may develop during the boxer's career or begin years after retirement and can be progressive. There are many similarities between Alzheimer's dementia and DP in terms of pathology (presence of tangles), anatomy (temporal lobe and basal nucleus of Meynert affected), neurochemistry (cholinergic defect) and symptoms. In DP pathological changes include cell loss in the cortex, cerebellum and *substantia nigra*. Moreover the presence of large numbers of neurofibrillary tangles throughout the temporal lobe was observed. These tangles are morphologically and ultrastructurally similar to those in Alzheimer's disease (AD). Although earlier reports on DP stressed the relative absence of senile plaques, a recent study using a sensitive immunohistochemical method has revealed many diffuse plaque-like lesions in this disease [2, 36]. Thus, it has been suggested that head injury may be a predisposing factor or environmental trigger for AD [35].

Address for correspondence: Wanda Gordon-Krajcer, PhD
Department of Neurochemistry, Medical Research Centre,
Polish Academy of Sciences,
ul. Pawińskiego 5, 02–106 Warszawa, Poland
tel/fax: (+48 22) 668 54 23, tel: (+48 22) 608 64 95

Although accumulation of β-amyloid protein (βA), β-amyloid precursor protein (β-APP) and appearance of bundles of paired helical filaments (PHF) — the neurofibrillary tangles (NF), were found in AD 100 years ago, little is known about the function of β-APP and the relation between neuronal damage and expression of β-APP in brain. Several investigators have addressed this issue by examining the effect of experimental lesions on β-APP expression in brain. For example, 2–4 days after a focal ischaemia insult, β-APP mRNA selectively increase in rat cortex [1], similar elevations in β-APP mRNA occur in rat cortex 7 days after lesion of the cholinergic projection from the basal forebrain [42]. Kalaria et al. [15], Pluta [32] and Wakita et al. [41] observed enhanced β-APP-immunoreactivity in rat hippocampus after ischaemic injury. Immunocytochemical analyses reveal increased β-APP expression several days following kainate administration, in part due to *de novo* expression in reactive astrocytes [17, 40]. A similar effect has been observed in the rat hippocampus lesioned by ibotenic acid injection [27]. On the other hand the trophic role of β-APP has been demonstrated in experiments on neuronal cultures [3, 28, 37, 43, 48].

Several authors [4, 7, 20, 24] suggested that excitotoxic mechanism could be involved in the pathophysiology of AD, but there is not enough direct evidence to establish the connection. It is conceivable that an excitotoxic process can explain primary degeneration of various types of neurones in AD. During the past few years, a variety of evidence has emerged indicating that the processing of β-APP is regulated by signal transduction pathways. Thus, phorbol esters (activators of protein kinase C) and okadaic acid (inhibitor of protein phosphatases 1 and 2A) increase β-APP metabolism and secretion [5, 6, 8, 11]. Also the first messengers, which activate the phospholipase C/protein kinase C cascade, increase the secretion of β-APP [29]. However, it has to be considered that activation of phospholipase C results not only in the upregulation of protein kinase C (through the formation of diacyglycerol), but also releases calcium from stores in the endoplasmic reticulum (ER) through the action of inositol 1,4,5-trisphosphate (IP_3).

It is known that stimulation of N-methyl-D-aspartate (NMDA) receptors, which induces a massive Ca^{2+} influx to neurones, results in an increase in the neuronal intracellular calcium $[Ca^{2+}]_i$ concentration [9, 21, 39, 44]. In addition, in many brain regions, e.g. in the hippocampus, NMDA-induces mobilisation of intracellular Ca^{2+} stores localised in ER, through the receptors sensitive to ryanodine (RyR) [22]. Increase of $[Ca^{2+}]_i$ triggers a number of calcium-dependent signal transduction pathways initiated by activation of protein kinases, proteases, phospholipases and release of various second messengers and metabolites. This, as well as depletion of Ca^{2+} stores in ER, may influence β-APP expression and metabolism [12, 13, 16, 25, 33, 34, 45, 47]. On the other hand excessive stimulation of excitatory amino acid receptors led to excitotoxic neuronal damage.

The aim of the present work was to characterise changes in the expression of some domains of β-APP in the rat hippocampus *in vivo* after stereotaxic microinjection of NMDA, glutamic acid or AMPA (alpha amino 3-hydroxy-5-methyl isoxazole-4-propionic acid) and to correlate these results with ultrastructural determinants of neuronal injury.

MATERIALS

Animals and preparation of hippocampal samples

Male Wistar rats (200–250 g b. w.) were anaesthetised with urethane (1.25 g/kg of body weight i.p.). During the experiment the rectal temperature of each animal was maintained at 36°C by means of a heating-pad. After stereotaxic microinjection of 1 μl of 1 mM, 2 mM or 5 mM NMDA, 1 mM or 2 mM glutamic acid, and 50 mM AMPA to CA1 of hippocampus, the animals were allowed to recover for: 0 min, 2h, 12h, 24h and 3 days. Stereotaxic co-ordinates of CA1: LR 2.0 mm, AP –4.8 mm and –3.0 mm from the cortex below bregma were established according to the stereotaxic atlas of Paxinos and Watson [30]. The position of the cannules was determined by macroscopic examination of the brain after each experiment. The injection of NMDA, glutamic acid and AMPA in the concentrations used in this study did not result in seizure activity.

A non-competitive NMDA receptor antagonist, *(+)-5-methyl-10,11-dihydro-5H-dibenzocyclohepten-5,10-imine maleate* (MK-801; 1 mg/kg i.p.) was injected intraperitoneally in some rats 30 min before intracerebral injection of NMDA or AMPA. Immediately after decapitation the rat brains were dissected on ice. Hippocampal CA1 regions and frontal brain cortex were isolated. An equal number of control animals received sham procedure (microinjection of PBS).

Antibodies raised against synthetic peptides corresponding to the amino acid residues of β-APP were used:

— mAb 2B8 against N-terminal domain of β-APP (98–116 aa) (1:1000); from "Sentek" Meryland, MO, USA;

— mAb 6E10 recognising (1–17 aa residues of βA) (597–613 aa) (1:1000) gift from Prof. Henry Wiśniewski, IBR, Staten Island, NY, USA;

— pAb against C-terminal domain of β-APP (643–695 aa) (1:1000) gift from Prof. Henry Wiśniewski, IBR, Staten Island, NY, USA;

— pAb against amyloid βA (1–40 aa residues of βA) (1:100) from Boehringer-Mannheim;

— mAb 468 recognising (17–24 aa residues of βA, 613–620 aa) gift from Prof. Henry Wiśniewski, IBR, Staten Island, NY, USA;

— pAb RAS 57 against C-terminal domain of β-APP (672–695 aa) (1:1000), gift from Prof. Henry Wiśniewski, IBR, Staten Island, NY, USA.

β-APP immunochemistry

β-APP immunoreactivity was determined by Western blotting. Briefly, aliquots of brain tissue homogenate containing approximately 40 μg protein were electrophoresed on tricine — SDS-polyacrylamide gels using 4% T 3% C stacking gel 10% T 3% C separating gel system for βA immunodetection [38] or on linear SDS-PAGE gels — 10% polyacrylamide for β-APP immunodetection [19]. Following the electrophoresis, proteins were transferred to nitrocellulose membrane and treated with anti-β-APP antibodies raised against synthetic peptides corresponding to various domains of β-APP (see above) followed by incubation with an appropriate secondary antibody. ECL Western Blotting Detection Reagent Kit (Amersham, UK) and Alkaline Phosphatase Conjugate Substrate Kit (Bio-Rad, USA) were used to visualise primary antibody complexes with β-APP. Immunoreactivity quantitation was performed by densitometric scanning with a model Ultra-Scan XL laser densitometer (Pharmacia LKB Biotechnology, Uppsala, Sweden).

Electron microscopy

The animals after experiments were sacrificed by transcardiac perfusion with 2.5 percent solution of glutaraldehyde in 0.1 M cacodylate buffer, pH 7.4. Blocks of brain tissue containing CA1 sector, hippocampus and cerebral cortex were fixed for 2 h in 2.5 percent of glutaraldehyde solution, washed in 0.1 M cacodylate buffer and than postfixed in 2.0 percent osmium tetroxide in cacodylate buffer. The sections were dehydrated in a routine way in ethanol solutions, transferred to propylene oxide, and finally embedded in Epon-812. Ultrathin sections were counterstained with uranyl acetate and lead citrate and examined in JEOL 1200 EX electron microscope.

Ultracytochemistry

Cytochemical Ca^{2+}-localisation was performed by the phosphate pyroantimonate method [23]. The animals were perfused through the heart with 90 mM potassium oxalate in 1.9% sucrose adjusted to pH 7.4 with KOH, at 37 °C for 2 min, followed by 3% glutaraldehyde, 0.5% paraformaldehyde, 90 mM potassium oxalate, 1.9% sucrose (pH 7.4) for 1 h at a constant perfusion rate. At the end of the perfusion, hippocampus and cerebral cortex were removed and incubated in the same fixative solution at 4 °C for 2 h. Next, the samples were soaked in 90 mM potassium oxalate in 1.9% sucrose, pH 7.4, postfixed in 1% osmium tetroxide and 2% potassium pyroantimonate for 2 h at room temperature. Unreacted potassium pyroantimonate was washed out by rinsing the tissue for 15 min in water adjusted to pH 10 with KOH. Subsequently the samples were dehydrated in alcohol and embedded in Epon 812. Ultrathin sections were prepared on LKB Nova ultratome, stained with uranyl acetate and lead citrate to enhance contrast and examined with JEOL 1200 EX electron microscope.

The specificity of the oxalate-pyroantimonate reaction in our hands was previously tested by immersion of sections in a solution containing 10 mM of the calcium chelator ethylene glycol-bis-(β-aminoethyl)-N,N'-tetraacetic acid (EGTA). EGTA treatment, in turn, was controlled by incubation of sections for 1h at 60 °C in distilled water.

RESULTS

Biochemical study

Our immunochemical analysis showed three labelled species of β-APP in the rat brain. The major species has a molecular mass of 110 kDa and the two minor species have molecular masses of 130 and 95 kDa. The anti β-APP proteins showed a similar pattern in homogenates of the CA1 and of the cortex, although much less immunoreactivity could be detected in cortex.

In homogenates of the rat CA1 sector of the hippocampus and of the cortex, collected 2 hrs after 1 mM, 2 mM or 5 mM NMDA or 1 mM or 2 mM glutamic acid injection, we did not detect any significant changes in immunoreactivities with antibodies specific to different domains of β-APP compared to those in sham-treated rats. The increased immunoreactivity with antibody against the extracellular N-terminal domains (98–116 amino acid) of β-APP in CA1 and cortex was observed 12 hrs after 5 mM NMDA application. This moderate enhancement of the immunoreactivity remained during the next 3 days of recovery (Fig. 1). The immunoreactivity of β-APP in CA1 increased twofold within 12 hrs, threefold ($p < 0.05$) within 24 hrs and 4.5 fold ($p < 0.05$) within 3 days after 5 mM NMDA injection compared with sham operated animals.

The immunoreaction with antibody against C-terminal domain of β-APP was less pronounced than with antibody against domains representing the extracellular part of the peptide (Fig. 2). A peak of immunoreactivity of the C-terminal forms of β-APP was seen at 12 hrs, where the immunoreactivity was

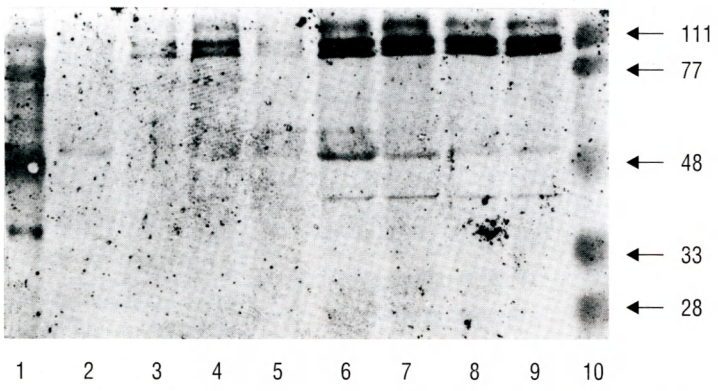

Figure 1. Western blot analysis of the rat brain CA1 hippocampus homogenates after 5 mM NMDA injection stained with mAb against N-terminal domain of β-APP (98–116 aa). Lane: 1, 10 — standards; 2 — 0 min after injection; 3 — 2 h after injection; 4 — 24 h after injection; 5 — 12 h after injection; 6–9 — 3 days after injection.

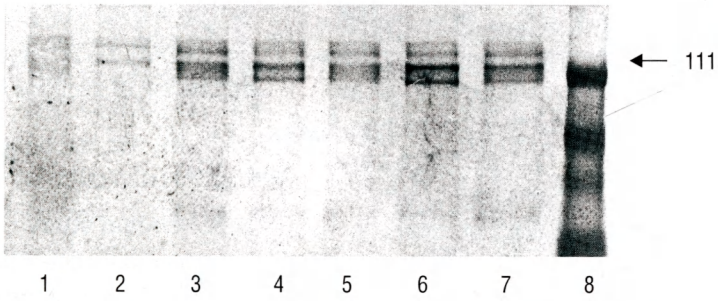

Figure 2. Western blot analyses of the rat brain CA1 hippocampus homogenates after 5 mM NMDA injection stained with pAbs (RAS 57) against carboxyl-terminal domain of β-APP (672–695 aa). Lane: 1 — 0 min after injection; 2 — 2 h after injection; 3 — 12 h after injection; 4 — 24 h after injection; 5 — 24 h after injection; 6 — 3 days after injection; 7 — 3 days after injection; 8 — standards.

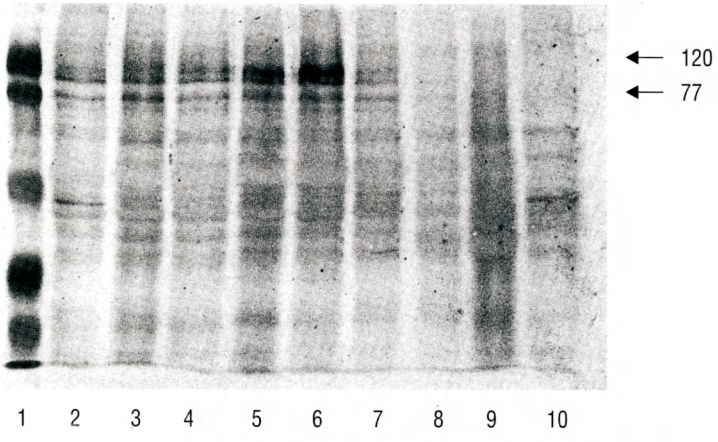

Figure 3. Western blot analyses of β-APP domains of CA1 hippocampus homogenates after 5 mM NMDA or 2 mM glutamic acid injection. Homogenates stained with mAb against β-APP (643-695 aa). Lane: 1 — prestained standards; 2 — 2 h after 5 mM NMDA injection; 3 — 12 h after 5 mM NMDA injection; 4 — 24 h after 5 mM NMDA injection; 5 — 3 days after 5 mM NMDA injection; 6 — 3 days after 2 mM glutamic acid injection; 7 — 24 h after 2 mM glutamic acid injection; 8 — 12 h after 2 mM glutamic acid injection; 9 — 2 h after 2 mM glutamic acid injection; 10 — 0 h after 2 mM glutamic acid injection.

enhanced twofold ($p < 0.05$) compared with sham operated controls. These changes were more evident after NMDA than after glutamic acid application (Fig. 3).

Similar results to those observed with antibody against C-terminal domain of β-APP were obtained with mAb 6E10 specific to transmembrane epitopes

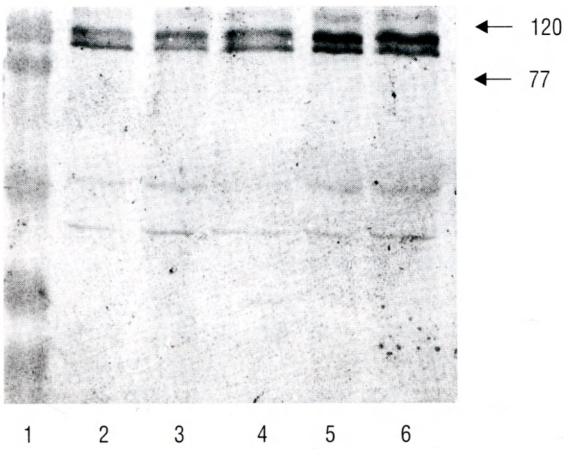

Figure 4. Western blot analysis of the rat brain CA1 hippocampus homogenates after 5 mM NMDA injection stained with mAb 6E10 against transmembrane domain of β-APP (597–613 aa). Lane: 1 – standards; 2 – 0 min after injection; 3 – 2 h after injection; 4 – 12 h after injection; 5 – 24 h after injection; 6 – 3 days after injection.

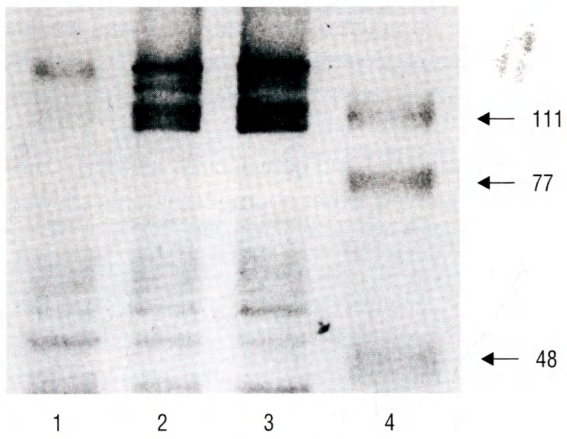

Figure 5. Western blot of the rat brain CA1 hippocampus homogenates 3 days after 5 mM NMDA injection and MK-801 prevention stained with pAb RAS 57 (672–695 aa). Lane: 1 – 3 days after NMDA injection and MK-801 application before experiment; 2 – 24 h after NMDA injection; 3 – 3 days after NMDA injection; 4 – standards.

of β-APP (597–613 amino acid). This immunoreaction increased twofold ($p < 0.05$) after 24 hrs and enhanced 2.5 fold ($p < 0.01$) 3 days after 5 mM NMDA (Fig. 4). To detect more precisely the role of glutamatergic receptors in modulation of β-APP expression, a non-competitive antagonist of NMDA receptor MK-801 was injected intraperitoneally 30 min before microinjection of NMDA. This treatment prevented β-APP expression in the hippocampus (Fig. 5), and in the cortex.

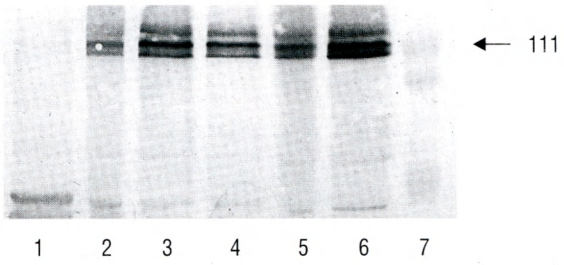

Figure 6. Western blot of β-APP in homogenates of CA1 hippocampus after 50 mM AMPA injection. Immunoreaction with mAb 6E10 (597–613 aa). Lane: 1 – sham control; 2 – 2 h after 50 mM AMPA injection; 3 –12 h after 50 mM AMPA injection; 4 – 24 h after 50 mM AMPA injection; 5 – 24 h after 50 mM AMPA injection; 6 – 3 days after 50 mM AMPA injection; 7 – prestained standard.

Injection of 50 mM AMPA to the CA1 of the hippocampus resulted in significant increase of the immunoreactivity for N-terminal and C-terminal epitopes of β-APP in the hippocampus (Fig. 6) and in the cortex. These immunofractions were enhanced twofold ($p < 0.01$) already 2 hr after AMPA. Its threefold ($p < 0.05$) increase was observed after 12 hrs and 24 hrs. After 3 days the signal of immunoreaction was maximal and increased fivefold ($p < 0.05$) compared to sham control animals. Pretreatment of the rats with MK-801 prevented AMPA-evoked changes in β-APP immunoreactivity in the hippocampus and cortex.

In all experimental groups immunoreactivity in homogenates with CA1 sector of the hippocampus and of the cortex were analysed with antibody 4G8 against βA protein epitop (669–676 aa). In none of these experiments was immunoreactivity detected.

Ultrastructural studies

After stereotaxic administration of saline into CA1 region of the hippocampus all types of neurones in CA1 region of the hippocampus were ultrastructurally normal. The astrocytes, glial elements and blood vessels showed also normal ultrastructure (Fig. 7).

Already 30 min after stereotaxic administration of NMDA marked changes in the ultrastructure of the neurones, glia, synapses and blood vessels were seen in the CA1. Abnormal neurones with clear cytoplasm, containing swollen polymorphic mitochondria, abundant cytoskeleton and, sporadically, bundles of short fibrils, were present. Some neurones showed dense cytoplasm and swollen mitochondria – so-called "dark" neurones (Fig. 8). Many astrocytes, especially in the perivascular region, showed different degrees of oedema (Fig. 9).

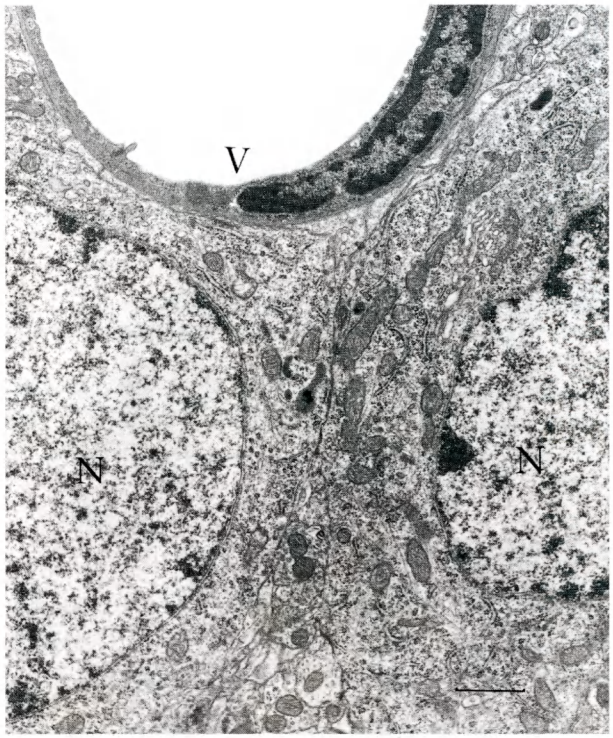

Figure 7. CA1. Control animal after stereotaxic administration of saline. Fragments of CA1 region of hippocampus with two pyramidal neurones (N), blood vessel (V) and neuropil ultrastructurally unchanged. Bar — 1 μm.

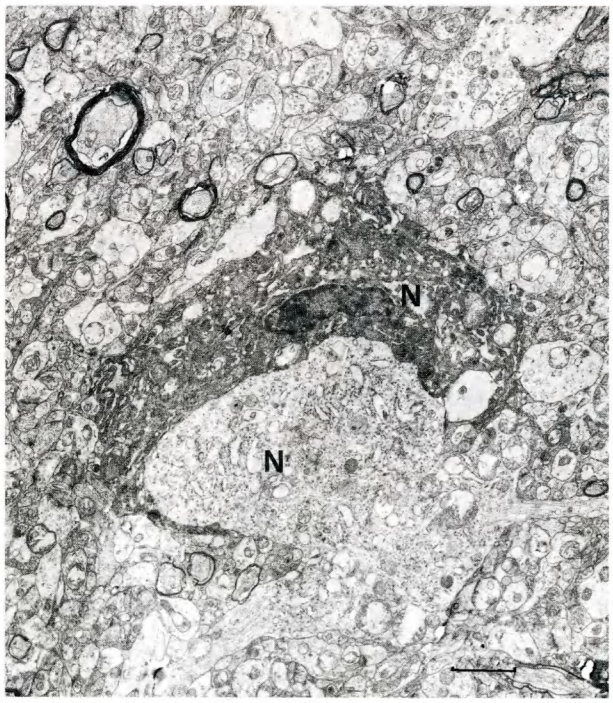

Figure 8. CA1 — 30 min after stereotaxic administration of NMDA. Note two ultrastructurally abnormal neurones (N), one with dense cytoplasm and swollen mitochondria, so-called "dark" neurone, the other with light cytoplasm containing swollen mitochondria and abundant cytoskeleton. Bar = 2 μm.

Ultrastructural abnormalities observed in the CA1 24 h after stereotaxic administration of NMDA encompassed an increased number of "dark" neurones and of the neurones with abundant cytoskeleton. In the distal part of axons, at the level of synapses, accumulation of bundles of neurofilaments was present in the synaptoplasma between synaptic vesicles (Fig. 10). The perivascular astrocytes were swollen. Other elements of the neuropil were ultrastructurally normal.

Histochemical studies employing the oxalate-pyroantimonate method for Ca^{2+} identification showed reaction product in mitochondria and cytoplasm of all swollen astrocytes. In neurones that showed abnormal ultrastructure with abundant cytoskeleton, the product of histochemical reaction was present in the mitochondria (Fig. 11).

Pretreatment of the rats with MK-801 presented ultrastructural alterations in hippocampus and cerebral cortex observed 24 h after stereotaxic administration of NMDA. No Ca^{2+} was seen in the neurones, astrocytes or other cellular elements of this region of the brain. The administration of MK-801 was weekly protective in neuropil of the hippocampal CA1 region. The frequencies of "dark" neurones or the neurones with electron lucent cytoplasm were lower. A small oedema of astrocytes and perivascular astrocytic processes was observed. Other neuropil elements showed normal ultrastructure.

Three days after stereotaxic administration of NMDA many neurones exhibited ultrastructural features of the activation of Golgi apparatus, in the vicinity of which numerous lysosomes were found. Lysosome-like or multivesicular (MV) bodies were present. Those neurones had a well-developed cytoskeleton. Abnormal accumulation of bundles of neurofilaments was observed. Sporadically, "dark" neurones were also encountered. The astrocytes, especially in the perivascular region, were swollen. The majority of synapses were normal (Fig. 12).

Histochemistry revealed the presence of Ca^{2+} in the ultrastructurally changed astrocytes. The reaction product was localised in the mitochondria as electron-dense granules in electron-dense mitochondrial matrix. Some ultrastructurally altered neurones with abundant cytoskeleton also contained the product of the histochemical reaction (Fig. 12, 13).

Seven days after stereotaxic administration of NMDA the ultrastructural changes in the CA1 observed in this group were similar to those seen after 3 days, but were less pronounced. The presence of Ca^{2+} in some mitochondria with electron-dense matrix was seen. In contrast to the group which was treated only

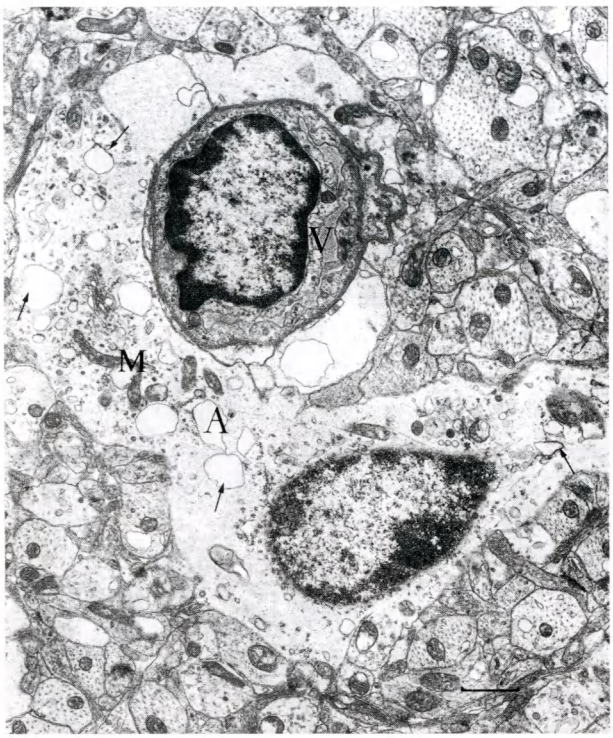

Figure 9. CA1 – 30 min after stereotaxic administration of NMDA. Swollen astrocyte (A) and astrocytic processes around blood vessel (V). Note swelling mitochondria (M) and dilation of some endoplasmic reticulum channels (arrows). Bar = 1 μm.

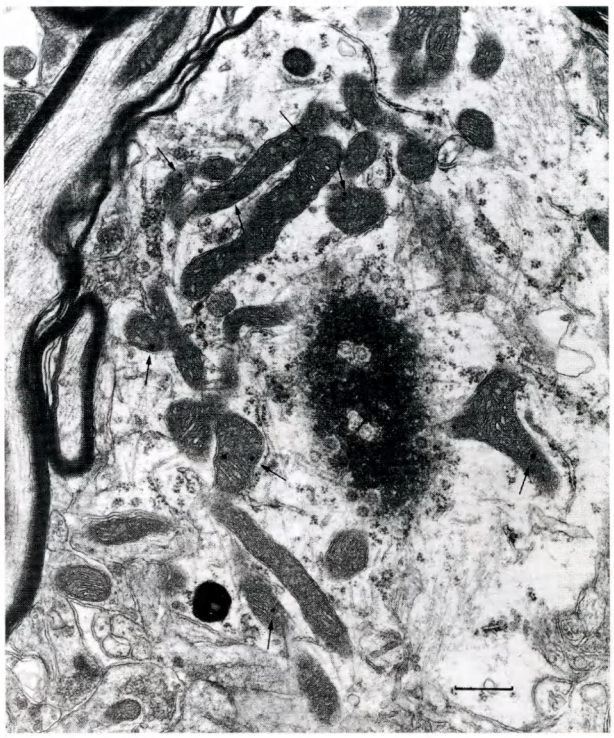

Figure 11. CA1 – 24 h after stereotaxic administration of NMDA. Identification of Ca^{++}. Note product reaction in mitochondria of the neurone with abnormal, abundant cytoskeleton. Bar = 500 nm.

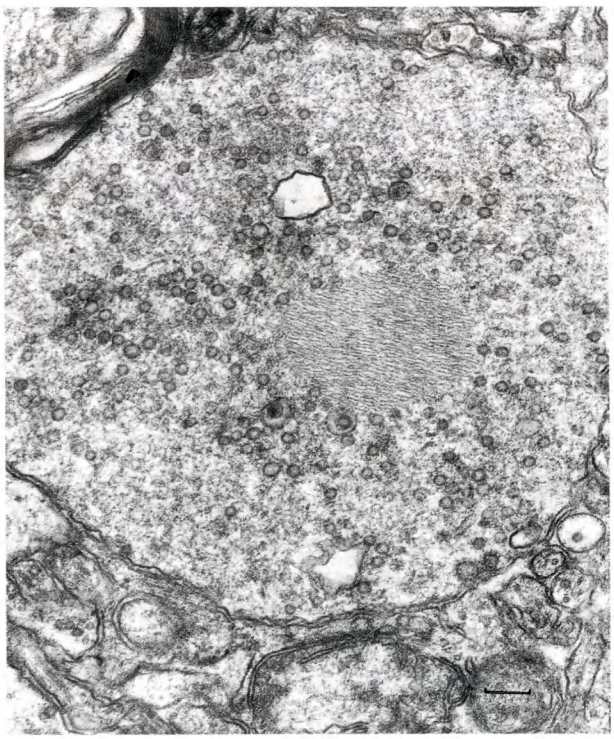

Figure 10. CA1 – 24 h after stereotaxic administration of NMDA. Note accumulation of neurofilaments in synaptoplasma between synaptic vesicles. Bar = 200 nm.

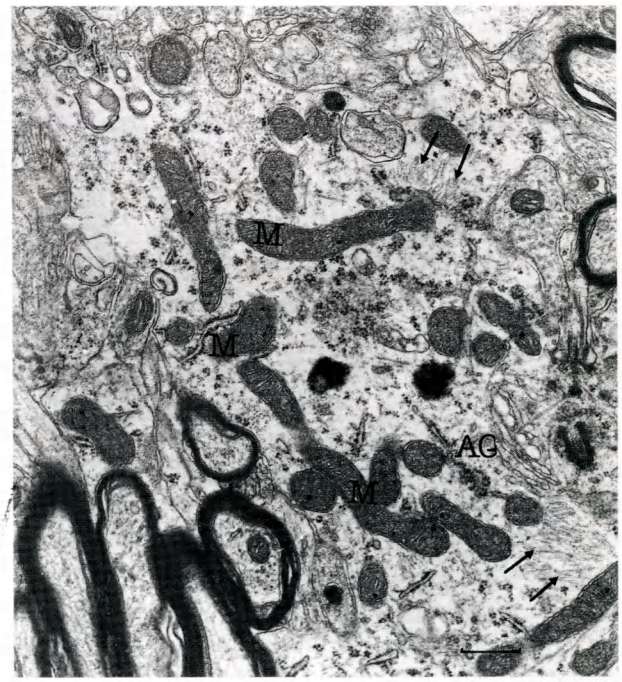

Figure 12. The neurone with activated Golgi apparatus (AG), with numerous lysosomes and lysosome-like bodies and well-developed cytoskeleton with bundles of neurofilaments (arrows). Note electron dense granules as a product reaction in mitochondria. Bar = 500 nm.

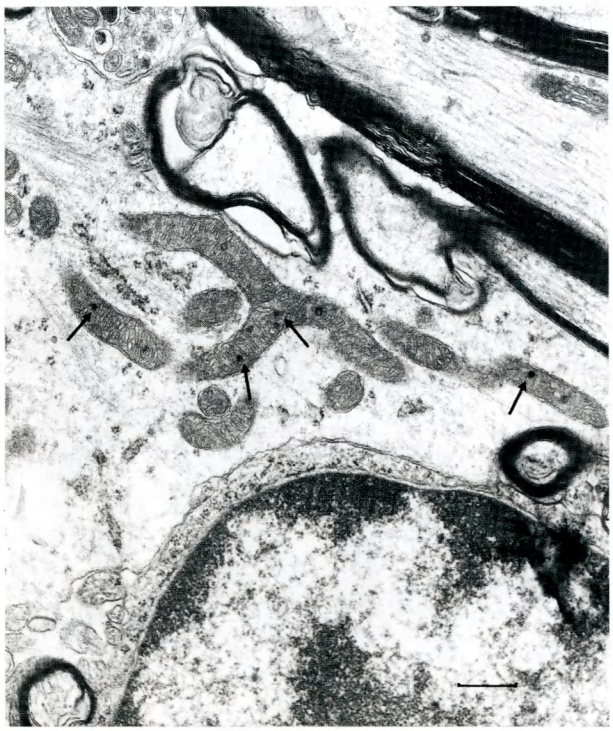

Figure 13. CA1 3 days after stereotaxic administration of NMDA. Identification of Ca^{++}. Mild swollen astrocyte with cytochemical product in electron-dense matrix of mitochondria (arrows). Bar = 500 nm.

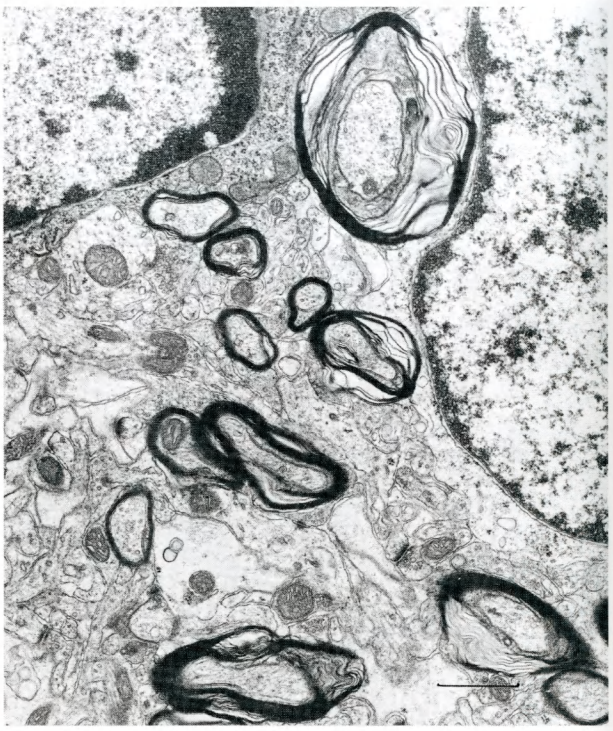

Figure 14. Cerebral cortex 24 h after stereotaxic administration of AMPA. Note a disintegration of myelin lamina arrangement dominated in nerve fibres. Bar = 1 μm.

with NMDA only a few neurones in the CA1 showed ultrastructural abnormalities 7 days after stereotaxic administration of NMDA preceded by i.p. injection of MK-801. Sporadically, swollen mitochondria were seen. Other subcellular elements were normal, but accumulation of synaptic vesicles was seen in swollen synapses. Oedema of perivascular astrocytes was present in a few blood vessels. "Dark" neurones were encountered sporadically.

Twenty-four hours after stereotaxic administration of AMPA into hippocampal CA1 region no ultrastructural changes were identified in the neurones or synapses of the CA1 hippocampal region. Glial and vascular elements were not altered, either. Histochemical studies for Ca^{2+} were negative in both hippocampus and cerebral cortex. However, the cerebral cortex contained astrocytes loaded with glycogen. After injection of AMPA, ultrastructural abnormalities were noted in many myelinated axonal fibres of cerebral cortex. A disintegration of myelin lamina arrangement dominated in the nerve fibres. Nevertheless, well-preserved myelinated and non-myelinated fibres were also observed (Fig. 14).

DISCUSSION

Results of this study demonstrated important differences between the pattern, intensity and cortical or hippocampal localisation of pathological ultrastructural changes in the rat brain, evoked by microinjections of NMDA and AMPA to the CA1 sector of the rat hippocampus. Both NMDA and AMPA induced remote tissue injury in the cortex, whereas only NMDA evoked morphological sings of some neuronal damage and oedema of glial cells, at the injection site. Immunochemical analysis of NMDA- and AMPA-induced changes in β-APP immunoreactivity indicates that both agonists of ionotropic excitatory amino acid receptors upregulate the expression of β-APP in the hippocampus and cortex without symptoms of its amyloidogenic processing. Thus, we did not find a relation between excitotoxic neuronal damage and expression of β-APP or amyloidogenesis.

In this electron microscopic study we observed distinct morphological and histochemical abnormalities in CA1 region of the hippocampus and of the cerebral cortex after injection of NMDA and AMPA. Clearly, morphological and biochemical changes evoked by NMDA and AMPA microinjection to the hippocampus, observed in

the CA1 sector of this structure, should be attributed to the direct effects of overstimulation of the NMDA and AMPA receptors by the injected agonists. On the contrary, remote changes in the brain cortex result most probably from the indirect excitation of the cortical neurones. The magnitude and localisation of changes after NMDA application were different than after AMPA. We observed ultrastructural changes in neurones and their axons, namely so-called "dark" neurones with dense cytoplasm and swollen mitochondria and neurones with light cytoplasm containing abundant cytoskeleton and also swollen mitochondria. Apart from mitochondrial changes, the other striking finding was accumulation of neurofilaments (NFs) in cytoplasm and axons of some neurones.

Although the role of NFs in the nervous system is not yet completely understood, several recent observations support the hypothesis that NFs are critically important in maintaining the structural integrity of neurones and their processes [46]. Therefore, altered neurones and axons with accumulation of neurofilaments appear to reflect degenerative changes that are a component of the toxicity process of NMDA. The presence of "dark" neurones in our experimental material indicates no resistant neurones to excitotoxic neuronal death mediated by glutamate or NMDA, described earlier by Dawson et al. [10]. In spite of many studies, a phenomenon of the occurrence of "dark" neurones in the brain still remains unclear. We can suppose that they represent phases of cell death. Another author drew attention to the probable contribution of "dark" neurones in apoptosis [14].

NMDA-induced changes concern not only neurones but also glial cells. In an early period after injection perivascular oedema and cerebral macrophages containing phagolysosomes were present. Prominent morphological and cytochemical changes were observed in neuronal and glial mitochondria. In many ultrastructurally changed neurones and glial cells, accumulation of calcium [Ca^{++}] was exclusively confined to mitochondria. Here, we did not find any major differences between cortical and hippocampal mitochondria. Numerous mitochondria demonstrated swelling or NMDA-induced calcium accumulation. Under control conditions mitochondria contained only a few calcium deposits using oxalate – pyroantimonate staining with electron microscopy. We observed that mitochondrial calcium sequestration correlated with ultrastructural signs of cellular damage. The mitochondrial sequestration system is able to inactivate substantial amounts of calcium ions but once the mitochondrial respiratory capacity is overrun, oxidative phosphorylation is inhibited and cellular energy state breaks down [26, 31].

In a parallel set of experiments we investigated the influence of AMPA injection into CA1 of the hippocampus on the ultrastructure of the cerebral cortex and the hippocampus. We observed the changes only in the cerebral cortex but not in the hippocampus. The striking finding was accumulation of glycogen in astroglial processes and unusual arrangement of myelin sheaths. In spite of relatively high doses of AMPA injected to the hippocampus the magnitude of changes after AMPA was lower than after NMDA. Since transynaptic propagation of the hippocampal hiperexcitation evoked by AMPA seems to be responsible for pathological changes in the cortex, their local mechanism may be common for NMDA and AMPA and depend on excessive release of glutamate from the presynaptic terminals and overstimulation of all types of postsynaptic glutamate receptors. In this case intensity of the cortical changes may be dependent on the level of hippocampal excitation. It is known that AMPA is less toxic to neurones than NMDA and usually requires a much longer agonist exposure to induce lethal excitotoxic changes [18].

Our study demonstrated that injections of NMDA to CA1 of hippocampus resulted in the increased expression of N-terminal and C-terminal fragments of β-APP and of the transmembrane epitope of βA (597–613 aa) in the CA1 and cortex, although immunoreaction in the cortex was much less intensive. The increase of immunoreactivity was dependent on NMDA concentration and sensitive to inhibition by MK-801, an antagonist of NMDA receptors. This suggests the primary role of NMDA receptor in regulation of β-APP expression.

β-APP immunoreactivity was also markedly enhanced in the cortex and hippocampus after AMPA injection to the hippocampus. Antibodies to different domains of β-APP gave comparable results for AMPA and NMDA, however antibodies towards the carboxyl-terminus of APP were more reactive after AMPA than NMDA injection. Interestingly, these effects were sensitive to systemic MK-801 administration, indicating that in both structures indirect activation of the NMDA receptors participates in the induction of β-APP.

Comparative analysis of the results indicates that our morphological changes were parallel with biochemical findings. After stereotaxic injection of NMDA to the hippocampus the ultrastructural neuronal changes in the hippocampus and cortex (injury of neurones leading to their degeneration and loss) were observed. These changes were accompanied by enhancement of the expression of β-APP in the hippocampus and cortex.

On the other hand, after AMPA injection overexpression of β-APP was also detected in these structures, whereas ultrastructural changes were found only in the cortex. Thus, there is a clear discrepancy between the extent and location of neuronal damage and β-APP hyperexpression. Our results did not provide any data suggesting relation between neurodegeneration and enhanced expression of β-APP. Moreover antibody 4G8 against βA protein epitop (669–676 aa) did not detect free βA in the cortex and hippocampus, which indicates that β-APP was not processed into βA protein, in spite of extensive excitotoxicity and even neurodegeneration. Thus, it seems that overexpression of β-APP observed after microinjection of excitotoxins may be rather attributed to compensatory mechanisms induced by NMDA- and AMPA-evoked overexcitation. In fact, neurotrophic properties of β-APP were demonstrated in recent *in vitro* studies.

To conclude, the results of this study demonstrate that excessive stimulation of ionotropic excitatory amino acid receptors NMDA and AMPA in the rat hippocampus enhances the expression of β-APP in the hippocampus and cerebral cortex, without symptoms of amyloidogenesis. Since excitotoxic neuronal damage was observed only after NMDA application, but not after AMPA receptor stimulation, in this experimental model in the rat brain there is no relation between excitotoxic neurodegeneration and hyperexpression or amyloidogenic processing of β-APP.

ACKNOWLEDGEMENTS

We thank Prof. Jerzy Łazarewicz and Dr Stanisław Chrapusta for helpful comments and discussion of this manuscript. This study was supported by the Polish State Committee for Scientific Research grant No 4.P05A.059.08.

REFERENCES

1. Abe K, Tanzi RE, Kogure K (1991) Selective induction of Kunitz-type protease inhibitor domain-containing amyloid precursor protein mRNA after persistent focal ischemia in rat cerebral cortex. Neurosci. Lett, 125: 172–174.
2. Allsop D, Haga S, Bruton C, Ishii T, Roberts GW (1990) Neurofibrillary tangles in some cases of dementia pugilistica share antigens with amyloid β-protein of Alzheimer's disease. Am J Pathol, 136: 255–260.
3. Araki W, Kitaguchi N, Tokushima Y, Ishii K, Aratake H, Shimohama S, Nakamura S, Kimura J (1991) Trophic effect of β-amyloid precursor protein on cerebral cortical neurons in culture. Biochem Biophys Res Commun, 181: 265–271.
4. Busciglio J, Gabuzda D, Yankner BA (1989) Inhibition of beta amyloid production by activation of protein kinase C. Soc Neurosci, 19: 1276 Abst.
5. Buxbaum JD, Gandy S, Cicchetti P, Ehrlich ME, Czernik AJ, Fracasso RP, Ramabhadran TV, Unterbeck AJ, Grenngard P (1990) Processing of Alzheimer beta-A4 amyloid precursor protein-modulation by agents that regulate protein phosphorylation. Proc Natl Acad Sci USA, 87: 6003–6006.
6. Buxbaum JD, Oishi M, Chen HJ, Pinkas-Kramarski KR, Jaffe EA, Gandy SL, Greengard P (1992) Cholinergic agonists and interleukin 1 regulate processing and secretion of the Alzheimer β/A4 amyloid precursor protein. Proc Natl Acad Sci USA, 89: 10075–10078.
7. Buxbaum JD, Ruefli AA, Parker CA, Cypess AM, Greengard P (1994) Calcium regulates processing of the Alzheimer amyloid protein precursor in a protein kinase C — independent manner. Proc Natl Acad Sci USA, 91: 4489–4493.
8. Caporaso GL, Gandy SE, Buxbaum JD, Ramabhadran TV, Greengard P (1992) Protein phosphorylation regulates secretion of Alzheimer β/A4 amyloid protein. Proc Natl Acad Sci USA, 89: 3055–3059.
9. Choi DW (1988) Calcium-mediated neurotoxicity: relationship to specific channel types and role in ischemic damage. Trends Neurosci, 11: 465–469.
10. Dawson VL, Dawson TM, Bartley DA, Uhl GR, Synder SH (1993) Mechanism of nitric oxide-mediated neurotoxicity in primary brain cultures. J Neurosci, 13: 2651–2661.
11. Gillespie SL, Golde TE, Younkin SG (1992) Secretory processing of the Alzheimer amyloid β/A4 protein precursor is increased by protein phosphorylation. Biochem Biophys Res Commun, 187: 1285–1290.
12. Guo Q, Furukawa K, Sopher BL, Pham DG, Xie J, Robinson N, Martin GM, Mattson MP (1996) Alzheimer's PS-1 mutation perturbs calcium homeostasis and sensitizes PC 12 cells to death induced by amyloid β-peptide. Neuroreport, 8: 379–383.
13. Guo Q, Sopher BL, Pham DD, Furukawa K, Robinson N, Martin GM, Mattson MP (1997) Alzheimer's presenilin mutation sensitizes neural cells to apoptosis induced by trophic factor withdrawal and amyloid β-peptide: involvement of calcium and oxyradicals. J Neurosci, 17: 4212–4222.
14. Iwanowski L (1988) Apoptosis and dark neurons. Neuropatol Pol, 26: 573–579.
15. Kalaria RN, Bhatti SU, Palatinsky EA, Pennington DH, Shelton ER, Chan HW, Perry G, Lust WD (1993) Accumulation of the β-amyloid precursor protein at sites of ischemic injury in rat brain. Neuroreport, 4: 211–214.
16. Katayama T, Imaizumi K, Sato N, Miyoshi K, Kudo T, Hitomi J, Morihara T, Yoneda T, Gomi F, Mori Y, Nakano J, Takeda J, Tsuda T, Itoyama Y, Murayama O, Takashima A, St. George-Hyslop P, Takeda M, Tohyama M (1999) Presenilin-1 mutations downregulate the signalling pathway of the unfolded protein response. Nature Cell Biol, 1: 479–485.
17. Kawarabayashi T, Shoji M, Harigaya M, Yamaguchi H, Hirai S (1991) Expression of APP in the early stage of brain damage. Brain Res, 563: 334–338.
18. Koh JY, Goldberg MP, Hartley DM, Chi DW (1990) Non-NMDA receptor mediated neurotoxicity in cortical culture. J Neurosci, 10: 693–705.
19. Laemmli UK (1970) Cleavage of structural proteins during the assembly of the head of bacteriophage T4. Nature, 227: 680–685.
20. Lee R, Wurtman RJ (1997) Metabotropic glutamate receptors increase amyloid precursors protein processing in astrocytes: inhibition by cyclic AMP. J Neurochem, 68: 1830–1835.

21. Łazarewicz JW, Hagberg H, Hamberger A (1986) Extracellular calcium in the hippocampus of unanesthetized rabbits monitored with dialysis-perfusion. J Neurosci Meth, 15: 317–328.
22. Łazarewicz JW, Rybkowski W, Sadowski M, Ziembowicz A, Alaraj M, Wegiel J, Wisniewski HM (1998) N-methyl-D-aspartate receptor-mediated, calcium-induced calcium release in rat dentate gyrus/CA4 in vivo. J Neurosci Res, 51: 76–84.
23. Mata M, Staple J, Fink DJ (1987) Ultrastructural distribution of Ca^{++} within neurons. An oxalate pyroantimonate study. Histochemistry, 87: 339–349.
24. Mattson MP, Cheng B, Davis D, Bryant K, Lieberburg I, Rydel RE (1992) β-Amyloid peptides destabilize calcium homeostasis and render human cortical neurons vulnerable to excitotoxicity. J Neurosci, 12: 379–389.
25. Mattson MP, Guo Q, Furukawa K, Pedersen WA (1998) Presenilins, the endoplasmic reticulum and neuronal apoptosis in Alzheimer's disease. J Neurochem, 70: 1–14.
26. Mignotte B, Vayssiere J-L (1998) Mitochondria and apoptosis. Eur J Biochem 252: 1–15
27. Nakamura Y, Takeda M, Niigawa H, Hariguchi S, Nishimura T (1992) Amyloid β-protein precursor deposition in rat hippocampus lesioned by ibotenic acid injection. Neurosci Lett, 136: 95–98.
28. Ninomiya H, Roch JM, Jin LW, Saitoh T (1994) Secreted form of amyloid β/A4 protein precursor (APP) binds to two distinct APP binding sites on rat B103 neuron-like cells through two different domains, but only one site is involved in neurotrophic activity. J Neurochem, 63: 495–500.
29. Nitsch RM, Slack BE, Wurtman RJ, Growdon JH (1992) Release of Alzheimer amyloid precursor derivatives stimulated by activation of muscarinic acetylcholine receptors. Science, 258: 304–307.
30. Paxinos G, Watson C (1982) The rat brain in stereotaxic coordinates. Academic, Sydney.
31. Peachey L D (1964) Electron microscopic observations on the accumulation of divalent cations in intra-mitochondrial granules. J Cell Biol, 20: 95–109.
32. Pluta R (2000) No effect of anti-oxidative therapy on cerebral amyloidosis following ischemia-reperfusion brain injury. Folia Neuropathol, 38, 4:188–190.
33. Pollard HB, Arispe N, Rojas E (1995) Ion channel hypothesis for Alzheimer amyloid peptide neurotoxicity. Cell Mol Neurobiol, 15: 513–526.
34. Querfurth HW, Selkoe DJ (1994) Calcium ionophore increases amyloid β peptide production by cultured cells. Biochemistry, 33: 4550–4561.
35. Roberts GW (1988) Immunocytochemistry of neurofibrillary tangles in dementia pugilistica and Alzheimer's disease: evidence for common genesis. Lancet, 2: 8626/8627: 1456–1457.
36. Roberts GW, Allsop D, Bruton C (1990) The occult aftermath of boxing. J Neurol Neurosurg Psych, 53: 373–378.
37. Roch JM, Masliah E, Roch-Levecq AC, Sundsmo MP, Otero DAC, Veinbergs I, Saitoh T (1994) Increase of synaptic density and memory retention by a peptide representing the trophic domain of the amyloid β/A4 protein precursor. Proc. Natl Acad Sci USA, 91: 7450–7454.
38. Schagger H, von Jagow G (1987) Tricine-sodium dodecyl sulphate-palyacrylamide gel electrophoresis for the separation of protein in the range from 1 to 100 kDa. Anal Biochem, 166: 368–379.
39. Siesjö BK (1988) Historical overview. Calcium, ischemia and death of brain cells. Ann NY Acad Sci, 522: 638–661.
40. Siman R, Card JP, Nelson RB, Davis LG (1989) Expression of beta-amyloid precursor protein in reactive astrocytes following neuronal damage. Neuron, 3: 275–285.
41. Wakita H, Tomimoto H, Akiguchi I, Ohnishi K, Nakamura S, Kimura J (1992) Regional accumulation of amyloid β/A4 protein precursor in the gerbil brain following transient cerebral accumulation. Neurosci Lett, 146: 135–138.
42. Wallece WC, Bragin V, Robakis NK, Sambmurti K, Vanderputten D, Merril CR, Davis KL, Santucci AC, Haroutunian V (1991) Increased biosynthesis of Alzheimer amyloid precursor protein in the cerebral cortex of rats with lesions of the nucleus basalis of Meynert. Mol Brain Res, 10: 173–178.
43. Whitson JS, Selkoe DJ, Cotman W (1989) Amyloid beta protein enhances the survival of hippocampal neurons in vitro. Science, 243: 1488–1490.
44. Wieloch T (1985) Endogenous excitotoxins as possible mediators of ischemic and hypoglycemic brain damage. Epilepsia, 26: 501.
45. Xia W, Zhang J, Perez R, Koo EH, Selkoe DJ (1997) Interaction between amyloid precursor protein and presenilins in mammalian cells: implications for the pathogenesis of Alzheimer's disease. Proc Natl Acad Sci USA, 94: 8208–8213.
46. Xu Z, Dong D L-Y, Cleveland D (1994) Neuronal intermediate filaments: new progress on an old subject. Curr Opin Neurobiol, 4: 655–661.
47. Yang YN, Turner RS, Gant JR (1998) The chaperone PIP/GRP 78 binds to amyloid precursor protein and decreases A-beta-40 and A-beta-42 secretion. J Biol Chem, 273, 25552–25555.
48. Yankner BA, Duffy LK, Kirschner DA (1990) Neurotrophic and neurotoxic effects of amyloid β protein: reversal by tachykinin neuropeptides. Science, 250: 279–282.

Publikacja 2

VIA MEDICA
ORIGINAL ARTICLE
Vol. 40, No. 1, pp. 2–
Copyright © 2002 Via Medica
ISSN 1641–4640

N-methyl-d-aspartate receptor-mediated processing of β-amyloid precursor protein in rat hippocampal slices: *in vitro* — superfusion study

Wanda Gordon-Krajcer, Elżbieta Salińska, Jerzy W. Łazarewicz

Department of Neurochemistry, Medical Research Centre, Polish Academy of Sciences, Warszawa, Poland

Abnormal proteolytic degradation of the β amyloid precursor protein (β-APP) may result in accumulation of potentially neurotoxic β amyloid (βA). The role of various receptors in the regulation of β-APP processing has been suggested. This study aimed to determine how NMDA receptors and Ca^{2+} ions regulate proteolysis of β-APP in rat hippocampus in vitro. Adult rat hippocampal slices were superfused with NMDA-containing media, and immunoreactivity of soluble β-APP derivatives was detected in dialysates. Application of 100 μM and 250 μM NMDA for 20 min in Ca^{2+}-containing medium induced dose-dependent release of amino-terminal β-APP derivatives, and a fragment of Aβ sequence, whereas carboxy-terminal fragments of β-APP were only slightly detected. This indicates activation of β-APP processing, and release of its soluble cleavage products. This effect was inhibited by NMDA receptor antagonist 1 μM MK-801 and 100 μM CPP in Ca^{2+}-free medium, thus indicating that NMDA receptors and calcium ions mediate proteolytic non-amyloidogenic degradation of the β-APP.

key words: NMDA receptors, calcium, β-amyloid precursor protein, α-secretase

INTRODUCTION

In brains of patients with Alzheimer's disease (AD) the amyloid β-protein (βA) is accumulated in the core of senile plaques, which seems to be related to the pathogenic processes of this disease. This protein is a proteolytic derivative of amyloid β-protein precursor (β-APP). Although the expression and metabolism of βA and of β-APP have been intensively studied, their role is still to be clarified. βA has been reported to have neurotrophic as well as neurotoxic effects [25, 26], whereas Koh et al. [12] noticed that βA alone is not neurotoxic to cultured murine cortical neurones, but increases their vulnerability to excitatory amino acids (EAA). Mattson et al. [16] suggested that there is a link between EAA, calcium and amyloid protein in the pathogenesis of AD.

Proteolytic processing of β-APP and the regulatory part of proteases (known as α/β/γ secretases) involved in the process is believed to be crucial to the understanding of AD [1, 4, 10, 20, 21, 24]. Various receptors, particularly cholinergic and interleukin receptors, have been found to play a fundamental role in the regulation of β-APP processing [3, 18, 19].

Several investigators have addressed the question of the functional roles of β-APP by examining the effects of experimental lesions on β-APP expression in brain. Arendash et al. [2] described late occurring pathological changes resembling neuritic plaques and neurofibrillary tangles in various limbic and neocortical regions of rat brain 14 months following kainic acid injection into the basal forebrain. Other reports described elevated

Address for correspondence: Dr Wanda Gordon-Krajcer
Medical Research Centre
ul. Pawińskiego 5, 02-106 Warszawa, Poland
tel: (+48 22) 608 64 95, fax: (+48 22) 668 54 23

expression of β-APP mRNA or protein in brain several days following experimental lesions evoked by ibotenic or kainic acid injection [11, 17]. In conditions of enhanced β-APP expression, its abnormal processing may result in the accumulation of amyloid proteins. The fundamental physiological and pathological role of excitatory amino acid receptors in excitatory synaptic transmission, developmental plasticity, learning and memory formation, but also in neurodegeneration, might suggest the relation between the activation of glutamatergic receptors and the abnormal processing of amyloid precursor protein β-APP.

The aim of this study was to determine if NMDA receptors and Ca^{2+} ions regulate proteolysis of β-APP in superfused rat hippocampal slices in vitro.

MATERIAL AND METHODS

Animals and preparation of hippocampal slices

Male Wistar rats (200–250 g b.w.) anaesthetised with ketamine (85 mg/kg of body weight i.m.) were decapitated. Brains were immediately removed and chilled in cold (4 °C) Krebs-Ringer (K-R) bicarbonate buffer, pH 7.4. Hippocampal slices were prepared in a cold room with McIllwain tissue chopper set on 300 μm thickness and collected into a chilled buffer containing 1 mM ketamine to avoid premature uncontrolled stimulation of NMDA receptors during tissue trauma.

Superfusion

Slices were preincubated for 15 min at 37 °C in continuously oxygenated K-R buffer containing 1.2 mM Ca^{2+}. Then buffer was decanted and slices were placed in chambers of the 6-channel Superfusion 600 system (Brandel, Gaithesburg, MA, USA). Slices were equilibrated by 30-min superfusion at a flow rate of 0.8 ml/min with oxygenated K-R bicarbonate buffer pH 7.4, Mg^{2+}-free, containing 1.2 mM $CaCl_2$ at 37 °C. Then superfusates were collected for 20 min, followed by 20-min pulses of experimental media (see below). After this, standard superfusion conditions were reestablished for 20 min. Experimental media contained: (1) 100 μM NMDA in Krebs-Ringer buffer containing 1.2 mM $CaCl_2$, (2) 250 μM NMDA in Krebs-Ringer buffer containing 1.2 mM $CaCl_2$, (3) 250 μM NMDA in Krebs-Ringer buffer Ca^{2+}-free, (4) 250 μM NMDA in Krebs-Ringer buffer containing 1.2 mM $CaCl_2$ and 1 μM MK-801, (5) 250 μM NMDA in Krebs-Ringer buffer containing 1.2 mM $CaCl_2$ and 100 μM CPP. Control media: (1) Krebs-Ringer buffer containing 1.2 mM $CaCl_2$, (2) Krebs-Ringer buffer Ca^{2+}-free were applied in parallel to corresponding experimental media.

Immunoblot analysis

Aliquots of superfusates collected in 20 min intervals were mixed with phenylmethylsulfonyl fluoride at final concentration of 250 μM. After centrifugation at 10,000 g for 30 min, supernatants were dialysed against water at 4 °C using cellulose dialysis bags, lyophilised, reconstituted in SDS-containing gel loading buffer, and boiled for 5 min. Total protein contents of superfused slices was measured by the method of Lowry et al. [15]. Reconstituted superfusate proteins, equivalent to 500 ug of protein content in corresponding slices, were electrophoresed on linear SDS 12% polyacrylamide gels by the method of Laemmli [13], and electroblotted onto nitrocellulose membranes (Bio-Rad, Richmond, CA). Membranes were blocked with 5% (w/v) non-fat dried milk in TBS and incubated overnight at 4 °C with the following antibodies diluted in TBST: pAb APP (98–116), mAb APP (282–364), mAb APP (597–613) and pAb APP (672–695).

Alkaline phosphatase-labelled goat anti-rabbit IgG 1:3000 (Bio-Rad) or alkaline phosphatase-labeled goat anti-mouse IgG 1:3000 (Bio-Rad) were used as a secondary antibody. Immunoblots were developed with nitro-blue tetrazolium and 5-bromo-4-chloro-3-indolyl phosphate (Bio-Rad, Richmond, CA, USA). The secondary horseradish peroxidase-linked antibodies were visualised by enhanced chemiluminescence (ECL, Amersham).

RESULTS

Superfusates of adult rat hippocampal slices contained immunoreactive material that was detected with the antibodies raised against β-APP (98–116) and (282–364) (Fig. 1, 2) amino acid domains, with apparent molecular masses ranging from 98 kDa to 130 kDa. In agreement with the previous finding of Nitsch et al. [18], the major band migrated at about 120 kDa. Western blot analysis of the same proteins collected in superfusates of hippocampal slices under control and experimental conditions using antibodies against the carboxyl-terminal fragments of β-APP (672–695) indicated only slight immunoreaction. However immunoreactivity of this carboxy-terminal fragment of β-APP was detected in homogenates from rat hippocampal slices. Thus, full-length β-APP is present in adult rat hippocampal slices in vitro, but during incubation they exclusively release the soluble amino-terminal, but not carboxy-terminal β-APP derivatives.

Application of 100 and 250 μM NMDA in a 20-min pulse in Ca^{2+}-containing medium stimulated release of the amino-terminal β-APP derivatives (282–364) in a dose-dependent manner (Fig. 1, lanes G, H, D, E). The

enhanced release of amino-terminal β-APP fragments (282–364), evoked by 250 μM NMDA was prevented by addition of 1 μM MK-801 or 100 μM CPP, which are non-competitive and competitive antagonists of NMDA receptors, respectively (Fig. 2, lanes H, I, J). The release of soluble amino-terminal β-APP cleavage products evoked by application of NMDA in calcium-free K-R buffer was significantly inhibited as compared to the effect of corresponding NMDA concentration given in calcium-containing medium (Fig. 2, lanes C, D, E, F, H). The application of a Ca^{2+}-free K-R superfusion medium without NMDA resulted in a decrease in contents of soluble β-APP fragments in superfusates (Fig. 2, lanes B and G).

Analysis of superfusates of rat hippocampal slices collected during and particularly after application of 100 and 250 μM NMDA in Ca^{2+} containing K-R medium detected appearance of β-APP domain (597–613), which represents amino acid sequence of βA fragment situated at the amino-terminal part of amyloid protein, outside the "secretase" splitting. Immunoreactivity of this material was dependent on NMDA concentration (Fig. 3).

DISCUSSION

The increase in the release of soluble amino-terminal β-APP domains during and after 20-min NMDA stimulation of hippocampal slices *in vitro* certainly reflects accelerated processing of β-APP pre-existing in slices. Within these time limits enhancement of β-APP gene expression may be certainly excluded [18] but in this study we did not address the question of NMDA receptor-mediated increase in β-APP gene expression in brain.

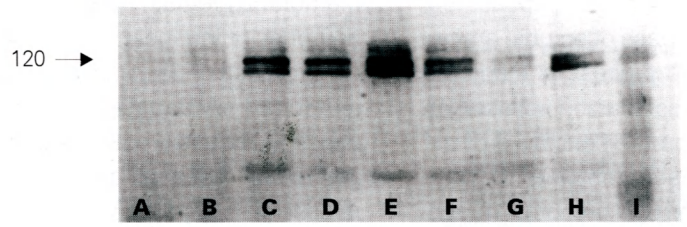

Figure 1. Western blot analyses of b-APP domains in superfusates of rat hippocampal slices before, during and after 20 min pulses of experimental media. Superfusate proteins were electrophoresed stained with mAb against APP (282–364). Control — K-R buffer containing 1.2 mM $CaCl_2$ (lane A). Krebs-Ringer (K-R) buffer containing 1.2 mM $CaCl_2$ — before appropriate pulses (lane B), 100 μM NMDA in K-R buffer containing 1.2 mM $CaCl_2$ during pulse (lane G) and after pulse (lane H), 250 μM NMDA in K-R buffer containing 1.2 mM $CaCl_2$ during pulse (lanes C, D) and after pulse (lane E). Prestained standards used to locate molecular weights (lane I).

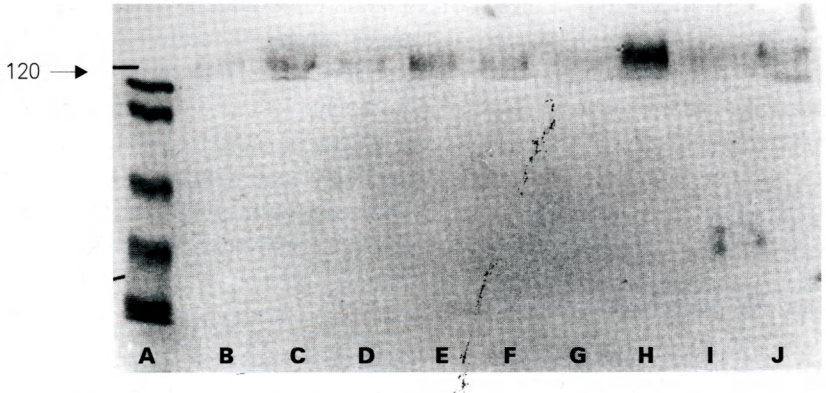

Figure 2. Western blot analyses of b-APP in superfusates of rat hippocampal slices collected during 20-min pulses of experimental media. Monoclonal Ab to N-terminal b-APP (282–364) was used. Prestained standards, were used to locate molecular weights (lane A). Krebs-Ringer buffer (K-R), Ca^{2+}-free (lane B), 250 μM NMDA in Ca^{2+}-free K-R (lanes C, E), 100 μM NMDA in Ca^{2+}-free K-R containing (lane D) and in Ca^{2+}-containing K-R (lane F), K-R buffer containing 1.2. mM $CaCl_2$ (lane G), 250 μM NMDA in K-R buffer containing 1.2 mM $CaCl_2$ (lane H), 250 μM NMDA in K-R buffer containing 1.2 mM $CaCl_2$ and 100 μM CPP (lane I), 250 μM NMDA in K-R buffer containing 1.2 mM $CaCl_2$ and 1 μM MK-801 (lane J).

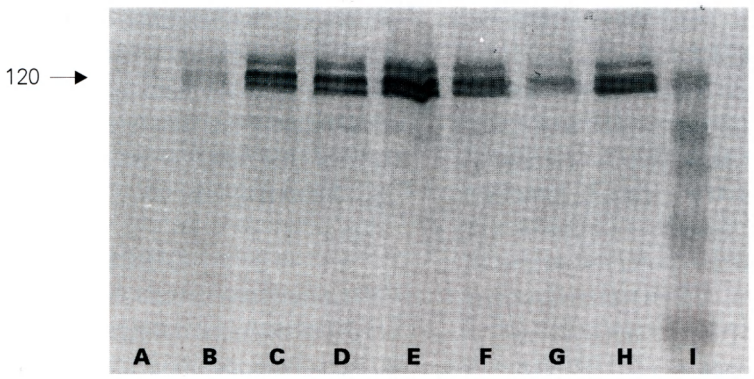

Figure 3. Western blot analysis of β-APP domains in superfusates collected before, during and after 20-min NMDA pulses. Monoclonal Ab against b-APP (597–613) was used. Krebs-Ringer buffer (K-R) containing 1.2 mM $CaCl_2$ before appropriate pulse (lane A), 100 μM NMDA in K-R containing 1.2 mM $CaCl_2$ during pulse (lanes B, G) and after pulse (lanes C, H), 250 μM NMDA in K-R buffer containing 1.2 mM $CaCl_2$ during pulse (lanes D, F) and after pulse (lane E). Prestained standards were used to locate molecular weights (lane I).

This study demonstrates that in the hippocampal slices in vitro NMDA induces release of soluble amino-terminal β-APP fragments. This process is mediated by NMDA receptors. The latter conclusion is based on NMDA dose-dependence and on the sensitivity of the release of β-APP amino-terminal to inhibition by competitive and non-competitive NMDA receptor antagonists. It should be stressed that hippocampal slices were superfused in the absence of Mg^{2+} in the medium. The other feature of this effect is its Ca^{2+} – dependence: our results indicate that Ca^{2+} ions mediate NMDA receptor-dependent regulation of β-APP processing in the hippocampus. These findings extended the previous results of Nitsch et al. [18], who suggested that β-APP degradation evoked by electrical depolarisation of hippocampal slices is mediated by neurotransmitter receptors. However, these authors did not address the question of Ca^{2+} – dependence and discussed their findings exclusively in terms of the involvement of cholinergic stimulation.

The discussion of our results should include the possibility that NMDA receptor-mediated release of β-APP fragments from the rat hippocampal slices reflects non-selective release of cellular proteins evoked by excitotoxic neuronal injury. In fact, increased release of protein to superfusates of slices submitted to NMDA stimulation was noticed. However selective release to superfusates of extracellular amino-terminal domains of β-APP indicates that NMDA in the presence of Ca^{2+} triggers specific proteolytic degradation of the precursor protein. Lack of any traces of carboxy-terminal fragments of β-APP in superfusates indicates that plasma membranes remain intact, which prevents efflux from neurones of intracellular carboxy-terminal fragments.

Exclusion of Ca^{2+} ions from the incubation medium, although instrumental in studies on calcium-dependence of various processes, according to some investigators may result in non-specific cell injury and protein release [14, 18]. This is however a controversial issue. The harmful effects of such media were denied by others, who indicated that extracellular calcium protects neurones from early damage in vitro [7]. In fact we did not observe any increase in the release of β-APP fragments in Ca^{2+}-free media, whereas NMDA-induced release was inhibited in these conditions.

The exact mechanism of proteolytic degradation of β-APP, which is mediated by NMDA receptors and Ca^{2+}, remains to be directly determined. However our data, namely the specific pattern of β-APP fragments released to superfusates, may give preliminary suggestions on the mechanism of β-APP processing. The presence in superfusates of β-APP amino-terminal domains and of the amino acid sequence of βA (597–613), which is characteristic for the amino-terminal part of β-amyloid protein, but the virtual absence of intracellular carboxy-terminal domains, indicates the involvement of "secretase" type of proteolysis, which splits β-APP inside βA molecule [5, 22, 23]. This process, non-amyloidogenic in nature, may be ascribed to the activation of a Ca^{2+} dependent α-secretase known to be located in neuronal pleasure membranes [4, 21]. It is well known that amyloidogenic β-APP degradation leads to release of carboxy-terminal fragments of β-APP, containing intact βA sequence [6, 8, 9].

To sum up, the results of these studies indicate that NMDA receptors modulate the activity of β-APP degradation in the rat hippocampus. Calcium ions are directly involved in mediating NMDA receptor-dependent regulation of protease(s) that process β-APP. This proteolytic degradation of β-APP seems to be non-amyloidogenic.

ACKNOWLEDGEMENTS

This study was supported by the Polish State Committee for Scientific Research grant No 4.P05A.059.08.

REFERENCES

1. Annaert W, De Strooper B (2000) Neuronal models to study amyloid precursor protein expression and processing *in vitro*. Biochim Biophys Acta, 1502: 53–62.
2. Arendash GW, Millard WJ, Dunn AJ, Meyer EM (1987) Long-term neuropathological and neurochemical effects of nucleus basalis lesions in the rat. Science, 238: 952–956.
3. Buxbaum JD, Oishi M, Chen HI, Pinkas-Kramski R, Jaffe EA, Gandy SE, Greengard P (1992) Cholinergic agonists and interleukin 1 regulate processing and secretion of the Alzheimer β/A4 amyloid protein precursor. Proc Natl Acad Sci USA, 89: 10075–10078.
4. Chen M (1997) Alzheimer's α-secretase may be calcium-dependent protease. FEBS Lett, 417: 163–167.
5. Esch FS, Keim PS, Beattie EC, Blacher RW, Culwell AR, Oltersdorf T, McClure D, Ward PJ (1990) Cleavage of amyloid beta peptide during constitutive processing of its precursor. Science, 248: 1122–1124.
6. Estus S, Golde TE, Kunishita T, Blades D, Lowery D, Eisen M, Usiak M, Qu X, Tabira T, Greenberg BD, Younkin SG (1992) Potentially amyloidogenic carboxyl-terminal derivatives of the amyloid protein precursor. Science, 255: 726–728.
7. Feig S, Lipton P. (1990) N-methyl-D-aspartate activation and Ca^{2+} account for poor pyramidal cell structure in hippocampal slices. J Neurochem, 55: 473–483.
8. Golde T, Estus S, Younkin L, Selkoe D, Younkin S (1992) Processing of the amyloid protein precursor to potentially amyloidogenic derivative. Science, 255: 728–730.
9. Haass C, Koo E, Mellon A, Hung A, Selkoe D (1992) Targeting of cell-surface β-amyloid precursor protein to lysosomes: alternative processing into amyloid-bearing fragments. Nature, 357: 500–503.
10. Haass C, Schlossmacher M, Hung A, Vigo-Pelfrey C, Mellon A, Ostaszewski B, Lieberburg I, Koo BM, Schenk D, Teplow D, Selkoe D (1992) Amyloid β-peptide is produced by cultured cells during normal metabolism. Nature, 359: 322–325.
11. Iverfeldt K, Walaas SI, Greengard P (1993) Altered processing of Alzheimer amyloid precursor protein in response to neuronal degeneration. Proc Natl Acad Sci USA, 90: 4146–4150.
12. Koh J, Yang LL, Cotman CW (1990) β-Amyloid protein increases the vulnerability of cultured cortical neurons to excitotoxic damage. Brain Res, 533: 315–320.
13. Laemmli UK (1970) Cleavage of structural proteins during the assembly of the head of bacteriophage. Nature, 277: 680–685.
14. Lonart G, Zigmond MJ (1991) Incubation of tissue slices in the absence of Ca^{2+} and Mg^{2+} can cause nonspecific damage. J Neurochem, 56: 1445–1448.
15. Lowry OH, Rosebrough AL, Farr AL, Randal RJ (1951) Protein measurement with the Folin phenol reagent. J Biol Chem, 193: 265–275.
16. Mattson MP, Cheng B, Davis D, Bryant K, Lieberburg I, Rydel R (1992) β-Amyloid peptides destabilize calcium homeostasis and render human cortical neurons vulnerable to excitotoxicity. J Neurosci, 12: 376–389.
17. Nakamura Y, Takdeda M, Niigawa H, Hariguchi S, Nishimura T (1992) Amyloid β-protein precursor deposition in rat hippocampus lesioned by ibotenic acid injection. Neurosci Lett, 136: 95–98.
18. Nitsch RM, Farber SA, Growdon JH, Wurtman RJ (1993) Release of amyloid β-protein precursor derivatives by electrical depolarization of rat hippocampal slices. Proc Natl Acad Sci USA, Neurobiology, 90: 5191–5193.
19. Nitsch RM, Slack BE, Wurtman RJ, Growdon JH (1992) Production of the Alzheimer amyloid β-protein by normal proteolytic processing. Science, 258: 303–307.
20. Parvathy S, Hussain I, Karran EH, Turner AJ, Hooper NM (1998) Alzheimer's amyloid precursor protein α-secretase is inhibited by hydroxamic acid-based zinc metalloprotease inhibitors: similarities to the angiotensin converting enzyme secretase. Biochemistry, 37: 1680–1685.
21. Parvathy S, Hussain I, Karran EH, Turner AJ, Hooper NM (1999) Cleavage of Alzheimer's amyloid precursor protein by α-secretase occurs at the surface of neuronal cells. Biochemistry, 38: 9728–9734.
22. Shoji M, Golde T, Ghiso J, Cheung T, Estus S, Shaffer L, Cai X, McKay D, Tinter R, Fraginone B, Younkin S (1992) Production of the Alzheimer amyloid β-protein by normal proteolytic processing. Science, 258: 126–129.
23. Sisodia SS, Koo EH, Beyreuther K, Unterbeck A, Proce DL (1990) Evidence that β-amyloid protein in Alzheimer's disease is not derived by normal processing. Science, 248: 492–495.
24. Skovronsky DM, Moore BD, Milla ME, Doms RW, Lee VMY (2000) Protein kinase C-dependent α-secretase competes with beta-secretase for cleavage of amyloid-β precursor protein in the trans-golgi network. J Biol Chem, 275 (4): 2568–2575.
25. Yankner BA, Dawes LR, Fisher S, Villa Komaroff L, Oster Granite ML, Neve RL (1989) Neurotoxicity of a fragment of the amyloid precursor associated with Alzheimer's disease. Science, 245: 417–420.
26. Yankner BA, Duffy LK, Kirschner DA (1990) Neurotrophic and neurotoxic effects of amyloid β protein: reversal by tachykinin neuropeptides. Science, 250: 279–282.

Publikacja 3

ELSEVIER

Brain Research 856 (2000) 163–175

BRAIN RESEARCH

www.elsevier.com/locate/bres

Research report

Conformation of paired helical filaments blocks dephosphorylation of epitopes shared with fetal tau except Ser199/202 and Ser202/Thr205

W. Gordon-Krajcer [1], L.-S. Yang, H. Ksiezak-Reding *

Department of Pathology, Rm. F-538, Albert Einstein College of Medicine, 1300 Morris Park Avenue, Bronx, NY 10461, USA

Accepted 23 November 1999

Abstract

To determine if the high phosphate content of paired helical filaments (PHFs) in Alzheimer's disease (AD) is a result of limited access to filament phosphorylation sites, we studied in vitro dephosphorylation of intact PHFs, PHFs with filamentous structure abolished by formic acid treatment (PHF_{FA}) and fetal human tau protein. Samples were treated with alkaline phosphatase for up to 24 h at 37°C and then immunoblotted with eight well characterized tau antibodies, that recognize two phosphorylation-insensitive sites and six phosphorylation-sensitive epitopes at Thr181, Ser199/202, Ser202/Thr205, Thr231, Ser262/356 and Ser396/404. Intact PHFs were effectively dephosphorylated only at the two N-terminal epitopes Ser199/202 and Ser202/Thr205, with little change in electrophoretic mobility. In contrast, PHF_{FA} were dephosphorylated at all epitopes, with particular effectiveness at those in the C-terminus and with significant increase in electrophoretic mobility. The fetal tau epitopes were effectively dephosphorylated except at Thr181 and Thr231 with marked increase in mobility. The extent of dephosphorylation of PHF_{FA} was equal or more effective than in fetal tau, except for Thr181 that was minimally dephosphorylated in both proteins. The results indicate that intact PHFs, but not PHF_{FA} or fetal tau display differential dephosphorylation of the N- and C-terminal epitopes. The results confirm that the filamentous conformation may significantly contribute to hyperphosphorylation of PHFs in the C-terminus. The filamentous conformation, however, does not limit access to two N-terminal epitopes Ser199/202 and Ser202/Thr205. The access to these sites in AD may be limited by other factors, e.g., inhibition of phosphatase binding.

Keywords: Alzheimer's disease; Formic acid; Paired helical filament; Phosphatase; Tau protein

1. Introduction

Highly phosphorylated microtubule associated protein tau is the major constituent of paired helical filaments (PHFs) found in Alzheimer's disease (AD) brain [13,17,40]. Phosphorylation is considered to be an important step in dysfunction of PHF-tau because (i) PHF-tau is unable to bind to microtubules [21,64] and (ii) phosphorylation inhibits the ability of normal tau to promote microtubule assembly [3,33,61]. The total phosphate content of PHFs, approximately 6–8 mol P/mol protein [23,26], is as high as that of fetal tau [22] but the number of phosphorylation sites and extent of phosphorylation differ. Phosphopeptide analysis and other techniques reveal the presence of ~22 phosphorylated sites in PHF-tau and only 12–13 in fetal tau [20,40]. Thus PHF-tau contains approximately nine more phosphorylated sites than fetal tau and is recognized by a greater number of phosphorylation-dependent antibodies, including AT100 [65]. The majority of phosphorylation sites, however, are common to both fetal tau and PHF-tau proteins and can be detected with the same antibodies [36,38].

It is still unclear whether the hyperphosphorylation of PHF-tau in AD results from an increase of protein kinase activities, from an impairment of protein phosphatase activities, or from other factors [54]. The presence of mitotic epitopes have been demonstrated in PHF-tau [57] suggesting that re-emergence of mitotic events and re-expression of specific kinases in AD may play a role in hyperphosphorylation. There is also evidence implicating deficiency in the phosphatase system to be responsible for hyperphosphorylation of PHF-tau [16,44]. Moreover, there is mounting evidence that hyperphosphorylation may result from a

* Corresponding author. Fax: +1-718-430-8541; e-mail: reding@aecom.yu.edu

[1] Dr. W. Gordon-Krajcer is a visiting scientist from the Department of Neurochemistry, Medical Research Centre of the Polish Academy of Science, 02-106 Warsaw, Poland.

0006-8993/00/$ - see front matter
PII: S0006-8993(99)02391-4

filamentous conformation of PHFs that blocks access of phosphatases to phosphorylation sites. For example, with an excess amount of phosphatases and prolonged incubation time in vitro, only minimal dephosphorylation of PHFs was achieved [26]. The sensitivity to phosphatase has been dramatically improved, however, in PHFs subjected to treatment with guanidine, a chaotropic agent known to destroy filamentous conformation of PHFs [8,13,61,64]. Other reagents, e.g., formic acid or perchloric acid (PCA), are also commonly used to release amorphous PHF-tau protein from native PHFs [34,63] but it is unknown whether these reagents also increase reactivity with phosphatases.

Although PHFs have been subjected to dephosphorylation by a number of phosphatases including protein phosphatase 1, 2A and 2B, comparative studies of the effects of filamentous conformation on accessibility of the phosphatases have been limited [59,61]. The purpose of the present studies was to determine the role of filamentous conformation in hyperphosphorylation of different regions of PHF-tau. To establish extent of phosphorylation and effectiveness of phosphatase a panel of phosphate-dependent antibodies was used. The time course of dephosphorylation was examined in isolated intact PHFs (filamentous conformation), formic acid-treated PHFs (PHF_{FA}, amorphous conformation) and human fetal tau isolated with or without acid treatment. Broad specificity alkaline phosphatase [47] was used to minimize the selectivity and maximize accessibility of phosphorylation sites. It was found that in intact PHFs, the C-terminal phospho-epitopes and two P-Thr epitopes in the N-terminus and mid-region are not accessible to dephosphorylation and that destruction of filamentous conformation with formic acid enhances the reactivity to phosphatase. The N-terminal phospho-epitopes located at Ser199/202 and Ser202/Thr205, however, are dephosphorylated as effectively as those in PHF_{FA} or fetal tau preparations. Since the endogenous phosphatases fail to dephosphorylate these epitopes in PHFs in situ, the access to these sites in AD may be limited by other factors.

2. Materials and methods

2.1. Materials

Alkaline phosphatase (*Escherichia coli*, type III) was obtained from Sigma (St. Louis, MO, USA). Enhanced chemiluminescence system (ECL) was purchased from Amersham Life Science (Arlington Heights, IL, USA), 70% PCA and 88% formic acid were from Fisher Scientific (Pittsburgh, PA, USA). Tau 14 antibody was obtained commercially (Zymed Laboratories, CA, USA). Secondary antibodies conjugated to horseradish peroxidase were from Vector Laboratories (Burlingame, CA, USA). Copper grids for electron microscopy (EM) were purchased from Fullam (Latham, NJ, USA). Carnation brand of fat-free dried milk was used.

2.2. Tissue

Brain tissue was obtained from two AD patients, one 63- and one 80-year-old woman, with post-mortem delay of 4 and 5.5 h, respectively. Tissue was derived from frontal and temporal lobes, respectively, and contained up to 20 neurofibrillary tangles per 40 × objective field. The diagnosis of AD was based on age-dependent modified criteria. Brains from aborted fetuses were obtained at 19–21 weeks of gestation. Tissue was stored frozen at −80°C. Protocols for the use of human material were approved by the Committee for Clinical Investigation.

2.3. PHF and fetal tau preparations

PHF preparations were obtained from AD brains as Sarcosyl-insoluble $100\,000 \times g$ pellet as previously described [29]. Preparations of fetal tau were obtained from fetal brain tissue by two protocols. In protocol one, the initial $15\,000 \times g$ brain extract was subjected to heat and 2.5% PCA treatments [28]; this preparation was designated as fetal tau_{PCA}. In protocol two, heat and acid treatments were not used. Instead, the initial $15\,000 \times g$ brain extract was subjected to ammonium sulfate fractionation as described [33]. Tau fraction which precipitated between 35% and 50% ammonium sulfate saturation was collected and designated as fetal tau_N.

2.4. SDS-PAGE and immunoblotting

Electrophoresis was performed using 10% polyacrylamide gels. Separated proteins were electrotransferred onto nitrocellulose membranes and incubated with 5% non-fat milk in 10 mM Tris/HCl, pH 7.4 and 150 mM NaCl (TBS) to block non-specific binding sites. Prior to incubations with milk, some membranes were incubated with alkaline phosphatase (10 IU/ml) in 0.1 M Tris/HCl buffer, pH 8 with 1 mM phenylmethylsulfoxyfluoride (PMSF) for 1 h at 37°C. Membranes were incubated with primary antibodies for 1–2 h at 25°C and then with secondary antibodies conjugated to horseradish peroxidase for 1 h. Both primary and secondary antibodies were diluted in 5% milk–TBS. Specific protein signals were detected using ECL reagents.

2.5. Alkaline phosphatase and formic acid treatments

Samples (1 mg/ml) of PHF or fetal tau were incubated with alkaline phosphatase (18 IU/ml) for 0–24 h at 37°C in buffer containing 0.1 M Tris/HCl, pH 8.0 and 1 mM PMSF. The reaction was terminated by addition of SDS–sample buffer and boiling for 5 min. Formic acid treatment

was performed by mixing PHF samples with 10 vol. of 88% formic acid. After incubation for 1 h at 25°C, samples were diluted with distilled water to a final concentration of 20% formic acid and then lyophilized. Freeze-dried samples were suspended in the original volume of 0.1 M Tris/HCl, pH 7.5 and pH-re-adjusted with 1 N NaOH if required.

2.6. Antibodies

Monoclonal antibodies were used that recognize distinct regions of the tau molecule (Table 1). All antibodies except Alz 50, Tau 14 and Tau-1 were previously shown to recognize specific phosphorylated amino acid residues. Tau-1 has been demonstrated to bind a non-phosphorylated tau epitope that no longer binds this antibody after phosphorylation.

2.7. Quantitative analysis

The intensity of immunoreactivity was quantified on nitrocellulose membranes and ECL X-ray films by densitometric scanning using a LKB Ultrascan XL Enhanced Laser Densitometer (Pharmacia, Uppsala, Sweden). Decreases of immunoreactivity in samples subjected to phosphatase were referred to control samples not treated with phosphatase (100% immunoreactivity). Increases of Tau-1 immunoreactivity were quantified against control samples (100% immunoreactivity), which were subjected to extensive dephosphorylation with alkaline phosphatase on electroblots prior to immunostaining (see Section 2.4).

2.8. Electron microscopy

Samples of PHF (25–50 μl) were deposited for 5 min on 200 mesh copper grids precoated with Formvar and carbon, stained with 2% uranyl acetate for another 5 min and examined using a JEOL 100CX electron microscope.

3. Results

3.1. Ultrastructural characterization of intact PHFs and PHF_{FA}

Control, untreated preparations defined as intact PHFs were examined by EM and shown to contain an abundance of short and dispersed filaments characteristic of PHFs from AD (Fig. 1A). The filaments were approximately 20 nm wide at the maximum width and narrowed to 10 nm width at regular intervals every 80 nm. The length of filaments varied from approximately 80 to 600 nm. The ultrastructural characteristics of intact PHFs were comparable to those reported in previous studies [29]. In contrast, preparations of PHFs that were treated with formic acid were devoid of filaments. Instead, they displayed amorphous material as well as structures resembling filamentous ghosts (arrows), with filaments characteristic of PHFs absent (Fig. 1B). Formic acid treatment, therefore, destroyed fibrillary structure of PHFs and preparations of PHF_{FA} could be defined as amorphous or non-filamentous fractions. Effects of formic acid treatment on ultrastructure of PHFs are similar to those reported previously [63].

3.2. Characterization of intact PHFs and PHF_{FA} by immunoblotting

Intact PHFs and PHF_{FA} were examined by Western blotting with antibodies to phosphorylated and non-phosphorylated epitopes spanning the length of the tau molecule (Table 1). As illustrated in Fig. 2, the antibodies to phosphorylated epitopes are categorized into two groups depending on the epitope location, those at the N-terminus (Tau-1 and AT8) and those at the C-terminus (PHF-1 and 12E8). A third group identified as recognizing epitopes containing P-Thr is located in the middle of the tau molecule (AT270 and AT180). This group is considered separately based on its unique pattern of dephosphorylation. The two preparations of PHFs demonstrated immuno-

Table 1
List of monoclonal antibodies used in the present studies. The location of epitopes refers to the longest tau isoform containing 441 amino acid residues [14]. Phosphate dependence is defined as a requirement for a P-Ser or P-Thr residue

Antibody	Location of epitope	Phosphate dependence	Dilution (blotting)	References
Alz 50	5–8	None[a]	1:10	[28]
Tau 14	141–178	None	1:1000	[24]
AT270	181	Thr181	1:2000	[11]
Tau-1	199–202	Ser199/202[b]	1:10	[24]
AT8	202–205	Ser202/Thr205	1:200	[12]
AT180	231	Thr231	1:2000	[11]
12E8	262/356	Ser262/356	1:200	[51]
PHF-1	396/404	Ser396/404	1:200	[42]

[a] Binding is improved by the presence of microtubule binding domain [4].
[b] Binding is blocked by phosphorylation of Ser199/202.

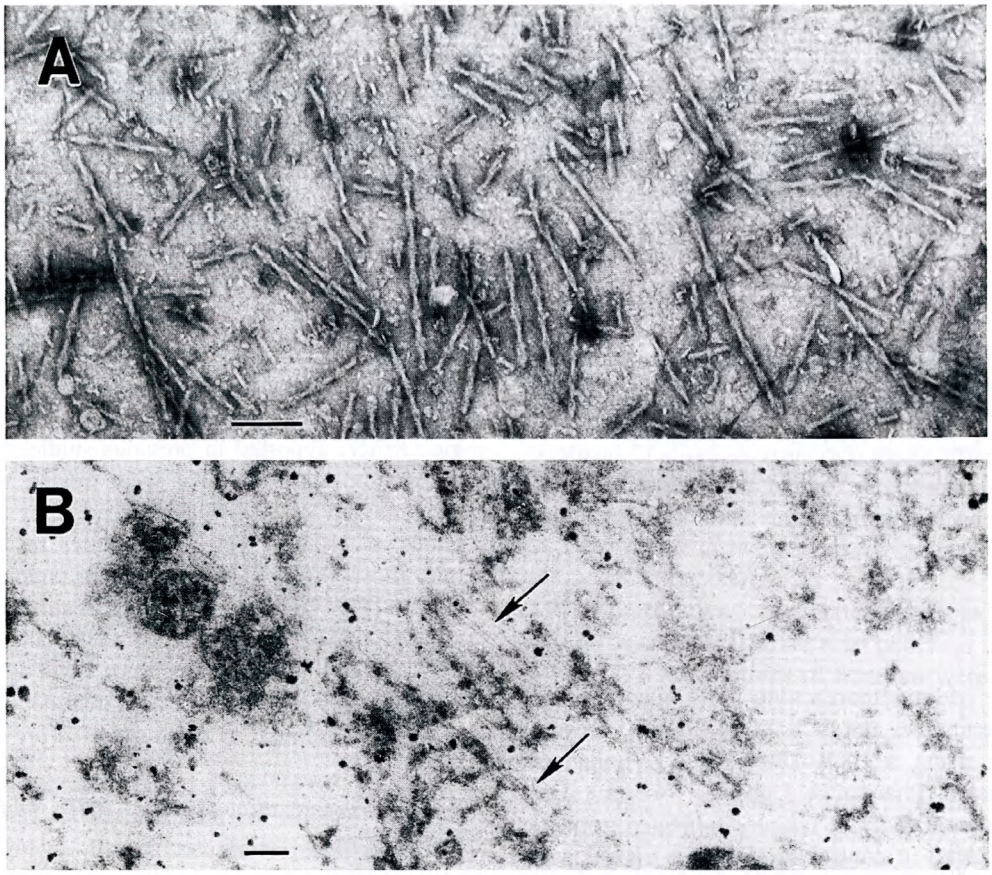

Fig. 1. Electron micrographs of intact PHFs (A) and PHF_{FA} (B) stained with uranyl acetate. PHF-enriched fractions were isolated from AD brain and they were either not treated (intact PHFs) or treated with formic acid (PHF_{FA}) before EM examination. In (A), abundant short and dispersed filaments typical of PHFs from AD are seen. In (B), amorphous material predominates with structures resembling filament ghosts (arrows), indicating that formic acid treatment destroyed the fibrillary structure of PHFs. Scale bars correspond to 200 nm (JEOL 100CX).

reactivity with both antibodies to phosphorylated and non-phosphorylated epitopes consistent with our previous reports [63]. In preparations of intact PHFs four immunoreactive polypeptides 60-, 63–64- and 68-kDa could be distinguished (Fig. 3A, 0 time), the 63- and 64-kDa polypeptides migrating either as a closely spaced doublet or in some blots as a single wide band. The PHF-tau polypeptides were not immunoreactive with Tau-1 unless the blots were pretreated with phosphatase, an observation indicating that the Tau-1 epitope was blocked by phosphorylation. The samples also displayed high molecular weight material as a smear from the top of the gel to approximately 68 kDa and degraded 45–58-kDa tau fragments. The treatment of PHFs with formic acid had no major effect on the electrophoretic migration pattern of PHF-tau polypeptides (Fig. 3B, 0 time).

Fig. 2. A diagram illustrating the location of epitopes to phosphorylation-sensitive antibodies used in the present studies. The antibodies were separated into three groups depending on the location and specificity of the epitopes: (a) N-terminal: Tau-1 and AT8, (b) C-terminal: 12E8 and PHF-1, and (c) P-Thr-sites specific: AT270 and AT180. The location refers to the longest tau isoform containing 441 amino acid residues.

3.3. Time course of dephosphorylation of intact PHFs and PHF_{FA}

To determine the effect of the filamentous conformation on the rate of dephosphorylation, both intact PHFs and PHF_{FA} were incubated for intervals up to 24 h at 37°C with alkaline phosphatase (*E. coli*) at a constant protein:enzyme ratio. The 24-h incubations resulted in a minimal decrease of total tau immunoreactivity using Tau 14 (Fig. 3A and B) and Alz 50 (not shown). Increases in proteolytic fragments were not observed, confirming a limited degradation of tau. Incubation with phosphatase did accelerate electrophoretic mobility of the PHF-tau polypeptides resulting in a downward shift of all immunoreactive bands. With

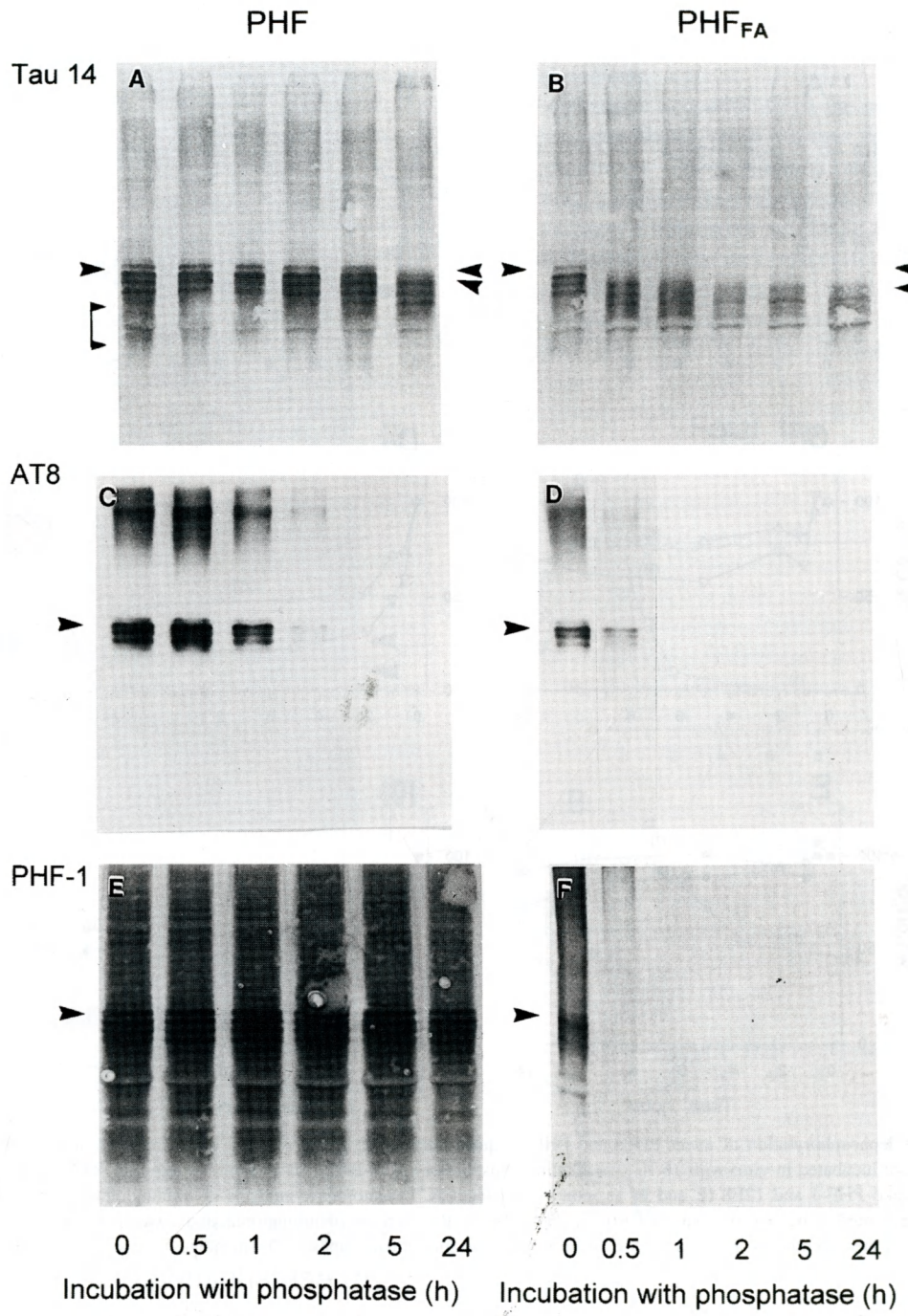

Fig. 3. Time course of dephosphorylation of intact PHFs and PHF$_{FA}$: selected Western blots. Samples of intact PHFs (A, C and E) or PHF$_{FA}$ (B, D and F) were incubated in vitro with 18 IU/ml alkaline phosphatase for 0–24 h and aliquots containing 0.5–1 μg protein/lane immunoblotted with Tau 14 (A and B) to detect tau protein or with AT8 (C and D) and PHF-1 (E and F) to detect specific phosphorylated epitopes as described in Section 2. At 0 time (controls), the location of PHF-tau polypeptides 60–68 kDa is marked by a single arrowhead. In (A), immunoreactive tau fragments 45–58 kDa are marked. The mobility of PHF-tau polypeptides increases following dephosphorylation and the shift is indicated by double arrowheads (24 h).

intact PHFs, a shift was weakly noticeable only after 24 h, but in PHF$_{FA}$ the shift was apparent as early as 0.5 h. Judging by the extent of the shift, dephosphorylation of PHF$_{FA}$ was faster and more extensive than with intact PHFs. This was confirmed by blotting with phosphate-dependent antibodies in selected immunoblots (Fig. 3C–D) and in densitometric data of all blots (Fig. 4). For example, with intact PHFs, the AT8 immunoreactivity was only partially decreased within 1 h, whereas with PHF$_{FA}$ it was practically abolished during the same period (Fig. 3C–D). Similar observations were noted using N-terminal antibody, Tau-1. The restoration of immunoreactivity with

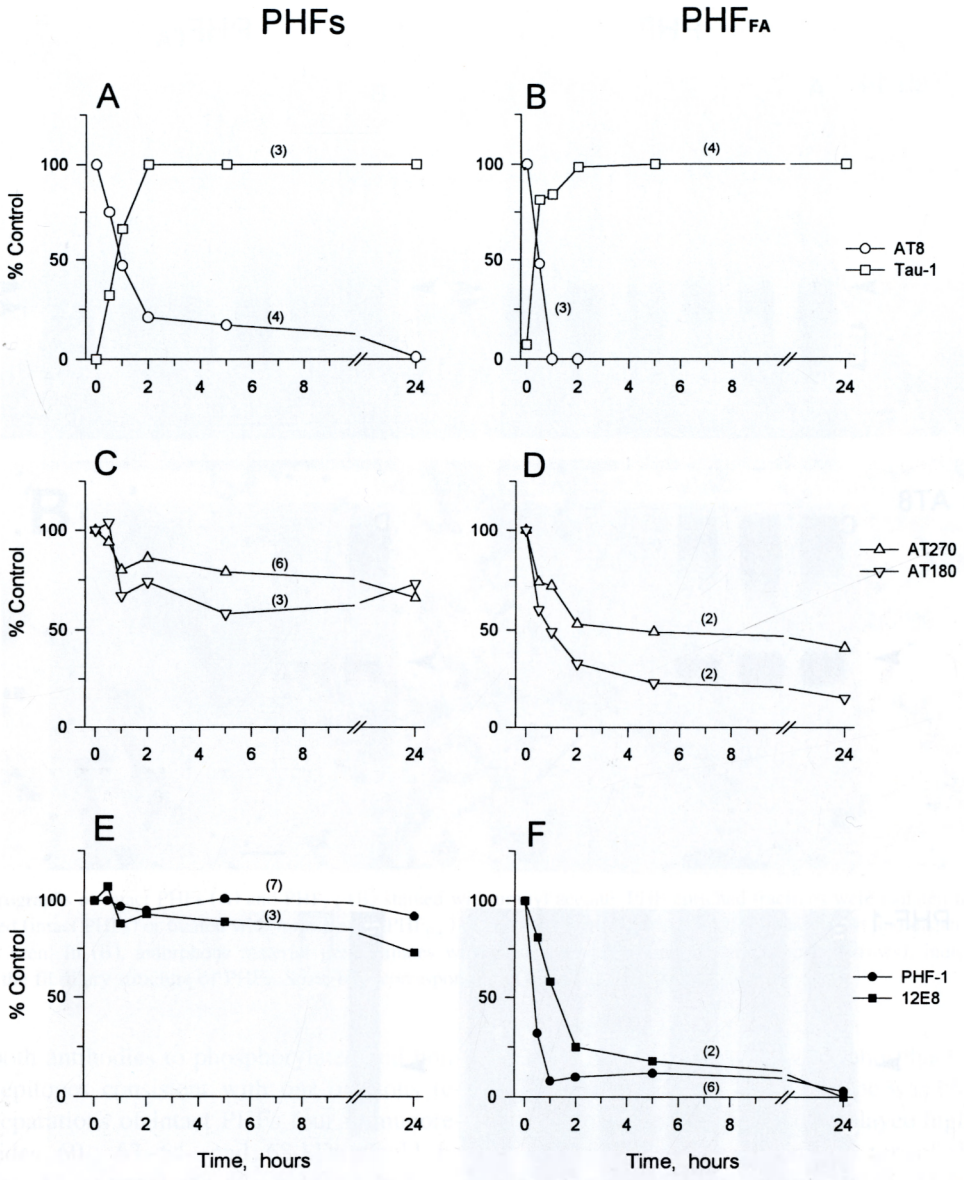

Fig. 4. Time course of dephosphorylation of intact PHFs and PHF_{FA}: quantitative analysis of Western blots. Samples of intact PHFs (A, C and E) or PHF_{FA} (B, D and F) were incubated in vitro with 18 IU/ml alkaline phosphatase for 0–24 h and immunoblotted with AT8 and Tau-1 (A and B), AT270 and AT180 (C and D) and PHF-1 and 12E8 (E and F) as indicated in legends. Densitometric analysis of immunoblots was performed as described in Section 2 and values presented in percent of controls (0 time). With Tau-1, the increase of immunoreactivity was quantified. Values are means for the number of experiments in the parentheses. For clarity, S.E. were omitted. In individual graphs, S.D. (or ranges) are similar to those in Table 2.

Tau-1, as a result of dephosphorylation, was found to be approximately one half as rapid in intact PHFs as in PHF_{FA} (Fig. 4A–B). The difference between the two preparations in the rate of dephosphorylation was largest for the C-terminal epitopes. With intact PHFs, the immunoreactivity with the PHF-1 antibody remained unchanged during 24 h of incubation, indicating minimal dephosphorylation, whereas with PHF_{FA} the immunoreactivity was abolished by 1 h, indicating fast and effective dephosphorylation (Fig. 4E–F). Observations with C-terminal antibody 12E8 were similar, reflecting the specific effect of formic acid treatment on enhancing dephosphorylation of both C-terminal epitopes (Fig. 4E–F). Collectively, these results demonstrate that destruction of the filamentous structure of PHFs by formic acid results in only a partially increased effectiveness of dephosphorylation of the N-terminal sites but a greatly improved dephosphorylation of the C-terminal sites.

Dephosphorylation of epitopes containing P-Thr is also enhanced by formic acid treatment. Quantitative densitometry of the AT180 and AT270 immunoblots showed a moderate dephosphorylation of intact PHFs (27–34% in 24 h) and pronounced dephosphorylation of PHF_{FA} (59–85% in 24 h) (Fig. 4C–D) indicating an approximately two-fold faster dephosphorylation of the P-Thr sites in non-filamentous than filamentous preparations. However, dephos-

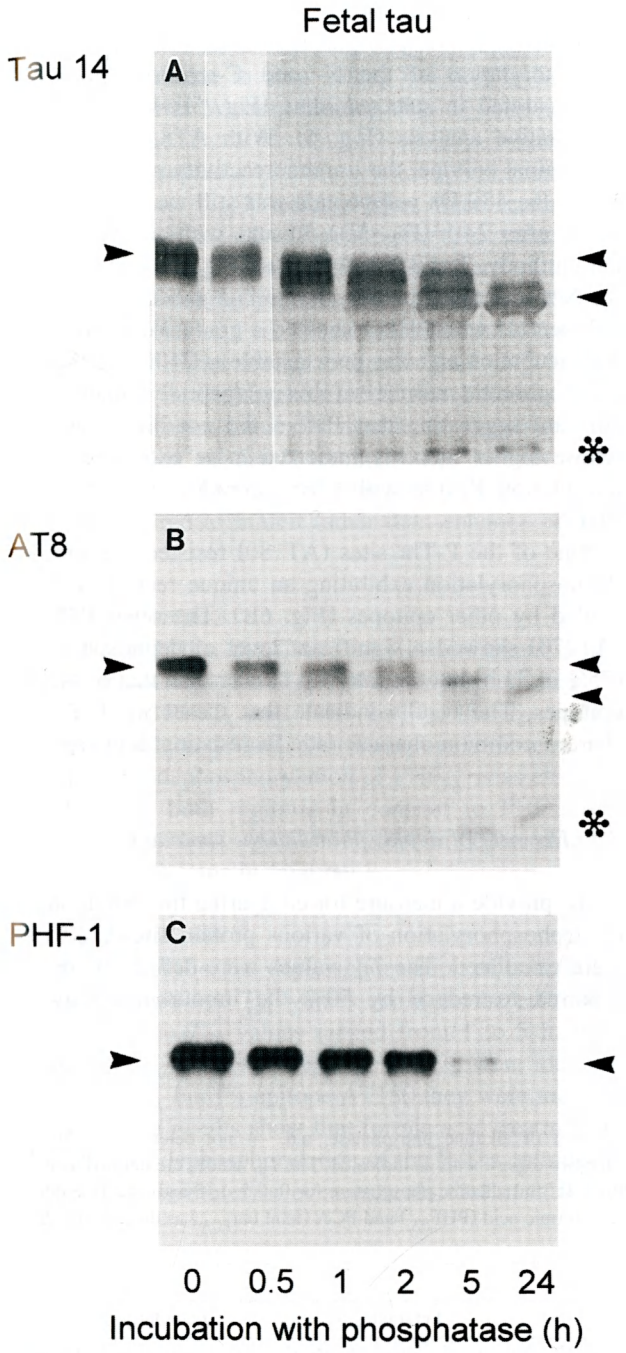

Fig. 5. Time course of dephosphorylation of human fetal tau: selected Western blots. Samples of fetal tau_{PCA} were incubated in vitro with 18 IU/ml alkaline phosphatase for 0–24 h and 0.5–1 μg protein/lane immunoblotted with Tau 14 (A) to detect tau protein or AT8 (B) and PHF-1 (C) to detect specific phospho-epitopes as described in Section 2. At 0 time (controls), the location of the 55-kDa polypeptide of fetal tau is marked by a single arrowhead. The increase in mobility following dephosphorylation is indicated by double arrowheads (24 h). Asterisk denotes degraded tau fragments 36–39 kDa.

phorylation of P-Thr sites was less extensive than at P-sites in N- and C-terminals. Thus P-Thr epitopes are characterized by a less dynamic dephosphorylation pattern.

3.4. Time course of dephosphorylation of fetal tau

3.4.1. Controls

To determine accessibility of the selected phospho-epitopes in normal tau proteins, two fetal tau preparations were employed. These preparations were isolated with (fetal tau_{PCA}) and without (fetal tau_{N}) acid treatment. Both fetal tau preparations were similar in their immunoreactivity on Western blots and susceptibility to phosphatase. They usually showed a major 55-kDa polypeptide as a single broad band but occasionally a doublet was weakly discerned (Fig. 5A, 0 time, arrowhead). The 55-kDa

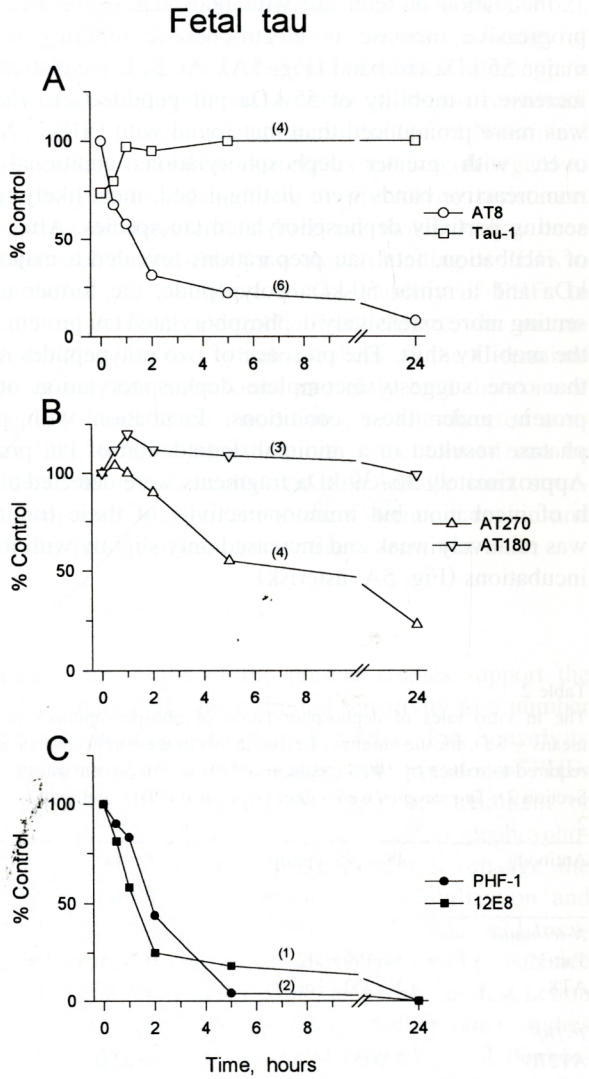

Fig. 6. Time course of dephosphorylation of human fetal tau: quantitative analysis of Western blots. Samples of fetal tau_{PCA} were incubated in vitro with 18 IU/ml alkaline phosphatase for 0–24 h and immunoblotted with AT8 and Tau-1 (A), AT270 and AT180 (B) and PHF-1 and 12E8 (C) as indicated in legends. Densitometric analysis of immunoblots was performed as described in Section 2 and values presented in percent of controls (0 time). With Tau-1, the increase of immunoreactivity was quantified. Values are means for the number of experiments in the parentheses. For clarity, S.E. were omitted. In individual graphs, S.D. (or ranges) are similar to those in Table 2.

polypeptide was immunoreactive with all tau antibodies used in these studies, including Tau-1 (Fig. 6A). Quantitative analysis of blots subjected to phosphatase treatment showed that approximately 26% to 63% of fetal tau protein was phosphorylated at the Tau-1 site, confirming previous reports [22,63]. Fetal tau was probably also partially phosphorylated at another N-terminal site judging by a relatively weak immunoreactivity with AT8 (Fig. 5B). With remaining sites, however, immunoreactivity alone was insufficient to distinguish between partial and complete phosphorylation.

3.4.2. Change in mobility

Incubation of fetal tau with phosphatase resulted in a progressive increase in electrophoretic mobility of the major 55-kDa tau band (Fig. 5A). At 24 h incubation, the increase in mobility of 55-kDa polypeptide (arrowheads) was more pronounced than that found with PHF_{FA}. Moreover, with greater dephosphorylation, additional immunoreactive bands were distinguished, most likely representing partially dephosphorylated tau species. After 24 h of incubation, fetal tau preparations revealed a major 48-kDa and a minor 50-kDa polypeptide, the former representing more extensively dephosphorylated tau protein from the mobility shift. The presence of two polypeptides rather than one suggests incomplete dephosphorylation of tau protein under these conditions. Incubation with phosphatase resulted in a minimal degradation of tau protein. Approximately 36–39-kDa fragments were detected after 1 h of incubation but immunoreactivity of these fragments was relatively weak and increased only slightly with longer incubations (Fig. 5A, asterisk).

3.4.3. Phospho-epitopes

Incubation with phosphatase resulted in a stepwise dephosphorylation of the N- and C-terminal epitopes as demonstrated in selected blots (Fig. 5B–C) and in their quantitative analysis (Fig. 6). With AT8, binding to an N-terminal epitope, the immunoreactivity gradually diminished; the 48-kDa polypeptide was still weakly immunoreactive after 24 h (Fig. 5B). Results with another N-terminal antibody, Tau-1, were similar (Fig. 6A). In contrast to the N-terminal antibodies, the immunoreactivity of 55-kDa polypeptide with PHF-1 showed a gradual decrease during 5 h incubation and was undetectable at 24 h (Fig. 5C). The electrophoretic mobility of this polypeptide remained fairly constant suggesting that PHF-1 did not bind tau species whose higher mobility indicated more extensive dephosphorylation. Results with 12E8 were identical to those with PHF-1.

One of the P-Thr sites (AT180) resisted even minimal dephosphorylation exhibiting an unique resistance, unparalleled by other epitopes (Fig. 6B). The other P-Thr site (AT270) showed a significant level of dephosphorylation (75% at 24 h) but the rate was slower than that of other tau epitopes. The results indicate that these two P-Thr sites share a common characteristic in resisting dephosphorylation.

3.5. The rate of dephosphorylation: summary

To provide a measure for comparing the extent and rate of dephosphorylation of various protein sites, T_{50} values were calculated. The T_{50} values were defined as the time required to reduce by 50% the immunoreactivity of a

Table 2
The in vitro rates of dephosphorylation of phospho-epitopes of tau in the presence of alkaline phosphatase. n.d. — not determined. Values are means ± S.D. for the number of experiments in the parentheses or means ± range for two experiments as indicated. The T_{50} values are defined as the time required to reduce by 50% immunoreactivity of tau protein during incubation with 18 IU/ml alkaline phosphatase for 0, 0.5, 1, 5 and 24 h (see details in Section 2). Tau samples were either not treated (PHFs and fetal tau_N) or treated with formic acid (PHF_{FA}) and PCA (fetal tau_{PCA}) as described in Section 2

Antibody	Phospho-epitope	T_{50} (h)			
		PHFs	PHF_{FA}	Fetal tau_N	Fetal tau_{PCA}
N-terminus					
Tau-1[a]	Ser199/202	0.7 ± 0.3 (3)	0.3 ± 0.1 (4)**	0.4 ± 0.2 (4)[b]*	0.7 ± 0.1 (4)[c]
AT8	Ser202/Thr205	0.9 ± 0.3 (4)	0.4 ± 0.3 (3)**	n.d.	1.7 ± 0.7 (6)
P-Thr					
AT270	Thr181	> 24 (6)	~ 5 (2)	n.d.	~ 5 (4)
AT180	Thr231	> 24 (3)	~ 1 (2)	n.d.	> 24 (3)
C-terminus					
2E8	Ser262/356	> 24 (3)	1.2 ± 0.5 (2)	0.4 ± 0.1 (3)	2.6 (1)
PHF-1	Ser396/404	> 24 (7)	0.4 ± 0.3 (6)	0.3 ± 0.1 (4)	1.8 ± 0.2 (2)

[a] Increases of the immunoreactivity were considered.
[b] Increases were from 37% (0 min) of the maximal immunoreactivity.
[c] Increases were from 74% (0 min) of the maximal immunoreactivity.
** $P < 0.001$ vs. fetal tau_{PCA} and $P > 0.05$ vs. PHFs and fetal tau_N.
* $P < 0.05$ vs. fetal tau_{PCA}.

phosphorylated site in vitro, under the specific dephosphorylating conditions. In several cases, T_{50} values could only be approximated due to slow rates. The results listed in Table 2 summarize Western blotting data.

3.5.1. The N-terminus

In all proteins, the N-terminal sites were sensitive to dephosphorylation as seen from the low T_{50} values. For intact PHFs, the T_{50} values (0.7–0.9 h) were similar to those for both fetal tau proteins (0.4–1.7 h). For PHF_{FA}, the T_{50} values (0.3–0.4 h) were lower than those for fetal tau_{PCA} (0.7–1.7 h) but similar to that for fetal tau_N (0.4 h). The difference in dephosphorylation rate between PHFs and PHF_{FA} was not statistically significant, suggesting that dephosphorylation of the N-terminal sites is only minimally enhanced by formic acid treatment. In fetal tau, acid treatment appeared to inhibit rather than enhance dephosphorylation.

3.5.2. The C-terminus

With intact PHFs, the C-terminus was resistant to dephosphorylation and the T_{50} values were too high to estimate. With PHF_{FA} and fetal tau_{PCA}, the T_{50} values were comparable and similar to those for the N-terminus, suggesting that dephosphorylation of PHF_{FA} is as effective as fetal tau in both regions. In contrast to PHFs, acid treatment was without significant effect on dephosphorylation of the C-terminus in fetal tau.

3.5.3. The P-Thr sites

With intact PHFs, the dephosphorylation of both P-Thr sites was blocked and T_{50} values could not be estimated. With PHF_{FA}, the T_{50} values ranged from 1 to 5 h. With fetal tau, the T_{50} values for epitope AT270 were identical to that in PHF_{FA} but for epitope AT180 they were too high to estimate. The results show that formic acid treatment of PHFs enhances dephosphorylation of the P-Thr epitopes to the level that resembles or even exceeds that in fetal tau.

4. Discussion

In the present studies, dephosphorylation rates of six phosphorylated epitopes were examined in preparations of PHFs containing intact filaments and in preparations treated with formic acid containing amorphous PHF-tau material. The destruction of the filamentous structure of PHFs following formic acid treatment dramatically increased susceptibility to dephosphorylation of two C-terminal epitopes (Ser262/356 and Ser396/404), improved that of P-Thr sites (Thr181 and Thr231) and only minimally affected this property of two N-terminal epitopes (Ser199/202 and Ser202/Thr205). Dephosphorylation rates of PHF_{FA} were either comparable or even more rapid than those of human fetal tau — a protein with similar phosphate content but lacking the filamentous conformation. In contrast to PHFs, acid treatment of fetal tau had no stimulatory effect on dephosphorylation rates of the N-terminal as well as the C-terminal epitopes.

4.1. Filamentous conformation

The results of the present studies show a significant interference of filamentous conformation with dephosphorylation of PHFs and are consistent with previous studies showing an inhibitory effect of filamentous conformation on the biological activity and proteolytic processing of PHF-tau, the major protein component of PHFs. For example, filamentous conformation was implicated in the resistance of PHFs to calpain-mediated proteolysis [39,62]. This resistance was attributed mainly to inaccessibility of the C-terminal region to enzyme digestion although a limited susceptibility of the N-terminal region remained. The differential effect of calpain on the C and N-terminal regions closely resembles our observations with regard to dephosphorylation. In addition to proteolytic resistance, filamentous arrangement of PHF-tau molecule has been reported to be responsible for a limited binding of PHFs to microtubules and contribute to the inability of PHFs to promote microtubule assembly. Furthermore, the microtubule-binding domain, which localizes to the C-terminal region of tau, has been found to tightly bind the core of filaments [6] and to be inaccessible to site-directed antibodies [27]. Intact PHFs therefore, once formed can be considered as metabolically and functionally inert structures, especially with regard to the C-terminal region and to a lesser but significant extent the N-terminus.

4.2. The N-terminal epitopes

Indeed, the results of the present studies support the view that intact PHFs have limited sensitivity to a number of specific phosphatases [59,61]. Such a low sensitivity was attributed earlier to filamentous conformation of PHFs alone [61,64] and necessity for guanidine treatment or extensive sonication [21] to achieve effective dephosphorylation of PHFs. Both of these conditions change the ultrastructure of PHFs: guanidine by solubilization and sonication by fragmentation of fibrils. Formic acid treatment in the present studies has also been found to enhance dephosphorylation of PHFs coincident with the destruction of PHF ultrastructure. It is unclear whether other studies using intact filaments to determine the effect of dephosphorylation on the migration pattern of PHF-tau polypeptides have been able to achieve full dephosphorylation of PHFs [13]. In the view of the present studies and other reports, the C-terminal sites are likely to remain highly phosphorylated since the effectiveness of phosphatase in intact PHFs is limited to some of the N-terminal epitopes.

With PHF_{FA}, dephosphorylation rates of the two N-terminal epitopes resemble that of Tau-1 epitope of fetal tau_N but exceed those of N-terminal epitopes of fetal

tau_{PCA}. This difference probably reflects dissimilar conformation of amorphous PHFs (or fetal tau_N) and fetal tau_{PCA}. Structural studies indicate that acid-treated tau assumes random coil conformation and is ''natively denatured'' with little evidence of secondary structure [5,50], but comparable structural studies of PHF_{FA} are not available. Amorphous PHF-tau may not have a random coil conformation due to elongation and stiffness of the molecule following hyperphosphorylation [18,32]. The difference in conformation could explain faster dephosphorylation rates of all sites examined in PHF_{FA} compared with fetal tau_{PCA}. It is unlikely that faster rates could result solely from non-specific changes produced by acid treatment [63] since acid-treated fetal tau is dephosphorylated at similar or slower rates than the untreated protein.

4.3. Access to phosphatases

The present studies demonstrate that intact PHFs and fetal human tau (including both fetal tau_{PCA} and fetal tau_N) exhibit similar in vitro dephosphorylation rates at the two N-terminal sites. Such similarity strongly suggests that filamentous conformation has no inhibitory effect on dephosphorylation at these sites. N-terminal sites are located at the periphery of filaments and therefore should be more accessible to phosphatases than the C-terminal or other sites buried in the filament core. Since N-terminal sites are readily available to dephosphorylation in vitro, it is unclear why they remain highly phosphorylated in AD brain tissue after a long post-mortem delay. Interestingly, a high level of phosphorylation, apparently maximal in case of Tau-1 site, has been a hallmark of neurofibrillary changes in AD [17,25].

There are several potential explanations for a high level of phosphorylation at Tau-1/AT8 sites: a reduction of phosphatase activities in AD, displacement/sequestration of phosphatases, and a binding of specific kinases by PHFs. The first explanation, a reduction of phosphatase activity per se [16], although an attractive explanation, would not account for a complete rather than partial phosphorylation of Tau-1/AT8 sites.

The second explanation suggests that phosphatase activity may be either sequestered from PHFs or locally inhibited. The potential phosphatases include phosphatases 1, 2A and 2B, although phosphatase 2A has been postulated to be a major tau phosphatase in vivo [52]. All three phosphatases are able to dephosphorylate the Tau-1/AT8 sites in normal tau protein [41], in non-PHF pool of AD tau [15,60] or in guanidine-treated PHFs [8,61]. With the exception of phosphatase 2B, these phosphatases are also active on intact PHFs [61]. If Tau-1/AT8 phosphatase were sequestered in other cell compartments it could not dephosphorylate PHFs. It is interesting to note, however, that both phosphatases 1 and 2A as well as phosphatase 2B are found to co-localize with neurofibrillary tangles [2,43]. These observations suggest that although a potential phosphatase is present in the vicinity of PHFs it may be blocked from accessing phosphorylated sites in PHFs. Moreover, its binding may be defective and lower in affinity than that in normal tau [31,52]. It is not known whether tau protein phosphatases are able to tightly associate with PHFs. Recent studies suggest that association of phosphatases with PHFs may be severely disrupted. In those studies, phosphatase 2A was found to bind with high affinity to a specific sequence in tau and the binding sequence coincided with the microtubule binding domain [53]. If binding of phosphatase 2A requires the microtubule binding domain of tau to be accessible, incorporation of the microtubule binding domain to the core of filaments could prevent the phosphatase from binding to intact PHFs.

With regard to the third explanation, binding of kinases, PHFs have been reported to bind kinases non-covalently, and a number of such protein kinases have been identified. They include a cdc2-related kinase [35], mitogen-activated protein kinase (Mapk/Erk) [46,55], cdk5 kinase [45], casein kinase II [37], recently described casein kinase 1, which is tightly associated with isolated PHFs [10,30], and others [56,57]. There is therefore a good possibility that protein kinase(s) strongly associated with PHFs may physically block phosphatases from the Tau-1/AT8 sites, and thus maintain their highly phosphorylated condition.

4.4. Fetal tau

Dephosphorylation of the six phospho-epitopes of fetal tau examined in the present studies showed similar rates for both the C- and N-terminal epitopes and slower rates for P-Thr sites. The slower rate for P-Thr sites is probably not caused by a lower activity of these sites since alkaline phosphatase from *E. coli* hydrolyses many different phosphate esters at nearly the same rate [47]. The results suggest rather that the availability of P-Thr sites in tau may depend on their local environment, e.g., the fetal tau molecule may contain a phosphatase-inaccessible fold around P-Thr sites. This may be particularly relevant to the phospho-epitope at Thr181, which was practically unreactive in fetal tau. A slower dephosphorylation rate of this site was previously reported and found to be unrelated to the type of phosphatase, including phosphatases 2A and 2B [61] or endogenous phosphatases in brain tissue [38]. This site may play a specific role, namely, by intermolecular bridging between a proline-rich region and the microtubule-binding domain [4]. Other neighbouring sites, however, are readily attacked by phosphatase, including Ser199/202, Ser202/Thr205 and the other P-Thr site (Thr231).

The present results support the view that phosphorylation of PHFs precedes [1] rather than follows [48] polymerization. The main argument is that only a severe change in ultrastructure of PHFs such as acid- or guanidine-induced depolymerization would allow for effective dephosphorylation and possible re-phosphorylation. Is

phosphorylation necessary to form filaments, or is it only sufficient? Several in vitro assembly studies indicate that phosphorylation of tau is not necessary for PHF formation [7] and that it may even protect against aggregation [49]. Furthermore, non-phosphorylated tau can be induced to aggregate by simply adding polyanions (e.g., heparin [19]), or by using tau fragments containing only the repeat region [9]. However, since considerable evidence shows that phosphorylation of tau precedes polymerization of PHFs in vivo [1,58], the role of phosphorylation in the assembly of filaments now needs to be fully determined.

In conclusion, the results of these studies indicate that the filamentous conformation does not limit access to certain phosphorylation sites in the N-terminus (e.g., Tau-1/AT8) whereas it restricts access to the C-terminal region. The profound effect of filamentous conformation on restricting the C-terminal dephosphorylation combined with defective interactions of the N-terminal sites with phosphatases are likely to play a significant role in the accumulation of hyperphosphorylated PHF-tau in metabolically and functionally inert PHFs of AD.

Acknowledgements

The authors would like to thank Drs. Peter Davies for providing antibodies Alz 50 and PHF-1, Peter Seubert of Athena Neurosciences, for supplying 12E8 antibody, and Andre Van De Voorde and Eugeen Vanmechelen of Innogenetics, Belgium for a generous gift of antibodies AT8, AT180 and AT270. We thank Dr. Maurice Rapport for his valuable editorial comments on the manuscript. These studies were supported by National Institute of Neurologic Disorders and Stroke (NS35254) and The Alzheimer's Association (RG3-96-085).

References

[1] C. Bancher, C. Brunner, H. Lassmann, H. Budka, K. Jellinger, G. Wiche, F. Seitelberger, I. Grundke-Iqbal, K. Iqbal, H.M. Wisniewski, Accumulation of abnormally phosphorylated tau precedes the formation of neurofibrillary tangles in Alzheimer's disease, Brain Res. 477 (1989) 90–99.

[2] M.L. Billingsley, C. Ellis, R.L. Kincaid, J. Martin, M.L. Schmidt, V.M.-Y. Lee, J.Q. Trojanowski, Calcineurin immunoreactivity in Alzheimer's disease, Exp. Neurol. 126 (1994) 178–184.

[3] G.T. Bramblett, M. Goedert, R. Jakes, S.E. Merrick, J.Q. Trojanowski, V.M.-Y. Lee, Abnormal tau phosphorylation at Ser396 in Alzheimer's disease recapitulates development and contributes to reduced microtubule binding, Neuron 10 (1993) 1089–1099.

[4] G. Carmel, E.M. Mager, L.I. Binder, J. Kuret, The structural basis of monoclonal antibody Alz50s selectivity for Alzheimer's disease pathology, J. Biol. Chem. 271 (1996) 32789–32795.

[5] D.W. Cleveland, S.-Y. Hwo, M.W. Kirschner, Physical and chemical properties of purified tau factor and the role of tau in microtubule assembly, J. Mol. Biol. 116 (1977) 227–247.

[6] T. Crowther, M. Goedert, C.M. Wischik, The repeat region of microtubule-associated protein tau forms part of the core of the paired helical filament of Alzheimer's disease (Review), Ann. Med. 21 (1989) 127–132.

[7] R.A. Crowther, O.F. Olesen, M.J. Smith, R. Jakes, M. Goedert, Assembly of Alzheimer-like filaments from full-length tau protein, FEBS Lett. 337 (1994) 135–138.

[8] G. Drewes, E.-M. Mandelkow, K. Baumann, J. Goris, W. Merlevede, E. Mandelkow, Dephosphorylation of tau protein and Alzheimer paired helical filaments by calcineurin and phosphatase-2A, FEBS Lett. 336 (1993) 425–432.

[9] P. Friedhoff, M. von Bergen, E.M. Mandelkow, P. Davies, E. Mandelkow, A nucleated assembly mechanism of Alzheimer paired helical filaments, Proc. Natl. Acad. Sci. U. S. A. 95 (1998) 15712–15717.

[10] N. Ghoshal, J.F. Smiley, A.J. DeMaggio, M.F. Hoekstra, E.J. Cochran, L.I. Binder, J. Kuret, A new molecular link between the fibrillar and granulovacuolar lesions of Alzheimer's disease, Am. J. Pathol. 155 (1999) 1163–1172.

[11] M. Goedert, R. Jakes, R.A. Crowther, P. Cohen, E. Vanmechelen, M. Vandermeeren, P. Cras, Epitope mapping of monoclonal antibodies to the paired helical filaments of Alzheimer's disease: identification of phosphorylation sites in tau protein, Biochem. J. 301 (1994) 871–877.

[12] M. Goedert, R. Jakes, E. Vanmechelen, Monoclonal antibody AT8 recognises tau protein phosphorylated at both serine 202 and threonine 205, Neurosci. Lett. 189 (1995) 167–169.

[13] M. Goedert, M.G. Spillantini, N.J. Cairns, R.A. Crowther, Tau proteins of Alzheimer paired helical filaments: abnormal phosphorylation of all six brain isoforms, Neuron 8 (1992) 159–168.

[14] M. Goedert, M.G. Spillantini, R. Jakes, D. Rutherford, R.A. Crowther, Multiple isoforms of human microtubule-associated protein tau: sequences and localization in neurofibrillary tangles of Alzheimer's disease, Neuron 3 (1989) 519–526.

[15] C.X. Gong, I. Grundke-Iqbal, K. Iqbal, Dephosphorylation of Alzheimer's disease abnormally phosphorylated tau by protein phosphatase-2A, Neuroscience 61 (1994) 765–772.

[16] C.X. Gong, S. Shaikh, J.-Z. Wang, T. Zaidi, I. Grundke-Iqbal, K. Iqbal, Phosphatase activity toward abnormally phosphorylated tau: decrease in Alzheimer disease brain, J. Neurochem. 65 (1995) 732–738.

[17] I. Grundke-Iqbal, K. Iqbal, Y.C. Tung, M. Quinlan, H.M. Wisniewski, L.I. Binder, Abnormal phosphorylation of the microtubule-associated protein tau (tau) in Alzheimer cytoskeletal pathology, Proc. Natl. Acad. Sci. U. S. A. 83 (1986) 4913–4919.

[18] T. Hagestedt, B. Lichtenberg, H. Wille, E.-M. Mandelkow, E. Mandelkow, Tau protein becomes long and stiff upon phosphorylation: correlation between paracrystalline structure and degree of phosphorylation, J. Cell Biol. 109 (1989) 1643–1651.

[19] M. Hasegawa, R.A. Crowther, R. Jakes, M. Goedert, Alzheimer-like changes in microtubule-associated protein Tau induced by sulfated glycosaminoglycans. Inhibition of microtubule binding, stimulation of phosphorylation, and filament assembly depend on the degree of sulfation, J. Biol. Chem. 272 (1997) 33118–33124.

[20] M. Hasegawa, M. Morishima-Kawashima, K. Takio, M. Suzuki, K. Titani, Y. Ihara, Protein sequence and mass spectrometric analyses of tau in the Alzheimer's disease brain, J. Biol. Chem. 267 (1992) 17047–17054.

[21] K. Iqbal, T. Zaidi, C. Bancher, I. Grundke-Iqbal, Alzheimer paired helical filaments. Restoration of the biological activity by dephosphorylation, FEBS Lett. 349 (1994) 104–108.

[22] A. Kenessey, S.H. Yen, The extent of phosphorylation of fetal tau is comparable to that of PHF-tau from Alzheimer paired helical filaments, Brain Res. 629 (1993) 40–46.

[23] E. Kopke, Y.C. Tung, S. Shaikh, A.C. Alonso, K. Iqbal, I. Grundke-Iqbal, Microtubule-associated protein tau. Abnormal phosphorylation of a non-paired helical filament pool in Alzheimer disease, J. Biol. Chem. 268 (1993) 24374–24384.

[24] K.S. Kosik, L.D. Orecchio, L.I. Binder, J. Trojanowski, V.M.-Y. Lee, G. Lee, Epitopes that span the tau molecule are shared with paired helical filaments, Neuron 1 (1988) 817–825.
[25] H. Ksiezak-Reding, L.I. Binder, S.-H. Yen, Immunochemical and biochemical characterization of tau proteins in normal and Alzheimer's disease brains with Alz 50 and Tau-1, J. Biol. Chem. 263 (1988) 7948–7953.
[26] H. Ksiezak-Reding, W.K. Liu, S.H. Yen, Phosphate analysis and dephosphorylation of modified tau associated with paired helical filaments, Brain Res. 597 (1992) 209–212.
[27] H. Ksiezak-Reding, K. Morgan, D.W. Dickson, Tau immunoreactivity and SDS solubility of two populations of paired helical filaments that differ in morphology, Brain Res. 649 (1994) 185–196.
[28] H. Ksiezak-Reding, R. Leibowitz, R. Bowser, P. Davies, Binding of Alz 50 depends on Phe8 in tau synthetic peptides and varies between native and denatured tau proteins, Brain Res. 697 (1995) 63–75.
[29] H. Ksiezak-Reding, J.S. Wall, Mass and physical dimensions of two distinct populations of paired helical filaments, Neurobiol. Aging 15 (1994) 11–19.
[30] J. Kuret, G.S. Johnson, D. Cha, E.R. Christenson, A.J. DeMaggio, M.F. Hoekstra, Casein kinase 1 is tightly associated with paired helical filaments isolated from Alzheimer's disease brain, J. Neurochem. 69 (1997) 2506–2515.
[31] H. Liao, Y. Li, D.L. Brautigan, G.G. Gundersen, Protein phosphatase 1 is targeted to microtubules by the microtubule-associated protein tau, J. Biol. Chem. 273 (1998) 21901–21908.
[32] B. Lichtenberg, E.-M. Mandelkow, T. Hagestedt, E. Mandelkow, Structure and elasticity of microtubule-associated protein tau, Nature 334 (1988) 359–362.
[33] G. Lindwall, R.D. Cole, The purification of tau protein and the occurrence of two phosphorylation states of tau in brain, J. Biol. Chem. 259 (1984) 12241–12245.
[34] W.-K. Liu, H. Ksiezak-Reding, S.H. Yen, Abnormal proteins from Alzheimer's disease brain. Purification and amino acid analysis, J. Biol. Chem. 266 (1991) 21723–21727.
[35] W.-K. Liu, R. Williams, F.L. Hall, D.W. Dickson, S.H. Yen, Detection of a cdc2-related kinase with Alzheimer paired helical filaments, Am. J. Pathol. 146 (1995) 228–238.
[36] S. Lovestone, C.H. Reynolds, The phosphorylation of tau: a critical stage in neurodevelopment and neurodegenerative processes, Neuroscience 78 (1997) 309–324.
[37] E. Masliah, D.S. Iimoto, M. Mallory, T. Albright, L. Hansen, T. Saitoh, Casein kinase II alteration precedes tau accumulation in tangle formation, Am. J. Pathol. 140 (1992) 263–268.
[38] E.S. Matsuo, R.-W. Shin, M.L. Billingsley, A. Van deVoorde, M. O'Connor, J.Q. Trojanowski, V.M.-Y. Lee, Biopsy-derived adult human brain tau is phosphorylated at many of the same sites as Alzheimer's disease paired helical filament tau, Neuron 13 (1994) 989–1002.
[39] M. Mercken, F. Grynspan, R.A. Nixon, Differential sensitivity to proteolysis by brain calpain of adult human tau, fetal human tau and PHF-tau, FEBS Lett. 368 (1995) 10–14.
[40] M. Morishima-Kawashima, M. Hasegawa, K. Takio, M. Suzuki, H. Yoshida, K. Titani, Y. Ihara, Poline-directed and nonproline-directed phosphorylation of PHF-tau, J. Biol. Chem. 270 (1995) 823–829.
[41] T. Ono, H. Yamamoto, K. Tashima, H. Nakashima, E. Okumura, K. Yamada, S. Hisanaga, T. Kishimoto, T. Miyakawa, E. Miyamoto, Dephosphorylation of abnormal sites of tau factor by protein phosphatases and its implication for Alzheimer's disease, Neurochem. Int. 26 (1995) 205–215.
[42] L. Otvos, L. Feiner, E. Lang, G.I. Szendrei, M. Goedert, V.M.-Y. Lee, Monoclonal antibody PHF-1 recognizes tau protein phosphorylated at serine residues 396–404, J. Neurosci. 39 (1994) 669–673.
[43] J.J. Pei, E. Sersen, K. Iqbal, I. Grundke-Iqbal, Expression of protein phosphatases (PP-1, PP-2A, PP-2B and PTP-1B) and protein kinases (MAP kinase and P34cdc2) in the hippocampus of patients with Alzheimer disease and normal aged individuals, Brain Res. 655 (1994) 70–76.
[44] J.J. Pei, C.X. Gong, K. Iqbal, I. Grundke-Iqbal, Q.L. Wu, B. Winblad, R.F. Cowburn, Subcellular localization of protein phosphatases and abnormally phosphorylated tau in the temporal cortex from Alzheimer's disease and control brains, J. Neural Transm. 105 (1998) 69–83.
[45] J.J. Pei, I. Grundke-Iqbal, K. Iqbal, N. Bogdanovic, B. Winblad, R. F Cowburn, Accumulation of cyclin-dependent kinase 5 (cdk5) in neurons with early stages of Alzheimer's disease neurofibrillary degeneration, Brain Res. 797 (1998) 267–277.
[46] S.L. Pelech, J.S. Sanghera, Mitogen-activated protein kinases: versatile transducers for cell signaling (Review), Trends Biochem. Sci. 17 (1992) 233–238.
[47] T.W. Reid, I.B. Wilson, *E. coli* alkaline phosphatase, in: P.D. Boyer (Ed.), The Ezymes, Vol. 4, Academic Press, Orlando, (1971) 373–415.
[48] J. Savory, Y. Huang, M.M. Herman, M.R. Wills, Quantitative image analysis of temporal changes in tau and neurofilament proteins during the course of acute experimental neurofibrillary degeneration; non-phosphorylated epitopes precede phosphorylation, Brain Res. 707 (1996) 272–281.
[49] A. Schneider, J. Biernat, M. von Bergen, E. Mandelkow, E.M. Mandelkow, Phosphorylation that detaches tau protein from microtubules (Ser262, Ser214) also protects it against aggregation into Alzheimer paired helical filaments, Biochemistry 38 (1999) 3549–3558.
[50] O. Schweers, E. Schonbrunn-Hanebeck, A. Marx, E. Mandelkow, Structural studies of tau protein and Alzheimer paired helical filaments show no evidence for β-structure, J. Biol. Chem. 269 (1994) 24290–24297.
[51] P. Seubert, M. Mawal-Dewan, R. Barbour, R. Jakes, M. Goedert, G.V.W. Johnson, J.M. Litersky, D. Schenk, I. Lieberburg, J.Q. Trojanowski, V.M.-Y. Lee, Detection of phosphorylated Ser262 in fetal tau, adult tau, and paired helical filament tau, J. Biol. Chem. 270 (1995) 18917–18922.
[52] E. Sontag, V. Nunbhakdi-Craig, G. Lee, G.S. Bloom, M.C. Mumby, Regulation of the phosphorylation state and microtubule-binding activity of tau by protein phosphatase 2A, Neuron 17 (1996) 1201–1207.
[53] E. Sontag, V. Nunbhakdi-Craig, G. Lee, R. Brandt, C. Kamibayashi, J. Kuret, C.L. White, M.C. Mumby, G.S. Bloom, Molecular interactions among protein phosphatase 2A, tau, and microtubules. Implications for the regulation of tau phosphorylation and the development of tauopathies, J. Biol. Chem. 274 (1999) 25490–25498.
[54] J.Q. Trojanowski, V.M.-Y. Lee, Phosphorylation of paired helical filament tau in Alzheimer's disease neurofibrillary lesions: focusing on phosphatases, FASEB J. 9 (1995) 1570–1576.
[55] J.Q. Trojanowski, M. Mawal-Dewan, M.L. Schmidt, J. Martin, V.M.-Y. Lee, Localization of the mitogen activated protein kinase ERK2 in Alzheimer's disease neurofibrillary tangles and senile plaque neurites, Brain Res. 618 (1993) 333–337.
[56] I. Vincent, P. Davies, A protein kinase associated with paired helical filaments in Alzheimer's disease, Proc. Natl. Acad. Sci. U. S. A. 89 (1992) 2878–2882.
[57] I. Vincent, G. Jicha, M. Rosado, D.W. Dickson, Aberrant expression of mitotic cdc2/cyclin B1 kinase in degenerating neurons of Alzheimer's disease brain, J. Neurosci. 17 (1997) 3588–3598.
[58] I. Vincent, J.H. Zheng, D.W. Dickson, Y. Kress, P. Davies, Mitotic phosphoepitopes precede paired helical filaments in Alzheimer's disease, Neurobiol. Aging 19 (1998) 287–296.
[59] J.Z. Wang, C.X. Gong, T. Zaidi, I. Grundke-Iqbal, K. Iqbal, Dephosphorylation of Alzheimer paired helical filaments by protein phosphatase-2A and -2B, J. Biol. Chem. 270 (1995) 4854–4860.
[60] J.Z. Wang, I. Grundke-Iqbal, K. Iqbal, Restoration of biological activity of Alzheimer abnormally phosphorylated tau by dephospho-

rylation with protein phosphatase-2A, -2B and -1, Brain Res. Mol. Brain Res. 38 (1996) 200–208.
[61] H. Yamamoto, M. Hasegawa, T. Ono, K. Tashima, Y. Ihara, E. Miyamoto, Dephosphorylation of fetal tau and paired helical filaments-tau by protein phosphatases 1 and 2A and calcineurin, J. Biochem. 118 (1995) 1224–1231.
[62] L.-S. Yang, H. Ksiezak-Reding, Calpain-induced proteolysis of normal human tau and tau associated with paired helical filaments, Eur. J. Biochem. 233 (1995) 9–17.
[63] L.-S. Yang, W. Gordon-Krajcer, H. Ksiezak-Reding, Tau released from paired helical filaments with formic acid or guanidine is susceptible to calpain-mediated proteolysis, J. Neurochem. 69 (1997) 1548–1558.
[64] H. Yoshida, Y. Ihara, Tau in paired helical filaments is functionally distinct from fetal tau: assembly incompetence of paired helical filament-tau, J. Neurochem. 61 (1993) 1183–1186.
[65] Q. Zheng-Fischhofer, J. Biernat, E.-M. Mandelkow, S. Illenberger, R. Godemann, E. Mandelkow, Sequential phosphorylation of Tau by glycogen synthase kinase-3beta and protein kinase A at Thr212 and Ser214 generates the Alzheimer-specific epitope of antibody AT100 and requires a paired-helical-filament-like conformation, Eur. J. Biochem. 252 (1998) 542–552.

Publikacja 4

Journal of Neurochemistry
Lippincott–Raven Publishers, Philadelphia

Tau Released from Paired Helical Filaments with Formic Acid or Guanidine Is Susceptible to Calpain-Mediated Proteolysis

Liang-Sheng Yang, Wanda Gordon-Krajcer, and Hanna Ksiezak-Reding

Department of Pathology, Albert Einstein College of Medicine, Bronx, New York, U.S.A.

Abstract: Paired helical filaments (PHFs), a characteristic neuropathologic finding in Alzheimer's disease brain, are abnormal fibrillary forms of hyperphosphorylated tau (PHF-tau), which have been shown to be highly resistant to calpain digestion. Either excessive phosphorylation or fibrillary arrangement of tau proteins in PHFs may play a role in proteolytic resistance by limiting access to calpain recognition/digestion sites. To determine the contribution of the fibrillary conformation, isolated PHFs were subjected to treatment with either formic acid or guanidine. Both procedures effectively abolished the fibrillary structure of PHF but preserved PHF-tau immunoreactivity using a panel of antibodies that recognize nonphosphorylated and phosphorylated epitopes. These treatments also significantly increased the sensitivity of PHF-tau polypeptides to calpain proteolysis as shown by significant decreases in the half-life ($t_{1/2}$) from the infinite with native PHF to 44 min and 4.4 min in formic acid- or guanidine-treated samples, respectively. In contrast, the sensitivity of normal fetal tau (3.4 min) was either decreased (5.9 min) or unaffected (3.6 min) by similar treatment. Our results indicate that after guanidine treatment, the sensitivity of PHF to calpain resembles that of fetal tau. These results strongly suggest that the fibrillary structure of PHF-tau, rather than hyperphosphorylation, is the major factor responsible for the resistance of abnormal filaments to calpain-mediated proteolysis. **Key Words:** Alzheimer's disease—Calpain—Formic acid—Guanidine—Paired helical filaments—Tau.
J. Neurochem. **69,** 1548–1558 (1997).

Calcium-activated neutral proteinases I and II (calpains; EC 3.4.22.17) have been postulated to play an important role in the degradation of neuronal cytoskeletal proteins including spectrin (Seubert et al., 1987; Siman et al., 1987); microtubule-associated protein 2 (MAP-2) (Sandoval and Weber, 1978; Johnson et al., 1992) and tau (Johnson et al., 1989). Several other roles of calpain have also been suggested, for example, in regulating the activity of proteins involved in signal transduction pathways such as protein kinases and phosphatases (Nixon, 1989; Wang et al., 1989) as well as a potential role in programmed cell death (Squier et al., 1994). Calpain I and II are nonlysosomal thiol proteinases characterized by distinct Ca^{2+} requirements, either in micromolar or millimolar range, respectively. In the presence of increased calcium concentrations, inactive forms of calpain undergo autoproteolytic cleavage and concomitant activation (Baki et al., 1996). Other mechanisms for calpain activation based on the translocation of calpain to the membrane and return to the quiescent state after dissociating from it have also been proposed (Molinari et al., 1994). An elevated activation ratio of calpain I has been demonstrated in Alzheimer's disease (AD) brain (Saito et al., 1993) possibly resulting from alterations in calcium homeostasis associated with this disorder (Mattson, 1994). Calpains have thus been suggested to be potential mediators of calcium-induced neuronal degeneration.

Proteins with high PEST scores [e.g., rich in sequences with proline (P), glutamic and aspartic acid (E), serine (S), and threonine (T)] and containing Ca^{2+}/calmodulin-binding regions have been shown to be preferential calpain substrates (Wang et al., 1989). MAPs including tau fall into this category. Tau proteins contain two amino acid sequences with high PEST scores surrounding the Ca^{2+}/calmodulin-binding region, which also coincides with the microtubule-binding domain (Lee and Wolff, 1984; Padilla et al., 1990). Immunoblotting analysis of calpain-proteolyzed tau fragments has localized most of the proteolytic sites to the C-terminal region of normal tau and within that region, primarily within the microtubule

Received March 4, 1997; revised manuscript received May 16, 1997; accepted May 20, 1997.

Address correspondence and reprint requests to Dr. H. Ksiezak-Reding at Department of Pathology, Room F-538, Albert Einstein College of Medicine, 1300 Morris Park Avenue, Bronx, NY 10461, U.S.A.

Dr. W. Gordon-Krajcer is a visiting scientist from the Department of Neurochemistry, Medical Research Centre of the Polish Academy of Science, 02-106 Warsaw, Poland.

Abbreviations used: AD, Alzheimer's disease; calpain, calcium-activated neutral proteinase; DAB, 3,3′-diaminobenzidine; ECL, enhanced chemiluminescence; EM, electron microscopy; MAP, microtubule-associated protein; PAGE, polyacrylamide gel electrophoresis; PHF, paired helical filaments; PEST, proline (P), glutamic and aspartic acid (E), serine (S), and threonine (T); SDS, sodium dodecyl sulfate.

binding domain (Yang and Ksiezak-Reding, 1995). Recent studies of calpain-mediated proteolysis revealed that PEST sequences do not always influence substrate susceptibility and that accessibility of calmodulin binding region appears to be critical for substrate proteolysis (Molinari et al., 1995).

Abnormal, fibrillary forms of tau proteins known as paired helical filaments (PHFs), accumulate in the brains of individuals affected with AD (Kidd, 1963; Grundke-Iqbal et al., 1986) and certain other neurodegenerative disorders (Trojanowski et al., 1993), including corticobasal degeneration (Feany et al., 1995), progressive supranuclear palsy (Flament et al., 1991), and Pick's disease (Murayama et al., 1990; Delacourte et al., 1996). The pathologic accumulation of PHFs could be the result of impairments in proteolytic degradation pathways in these various neurodegenerative disorders. Administration of proteolytic inhibitors to animals appears to support such a hypothesis because certain features of neurodegenerative process can be observed in these subjects (Ivy, 1992). However, postmortem analysis of brain tissue from patients with neurodegenerative diseases has shown that the activity of many proteolytic enzymes is increased (Backstrom et al., 1992; Saito et al., 1993) rather than decreased, suggesting that enhanced proteolytic resistance of accumulating proteins may be an important contributing factor in the neurodegenerative process. Previous results from this (Yang and Ksiezak-Reding, 1995) and other laboratories (Mercken et al., 1995) have provided experimental evidence for this hypothesis by demonstrating enhanced proteolytic resistance of fibrillary forms of tau in vitro in comparison with normal tau proteins. According to those studies, calpain recognition/digestion sites may be blocked in PHFs.

In vitro and in situ phosphorylation of certain amino acid residues has been found to reduce the rate of proteolytic degradation of normal tau by calpain (Litersky and Johnson, 1992, 1995). Therefore, the high phosphate content of fibrillary tau as shown by immunocytochemistry, western blotting, and direct phosphate analysis (Grundke-Iqbal et al., 1986; Ksiezak-Reding et al., 1992; Kopke et al., 1993), may be a major factor in the higher resistance of PHFs to proteolytic degradation. Recently, however, such a role for hyperphosphorylation has been questioned (Mercken et al., 1995; Yang and Ksiezak-Reding, 1995).

In the present study, we sought to determine directly the contribution of fibrillary conformation in the resistance of PHFs to calpain proteolysis. We used two different reagents, formic acid and guanidine, to abolish the fibrillary structure of PHFs. We observed that both these treatments were very effective in increasing the sensitivity of PHFs to calpain. In particular, with guanidine treatment, the sensitivity of PHFs to degradation by calpain was comparable with that observed with fetal tau, with similar high phosphate content.

MATERIALS AND METHODS

Materials

Alkaline phosphatase (*Escherichia coli,* type III) and calpain II (rabbit skeletal muscle) were obtained from Sigma (St. Louis, MO, U.S.A.). Enhanced chemiluminescence system (ECL) and 10-nm immunogold were purchased from Amersham Life Science Inc. (Arlington Heights, IL, U.S.A.) and 88% formic acid was from Fisher Scientific (Pittsburgh, PA, U.S.A.). Substrates for phosphatase (5-bromo-4-chloro-3-indolylphosphate and nitro blue tetrazolium; one-component substrates) were obtained from Kirkegaard and Perry Laboratories (Gaithersburg, MD, U.S.A.). VectaStain kits were from Vector Laboratories (Burlingame, CA, U.S.A.). Copper grids for electron microscopy (EM) were purchased from Fullam Inc. (Latham, NJ, U.S.A.).

Tissue

Brain tissue was obtained from two AD patients, a 74-year-old woman and a 78-year-old man. Postmortem delays were 5 and 8 h, respectively. Tissue was derived from frontal and temporal lobes and contained two to 12 neurofibrillary tangles per 40× objective field. The diagnosis of AD was based on age-dependent modified criteria (Khachaturian, 1985). Brains from aborted fetuses were ~19–21 weeks of gestation. Tissue was stored frozen at −80°C until used. Protocols for the use of human material were approved by the Committee for Clinical Investigation.

PHFs and fetal tau

Protein fractions enriched in PHFs were obtained from AD brains as Sarcosyl-insoluble 100,000-*g* pellets according to previously described procedures (Ksiezak-Reding and Wall, 1994). In some experiments, further purification of PHFs on sucrose density gradients was performed and fraction A2, which sedimented in a 1 *M* sucrose layer, was collected. Fetal tau was obtained by heat and perchloric acid treatments as previously reported (Ksiezak-Reding et al., 1992). In some experiments, fetal tau was subjected to dephosphorylation by incubation of samples with alkaline phosphatase (15 IU/mg of protein/ml) for 24 h at 37°C in buffer containing 0.1 *M* Tris-HCl, pH 8, and 1 m*M* phenylmethylsulfonyl fluoride.

Digestion with calpain

PHF preparations or fetal tau were incubated for 0–90 min at 30°C with or without calpain in a buffer containing 50 m*M* Tris-HCl, pH 7.5, 100 m*M* NaCl, 2 m*M* dithiothreitol, 1 m*M* EDTA, and 5 m*M* $CaCl_2$. Calpain was used at 3.3 U/mg of protein and a calpain to protein ratio was kept constant at 1:1. The reaction was initiated by the addition of $CaCl_2$. In samples prepared for sodium dodecyl sulfate–polyacrylamide gel electrophoresis (SDS-PAGE), the reaction was terminated by the addition of SDS-sample buffer and boiling for 5 min. After cooling, were samples were spun at 10,000 *g* for 5 min and SDS-soluble supernatants were loaded onto gels. In samples subjected to EM, the reaction was terminated by the addition of 20 m*M* EGTA and cooling on ice.

Gel electrophoresis and immunoblotting

Electrophoresis was performed using 10% polyacrylamide SDS-PAGE (minigels). Separated proteins were electrotransferred onto nitrocellulose membrane, incubated with 5% fat-free milk (Carnation), and subjected to immunoblotting with tau antibodies. In some experiments, electroblots were

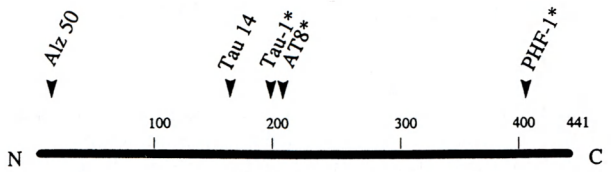

FIG. 1. Schematic diagram of the longest tau isoform and epitopes for the antibodies used in the present studies. Asterisks mark epitopes that are phosphorylated in PHFs. The respective amino acid sequences marked with arrows are recognized by Alz 50 (Ksiezak-Reding et al., 1995), Tau 14 and Tau-1 (Kosik et al., 1988), AT8 (Biernat et al., 1992), and PHF-1 (Otvos et al., 1994) in the longest human tau isoform (Goedert et al., 1989). For the AT8 and PHF-1 binding, phosphorylated serine(s) is required, whereas for the Tau-1 binding nonphosphorylated serine is needed. In addition to the N-terminal tau region, efficient binding of Alz 50 depends on the other region in the C-terminus (Carmel et al., 1996; Jicha et al., 1997) not marked in the diagram.

incubated with alkaline phosphatase (10 IU/ml) for 2 h at 37°C before incubation with milk. Secondary antibodies were either peroxidase- or alkaline phosphatase-conjugated immunoglobulins or ABC VectaStain kit reagents. To detect bound immunoglobulins, either an ECL or individual substrates for peroxidase [hydrogen peroxide and 3,3′-diaminobenzidine (DAB)] or phosphatase (5-bromo-4-chloro-3-indolyl phosphate and tetrazolium blue; one-component substrates) were used.

Formic acid and guanidine treatments

Samples were treated with formic acid by mixing PHFs or fetal tau samples with 10 volumes of 88% formic acid for 1 h at room temperature. Samples were then diluted with distilled water to a 20% final concentration of formic acid and lyophilized for at least 24 h. Freeze-dried samples were suspended (reconstituted) in original volume of 0.1 *M* Tris-HCl, pH 7.5, and adjusted to pH 7.5 with NaOH. For guanidine treatment, samples of PHFs or fetal tau were incubated with 4 *M* guanidine-HCl for 1 h at room temperature. Samples were then dialyzed overnight at 4°C in the buffer containing 50 m*M* Tris-HCl, pH 7.5, 2 m*M* dithiothreitol, and 1 m*M* EDTA and then concentrated to the original volume by using Centriprep-30 (Amicon, Beverly, MA, U.S.A.). Both treatments had an inhibitory effect on solubility of proteins in SDS compared with that in untreated samples. The solubility of samples was examined after addition of SDS sample buffer containing SDS and β-mercaptoethanol (both at 2% final concentration) but no bromophenol blue, boiling for 5 min, and centrifugation at 10,000 *g* for 5 min at room temperature. The protein content in SDS-soluble supernatant or other fractions was determined by microassay (Bio-Rad Laboratories, Hercules, CA, U.S.A.).

Antibodies

Five monoclonal antibodies were used that recognize distinct regions of the tau molecule (Fig. 1). Alz 50 and PHF-1 were obtained from Dr. Peter Davies (Albert Einstein College of Medicine, Bronx, NY, U.S.A.). Tau-1 was provided by Dr. Lester Binder (Northwestern University Medical School, Chicago, IL, U.S.A.), AT8 was a generous gift from Innogenetics (Ghent, Belgium), and Tau 14 was obtained commercially (Zymed Laboratories, San Francisco, CA, U.S.A.). Antibodies were diluted in 5% fat-free milk in 10 m*M* Tris-HCl, pH 7.4, and 150 m*M* NaCl. Dilutions for immunoblotting were between 1:10 and 1:1,000.

Quantitative analysis

The intensity of immunoreactivity was quantified on nitrocellulose membranes or ECL x-ray films by densitometric scanning using an LKB Ultrascan XL Enhanced Laser Densitometer (Pharmacia, Uppsala, Sweden). In PHF samples, the region of 58–68 kDa corresponding to full-length polypeptides of PHF-tau was scanned, whereas in samples of fetal tau the major polypeptide region of 55 kDa was considered. Positive controls were identical samples without added calpain (100% immunoreactivity). For statistical analysis, Student's *t* test was used.

Electron microscopy and immunogold labeling

Samples of PHFs (25–50 μl) were deposited for 5 min on 200-mesh copper grids precoated with Formvar and carbon and stained for 5 min with 2% uranyl acetate. Before uranyl acetate staining, some samples were subjected to 10-nm immunogold labeling using antibody Tau 14 at 1:1,000 dilution as previously described (Ksiezak-Reding and Yen, 1991). Samples on grids were examined using JEOL 100CX and JEOL 100S electron microscopes.

RESULTS

PHF: formic acid and guanidine treatments

Untreated, native fractions of PHFs subjected to SDS-PAGE and western analysis (Fig. 2A) revealed the presence of three major polypeptides of PHF-tau of 60, 64, and 68 kDa. These polypeptides were immunoreactive with phosphorylation-dependent (AT8 and PHF-1) as well as with phosphorylation-independent antibodies (Alz 50 and Tau 14). These polypeptides, however, were not immunoreactive with Tau-1 unless prior phosphatase treatment of electroblots was performed. The overall pattern of immunoreactivity of PHF samples was consistent with that previously described (Ksiezak-Reding et al., 1992; Yang and Ksiezak-Reding, 1995). In addition to three major polypeptides of PHF-tau, a high molecular mass smear of ~200 kDa was also detected. The immunoreactivity of the smear was similar to that of the three polypeptides of PHF-tau, suggesting that this material contained PHF-tau polymers, a result of cross-linking, ubiquitination, or other posttranslational modifications of these polypeptides (Morishima and Ihara, 1994).

Immunoreactivity of PHF-tau polypeptides in samples treated with formic acid was observed as either diffuse staining of ~58–68 kDa, e.g., with Alz 50 or AT8, or as a distinct six-band pattern, e.g., with Tau 14 or PHF-1 (Fig. 2C). In this respect, the pattern of immunoreactivity differed from that of untreated controls. Moreover, the overall immunoreactivity of PHF-tau polypeptides and that of high molecular weight smear appeared to be reduced from that of untreated controls in spite of comparable protein content in both fractions. The reduction in immunoreactivity could be due to a lower solubility of formic acid treated proteins in SDS-sample buffer. The SDS-soluble su-

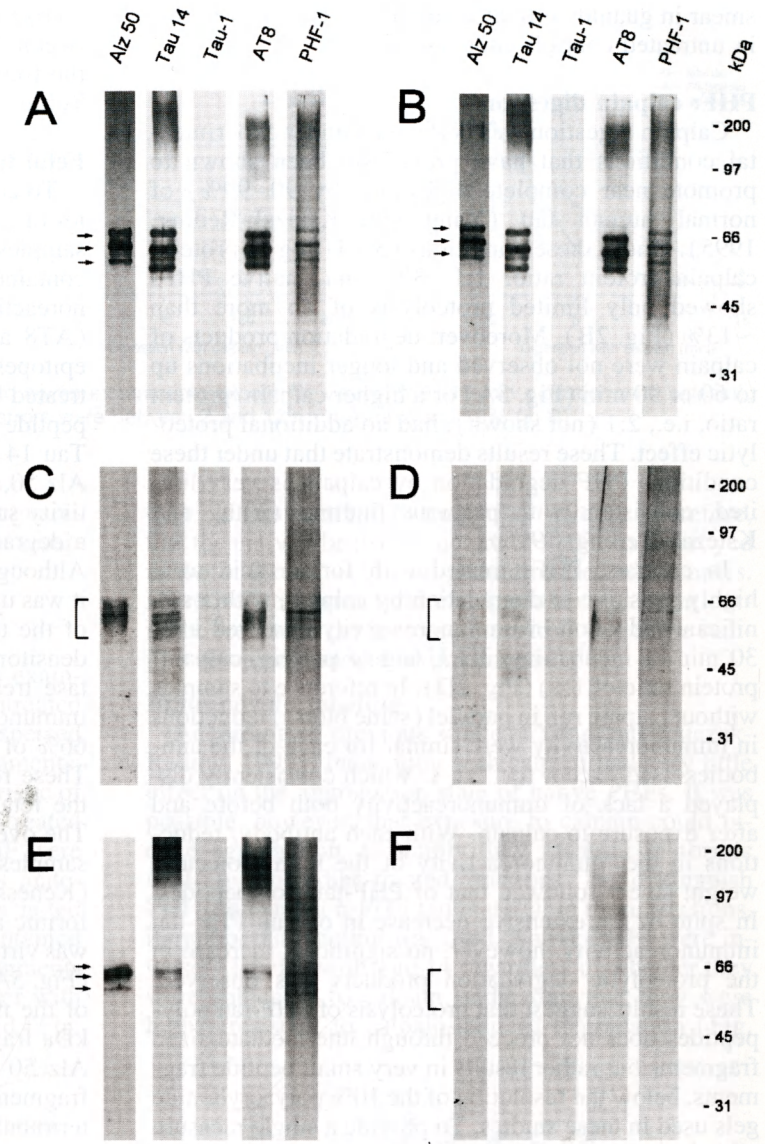

FIG. 2. Calpain digestion of native, formic acid-, or guanidine-treated PHFs (western blotting). Native (**A** and **B**), formic acid-treated (**C** and **D**), and guanidine-treated (**E** and **F**) samples of PHFs were incubated without (**left panels**) or with calpain (**right panels**) for 30 min at 30°C. Calpain concentration was 3.3 U/mg of protein/ml and the calpain/protein ratio was kept constant at 1:1. Proteins were separated by SDS-PAGE and immunoblotted with tau antibodies as indicated. Bound immunoglobulins were detected with ECL (E and F) or VectaStain. For each antibody and treatment, identical amounts of protein were used in samples with or without calpain. Moreover, samples with or without calpain were always run on the same gel to allow for a proper quantitation. The protein loading was between 2 and 6 μg/lane for most antibodies, except for PHF-1, which required only 0.2–0.6 μg/lane. The protein loading refers to the total protein content and does not reflect different solubility of PHF fractions in SDS-sample buffer used before electrophoresis. The polypeptides of PHF-tau migrated at 60, 64, and 68 kDa as a triplet (arrows) or a diffuse set of polypeptides (brackets). Molecular mass standards are indicated in kilodaltons.

pernatants prepared from these fractions were determined to contain 34% less protein ($n = 5$) than that in controls. These results suggest that some of PHF-tau polypeptides were irreversibly denatured by the treatment and remained in SDS-insoluble pellets. Formic acid-treated PHF displayed no immunoreactivity with Tau-1, indicating that this epitope remained phosphorylated similar to untreated samples. Although overall immunoreactivity of PHF-tau polypeptides presented a more diffuse pattern, there was no evidence for either partial amino-terminal degradation (Alz 50) or dephosphorylation. In particular, no alterations in electrophoretic mobility were observed with phosphorylation-dependent antibodies (PHF-1 or AT8) or increases in the immunoreactivity with phosphorylation-blocked antibody (Tau-1). We cannot rule out the possibility, however, that a small amount of PHF material underwent degradation.

PHF samples treated with guanidine displayed immunoreactivity that resembled that of the three major PHF-tau polypeptides of 60, 64, and 68 kDa, except that the 64-kDa polypeptide was present as a doublet and staining of the 60- and 68-kDa polypeptides was reduced (Fig. 2E). As with formic acid-treated PHFs, these changes could be due to a lower SDS solubility of the PHF material treated with guanidine (by 18%, $n = 5$), demonstrated with SDS-sample buffer supernatants. Moreover, some of the proteins could undergo guanidine-induced degradation. The immunoreactivity of the high molecular weight smear with Tau 14 and AT8 appeared stronger in guanidine-treated samples (detected with ECL) than in untreated controls (detected with DAB). This was due to the use of an ECL detection system, necessary with these samples (see below) rather than to the enhanced, guanidine-induced aggregation of PHFs. Using DAB, intensity of the

smear in guanidine-treated samples was similar to that in untreated controls (not shown).

PHF: calpain digestion

Calpain digestion was performed under experimental conditions that have previously been shown to promote near complete digestion (by 90–99%) of normal human tau (Yang and Ksiezak-Reding, 1995). Under these conditions (3.3 U/mg of protein; calpain/protein ratio, 1:1; 30 min), native PHFs showed only limited proteolysis of no more than ~13% (Fig. 2B). Moreover, degradation products of calpain were not observed and longer incubations up to 60 or 90 min (Fig. 3A) or a higher calpain/protein ratio, i.e., 2:1 (not shown), had no additional proteolytic effect. These results demonstrate that under these conditions PHF degradation by calpain is very limited, consistent with previous findings (Yang and Ksiezak-Reding, 1995).

In contrast, PHFs treated with formic acid were highly sensitive to degradation by calpain, with a significant reduction in immunoreactivity observed after 30 min of incubation (3.3 U/mg of protein, calpain/protein ratio of 1:1) (Fig. 2D). In reference to samples without calpain run in parallel (same blots), reductions in immunoreactivity were similar for each of the antibodies used except for Tau-1, which consistently displayed a lack of immunoreactivity both before and after exposure to calpain. With each antibody, reductions in the immunoreactivity of the high molecular weight smear followed that of PHF-tau polypeptides. In spite of the extensive decrease in overall PHF-tau immunoreactivity, however, no significant increase in the proteolytic degradation products was observed. These results suggest that proteolysis of PHF-tau polypeptides does not proceed through intermediate-sized fragments but rather results in very small peptide fragments, below the resolution of the 10% polyacrylamide gels used in these studies. To provide a single measure allowing us to compare susceptibility of various proteins to calpain, we calculated half-life ($t_{1/2}$) values. Although usually referred to processes in vivo, in our studies in vitro, the $t_{1/2}$ values were defined as the time required to reduce by 50% the content of full-length fetal tau or PHF-tau polypeptides under specific conditions (3.3 U of calpain/mg of protein at 30°C and a calpain/protein ratio of 1:1). Accordingly, considering decreases in PHF-tau polypeptides immunoreactivity during 10–90 min of incubation, an average $t_{1/2}$ of PHF treated with formic acid was calculated to be ~44 min (Fig. 3A and Table 1).

Guanidine-treated PHFs were even more sensitive to calpain digestion than formic acid-treated samples, and to detect tau immunoreactivity, it was necessary to use a more sensitive technique, ECL. After guanidine treatment, only traces of immunoreactivity were detectable after 30 min of exposure to calpain (Fig. 2F), and to accurately determine $t_{1/2}$ shorter incubation times were introduced. Time course experiments performed with incubations between 5 and 90 min revealed that an average $t_{1/2}$ for the four epitopes of tau was ~4.4 min (Fig. 3A and Table 1).

Fetal tau

To compare the proteolytic sensitivity of formic acid- or guanidine-treated PHFs with that of normal tau, samples of fetal tau were obtained. Untreated fetal tau contained a major 55-kDa polypeptide that was immunoreactive with antibodies to both phosphorylated (AT8 and PHF-1) and nonphosphorylated (Tau 14) epitopes as well as with Tau-1 antibody (Fig. 4). Untreated samples also contained a minor 52-kDa polypeptide that was reactive with two of the antibodies, Tau 14 and Tau-1, but lacked immunoreactivity with Alz 50, AT8, and PHF-1. This selective immunoreactivity suggests that the 52-kDa polypeptide represents a degraded or dephosphorylated 55-kDa polypeptide. Although fetal tau displayed Tau-1 immunoreactivity, it was unclear whether all the protein or only a fraction of the total protein bound Tau-1 antibody. However, densitometric analysis revealed that alkaline phosphatase treatment (before SDS-PAGE) increased Tau-1 immunoreactivity 1.5-fold, demonstrating that only 66% of native fetal tau bound the antibody ($n = 5$). These results suggest that approximately one-third of the fetal tau is phosphorylated at the Tau-1 epitope. The overall immunoreactivity of fetal tau in untreated samples was consistent with that reported previously (Kenessey and Yen, 1993). The immunoreactivity of formic acid- or guanidine-treated samples of fetal tau was virtually unchanged from that of untreated samples (Fig. 5A–C). In all samples, Alz 50 immunoreactivity of the major 55-kDa polypeptide and that of 36–39-kDa fragments were detected. The preservation of the Alz 50 immunoreactivity in 36–39-kDa endogenous fragments suggests that they derived from the amino-terminal region of tau.

A time course of proteolytic degradation revealed rapid degradation of fetal tau in all preparations. By 10–15 min, the immunoreactivity of the major 55-kDa polypeptide decreased to <20% of the control (Fig. 3B). The decreases were accompanied by increases in the immunoreactivity of 36–39-kDa polypeptides, which comigrated with the endogenous fragments (Fig. 5A–C). A newly generated 33-kDa fragment was most evident in formic acid-treated samples, suggesting that in these preparations tau was degraded at a slower rate (Fig. 5B, asterisk). The overall pattern of calpain-induced degradation products was similar to that described previously (Yang and Ksiezak-Reding, 1995). Based on values from two to seven experiments, the estimated $t_{1/2}$ for the Alz 50 epitope was ~3.4 min in controls and 3.6 min in guanidine-treated samples (Table 1). Formic acid-treated preparations were proteolyzed at a slower rate and the estimated $t_{1/2}$ was significantly higher (5.9 min, $p < 0.05$). These results indicate that formic acid treatment renders tau

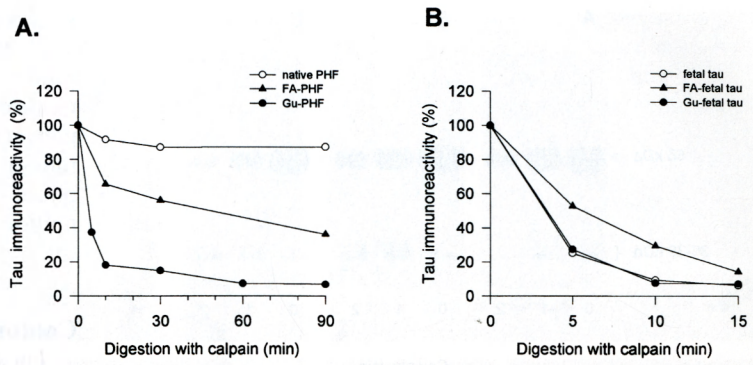

FIG. 3. Calpain digestion of PHF (**A**) and fetal human tau (**B**) in untreated (○—○), formic acid- (FA; ▲—▲), or guanidine- (Gu; ●—●) treated samples: quantitative analysis of immunoblots. Various preparations of PHF or fetal tau were digested for indicated periods of time with calpain (3.3 U/mg of protein/ml), proteins were separated by SDS-PAGE and immunoblotted with tau antibodies. Immunoreactivity of full-length polypeptides of PHF-tau between 60 and 68 kDa and a major 55-kDa polypeptide of fetal tau were quantified by densitometric scanning. In PHF samples, scanning was either for Alz 50 alone (guanidine-treated PHF) or Alz 50, Tau 14, AT8, and PHF-1 (native and formic acid-treated PHF). In fetal tau samples, scanning was for Alz 50. Values were expressed as percentage of control samples without added calpain and were from three to seven experiments except for values in B (15-min digestion with calpain), which were only from two experiments. The standard errors were between 2 and 12% (in A) or 2 and 10% (in B).

protein more resistant to calpain proteolysis, yet guanidine treatment induces no apparent difference in sensitivity.

Ultrastructure of PHFs after formic acid or guanidine

The ultrastructural appearance of PHFs was examined in uranyl acetate-stained samples. In untreated preparations, which had the appearance of a dispersed and nonaggregated population of individual filaments, twisted 15–20-nm-diameter filaments characteristic of PHF were observed (Fig. 6A). In formic acid-treated samples, twisted filaments characteristic of PHF were rarely detected (Fig. 6B). Instead, amorphous material, which resembled unwound filaments was noted (Fig. 6B, arrow). Guanidine-treated samples contained few filamentous structures. Instead, small fragments and granular material of ~5–20 nm in diameter with little resemblance to native PHFs were detected (Fig. 6C). Ultrastructural examination reveals, therefore, that the native fibrillary structure of PHF was destroyed in both formic acid- or guanidine-treated samples. Moreover, ultrastructural changes after treatment correlate well with the increased sensitivity of these samples to calpain-mediated proteolysis.

Immunogold labeling

According to previous studies (Yang and Ksiezak-Reding, 1995), incubation with calpain had very little effect on the aggregation state of native PHFs. It was possible, however, that exposure to calpain could induce aggregation of nonfibrillary material in formic acid- or guanidine-treated fractions. To distinguish PHF-tau from non-PHF-tau material in these fractions, immunogold labeling was used. Native PHFs were intensely labeled with Tau 14 regardless of whether they were subjected to calpain, indicating that they were highly resistant to calpain-induced degradation (Fig.

TABLE 1. *The half-life of PHF and fetal human tau before and after formic acid or guanidine treatments: calpain-mediated proteolysis*

Treatment	PHF	Fetal tau
None	⩾90 (4)	3.4 ± 0.2 (6)
Formic acid	44 ± 9 (4)	5.9 ± 1.0 (4)[a]
Guanidine	4.4 ± 1.0 (3)[b,c]	3.6 ± 0.4 (6)[d]

Samples were incubated with calpain 3.3 U/mg of protein for 0–90 min (PHF) or 0–15 min (fetal tau), separated on SDS-PAGE, and immunoblotted with tau antibodies. The $t_{1/2}$ values were estimated for full-length polypeptides of PHF-tau (60–68 kDa) or fetal tau (55 kDa) by densitometric scanning of respective areas on immunoblots and comparisons with controls (100%) containing no calpain (see also Figs. 2 and 5). For native and formic acid-treated PHFs, immunoblots with Alz 50, Tau 14, AT8, and PHF-1 were used. For fetal tau or guanidine-treated PHFs, immunoblots with Alz 50 were scanned. Values are means ± SEM in minutes for the number of experiments in the parentheses.

[a] $p < 0.05$ vs. other fetal tau samples.
[b] $p < 0.001$ vs. formic acid-treated PHFs.
[c] NS vs. tau samples.
[d] NS vs. not treated tau or guanidine-treated PHFs.

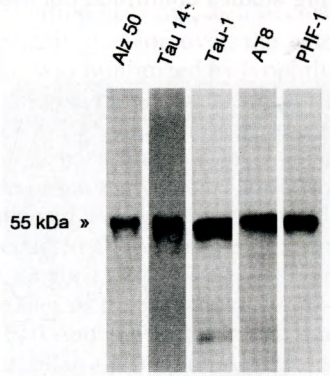

FIG. 4. Immunoreactivity of fetal tau on immunoblots (controls). Untreated samples of fetal tau were separated by SDS-PAGE and immunoblotted with tau antibodies as indicated. A major 55-kDa polypeptide was immunoreactive with all antibodies, but a minor 52-kDa component was immunoreactive only with Tau 14 and Tau-1. Fetal tau was phosphorylated in at least three epitopes, AT8, PHF-1, and Tau-1. As demonstrated with alkaline phosphatase treatment before SDS-PAGE, Tau-1 epitope was phosphorylated in at least one-third of the total protein (not shown). Protein loading was between 0.5 and 1 μg/lane.

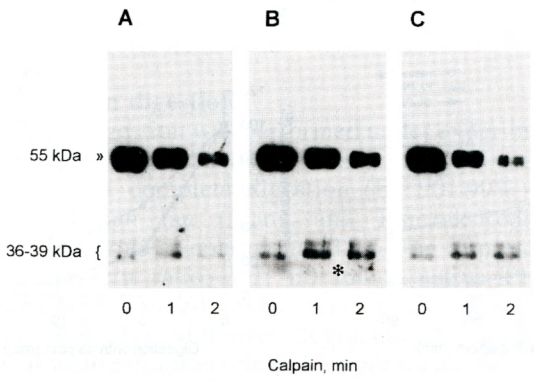

FIG. 5. Immunoreactivity of fetal tau during calpain digestion; untreated controls (**A**), formic acid-treated (**B**), or guanidine-treated samples (**C**). Samples of fetal tau were digested for 0, 1, and 2 min with calpain (3.3 U/mg of protein/ml) as indicated and immunoblotted with Alz 50. A decrease in the immunoreactivity of a major 55-kDa polypeptide was observed in all samples. An increase in the 36–39-kDa degradation products, which co-migrated with endogenous fragments, was most prominent in formic acid-treated samples. These samples also displayed a newly calpain-generated fragment of 33 kDa (asterisk). Protein loading was 1.4 μg/lane.

7A and B). Ultrastructurally, native PHFs remained mostly dispersed and nonaggregated. Formic acid-treated PHFs displayed immunogold labeling of both amorphous material and distorted filaments characteristic of these samples (Fig. 7C). With calpain digestion, the intensity of the gold label was generally diminished and aggregation of PHF material was minimal. Guanidine-treated samples displayed immunodecoration of structures resembling small fragments or amorphous material. With calpain digestion, very little ultrastructural features or aggregates were observed and immunogold particles were sparse. The results of immunolabeling studies confirmed our western analysis demonstrating that native PHFs were mostly insensitive to calpain digestion and that nonfibrillary preparations of PHF obtained with formic acid or guanidine treatments were, in contrast, highly sensitive to calpain-mediated proteolysis. Moreover, the results of immunogold studies suggest that proteolysis of the amorphous, nonfibrillary PHF material does not induce formation of filamentous or amorphous PHF aggregates.

DISCUSSION

Conformation and susceptibility to calpain

These studies provide direct evidence that PHFs, which are extremely resistant to calpain degradation in their native, fibrillar conformation, can be efficiently proteolyzed after treatment with either 88% formic acid or 4 *M* guanidine. This increase in proteolytic sensitivity is clearly associated with the destruction of the fibrillar structure, because a dramatic change from a fibrillar to nonfibrillar, amorphous conformation is observed with ultrastructural analysis. Despite the ultrastructural alterations, the native phosphorylation state of PHF was preserved in treated samples as demonstrated by binding of both phosphorylation-dependent and phosphorylation-blocked antibodies. These results suggest that with the phosphorylation state of PHF preserved, disruption of the filamentous structure significantly improves access to calpain recognition and digestion sites.

Comparisons of PHFs and normal fetal tau proteins treated with guanidine and subjected to calpain revealed a similar rate of proteolysis for both species of tau proteins ($t_{1/2}$ values of 4.4 min and 3.6 min, respectively). Thus, the proteolytic sensitivity of PHFs appeared to be restored to a level comparable with that of normal tau and in the absence of any significant biochemical alterations except for a small reduction (by 18%) in SDS solubility. As shown by western

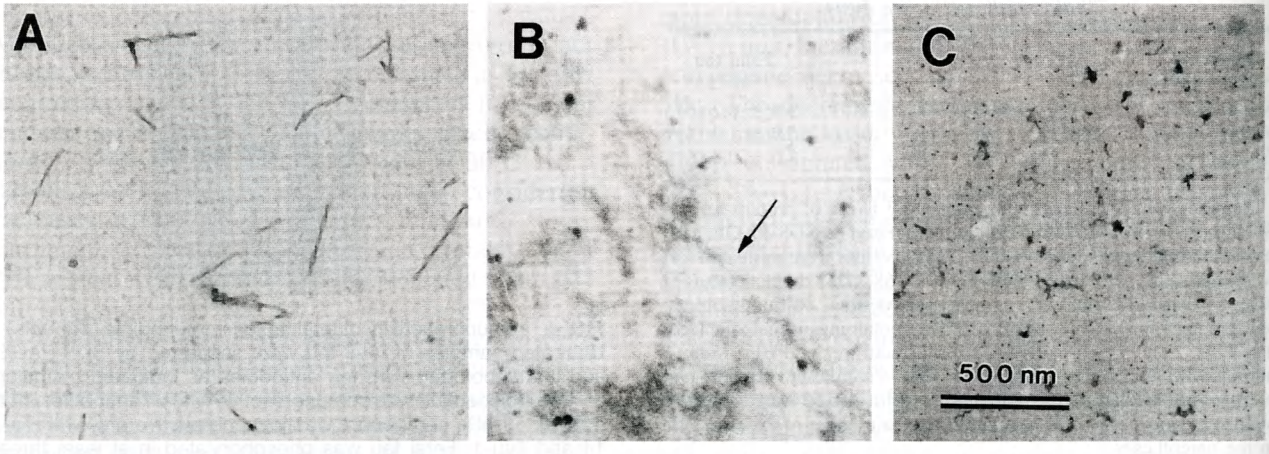

FIG. 6. Electron photomicrographs of native PHFs (**A**) and PHFs treated with formic acid (**B**) or guanidine (**C**), stained with 2% uranyl acetate. Note the presence of dispersed and short filaments characteristic of PHFs in A and the absence of filaments in B and C. In B, formic acid-treated samples display amorphous material and distorted filament-like structures (arrow). In C, material is predominantly amorphous or granular. Both treatments destroyed the ultrastructure of filaments. Scale bar represents 500 nm.

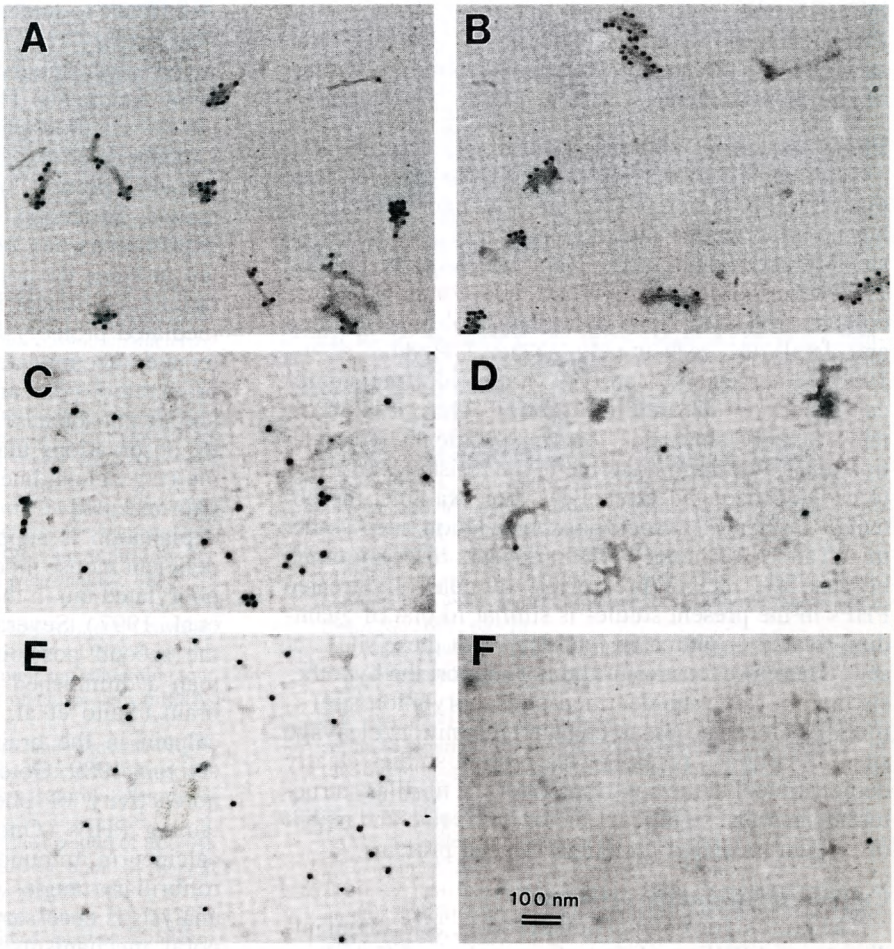

FIG. 7. Immunogold labeling of native PHFs (**A** and **B**), PHFs treated with formic acid (**C** and **D**), or guanidine (**E** and **F**) before and after calpain-induced proteolysis, respectively. Native PHFs display intense decoration of filaments with Tau 14 either before or after calpain digestion (3.3 U/mg of protein/ml, 30 min). In the absence of calpain, formic acid- or guanidine-treated samples show heavy labeling of amorphous material (in C and E, respectively). With calpain, immunogold labeling is either markedly reduced (as in D) or practically abolished (as in F). In calpain-digested material, formation of tau aggregates is not apparent. Samples were stained with uranyl acetate. Scale bar represents 100 nm.

analysis and electrophoretic mobility studies, guanidine treatment was without apparent effects on phosphorylation patterns of either fetal tau or PHF. The results of these proteolytic studies are similar to those obtained by other groups examining dephosphorylation of PHF. In these studies, guanidine-treated PHFs displayed a significantly increased sensitivity to phosphatase treatment, and in contrast to native PHFs (Ksiezak-Reding et al., 1992), could undergo efficient dephosphorylation (Goedert et al., 1992; Greenberg et al., 1992; Yoshida and Ihara, 1993). Moreover, guanidine-treated, dephosphorylated PHFs were biologically active and capable of promoting microtubule assembly similar to that observed with normal tau (Yoshida and Ihara, 1993). The inhibitory effect of guanidine treatment on solubility of PHFs in SDS has not been reported previously.

In comparison with PHFs treated with guanidine, formic acid-treated samples were less efficiently digested. This was observed with both fetal tau and PHF, suggesting that formic acid introduced changes in the protein structure that prolonged or inhibited proteolysis. For example, formic acid treatment is known to chemically interact with serine residue(s), resulting in formylation of the target residue (Klunk et al., 1994). This covalent modification, however, was not detected with our tau antibodies, e.g., as a decrease or increase in immunoreactivity. Moreover, the potential for such modifications was minimized by lyophilization of samples using diluted rather than concentrated solutions of formic acid. The dilution of formic acid before lyophilization has been found to reverse possible esterification and to promote hydrolysis of formylated derivatives (Klunk and Pettegrew, 1990). If minimal formylation occurred despite these precautions, it could explain the longer $t_{1/2}$ that was observed with calpain or explain either diffuse or a distinct six-band staining pattern of PHF-tau polypeptides on immunoblots. It could also explain the impaired solubility of PHFs in SDS-sample buffer and the fact that the SDS solubility was affected more by formic acid than guanidine treatment. It is uncertain whether formylation of serine has similar consequences in the structure and function of tau as mutation of serine to aspartate, reported to imitate phosphorylation-induced changes (Leger et al., 1997). A detailed mechanism of the interaction of formic acid with PHFs or tau is still forthcoming. Nevertheless, formic acid-treated PHFs displayed significant

improvement in proteolytic sensitivity over native PHFs, suggesting that the abolition of the fibrillar structure was more significant than the inhibitory effect of formic acid alone.

Phosphorylation and susceptibility to calpain

With regard to normal tau, previous data indicate that phosphorylation of the Tau-1, AT8, or PHF-1 sites has no effect on the rate of calpain-mediated proteolysis (Mercken et al., 1995; Yang and Ksiezak-Reding, 1995). Furthermore, differences in the total phosphate content, from 2 to 7 mol phosphate/mol between adult and fetal tau, respectively (Ksiezak-Reding et al., 1992; Kenessey and Yen, 1993), also have no significant effects on the rate of digestion. Thus, it is uncertain whether "abnormal" or AD-specific phosphorylation plays any significant role in the resistance of PHFs to calpain-mediated proteolysis. For example, the potential influence of such phosphorylation sites (other than Tau-1, AT8, and PHF-1) appears to be minimal, because the rate of proteolysis of guanidine-treated PHFs in the present studies is similar to that of guanidine-treated or untreated fetal tau, with these sites absent. Therefore, our results do not support the hypothesis that an as-yet-unidentified phosphorylation site(s) in PHFs blocks access to calpain recognition/cleavage sites. In contrast, results of the present studies clearly demonstrate that the contribution of the fibrillary structure is the most significant factor in the rate and extent of calpain-mediated proteolysis of tau proteins.

Calpain degradation products

The proteolytic degradation of formic acid- or guanidine-treated PHFs and that of normal tau differs in at least two aspects. First, no intermediate degradation products of PHFs accumulate, presumably being rapidly proteolyzed to smaller fragments. In contrast, with normal tau, large amino-terminal fragments are very prominent during proteolysis and often remain undigested in the absence of parental polypeptides (Yang and Ksiezak-Reding, 1995). Second, the present studies demonstrate that in PHFs, both the amino- and carboxyl-terminal regions (e.g., Alz 50 and PHF-1) appear to be equally sensitive to calpain, whereas in normal tau the carboxyl terminus is distinctly more sensitive. These comparisons indicate that treatment with formic acid or guanidine alone does not restore to PHF all of the proteolytic properties of normal tau. In other studies using binding to tubulin as functional criteria, mechanical treatment such as sonication of PHFs (Iqbal et al., 1994) or treatment with guanidine (Yoshida and Ihara, 1993), both followed by dephosphorylation, resulted in practically full recovery of tau function.

Calpain and AD

It has been postulated that nonfibrillary, hyperphosphorylated PHF-tau accumulates in AD brains before formation of PHFs (Bancher et al., 1989; Kopke et al., 1993). Although this is a likely sequence of events, it is difficult to understand how a significant amount of nonfibrillary PHF-tau may accumulate without undergoing dephosphorylation or proteolytic digestion to small fragments. The sensitivity of nonfibrillary PHF-tau to alkaline phosphatase (Goedert et al., 1992; Greenberg et al., 1992; Yoshida and Ihara, 1993) or calpain (present studies) has already been demonstrated. To reconcile these apparent discrepancies, two explanations can be offered. (1) Unassembled PHF-tau proteins do not accumulate as monomers but are rapidly assembled into filaments, resistant to calpain-mediated proteolysis. (2) Unassembled PHF-tau proteins do accumulate as monomers but only in cells or brain regions that are deficient (or inhibited) in calpain and/or phosphatase. The first explanation is supported by observations that calpain-sensitive forms of PHF-tau (e.g., guanidine-treated, amorphous PHF) are calpain-insensitive in the fibrillary form. The second explanation is supported strongly in the calcineurin-deficient mouse model, in which accumulation of phosphorylated tau in the brain has been reported (Kayyali et al., 1997). Several other studies, however, challenge the second possibility, including an elevated rather than a diminished activation ratio of calpain in AD brain (Saito et al., 1993), a ubiquitous presence of calpain in the brain tissue, in particular in neurons (Nixon, 1989; Goto et al., 1994), an increased immunoreactivity of phosphatases in brain regions containing PHFs (Ono et al., 1995), or a presence of calcineurin immunoreactivity in association with neurofibrillary tangles (Billingsley et al., 1994). Further analysis is necessary to clarify the molecular and temporal mechanisms involved in the accumulation of PHFs in AD.

Acknowledgment: We thank Drs. Lester Binder and Peter Davies for the generous gift of monoclonal antibodies and Dr. Andre Van de Voorde from Innogenetics, Inc., for providing monoclonal antibody AT8. We also thank Drs. Dennis Dickson and William Lyman for their assistance in collecting autopsy samples, Dr. Michael Pollanen for helpful discussions, and Mrs. Rebecca L. Leibowitz for her assistance in preparing and characterizing tau. This study was supported by the National Institutes of Health grants NS30027 and NS35254.

REFERENCES

Backstrom J. R., Miller C. A., and Tökes Z. A. (1992) Characterization of neutral proteinases from Alzheimer-affected and control brain specimens: identification of calcium-dependent metalloproteinases from the hippocampus. *J. Neurochem.* **58,** 983–992.

Baki A., Tompa P., Alexa A., Molnar O., and Friedrich P. (1996) Autolysis parallels activation of μ-calpain. *Biochem. J.* **318,** 897–901.

Bancher C., Brunner C., Lassmann H., Budka H., Jellinger K., Wiche G., Seiteberger F., Grundke-Iqbal K., and Wisniewski H. M. (1989) Accumulation of abnormally phosphorylated tau precedes the formation of neurofibrillary tangles in Alzheimer's disease. *Brain Res.* **477,** 90–99.

Biernat J., Mandelkow E.-M., Schroter C., Lichtenberg-Kraag B.,

Steiner B., Berling B., Meyer H., Mercken M., Vandermeeren A., Goedert M., and Mandelkow E. (1992) The switch of tau protein to an Alzheimer-like state includes the phosphorylation of two serine-proline motifs upstream of the microtubule binding region. *EMBO J.* **11,** 1593–1597.

Billingsley M. L., Ellis C., Kincaid R. L., Martin J., Schmidt M., Lee V. M., and Trojanowski J. Q. (1994) Calcineurin immunoreactivity in Alzheimer's disease. *Exp. Neurol.* **126,** 178–184.

Carmel G., Mager E. M., Binder L. I., and Kuret J. (1996) The structural basis of monoclonal antibody Alz50's selectivity for Alzheimer's disease pathology. *J. Biol. Chem.* **271,** 32789–32795.

Delacourte A., Robitaille Y., Sergeant N., Buee L., Hof P. R., Wattez A., Laroche-Cholette A., Mathieu J., Chagnon P., and Gauvreau D. (1996) Specific pathological tau protein variants characterize Pick's disease. *J. Neuropathol. Exp. Neurol.* **55,** 159–168.

Feany M. B., Ksiezak-Reding H., Liu W.-K., Vincent I., Yen S.-H., and Dickson D. W. (1995) Epitope expression and hyperphosphorylation of tau proteins in corticobasal degeneration: differentiation from progressive supranuclear palsy. *Acta Neuropathol.* **90,** 37–43.

Flament S., Delacourte A., Verny M., Hauw J.-J., and Javoy-Agid F. (1991) Abnormal tau proteins in progressive supranuclear palsy. Similarities and differences with the neurofibrillary degeneration of the Alzheimer type. *Acta Neuropathol.* **81,** 591–596.

Goedert M., Spillantini M. G., Potier M. C., Ulrich J., and Crowther R. A. (1989) Cloning and sequencing of the cDNA encoding an isoform of microtubule-associated protein tau containing four tandem repeats: differential expression of tau protein mRNAs in human brain. *EMBO J.* **8,** 393–399.

Goedert M., Spillantini M. G., Cairns N. J., and Crowther R. A. (1992) Tau proteins in Alzheimer paired helical filaments: abnormal phosphorylation of all six brain isoforms. *Neuron* **8,** 159–168.

Goto K., Iwamoto T., and Kondo H. (1994) Localization of mRNAs for calpain and calpastatin in the adult rat brain by in situ hybridization histochemistry. *Brain Res.* **23,** 40–46.

Greenberg S. G., Davies P., Schein J. D., and Binder L. I. (1992) Hydrofluoric acid-treated tauPHF proteins display the same biochemical properties as normal tau. *J. Biol. Chem.* **267,** 564–569.

Grundke-Iqbal I., Iqbal K., Tung Y. C., Quinlan M., Wisniewski H. M., and Binder L. I. (1986) Abnormal phosphorylation of the microtubule-associated protein tau in Alzheimer cytoskeletal pathology. *Proc. Natl. Acad. Sci. USA* **83,** 4913–4917.

Iqbal K., Zaidi T., Bancher C., and Grundke-Iqbal I. (1994) Alzheimer paired helical filaments. Restoration of the biological activity by dephosphorylation. *FEBS Lett.* **349,** 104–108.

Ivy G. O. (1992) Protease inhibition causes some manifestations of aging and Alzheimer's disease in rodent and primate brain. *Ann. NY Acad. Sci.* **674,** 89–102.

Jicha G. A., Bowser R., Kazam I. G., and Davies P. (1997) Alz-50 and MC-1, a new monoclonal antibody raised to paired helical filaments, recognize conformational epitopes on recombinant tau. *J. Neurosci. Res.* **48,** 128–132.

Johnson G. V. W., Jope R. S., and Binder L. I. (1989) Proteolysis of tau by calpain. *Biochem. Biophys. Res. Commun.* **163,** 1505–1511.

Johnson G. V. W., Litersky J. M., and Jope R. S. (1992) Degradation of microtubule-associated protein 2 and brain spectrin by calpain: a comparative study. *J. Neurochem.* **56,** 1630–1638.

Kayyali U. S., Zhang W., Yee A. G., Seidman J. G., and Potter H. (1997) Cytoskeletal changes in the brains of mice lacking calcineurin Aα. *J. Neurochem.* **68,** 1668–1678.

Kenessey A. and Yen S. H. (1993) The extent of phosphorylation of fetal tau is comparable to that of PHF-tau from Alzheimer paired helical filaments. *Brain Res.* **629,** 40–46.

Khachaturian Z. S. (1985) Diagnosis of Alzheimer's disease. *Arch. Neurol.* **42,** 1097–1105.

Kidd M. (1963) Paired helical filaments in electron microscopy of Alzheimer's disease. *Nature* **197,** 192–193.

Klunk W. E. and Pettegrew J. W. (1990) Alzheimer's β-amyloid protein is covalently modified when dissolved in formic acid. *J. Neurochem.* **54,** 2050–2056.

Klunk W. E., Xu C.-J., and Pettegrew J. W. (1994) NMR identification of the formic acid–modified residue in Alzheimer's amyloid protein. *J. Neurochem.* **62,** 349–354.

Kopke E., Tung Y.-C., Shaikh S., Iqbal K., and Grundke-Iqbal I. (1993) Microtubule-associated protein tau: abnormal phosphorylation prior to its assembly into paired helical filaments. *J. Biol. Chem.* **268,** 24374–24384.

Kosik K. S., Orecchio L. D., Binder L. I., Trojanowski J., Lee V. M.-Y., and Lee G. (1988) Epitopes that span the tau molecule are shared with paired helical filaments. *Neuron* **1,** 817–825.

Ksiezak-Reding H. and Wall J. S. (1994) Mass and physical dimensions of two distinct populations of paired helical filaments. *Neurobiol. Aging* **15,** 11–19.

Ksiezak-Reding H. and Yen S.-H. (1991) Structural stability of paired helical filaments requires microtubule-binding domains of tau: a model for self-association. *Neuron* **6,** 717–728.

Ksiezak-Reding H., Liu W.-K., and Yen S.-H. (1992) Phosphate analysis and dephosphorylation of modified tau associated with paired helical filaments. *Brain Res.* **597,** 209–212.

Ksiezak-Reding H., Leibowitz R. L., Bowser R., and Davies P. (1995) Binding of Alz 50 depends on Phe8 in tau synthetic peptides and varies between native and denatured tau proteins. *Brain Res.* **697,** 63–75.

Lee Y. C. and Wolff J. (1984) Calmodulin binds to both microtubule-associated protein 2 and tau proteins. *J. Biol. Chem.* **259,** 1226–1230.

Leger J., Kempf M., Lee G., and Brandt R. (1997) Conversion of serine to aspartate imitates phosphorylation-induced changes in the structure and function of microtubule-associated protein tau. *J. Biol. Chem.* **272,** 8441–8446.

Litersky J. M. and Johnson G. V. W. (1992) Phosphorylation by cAMP-dependent protein kinase inhibits the degradation of tau by calpain. *J. Biol. Chem.* **267,** 1563–1568.

Litersky J. M. and Johnson G. V. W. (1995) Phosphorylation of τ in situ: inhibition of calcium-dependent proteolysis. *J. Neurochem.* **65,** 903–911.

Mattson M. P. (1994) Calcium and neuronal injury in Alzheimer's disease. Contributions of β-amyloid precursor protein mismetabolism, free radicals, and metabolic compromise. *Ann. NY Acad. Sci.* **747,** 50–76.

Mercken M., Grynspan F., and Nixon R. A. (1995) Differential sensitivity to proteolysis by brain calpain of adult human tau, fetal human tau and PHF-tau. *FEBS Lett.* **368,** 10–14.

Molinari M., Anagli J., and Carafoli E. (1994) Ca^{2+}-activated neutral protease is active in the erythrocyte membrane in its nonautolyzed 80-kDa form. *J. Biol. Chem.* **269,** 27992–27995.

Molinari M., Anagli J., and Carafoli E. (1995) PEST sequences do not influence substrate susceptibility to calpain proteolysis. *J. Biol. Chem.* **270,** 2032–2035.

Morishima M. and Ihara Y. (1994) Posttranslational modifications of tau in paired helical filaments. *Dementia* **5,** 282–288.

Murayama S., Mori H., Ihara Y., and Tomonaga M. (1990) Immunocytochemical and ultrastructural studies of Pick's disease. *Ann. Neurol.* **27,** 394–405.

Nixon R. A. (1989) Calcium-activated neutral proteinases as regulators of cellular function. *Ann. NY Acad. Sci.* **568,** 198–208.

Ono T., Yamamoto J., Tashima K., Nakashima H., Okumura E., Yamada K., Hisanaga S., Kishimoto T., Miyakawa E., and Miyamoto E. (1995) Dephosphorylation of abnormal sites of tau factor by protein phosphatases and its implication for Alzheimer's disease. *Neurochem. Int.* **26,** 205–215.

Otvos L., Feiner L., Lang E., Szendrei G. I., Goedert M., and Lee V. M.-Y. (1994) Monoclonal antibody PHF-1 recognizes tau protein phosphorylated at serine residues 396-404. *J. Neurosci.* **39,** 669–673.

Padilla R., Maccioni R. B., and Avila J. (1990) Calmodulin binds to a tubulin binding site of the microtubule-associated protein tau. *Mol. Cell. Biochem.* **97,** 35–41.

Saito K.-I., Elce J. S., Hamos J. E., and Nixon R. A. (1993) Widespread activation of calcium-activated neutral proteinase (calpain) in the brain in Alzheimer disease: a potential molecular basis for neuronal degeneration. *Proc. Natl. Acad. Sci. USA* **90,** 2628–2632.

Sandoval I. V. and Weber K. (1978) Calcium-induced inactivation of microtubule formation in brain extracts. *Eur. J. Biochem.* **92,** 463–470.

Seubert P., Baudry M., Dudek S., and Lynch G. (1987) Calmodulin stimulates the degradation of brain spectrin by calpain. *Synapse* **1,** 16–21.

Siman R., Ahdoot M., and Lynch G. (1987) Ontogeny, compartmentation and turnover of spectrin isoforms in rat central neurons. *J. Neurosci.* **7,** 55–64.

Squier M. K. T., Miller A. C. K., Malkinson A. M., and Cohen J. J. (1994) Calpain activation in apoptosis. *J. Cell. Physiol.* **159,** 229–237.

Trojanowski J. Q., Schmidt M. L., Shin R. W., Bramblett G. T., Rao D., and Lee V. M.-Y. (1993) Altered tau and neurofilament proteins in neurodegenerative diseases: diagnostic implications for Alzheimer's disease and Lewy body dementias. *Brain Pathol.* **3,** 45–54.

Wang K. K. W., Villalobo A., and Roufogalis B. D. (1989) Calmodulin-binding proteins as calpain substrates. *Biochem. J.* **262,** 693–706.

Yang L.-S. and Ksiezak-Reding H. (1995) Calpain-induced proteolysis of normal human tau and tau associated with paired helical filaments. *Eur. J. Biochem.* **233,** 9–17.

Yoshida H. and Ihara Y. (1993) τ in paired helical filaments is functionally distinct from fetal τ: assembly incompetence of paired helical filaments. *J. Neurochem.* **61,** 1183–1186.

Publikacja 5

Cell Motility and the Cytoskeleton 47:236–252 (2000)

Induction of Alzheimer-Specific Tau Epitope AT100 in Apoptotic Human Fetal Astrocytes

Hanna Ksiezak-Reding,[1]* Deke He,[1] Wanda Gordon-Krajcer,[1] Yvonne Kress,[1] Sunhee Lee,[1] and Dennis W. Dickson[2]

[1]*Department of Pathology, Albert Einstein College of Medicine, Bronx, New York*
[2]*Mayo Clinic, Jacksonville, Florida*

In Alzheimer's and other neurodegenerative diseases, hyperphosphorylated tau accumulates in affected neuronal and glial cells in the form of paired helical filaments (PHFs). This tau binds antibody AT100, which recognizes the double phosphorylation site (Thr212/Ser214) that is not present in normal biopsy tau. In primary cultures, highly enriched (>98%) in astrocytes of human fetal brain, three polypeptides of 52, 64, and 70 kD showed immunoreactivity with tau antibodies against non-phosphorylated epitopes, accounting for 88, 12, and <1%, respectively, of the total reactivity. All three polypeptides were phosphorylated at the PHF-1 epitope but not at the epitopes Tau-1, 12E8, AT8, and AT100. Treatment of cultures with okadaic acid resulted in apoptosis characterized by the blebbing of the plasma membrane, condensation of nuclear chromatin, and fragmentation of the nucleus. This treatment also resulted in a 3- to 5-fold increase in the content of both tau protein and phosphorylation. The increases were observed in all phosphorylation sites examined, and included the AT100 site. The AT100 site has been proposed to be generated by protein kinase B/Akt and Cdc2. Since okadaic acid can induce an AD-like hyperphosphorylated state of normal tau in primary cultures of human brain cells, a simple cellular model is available permitting study of self-aggregation of tau and phosphorylation events characteristic of neurodegeneration. Cell Motil. Cytoskeleton 47:236–252, 2000.

Key words: primary cultures; okadaic acid; apoptosis; tau protein; Alzheimer's disease; tau phosphorylation

INTRODUCTION

Tau is a microtubule-associated protein that plays a role in microtubule assembly and stability [Lovestone and Reynolds, 1997]. Interactions of tau with microtubules are regulated by the length of the microtubule binding domain that may contain either 3 or 4 repeats, and by phosphorylation. Different phosphorylation sites play a specific role in the development of cell processes [Biernat and Mandelkow, 1999], in axonal transport [Ebneth et al., 1998], and in signal transduction [Lee et al., 1998]. In primary cell cultures, tau protein can be detected in neurons and oligodendrocytes [LoPresti et al., 1995; Ksiezak-Reding et al., 1997; Muller et al., 1997], but only a minimal level is found in astrocytes [Couchie et al., 1985]. Tau is also expressed in a number of transformed cell lines including PC12 [Davis and Johnson, 1999] and neuroblastomas [Chiang et al., 1993]. In unstimulated SY5Y neuroblastoma cells or in COS fibroblasts, constitutive expression of tau is low or undetectable [Lee et al., 1998; Sato-Harada et al., 1996].

In Alzheimer's disease (AD) and other neurodegenerative disorders, hyperphosphorylated tau protein

Contract grant sponsor: National Institute of Health; Contract grant number: NS35254; Contract grant number: NS07098; Contract grant sponsor: Alzheimer's Association; Contract grant number: RG3-96-085.

*Correspondence to: Hanna Ksiezak-Reding, Ph.D., Department of Pathology, Rm. F-538, Albert Einstein College of Medicine, 1300 Morris Park Avenue, Bronx, NY 10461.
E-mail: reding@aecom.yu.edu

Received 3 February 2000; Accepted 17 July 2000

accumulates in paired helical filaments (PHFs), a major constituent of abnormal neurofibrillary tangles [Goedert, 1998]. In AD, abnormal tau inclusions are found mostly in neurons, although in other disorders these inclusions are also found in glia, including both oligodendrocytes and astrocytes [Dickson et al., 2000]. PHFs contain more phosphorylated sites than normal tau and therefore immunoreact with more phosphate-dependent antibodies. The monoclonal antibody AT100 is a unique probe that recognizes abnormal PHF-tau polypeptides from AD brains but not polypeptides of normal phosphorylated tau from biopsy-derived samples [Matsuo et al., 1994; Hoffmann et al., 1997]. The AT100 epitope is generated in recombinant tau in vitro by sequential phosphorylation by two kinases: proline-dependent glycogen synthase kinase-3β (GSK-3β) at Thr212 and nonproline-dependent protein kinase A at Ser214 [Zheng-Fischhofer et al., 1998]. The generation of the AT100 epitope in a cell-free system requires a PHF-like conformation of tau induced by polyanions such as heparin, RNA, or poly(Glu).

Okadaic acid (OA) is a powerful inducer of apoptosis [Gjertsen and Doskeland, 1995] and a potent inhibitor of protein phosphatases (2A and 1). OA treatment increases the phosphorylation level of endogenous tau in both primary cell cultures [Arias et al., 1993; Litersky et al., 1996; Ho et al., 1997; Kim et al., 1999] and transformed cell cultures lacking tau transfection [Shea and Fischer, 1996; Bondareff et al., 1998; Xie et al., 1998]. Although this treatment could generate conformation- and phosphorylation-sensitive epitopes associated with PHFs, induction of the AT100 epitope has not been reported.

In the present studies, phosphorylation of the AT100 epitope has been achieved through OA treatment of primary cultures of astrocytes derived from human fetal brain. In parallel, OA treatment caused apoptosis of cultured astrocytes. To our knowledge, this is the first report describing the induction of an epitope specific for AD-type pathology in primary cell cultures or any cultured cells that avoids transfection of the cells with human cDNA [Zheng-Fischhofer et al., 1998; Mailliot et al., 1998a]. Our studies provide a simple and robust cellular model system to study self-aggregation of tau and phosphorylation events characteristic of neurodegeneration.

MATERIAL AND METHODS

Materials

Enhanced chemiluminescence system and 10-nm immunogold reagents were purchased from Amersham Life Science, Inc. (Arlington Heights, IL). Secondary antibodies conjugated to horseradish peroxidase were from BioRad (Redding, CA) and from Fisher Scientific (Pittsburgh, PA). Tetrazolium reagent 3-(4,5-dimethylthiazol-2-yl)-2,5-diphenyltetrazoliumbromide (MTT), Hoechst 33258, OA, and alkaline phosphatase (*Escherichia coli*, type III) were obtained from Sigma (St. Louis, MO). Fetal calf serum and antibiotic/antimycotic mixture were from Gibco (Grand Island, NY). Dulbecco's modified Eagle's medium (DMEM) was manufactured by BioWhittaker and purchased from Fisher Scientific. Lab-Tek chamber slides were from Nalge-Nunc International (Naperville, IL). Gel/Mount was obtained from Biomeda Corp. (Foster City, CA). Formvar-coated copper and nickel grids for electron microscopy (EM) were purchased from Fullam Inc. (Latham, NJ). Fat-free dry milk was from Carnation. Tau 14 and Tau 46 were from Zymed Laboratories, Inc., Tau-1 from Boehringer Mannheim (Indianapolis, IN), anti-glial fibrillary acidic protein (GFAP), anti-β-tubulin, and anti-vimentin from Sigma, anti-galactocerebroside (Gal C) from Chemicon International, Inc., anti-CD 68 from Upstate Biotechnology, and anti-neurofilaments (SMI-33 and SMI-34) from Sternberger Monoclonals, Inc.

Cell Culture

Human fetal brain tissue was obtained from elective termination of pregnancies (19–24 weeks of gestation) in a protocol approved by the Committee on Clinical Investigations. Fresh tissue was dissociated and cells isolated according to an established protocol [Lee et al., 1992]. Cultures were enriched in astrocytes and maintained for 3–4 months in a tissue culture medium containing DMEM with glucose (4.5 g/l) and L-glutamine (4 mM) supplemented with 10% heat-inactivated calf serum and antibiotic/antimycotic mixture in a 5% CO_2 humidified incubator at 37°C. Confluent cells were trypsinized and reseeded for up to four passages.

Okadaic Acid Treatment

Subconfluent cultures in 75-cm^2 tissue culture flasks and 8-well glass or plastic Lab-Tek chamber slides were treated with OA (50 and 250 nM) for 1, 5, and 24 h. The viability of the cells was determined using tetrazolium reagent MTT as described by Carmichael et al. [1987] with minor modifications [De Groot et al., 1997]. Briefly, control and OA-treated cells were incubated for 2 h at 37°C with fresh culture medium containing MTT (1 mg/ml). After the incubation, detached cells were collected by centrifugation (10 min, 10,000*g*, 25°C). Detached cells and cells in chambers were solubilized with dimethylsulfoxide using the total of 250 μl per chamber. Samples were transferred to ELISA plates and the 595-nm absorbance was measured. The viability of cells was expressed in the % of control values obtained with untreated cultures.

Immunocytochemistry and Nuclear Staining

Cells were fixed with 0.3% glutaraldehyde in a buffer (80 mM PIPES-Na, pH 6.8, 1 mM $MgCl_2$, 5 mM EGTA, and 0.1% saponin) for 10 min at 25°C as described [Drubin and Kirschner, 1986] and modified [Lee and Rook, 1992]. Cells were then subjected to $NaBH_4$ and glycine treatment, followed by incubation in cold methanol for 10 min, 0.3% hydrogen peroxide for 30 min, and TBS containing 5% milk and 0.1% Triton X-100 for 30–60 min. Cells were then incubated with primary and secondary antibodies diluted in 5% milk-TBS for 1 h each at 25°C. Secondary antibodies were conjugated to horseradish peroxidase. A freshly made solution of peroxidase substrates [0.5 mg/ml 3,3′-diaminobenzidine (DAB) and 0.3% hydrogen peroxide in 50 mM Tris/HCl, pH 7.6] was added to cells for 1–5 min or until a brown precipitate formed. Slides were then mounted in glycerol:TBS (1:1), sealed with nail polish or mounted in Gel/Mount, and examined under light microscope Olympus BH2. Nuclear staining was performed with cells fixed in 0.3% glutaraldehyde in buffer as described above. Fixed cells were washed twice in TBS and incubated in 5 μg/ml Hoechst 33258 in TBS for 30 min at 25°C. Cells were mounted in Gel/Mount and examined with a fluorescent microscope (Olympus BH2). Color slides were scanned using Polaroid Sprint Scanner, layered out and assembled using software program Corel.

Electron Microscopy

Cells grown on plastic Lab-Tek chamber slides were fixed and immunostained as described above. Cells were post-fixed in 1% osmium for 1 h, dehydrated, and embedded in araldite-epon. Ultrathin sections were cut and placed on Formvar-coated grids. Sections were examined in a JEOL 100CX electron microscope without additional staining. The number of cells found in OA-treated samples was very small. This was due to poor attachment of apoptotic cells to the plastic support in chamber slides. Therefore, post-embedding immunogold labeling was used as an alternative procedure. In this procedure, cells were grown in tissue culture flasks and then collected to obtain pellets as described in Cell Fractionation. Cells in pellets were fixed in 2% paraformaldehyde and 0.5% glutaraldehyde in phosphate buffered saline (PBS) for 20 min at 25°C. Unosmicated cells were dehydrated and embedded in araldite-epon. Ultrathin sections were cut and placed on Formvar-coated nickel grids. Sections on grids were subjected to de-eponization and immunogold labeling as described previously [Casadevall et al., 1998] except for using 1% bovine serum albumin and 4% milk in PBS as blocking solution. Samples were examined in a JEOL 100CX electron microscope after staining with lead citrate and uranyl acetate.

Cell Fractionation

Confluent cultures in 75-cm^2 tissue culture flasks were collected after treating with 250 nM OA for 24 h. Cells treated with vehicle served as control. Medium from OA-treated cultures was aspirated and centrifuged (10 min, 1,000*g*) to collect detached cells. Attached and suspended cells were processed separately. Cells in flasks were washed initially with PBS at 37°C and then scraped using a collection buffer [10 mM Tris/HCl, pH 7.8, 140 mM NaCl, 1 mM EDTA, 0.1 mM phenylmethylsulfoxyfluoride (PMSF), 0.2% sodium azide] [Chiang et al., 1993]. Collected cells were spun for 10 min at 1,000*g* and the pellets were suspended in urea buffer (6 M urea, 0.15 M NaCl, 10 mM Tris/HCl, pH 7.4, 1% β-mercaptoethanol, 2 mM EDTA, and 0.1 mM PMSF). Samples in urea buffer were designated as "total tau" fractions. In some experiments, the pellets were suspended in lysis buffer (20 mM MES-Na, pH 6.8, 80 mM NaCl, 1 mM $MgCl_2$, 2 mM EGTA, 10 mM NaH_2PO_4, 20 mM NaF, 0.1 mM PMSF, and 10 μg/ml leupeptin), kept at −20°C for 24 h, then thawed and centrifuged (15 min, 10,000*g*, 4°C) to obtain "S_1 fraction" ("postnuclear extract"). This fraction was supplemented with 2% NaCl and 2% β-mercaptoethanol, kept on ice for 30 min, and then boiled for 5 min. Samples were centifuged (20 min, 15,000*g*, 4°C) and the supernatant designated as "heat-stable" fraction was dialyzed 24 h at 4°C against 20 mM Tris/HCl, pH 7.4. Protein contents in the fractions were determined using Coomassie Blue binding assay of Bradford (Bio-Rad) adapted to microtiter ELISA plates.

Fetal Tau and PHF Preparations

Preparations highly enriched in fetal tau protein (≥59%) were obtained from 10 g human fetal brain tissue by heat and perchloric acid treatments [Ksiezak-Reding et al., 1995]. Fractions enriched in PHFs were obtained from 20 g of parietal cortex from AD brain (82-year-old female, 6 h postmortem delay) as sarcosyl-insoluble 100,000*g* pellets [Ksiezak-Reding and Wall, 1994].

Alkaline Phosphatase Treatment

Heat-stable fractions from cultured cells or fetal tau preparations (1 mg/ml) were incubated with alkaline phosphatase (20 IU/ml) for 5 h at 37°C in buffer [0.1 M Tris/HCl, pH 8.0, 5 mM EGTA, 1 mM PMSF, leupeptin (10 μg/ml), pepstatin A (1 μg/ml), and aprotinin (0.1 μg/ml)]. The reaction was terminated by addition of SDS-sample buffer and boiling for 5 min.

SDS-PAGE and Immunoblotting

Electrophoresis was performed using 10% polyacrylamide gels. The separated proteins were electro-

transferred onto nitrocellulose membranes. Non-specific binding sites were blocked with 5% milk in TBS for 1 h at 25°C. Membranes were incubated with primary antibodies for 1–2 h at 25°C and then with secondary antibodies conjugated to horseradish peroxidase for 1 h. Both primary and secondary antibodies were diluted in 5% milk-TBS. Specific protein signals were detected using enhanced chemiluminescence reagents.

Antibodies

Monoclonal antibodies were used that recognize phosphorylated and non-phosphorylated regions of the tau molecule. Alz 50 recognizes conformational epitope in the N-terminus of tau [Ksiezak-Reding et al., 1995; Carmel et al., 1996; Jicha et al., 1997] and PHF-1 recognizes phosphorylated Ser394/Ser404 [Otvos et al., 1994]. Numbering refers to the longest tau isoform containing 441 amino acid residues. AT8 and AT100 bind to phosphorylated sequences Ser202/Thr205 [Goedert et al., 1995] and Thr212/Ser214 [Hoffmann et al., 1997], respectively. 12E8 recognizes phosphorylated Ser262/Ser356 [Seubert et al., 1995]. Tau 14, Tau-1, and Tau 46 bind to non-phosphorylated sequences of tau 141-178, 199-202, and 428-441, respectively [Kosik et al., 1988; Carmel et al., 1996]. Binding of Tau-1, but not Tau 14 and Tau 46, is blocked by phosphorylation of the epitope. Polyclonal antibodies included E-2, E-3, and E-10, which were raised against specific regions of the tau molecule in exons 2, 3, and 10, respectively [Sergeant et al., 1997]. Other antibodies included anti-GFAP, anti-β-tubulin, anti-vimentin, Gal C, anti-CD 68, SMI-33, SMI-34, anti-myelin basic protein (polyclonal), anti-microtubule-associated protein 2 (AP-18), and others.

RESULTS

Characterization of Astrocyte-Enriched Cultures

The primary cultures from human fetal brain were highly enriched in astrocytes as determined by immunostaining for GFAP (Fig. 1A). GFAP-positive cells constituted more than 98% of the total cell population. Two morphologies of cells could be distinguished (Fig. 1A and D): flat polygonal cells characteristic of protoplasmic astrocytes and more elongated cells characteristic of fibrous astrocytes [Privat and Rataboul, 1986]. Occasionally Gal C-positive or myelin basic protein-positive cells were detected (not shown). Microglia (CD 68-positive) were rarely observed, contributing to less than 0.5–1% of the total population. The SMI-33 or SMI-34-positive cells with neuronal morphology and MAP-2 positive neurons constituted less than 2% of cells in cultures passaged two or more times. The morphological characteristics of the cultures were consistent with those described previously [Liu et al., 1994].

In control cultures, a pattern of immunostaining and immunogold labeling for GFAP and tubulin revealed a well-developed network of intermediate filaments and microtubules within the cells (Figs. 1 and 2). In the large polygonal cells, glial filaments were found as bundles or arrays near the nucleus and projecting towards the cell margins and cell processes (Fig. 2A). Microtubule arrays were distributed throughout the cytoplasm as a fine network with a denser pattern around the nucleus (Fig. 1D). Microtubules were often intermingled with glial filaments (Fig. 2C and D). Besides microtubules, tubulin label was also found in association with endoplasmic reticulum, which was identified by morphology. The appearance of the cytoskeleton was similar to that described previously in astrocytes [Eliasson et al., 1999] or cells in general [Fawcett, 1981]. In fibrous actrocytes, GFAP and tubulin staining were much stronger than in polygonal cells. Despite good morphological preservation of the cytoskeleton, immunogold labeling for tubulin in post-embedded material was less intense than that for GFAP (Fig. 2C and D). This could be due to differential sensitivity of epitopes to labeling technique since staining with peroxidase-DAB was comparable for both proteins (Fig. 1A and D).

Loss of Viability and Nuclear Changes Following Okadaic Acid Treatment

Treatment of cell cultures with OA resulted in a time- and dose-dependent loss of viability of cells as determined by MTT assay (Fig. 3). Within 1 h of treatment with 50 and 250 nM OA, cells lost approximately 20 and 40% viability, respectively. After 24 h, the losses were 48 and 60%. Changes in viability were parallel to alterations in cell morphology and both were consistent with apoptosis. The morphological changes included rounding of the cell shape and blebbing of the cell membrane (Fig. 1B and C). Condensation of nuclear chromatin and fragmentation of the nucleus were demonstrated with the DNA-binding dye Hoechst 33258 (Fig. 1H and I) and also with EM (Fig. 4A and B). Cells were often seen with two or more nuclear fragments (Fig. 4A).

Derangement of Cytoskeleton

Treatment of cultures with either 50 or 250 nM OA induced time- and concentration-dependent alterations in intensity and pattern of immunostaining for GFAP and other cytoskeletal proteins (Fig. 1B–F). The intensity of staining was increased with practically all the antibodies tested, including that for vimentin (not shown). Changes in the pattern of staining were consistent with disruption of the cytoskeletal network, as the cells adopted a rounded shape. Within 1 h of treatment, some cells already had a rounded appearance and displayed a num-

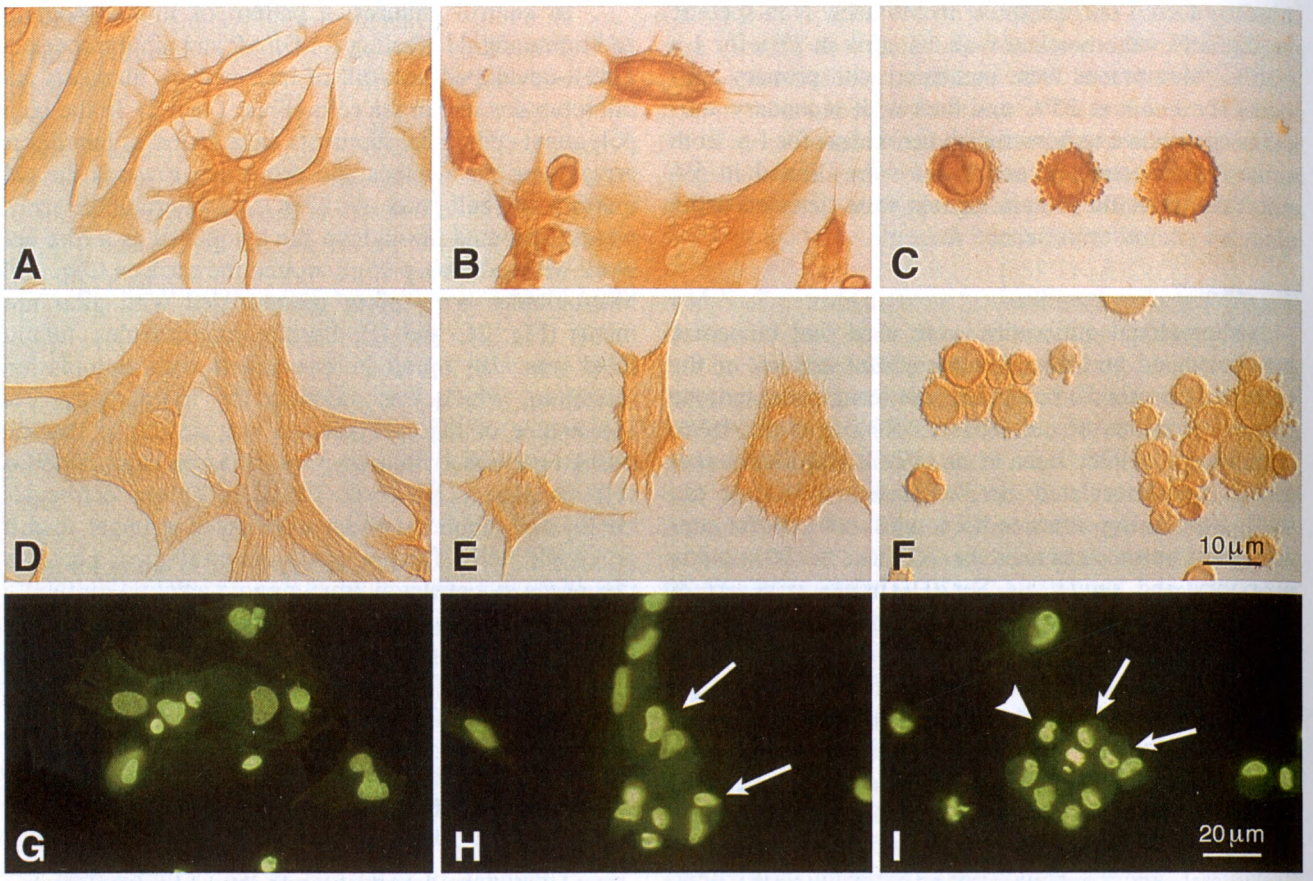

Fig. 1. Astroglia-enriched cultures immunostained for GFAP (**A–C**) and β-tubulin (**D–F**), and stained for DNA with Hoechst 33258 (**G–I**). Cells in culture were either not treated (A, D, and G) or treated with 250 nM OA for 1 h (B, E, and H) and 5 h (C, F, and I). Control GFAP-positive cells were mostly large flat polygonal or fibrous cells as seen in A and D. Changes in morphology induced by OA were consistent with apoptosis, including rounding of the cells and blebbing of the membrane. This is particularly evident in C and F. Note the intense immunostaining of the cytoskeletal ring in apoptotic cells. Fragmentation of nuclei (*arrowhead*) and condensation of chromatin into kidney-like shaped nuclei (*arrows*) are seen in I and H. Scale bar in F and I refers to A–F and G–I, respectively.

ber of short spike-like processes (Fig. 1B and E). Others showed distinctive blebbing of the plasma membrane. After 5 and 24 h incubations, most, if not all, of the cells were round and the cytoskeletal markers for GFAP and tubulin showed a ring underlying the cell membrane (Fig. 1C,F). A similar pattern of cytoplasmic staining was seen by EM examination of immunoperoxidase-DAB or immunogold labeled cells (arrow in Fig. 4A; see also Fig. 4C). Glial filaments were often seen arranged in characteristic swirls and tight weavy bundles (Fig. 4A, asterisks and insert). Morphologically, microtubules appeared distorted and difficult to distinguish in the massive accumulation of intermediate filaments (Fig. 4D, arrowheads). Some of the tubulin label was associated with endoplasmic reticulum (Fig. 4D, arrows) as in control cultures. In contrast to the robust peroxidase-DAB staining (Fig. 1 E,F), immunogold labeling for tubulin was weak, indicating different sensitivity of the two techniques.

Tau in Astrocytes: Light and Electron Microscopy

Tau staining was minimal in control cultures (Fig. 5). The immunostaining with PHF-1, AT8, and 12E8 antibodies was weak in the cytoplasm and nucleus/nucleolus at the light microscope level (Fig. 5A,C,E). At

Fig. 2. Electron micrographs of control astrocytes in culture stained with immunoperoxidase-DAB for GFAP (**A**) and PHF-1 (**B**) or labeled with 10-nm immunogold for GFAP (**C**), β-tubulin (**D**), and PHF-1 (**E,F**). Control astrocytes contain distinct bundles of glial filaments (*arrows* in A) surrounding the nucleus in a perinuclear rim and projecting towards cell processes. Glial filaments are interlaced with microtubules (*arrowheads* in C and D) and mitochondria. The PHF-1 label is associated with nuclear and nucleolar material, microtubules and endoplasmic reticulum (*arrows* in B, E, and F). N, nucleus; M, mitochondria; F, intermediate filaments; ER, rough endoplasmic reticulum; *arrowheads*, microtubules; *arrows*, details of labeling. JEOL 100CX.

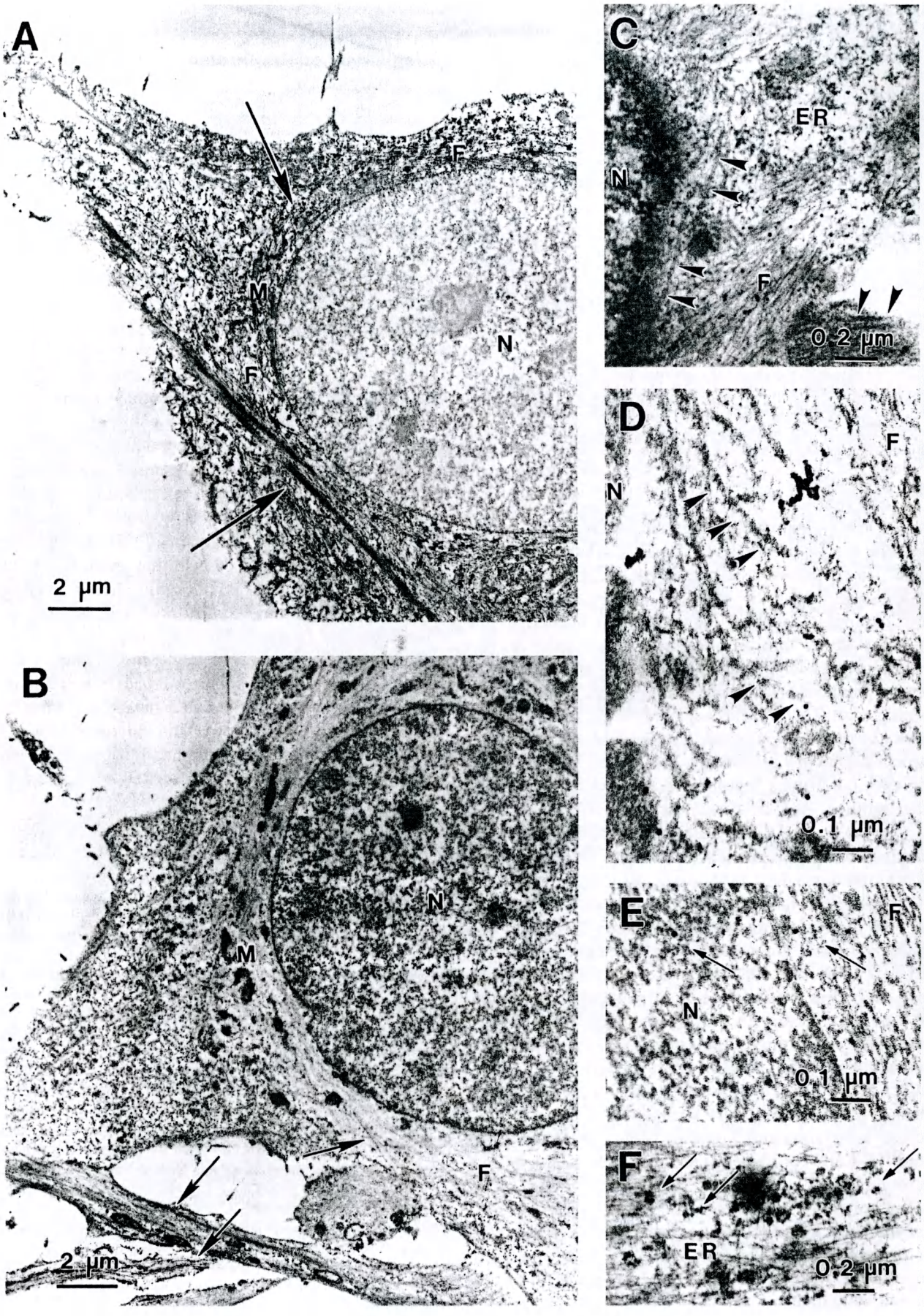

Figure 2.

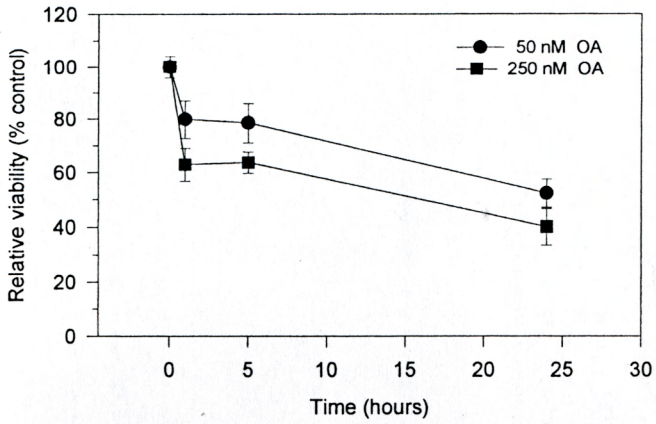

Fig. 3. MTT assay of cell viability. Astroglial-enriched cultures were treated with OA (50 and 250 nM) for 1, 5, and 24 h and viability of cells determined with the MTT assay as described in Materials and Methods. Results are expressed in % of control values (untreated cultures). Values are means ± SEM for 4–6 experiments.

the EM level, there was diffuse cytoplasmic and nuclear/nucleolar staining for PHF-1 (Fig. 2B). The cytoplasmic PHF-1 labeling was associated with microtubules and endoplasmic reticulum (Fig. 2E and F, arrows). The weak tau immunostaining indicates a low level of tau in astrocytes rather than an effect of fixation since an occasional neuron displayed robust tau immunoreactivity seen in long beaded-like processes (Fig. 5E, arrows). The staining with Tau 14 was negative, suggesting a lower affinity of binding compared to other antibodies. Control astrocytes showed no immunoreactivity with AT100 (Fig. 5G) confirming that this phosphorylated epitope is either minimal or absent in normal tau.

In OA-treated cells, tau immunostaining increased dramatically. The greatest increases were seen with phosphorylation-dependent antibodies, including AT8, 12E8, PHF-1, and most interestingly with AT100. The increase was also noticed, although less distinctly, with Tau 14, which recognizes a non-phosphorylated epitope. In contrast to cytoskeletal markers, tau immunostaining with most antibodies was diffuse throughout the cytoplasm and was also present in the nucleus (Fig. 5D). PHF-1 demonstrated a strong cytoplasmic labeling at the light microscope (Fig. 5B) and EM (Fig. 4B, arrows) levels. A distinct filamentous/membranous pattern in the cytoplasm (Fig. 4B, insert) and amorphous staining of the nucleus were apparent. Some of the cytoplasmic label with PHF-1 and AT100 was identified as that of distorted microtubules and endoplasmic reticulum (Fig. 4E and F). The microtubules were mostly concealed in the swirls of glial filaments (Fig. 4D). As with the tubulin label, immunogold labeling of tau was less intense than that with peroxidase-DAB, suggesting an interfering effect of the labeling technique.

Upregulation of Tau Protein Content and Phosphorylation

Controls. Immunoblotting was more sensitive than immunocytochemistry in detecting tau activity in cultured cells. By immunoblotting, the homogenates were found to contain three polypeptides (52, 64, 70 kD) that were immunoreactive with Tau 14 (Fig. 6A). Similar polypeptides were immunoreactive with Tau 46 (Fig. 7A) in heat-stable tau fractions. These fractions were obtained by heat treatment of postnuclear extracts to denature heat-sensitive proteins and enrich the heat-stable tau. The total tau activity and the percent contribution of individual bands were determined by densitometic scanning of immunoblots with both antibodies. The most abundant was the 52-kD polypeptide (approximately 88% of the total tau activity), with the 64- and 70-kD polypeptides accounting for the remaining 12% and < 1%, respectively. All three polypeptides were immunoreactive with PHF-1, but were either unreactive or only weakly reactive with antibodies against other phosphorylated epitopes (AT8, 12E8, and AT100) or with Alz 50 (Fig. 6A). These results indicate that control astrocytes have low tau expression and phosphorylation. In addition to tau reactive proteins, control homogenates showed a 45-kD reactive band. This band is non-specific since it also stained on blots developed without primary antibodies (Fig. 6A, arrowhead in lane marked None). An additional 76-kD polypeptide was also detected in some blots with Tau 46 (Fig. 7A, arrow). This polypeptide was low in abundance and could be unrelated to tau since it was not detected with Tau 14 and other tau antibodies.

Fig. 4. Electron micrographs of OA-treated astrocytes in culture stained with immunoperoxidase-DAB for GFAP (**A**) and PHF-1 (**B**) or labeled with 10-nm immunogold for GFAP (**C**), β-tubulin (**D**), PHF-1 (**E**), and AT100 (**F**). OA-treated astrocytes contain nuclear fragments as seen in A, where three nuclear fragments (N1, N2, and N3) can be distinguished, each with the intact nuclear membrane. Nuclear chromatin appears condensed and fragmented. In A and B, nuclear fragments close to the cell periphery appear to be located inside a bleb of the plasma membrane. Cells are filled with tightly packed glial filaments (*arrows* in A), which form swirls of fibers (*asterisks* and *inset* in A), heavily labeled for GFAP (C). The filaments are interwoven with distorted microtubules (*arrowheads* in D). Tubulin labeling is also associated with rough endoplasmic reticulum (*arrows* in D). PHF-1 stains nuclear chromatin in a fragmented nucleus, a mass of filamentous/memebranous material in the cytoplasm and rough endoplasmic reticulum (*inset* in B, *arrows* in B and E). The filamentous/membranous material resembling microtubules (*inset* in B, *arrowheads* in F) also labels for AT100 (F, *arrow*). N, nucleus; M, mitochondria; F, intermediate filaments; ER, rough endoplasmic reticulum; *arrowheads*, microtubules; *arrows*, details of labeling. Incubations with OA (250 nM) were for 24 h. **Insets** in A and B have a 3-fold magnification compared to background. **Insets** in D–F have the same magnification as background. JEOL 100CX.

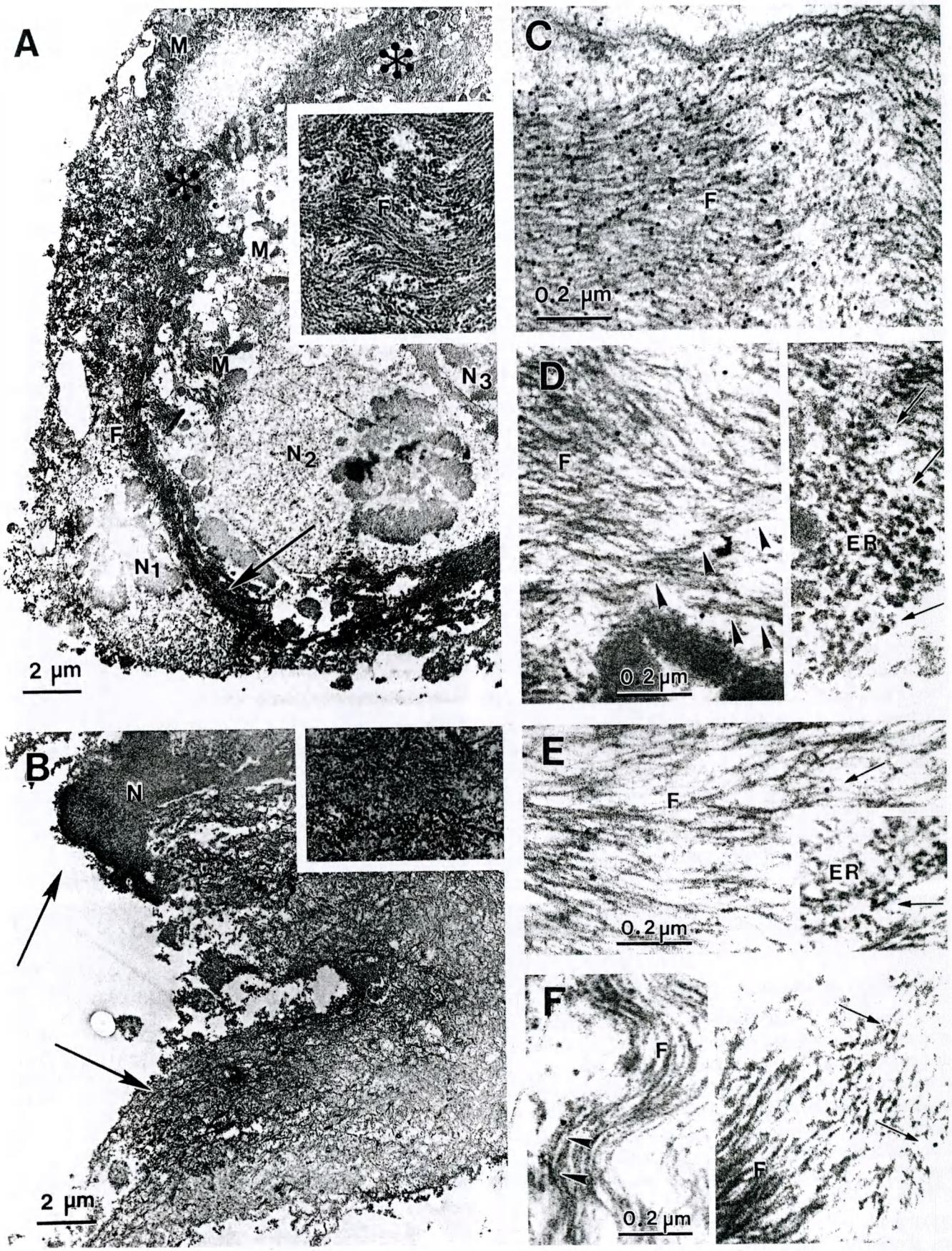

Figure 4.

OA-treated astrocytes. Homogenates and heat-stable fractions of OA-treated cultures displayed significant alterations in the staining pattern such as a shift in electrophoretic mobility as well as the appearance of new bands. The number of tau immunoreactive bands increased from three (52, 64, and 70 kD) to four (61, 64, 71, and 76 kD) (Figs. 6B and 7B). This alteration in pattern was most consistent with a higher level of phosphorylation since all four polypeptides in the OA-treated samples displayed significantly enhanced tau immunoreactivity with phosphorylation-dependent antibodies. The increases involved double phosphorylation sites at different regions of the molecule, especially including the AT100 epitope (Thr212/Ser214) as well as AT8 (Ser202/Thr205), 12E8 (Ser262/Ser356), and PHF-1 (Ser396/Ser404). Alz 50 immunoreactivity was associated mostly with the 61-kD polypeptide. Tau 14 and Tau 46 immunoreactivities were also markedly increased. By densitometric scanning, the increase in the total tau activity was estimated to be approximately 3.5-fold for cells that were attached (Fig. 6C, lane 3) and approximately 5-fold for cells that remained in the culture medium (Fig. 6C, lane 4). These results demonstrated that the amount of tau protein, and not merely phosphorylation, was elevated in OA-treated cultures.

Both control and OA-treated samples contained heat-stable tau proteins indicating that both phosphorylated and non-phosphorylated tau species are resistant to heat denaturation, consistent with previous reports [Schweers et al., 1994]. The results obtained with heat-stable fractions (Fig. 6C and D, lanes 5 and 6) were qualitatively similar to those obtained with homogenates (Fig. 6A and B), suggesting that the observed alterations in immunoreactivity and mobility are due to tau proteins rather than to cross-reactive proteins unrelated to tau. In comparison to homogenates, however, heat-stable fractions of OA-treated cultures showed less pronounced increases (approximately 1.5–1.6 fold), suggesting a lower content and therefore solubility of tau in these fractions.

Expression of Alternatively Spliced Exons

Controls. The presence of various isoforms of tau was examined with exon peptide-specific tau antibodies designated as E-10, E-2, and E-3. These antibodies reacted strongly with the recombinant tau (longest isoform) used as positive control (Fig. 7C). In heat-stable fractions from control cultures, the 52-kD polypeptide did not react with any exon peptide-specific antibodies (Fig. 7A, band 1); the 64 kD polypeptide was weakly reactive with E-10 and E-2, but not E-3 (band 2); and the 70 kD polypeptide was immunoreactive with all three antibodies (band 3). These results indicate that the 52-kD polypeptide (88% of the total reactivity) contains no sequences encoded by exons 2, 3, and 10 and is thus the shortest single tau isoform. The 64-kD polypeptide (12% of the total) is related to tau isoforms expressing exon 2 but little of exons 3 and 10. The 70-kD polypeptide (<1% of the total) contains isoforms with exons 2, 3, or 10 expressed. It is entirely possible that the 64- and 70-kD tau polypeptides (Fig. 7A, bands 2 and 3) contain more than one isoform or contain differentially phosphorylated forms of the shortest tau isoform. To test these possibilities, it will be necessary to use single isoform-specific antibodies or antibodies recognizing phosphorylation sites other than those examined in the present studies.

OA-treated astrocytes. In heat-stable fractions of OA-treated cultures, the pattern of immunoreactivity shows that the 61-kD polypeptide (Fig. 7B, band 1) represents the shortest tau isoform, the 62-kD polypeptide (band 2) contains isoforms with exons 10 and/or 2 but not exon 3, and the 71- and 76-kD polypeptides (bands 3 and 4) contain isoforms expressing two (exons 2 and 3) or three exons, respectively. In OA-treated cultures, the immunoreactivity of tau with E-10 increased approximately 1.6–2.1-fold as compared with controls. The increases, most evident for the 64- and 76-kD polypeptides (Fig. 7B, bands 2 and 4), resembled those for the total immunoreactivity with Tau 46/Tau 14 (1.5–1.6-fold), suggesting little preferential accumulation of isoforms expressing exon 10. Increases with E-2 and E-3 were less evident. This was not due to masking of epitopes by phosphorylation since treatment of samples with alkaline phosphatase for 24 h at 37°C did not improve the immunoreactivity with E-2, E-3, or E-10 (not shown). In summary, the increase in total tau protein could be due to factors other than selective changes in alternative gene splicing.

Tau in Cultured Astrocytes vs. Human Brain

Comparisons were made among tau proteins in cultured cells, in human fetal brain tissue, and in the PHF fraction from AD brain (Fig. 8). In control cultures, the major 52-kD polypeptide of tau migrated slightly below the major 55-kD polypeptide of fetal tau, consistent with a lower level of phosphorylation of the shortest tau isoform. The minor 64- and 70-kD bands, which were E-10, E-2, and E-3 reactive, were absent from fetal tau. The migration of the 61-kD polypeptide representing the shortest tau isoform was slower in OA-treated cultures than in fetal tau. This was consistent with a higher level of phosphorylation of tau in OA-treated cells. Indeed, the AT100 antibody detected the 61-kD polypeptide from cultures but was weak or absent in fetal brain samples (Fig. 6D, lane 1). Other phospho-epitopes including AT8, 12E8, and PHF-1 did not contribute to the differences in the migration pattern since these epitopes were

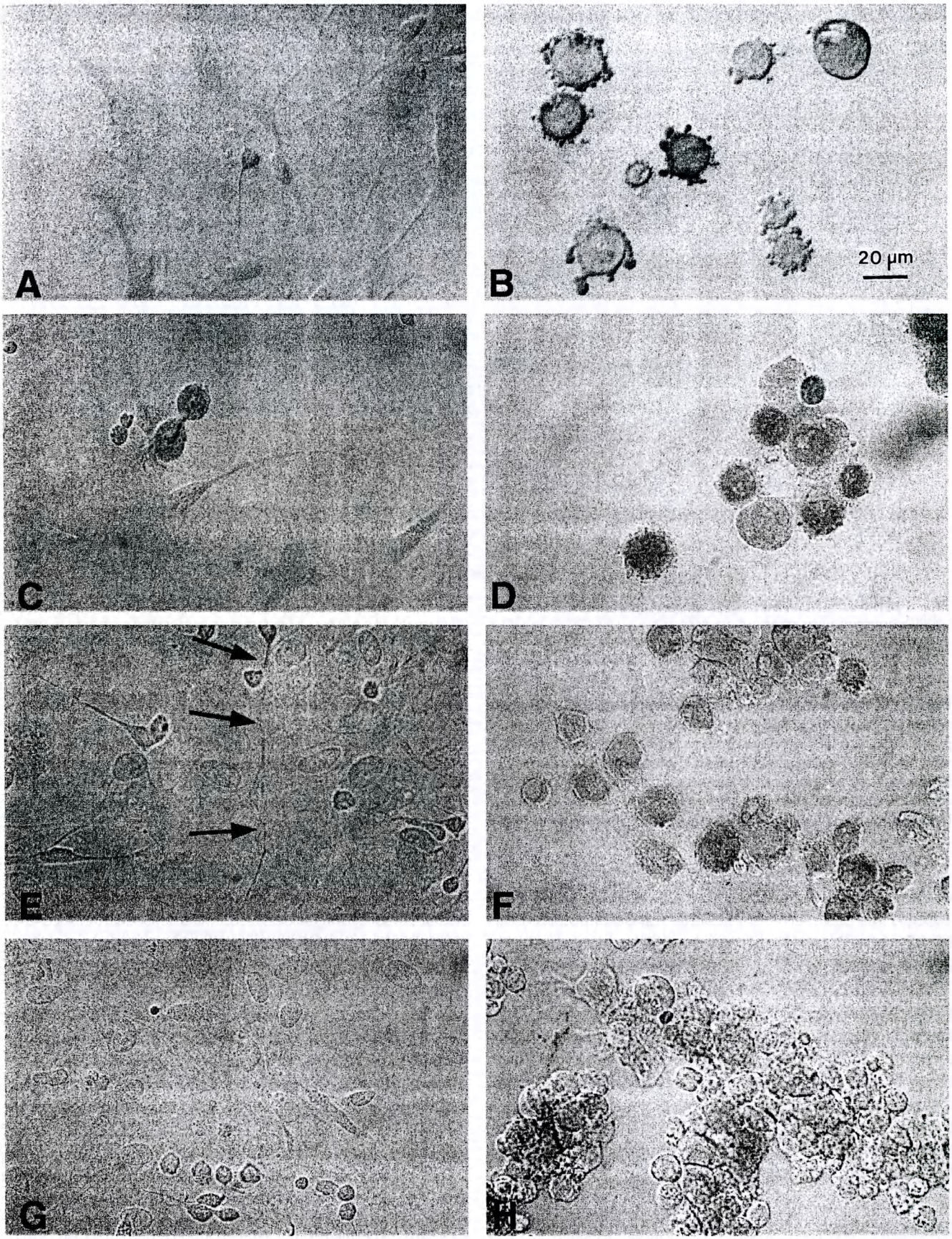

Fig. 5. Astroglia-enriched cultures immunostained for tau. **A,C,E,G:** Control cultures. **B,D,F,H:** OA-treated cultures. Antibodies against tau included PHF-1 (A and B), 12E8 (C and D), AT8 (E and F), and AT100 (G and H). Control cultures show either minimal staining (A and C) or no staining due to a low tau protein content and low phosphorylation. In E, cells are negative for AT8 except for a single cell, most likely of neuronal origin, displaying staining of the cytoplasm and neuritic process (*arrows*). The OA-treated cultures show a prominent but diffuse cytoplasmic staining with all tau antibodies. With PHF-1, the membrane blebs are also stained as seen in B. Incubations with OA (250 nM) were for 24 h except for 5 h in B.

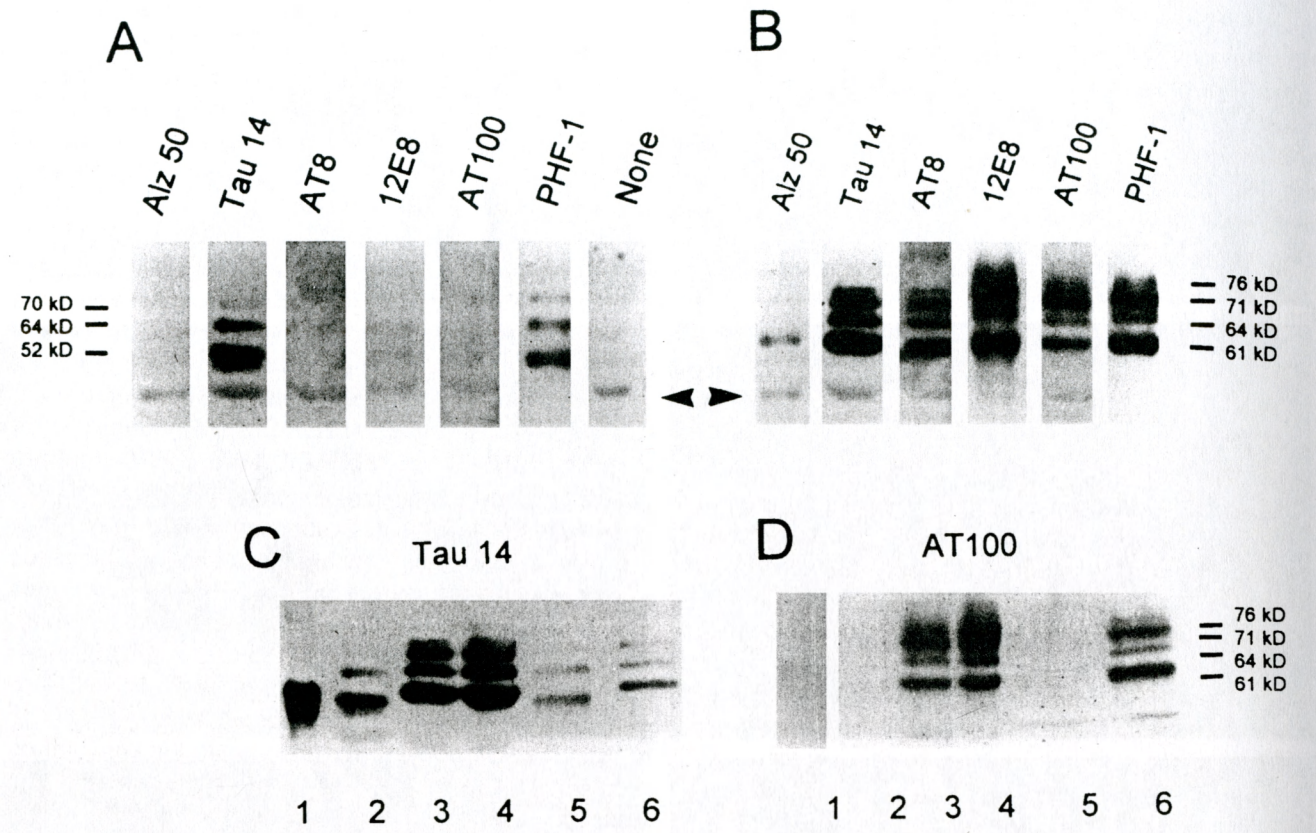

Fig. 6. Detection of tau in astroglia-enriched cultures. **A:** Control cultures. **B:** Cultures treated with OA (250 nM) for 24 h. Ten micrograms of protein of homogenates (urea buffer) were immunoblotted with antibodies against tau or without a primary antibody (None) as indicated. **C,D:** Immunoblots of various tau fractions with Tau 14 and AT100, respectively. **Lane 1**, tau preparation from human fetal brain; **lane 2**, control cell homogenate; **lane 3**, OA homogenate; **lane 4**, OA homogenate (detached cells only); **lane 5**, heat-stable extract of control cells; **lane 6**, heat-stable extract of OA-treated cells. The protein loading was 0.2 μg (lane 1), 10 μg (lanes 2, 3, and 4), and 2 μg (lanes 5 and 6). *Arrowheads* indicate a non-specific band stained in most blots. Three and four polypeptides of tau were identified in control and OA-treated cultures, respectively, with the molecular weight as indicated.

detected in both tau samples [see also Kenessey and Yen, 1993; Yang et al., 1997]. The PHF fraction contained the 60 kD, 64 kD and 68 kD polypeptides characteristic of PHF-tau from AD (Fig. 8) [Ksiezak-Reding and Wall, 1994; Goedert, 1998]. The migration pattern of PHF-tau polypeptides was strikingly similar to that from OA-treated cultures (61, 64, and 71 kD). This suggests a comparable phosphorylation state of both tau preparations. However, the relative content of individual bands differed between the preparations, e.g., the 64-kD polypeptide was only a minor band in cultured cells, suggesting that the contribution of individual tau isoforms is less comparable.

DISCUSSION

Cellular Tau

The major finding in the present studies is the induction of the AT100 epitope in cultures of normal human fetal astrocytes. This epitope is specific to PHFs from AD and other types of neurodegeneration [Ksiezak-Reding et al., 1996; Mailliot et al., 1998b] since it is absent in normal tau from biopsy brain samples. It has been suggested that generation of the AT100 epitope in cell-free systems requires a PHF-like conformation. However, we were unable to detect PHF-like filaments by EM examination of the apoptotic cells expressing the epitope. Instead, the apoptotic cells were filled with glial filaments in such abundance that they obscured other cytoskeletal elements, e.g., microtubules. Glial filaments could also mask PHFs. If present, PHFs are likely to be found in only small quantities and other methods may be required for detection. Interestingly, the PHF-1-immunoreactivity was associated with both nuclear material and filamentous/membranous structures in the cytoplasm. The presence of tau in the nucleus is compatible with earlier results [Brady et al., 1995; Greenwood and Johnson, 1995; Shea and Cressman, 1998]. In normal brains,

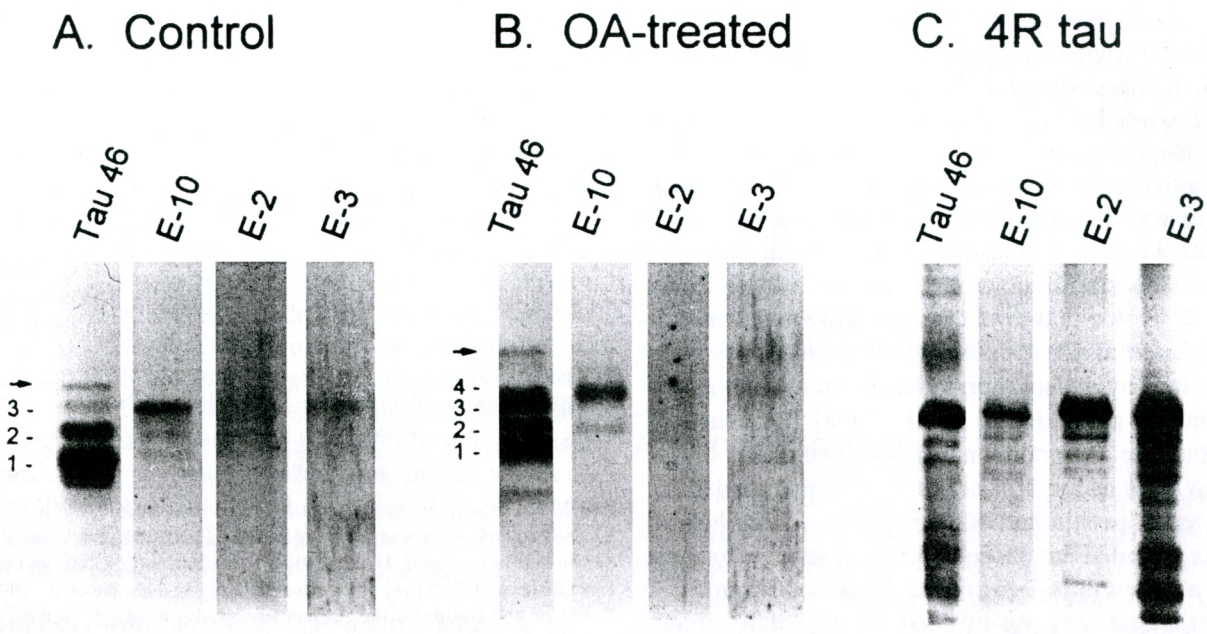

Fig. 7. Detection of tau isoforms with exon-peptide specific tau antibodies. A: Control astrocytes (Control); B: Cultures treated with OA (250 nM) for 24 h (OA-treated); C: Recombinant of the longest tau isoform (4R tau). Samples were heat-stable extracts (A and B) or purified preparations (C) immunoblotted with Tau 46, E-10, E-2 and E-3 antibodies as indicated. The protein loading was 2-4 μg (A and B) or 0.05-0.1 μg (C). Three and four polypeptides of tau were identified in control and OA-treated cultures, respectively, with the molecular weight as indicated in Fig. 6. An arrow marks a 76 kD polypeptide detected in some blots with Tau 46 but not other tau antibodies.

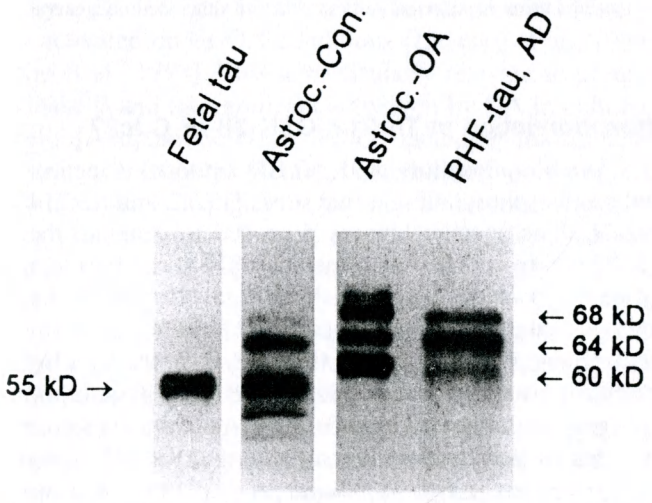

Fig. 8. Detection of various tau proteins with Tau 14. Lanes contain tau preparation from human fetal brain (Fetal tau); heat-stable extract from control astroglial cultures (Astroc.-Con.); heat-stable extract from OA-treated cultures (250 nM, 24 h) (Astroc.-OA); sarcosyl-insoluble fraction enriched in PHFs from AD brain (PHF-tau, AD). The protein loading was 5 μg except for fetal tau (0.2 μg). The molecular weight of fetal tau and PHF-tau triplet are indicated.

nuclear tau immunoreacts with AT100 [Gartner et al., 1998]. The role of phosphorylated tau in the nucleus is still unclear. In the cytoplasm, the PHF-1 immunoreactivity may represent tau tightly bound to cytoskeletal elements, especially tubulin (microtubules) and other proteins such as actin, GFAP, and non-receptor tyrosine kinase, fyn [Lee et al., 1998]. The binding of tau as well as tubulin to the endoplasmic reticulum is consistent with the fundamental role of microtubules and microtubule-associated proteins in the dynamic behavior of this and other organelles [Sato-Harada et al., 1996; Klopfenstein et al., 1998; Waterman-Storer and Salmon, 1998]. The precise molecular nature of the cytoskeletal and nuclear elements interacting with tau in apoptotic cells requires further study.

Apoptosis and Induction of AT100 Epitope

It is unclear whether type of cells, transfection with human tau cDNAs, OA treatment, or other factors are important for the induction of the AT100 phosphorylation. For example, AT100 immunoreactivity has been detected in untreated Sf9 insect cells transfected with human htau23 and htau40 cDNAs using the baculovirus vector [Zheng-Fischhofer et al., 1998]. The AT100 immunoreactivity has also been detected after OA treatment in COS-7 cells and in SY5Y neuroblastoma cell lines transfected with each of six human tau cDNAs [Mailliot et al., 1998a].

Our studies imply that events leading to induction of the AT100 epitope can be related either to apoptosis triggered by OA or to inhibition of OA-sensitive phosphatases. The distinction between these two effects of

OA on tau is not clear. Apoptosis induced by other methods, e.g., withdrawal of the nerve growth factor, resulted in increased phosphorylation of tau in PC12 cells and two human neuroblastoma cell lines, TR14 and N2T-N [Nuydens et al., 1997; Davis and Johnson, 1999]. Also treatment with sodium butyrate, another inducer of apoptosis, was associated with the hyperphosphorylation of tau in TR14 neuroblastoma cells [Nuydens et al., 1995]. However, in other studies, apoptosis triggered in PC12 cells by withdrawal of the nerve growth factor or in tau-transfected CHO cells by UV irradiation has been characterized by dephosphorylation of tau at the onset of the execution phase [Mills et al., 1998]. Sequence of events may be important in phosphorylation of tau in apoptosis. This factor still needs to be determined.

It has been reported that apoptosis induced by OA in differentiated and proliferating cells resembles incomplete or aberrant mitosis. For example, increases in Cdc2 and other kinases accompany decreases in certain protein phosphatases in apoptotic PC12 cells [Davis et al., 1997]. Induction of Cdk5 kinase is associated with neuronal death [Shirvan et al., 1998]. Upregulation of cyclins and other cell cycle markers occurs in postmitotic N2T-N cells as well as in proliferating TR14 cells undergoing apoptosis [Nuydens et al., 1998]. Since mitotic but not interphase cells phosphorylate tau at AD-specific sites [Vincent et al., 1996], it is reasonable to suggest that phosphorylation of the AT100 and other epitopes in astrocytes may reflect mitotic mechanisms triggered by apoptosis. Treatment with OA may be particularly effective in hyperphosphorylation of tau by playing a dual role: a trigger for apoptosis and inhibitor of tau phosphatases.

The OA-treated cells in our studies were far less viable than controls and contained significantly more Tau 14/Tau 46-immunoreactive protein. These results suggest that events accompanying apoptosis (e.g., reduction in viability and metabolism in general) additionally contribute to hyperphosphorylation of tau by slowing its degradation and prolonging its interaction with kinases [Vincent et al., 1994]. Some of the elevated tau content can be attributed to a spliced isoform of tau expressing exon 10. The increases, however, paralleled those of the total tau protein and are most likely due to a slower catabolism rather than changes in alternative splicing. Specific changes in alternative splicing stimulated by apoptosis have not been reported. On the other hand, tau protein content and tau mRNA expression were significantly increased in cultured cells using some [Barlow et al., 1994] but not all [Esclaire et al., 1998] apoptotic models. The effect of OA on expression of tau mRNA in astrocytes remains to be determined.

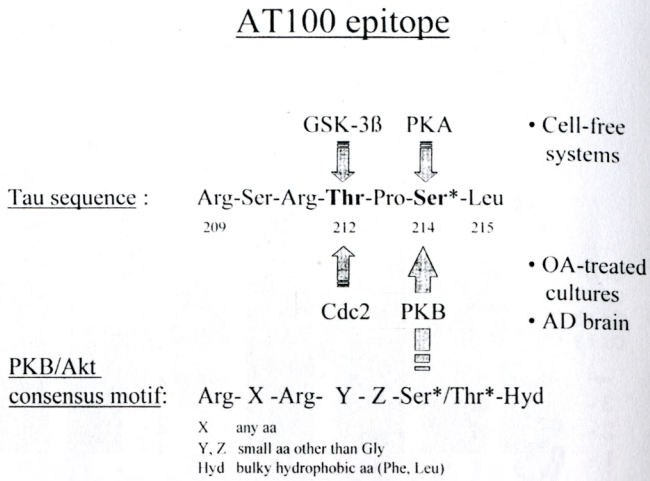

Fig. 9. Schematic diagram of the AT100 double phosphorylation site and two sets of kinases responsible for its phosphorylation, depending on the conditions used. Under cell-free conditions, GSG-3β and protein kinase A (PKA) may be involved [Zheng-Fischhofer et al., 1998]. Based on the results of the present sudies and results by others, we postulate that in OA-treated cells two other kinases—Cdc2-related kinase and protein kinase B (PKB)—are involved. These kinases are stimulated under OA conditions. Tau may be a substrate of protein kiase B since it contains a single consensus motif [Alessi et al., 1996] between Arg209 and Leu215, encompassing the region of the AT100 epitope as indicated. Protein kinase B is involved in the cell survival pathway [Dudek et al., 1997; Hemmings, 1997; Coffer et al., 1998] implying that AT100 phosphorylation may indicate activation of survival mechanisms in affected cells in AD and other neurodegenerations.

Phosphorylation at Thr212: GSK-3β or Cdc2?

Double-phosphorylated AT100 epitope is generated by phosphorylation at two sites, Thr212 and Ser214 (Fig. 9). The specific kinases proposed to generate the AT100 site in cell-free systems are GSK-3β and protein kinase A, respectively. Both kinases are found in the brain, although GSK-3β is considered to be mostly neuronal [Hangar et al., 1992]. GSK-3β is probably also present in astrocytes since it is involved in regulation of glycogen synthesis. The capacity to store and metabolize glycogen in astrocytes is unique among CNS cell types [Pellegri et al., 1996; Wiesinger et al., 1997] and in mature brain, glycogen is resticted to astrocytes [Hamprecht and Dringen, 1995].

There is an interesting issue related to the regulation of the activity of the two kinases involved, GSK-3β in particular. This enzyme plays a role in signal transduction [Woodgett et al., 1993; Welsh et al., 1996]. Its activity is subjected to intense positive and negative regulation, which involves phosphorylation at Tyr216 and Ser9, respectively [Hughes et al., 1993]. It is rather unlikely that OA induces prolonged Tyr216 phosphorylation and consequent activation of GSK-3β in astrocytes. In fact, OA treatment should induce inactivation of

this kinase as in human A431 epithelial cells [Saito et al., 1994]. Such inactivation may involve Ser9 phosphorylation via an upstream regulatory protein kinase B (also known as Akt), which is widely distributed in human brain and other tissues and plays an important role in cell signaling and survival [Dudek et al., 1997; Hemmings, 1997; Coffer et al., 1998]. Protein kinase B undergoes a 2- to 10-fold activation under OA conditions [Andjelkovic et al., 1996] and is likely to inactivate its physiological substrate, GSK-3β [Cross et al., 1995; van Weeren et al., 1998]. Therefore, proline-directed kinases other than GSK-3β may play a role in phosphorylating Thr212 of tau but their identity remains to be established [Lovestone et al., 1994; Ho et al., 1997]. Potential candidates are the apoptotic Cdc2-related kinases which are indirectly activated by OA [Liu et al., 1995; Vincent et al., 1997; Tanaka et al., 1998] and other members of the Cdc2 family, including Cdk5 [Patrick et al., 1999].

Phosphorylation at Ser214: Protein Kinase A or B?

Phosphorylation at Ser214 of recombinant tau in vitro has been attributed to protein kinase A [Scott et al., 1993; Zheng-Fischhofer et al., 1998; Jicha et al., 1999] although other non-proline-directed kinases may be involved as well [Mandelkow et al., 1995; Lovestone and Reynolds, 1997]. It is not clear whether protein kinase A is activated under OA conditions [Litersky et al., 1996; Xie et al., 1998]. This is particularly relevant to protein kinase B and its significant activation by OA in cultured cells [Andjelkovic et al., 1996], including human fetal astrocytes (Ksiezak-Reding, unpublished observation). As illustrated in Figure 9, tau may be an ideal substrate for protein kinase B as it contains a single consensus sequence motif required for efficient phosphorylation, Arg-X-Arg-Y-Z-Ser/Thr-Hyd, where X is any amino acid, Y and Z are small residues other than glycine, and Hyd is a bulky hydrophobic residue (Phe, Leu) [Alessi et al., 1996]. Such a motif encompasses the AT100 epitope, Arg-Ser-Arg-Thr-Pro-Ser214-Leu, suggesting that Ser214 of tau is likely to be under regulatory control by this kinase. Such regulation, however, remains to be determined. This is particularly important in neurodegenerative disorders associated with neuronal and glial apoptosis since protein kinase B plays a central role in a variety of critical biological functions, including protection from apoptosis [Coffer et al., 1998]. Phosphorylation at Ser214 may indicate an upregulation of protein kinase B activity in an effort to control cell survival. Furthermore, protein kinase B appears to be upregulated in terminally differentiated cells.

Our results suggest that apoptotic human astrocytes in culture can serve as a simple model for neuro- or glial degeneration in vitro. In such a model, it is necessary to use human material since alternative splicing of tau in humans differs from that in rodents [Grover et al., 1999]. Furthermore, cultured glial cells contain enough endogenous tau protein to perform biochemical and immunocytochemical studies without requiring transfection with human tau cDNA. They also contain kinases that are able to elicit AD-like specific phosphorylation as exemplified by induction of the AT100 epitope along with other phosphorylated sites. Protein kinase B represents one of the potential kinases linking Ser214 phosphorylation of tau to induction of cell-survival mechanisms.

ACKNOWLEDGMENTS

The authors thank Drs. Peter Davies (Albert Einstein College of Medicine, NY) for kindly providing monoclonal antibodies Alz 50 and PHF-1, André Delacourte and Luc Buée (INSERM U422, Lille Cedex, France) for exons 2, 3, and 10-specific antibodies, Lester Binder (Northwestern University, IL) for AP-18 antibody, Cedric Raine (Albert Einstein College of Medicine, NY) for anti-myelin basic protein, Peter Seubert (Athena Neurosciences, Inc., CA, and Elan Pharmaceuticals, Inc., CA) for the generous supply of 12E8, and A. Van de Voorde and E. Vanmechelen of Innogenetics, N.V. (Ghent, Belgium) for antibodies AT8 and AT100. The authors acknowledge Bradford K. Paulos, PhD, Meng Liang Zhao, MD, and Wa Shen for their effort in establishing human cell cultures. We thank Dr. Maurice Rapport for his comments on the manuscript and editorial corrections.

REFERENCES

Alessi DR, Caudwell FB, Andjelkovic M, Hemmings BA, Cohen P. 1996. Molecular basis for the substrate specificity of protein kinase B; comparison with MAPKAP kinase-1 and p70 S6 kinase. FEBS Lett 399:333–338.

Andjelkovic M, Jakubowicz T, Cron P, Ming XF, Han JW, Hemmings BA. 1996. Activation and phosphorylation of a pleckstrin homology domain containing protein kinase (RAC-PK/PKB) promoted by serum and protein phosphatase inhibitors. Proc Natl Acad Sci USA 93:5699–5704.

Arias C, Sharma N, Davies P, Shafit-Zagardo B. 1993. Okadaic acid induces early changes in microtubule-associated protein 2 and tau phosphorylation prior to neurodegeneration in cultured cortical neurons. J Neurochem 61:673–682.

Barlow S, Gonzales-Garay M, West R, Olmsted J, Cabral F. 1994. Stable expression of heterologous microtubule-associated proteins (MAPs) in chinese hamster ovary cells: evidence for differentiating roles of MAPs in microtubule organization. J Cell Biol 126:1017–1019.

Biernat J, Mandelkow EM. 1999. The development of cell processes induced by tau protein requires phosphorylation of serine 262 and 356 in the repeat domain and is inhibited by phosphorylation in the proline-rich domains. Mol Biol Cell 10:727–740.

Bondareff W, Matsuyama SS, Dell'Albani P. 1998. Production of paired helical filament, tau-like proteins by PC12 cells: a model of neurofibrillary degeneration. J Neurosci Res 52:498–504.

Brady RM, Zinkowski RP, Binder LI. 1995. Presence of tau in isolated nuclei from human brain. Neurobiol Aging 16:479–486.

Carmel G, Mager EM, Binder LI, Kuret J. 1996. The structural basis of monoclonal antibody Alz50's selectivity for Alzheimer's disease pathology. J Biol Chem 271:32789–32795.

Carmichael J, DeGraff WG, Gazdar AF, Minna JD, Mitchell JB. 1987. Evaluation of a tetrazolium-based semiautomated colorimetric assay: assessment of chemosensitivity testing. Cancer Res 47: 936–942.

Casadevall A, Cleare W, Feldmesser M, Glatman-Freedman A, Goldman DL, Kozel TR, Lendvai N, Mukherjee J, Pirofski LA, Rivera J, Rosas AL, Scharff MD, Valadon P, Westin K, Zhong Z. 1998. Characterization of a murine monoclonal antibody to Cryptococcus neoformans polysaccharide that is a candidate for human therapeutic studies. Antimicrob Agents Chemother 42: 1437–1446.

Chiang MF, Liu WK, Yen SH. 1993. Reversible heat-stress-related loss of phosphorylated Alzheimer-type epitopes in tau proteins of human neuroblastoma cells. J Neurosci 13:4854–4860.

Coffer PJ, Jin J, Woodgett JR. 1998. Protein kinase B (c-Akt): a multifunctional mediator of phosphatidylinositol 3-kinase activation. [Review] Biochem J 335:1–13.

Couchie D, Fages C, Bridoux AM, Rolland B, Tardy M, Nunez J. 1985. Microtubule-associated proteins and in vitro astrocyte differentiation. J Cell Biol 101:2095–3103.

Cross DA, Alessi DR, Cohen P, Andjelkovich M, Hemmings BA. 1995. Inhibition of glycogen synthase kinase-3 by insulin mediated by protein kinase B. Nature 378:785–789.

Davis PK, Johnson GVW. 1999. Energy metabolism and protein phosphorylation during apoptosis: a phosphorylation study of tau and high-molecular-weight tau in differentiated PC12 cells. Biochem J 340:51–58.

Davis PK, Dudek SM, Johnson GVW. 1997. Select alterations in protein kinases and phosphatases during apoptosis of differentiated PC12 cells. J Neurochem 68:2338–2347.

De Groot CJ, Langeveld CH, Jongenelen CA, Montagne L, Van Der Valk P, Dijkstra CD. 1997. Establishment of human adult astrocyte cultures derived from multiple sclerosis and control brain and spinal cord regions: immunophenotypical and functional characterization. J Neurosci Res 49:342–354.

Dickson DW, Liu WK, Ksiezak-Reding H, Yen SH. 2000. Corticobasal degeneration: neuropathologic and molecular considerations. In: Litvan I, Goetz C, Lang Á, editors. Corticobasal degeneration. Philadelphia: Lippincott-Raven Publishers p 9–27.

Drubin DG, Kirschner MW. 1986. Tau protein function in living cells. J Cell Biol 103:2739–2746.

Dudek H, Datta SR, Franke TF, Birnbaum MJ, Yao R, Cooper GM, Segal RA, Kaplan DR, Greenberg ME. 1997. Regulation of neuronal survival by the serine-threonine protein kinase Akt. Science 275:661–665.

Ebneth A, Godemann R, Stamer K, Illenberger S, Trinczek B, Mandelkow E. 1998. Overexpression of tau protein inhibits kinesin-dependent trafficking of vesicles, mitochondria, and endoplasmic reticulum: implications for Alzheimer's disease. J Cell Biol 143:777–794.

Eliasson C, Sahlgren C, Berthold C-H, Stakeberg J, Celis JE, Betsholtz, Eriksson JE, Pekny M. 1999. Intermediate filament protein partnership in astrocytes. J Biol Chem 274:23996–24006.

Esclaire F, Terro F, Yardin C, Hugon J. 1998. Neuronal apoptosis is associated with a decrease in tau mRNA expression. NeuroReport 9:1173–1177.

Fawcett DW. 1981. The cell. Philadelphia: W.B. Saunders Company. 743–855 p.

Gartner U, Janke C, Holzer M, Vanmechelen E, Arendt T. 1998. Postmortem changes in the phosphorylation state of tau-protein in the rat brain. Neurobiol Aging 19:535–543.

Gjertsen BT, Doskeland SO. 1995. Protein phosphorylation in apoptosis. [Review] Biochim Biophys Acta 1269:187–199.

Goedert M. 1998. Neurofibrillary pathology of Alzheimer's disease and other tauopathies. [Review] Prog Brain Res 117:287–306.

Goedert M, Jakes R, Vanmechelen E. 1995. Monoclonal antibody AT8 recognises tau protein phosphorylated at both serine 202 and threonine 205. Neurosci Lett 189:167–169.

Greenwood JA, Johnson GV. 1995. Localization and in situ phosphorylation state of nuclear tau. Exp Cell Res 220:332–337.

Grover A, Houlden H, Baker M, Adamson J, Lewis J, Prihar G, Pickering-Brown S, Duff K, Hutton M. 1999. 5′ splice site mutations in tau associated with the inherited dementia FTDP-17 affect a stem-loop structure that regulates alternative splicing of exon 10. J Biol Chem 274:15134–15143.

Hamprecht B, Dringen R. 1995. Energy metabolism. In: Kettenmann H, Ransom BR, editors. Neuroglia. New York and Oxford: Oxford University Press, p 473–487.

Hangar DP, Hughes K, Woodgett JR, Brion JP, Anderton BH. 1992. Glycogen synthase kinase-3 induces Alzheimer's disease-like phosphorylation of tau: generation of paired helical filament epitopes and neuronal localisation of the kinase. Neurosci Lett 147:58–62.

Hemmings BA. 1997. Akt signaling-linking membrane events to life and death decisions. Science 275:628–630.

Ho DT, Shayan H, Murphy TH. 1997. Okadaic acid induces hyperphosphorylation of tau independently of mitogen-activated protein kinase activation. J Neurochem 68:106–111.

Hoffmann R, Lee VMY, Leight S, Varga I, Otvos L Jr. 1997. Unique Alzheimer's disease paired helical filament specific epitopes involve double phosphorylation at specific sites. Biochemistry 36:8114–8124.

Hughes K, Nikolakaki E, Plyte SE, Totty NF, Woodgett JR. 1993. Modulation of the glycogen synthase kinase 3-family by tyrosine phosphorylation. EMBO J 12:803–808.

Jicha GA, Bowser R, Kazam IG, Davies P. 1997. Alz-50 and MC-1, a new monoclonal antibody raised to paired helical filaments, recognize conformational epitopes on recombinant tau. J Neurosci Res 48:128–132.

Jicha GA, Weaver C, Lane E, Vianna C, Kress Y, Rockwood J, Davies P. 1999. cAMP-dependent protein kinase phosphorylations on tau in Alzheimer's disease. J Neurosci 19:7486–7494.

Kenessey A, Yen SH. 1993. The extent of phosphorylation of fetal tau is comparable to that of PHF-tau from Alzheimer paired helical filaments. Brain Res 629:40–46.

Kim D, Su J, Cotman CW. 1999. Sequence of neurodegeneration and accumulation of phosphorylated tau in cultured neurons after okadaic acid treatment. Brain Res 839:253–262.

Klopfenstein DR, Kappeler F, Hauri HP. 1998. A novel direct interaction of endoplasmic reticulum with microtubules. EMBO J 17:6168–6177.

Kosik KS, Orecchio LD, Binder LI, Trojanowski J, Lee VMY, Lee G. 1988. Epitopes that span the tau molecule are shared with paired helical filaments. Neuron 1:817–825.

Ksiezak-Reding H, Wall JS. 1994. Mass and physical dimensions differ in two distinct populations of paired helical filaments. Neurobiol Aging 15:11–19.

Ksiezak-Reding H, Leibowitz R, Bowser R, Davies P. 1995. Binding of Alz 50 depends on Phe8 in tau synthetic peptides and varies between native and denatured tau proteins. Brain Res 697:63–75.

Ksiezak-Reding H, Tracz E, Yang LS, Dickson DW, Simon M, Wall JS. 1996. Ultrastructural instability of paired helical filaments from corticobasal degeneration as examined by scanning transmission electron microscopy. Am J Pathol 149:639–652.

Ksiezak-Reding H, Farooq M, Norton W, Yang LS, Dickson DW. 1997. A distinct subset of tau isoforms is expressed in bovine brain oligodendrocytes. Mol Biol Cell 8:263a.

Lee G, Rook SL. 1992. Expression of tau protein in non-neuronal cells: microtubule binding and stabilization. J Cell Sci 102: 227–237.

Lee G, Newman ST, Gard DL, Band H, Panchamoorthy G. 1998. Tau interacts with src-family non-receptor tyrosine kinases. J Cell Sci 111:3167–3177.

Lee SC, Liu W, Brosnan CF, Dickson DW. 1992. Characterization of primary human fetal dissociated central nervous system cultures with an emphasis on microglia. Lab Invest 67:465–476.

Litersky J.M, Johnson GV, Jakes R, Goedert M, Lee M, Seubert P. 1996. Tau protein is phosphorylated by cyclic AMP-dependent protein kinase and calcium/calmodulin-dependent protein kinase II within its microtubule-binding domains at Ser-262 and Ser-356. Biochem J 316:655–660.

Liu W, Shafit-Zagardo B, Aquino DA, Zhao M-L, Dickson DW, Brosnan CF, Lee S. 1994. Cytoskeletal alterations in human fetal astrocytes induced by interleukin-1β. J Neurochem 63: 1625–1634.

Liu WK, Williams RT, Hall FL, Dickson DW, Yen SH. 1995. Detection of a Cdc2-related kinase associated with Alzheimer paired helical filaments. Am J Pathol 146:225–238.

LoPresti P, Szuchet S, Papasozomenos SC, Zinkowski RP, Binder LI. 1995. Functional implications for the microtubule-associated protein tau: localization in oligodendrocytes. Proc Natl Acad Sci USA 92:10369–10373.

Lovestone S, Reynolds CH. 1997. The phosphorylation of tau: a critical stage in neurodevelopment and neurodegenerative processes. [Review] Neuroscience 78:309–324.

Lovestone S, Reynolds CH, Latimer D, Davis DR, Anderton BH, Gallo JM, Hanger D, Mulot S, Marquardt B, Stabel S, Woodgett JR, Miller CCJ. 1994. Alzheimer's disease-like phosphorylation of the microtubule-associated protein tau by glycogen synthase kinase-3 in transfected mammalian cells. Curr Biol 4:1077–1086.

Mailliot C, Bussiere T, Caillet-Boudin ML, Delacourte A, Buee L. 1998a. Alzheimer-specific epitope of AT100 in transfected cell lines with tau: toward an efficient cell model of tau abnormal phosphorylation. Neurosci Lett 255:13–16.

Mailliot C, Sergeant N, Bussiere T, Caillet-Boudin ML, Delacourte A, Buee L. 1998b. Phosphorylation of specific sets of tau isoforms reflects different neurofibrillary degeneration processes. FEBS Lett 433:201–204.

Mandelkow EM, Biernat J, Drewes G, Gustke N, Trinczek B, Mandelkow E. 1995. Tau domains, phosphorylation, and interactions with microtubules. [Review] Neurobiol Aging 16:355–362.

Matsuo ES, Shin RW, Billingsley ML, Van deVoorde A, O'Connor M, Trojanowski JQ, Lee VMY. 1994. Biopsy-derived adult human brain tau is phosphorylated at many of the same sites as Alzheimer's disease paired helical filament tau. Neuron 13: 989–1002.

Mills JC, Lee VMY, Pittman RN. 1998. Activation of a PP2A-like phosphatase and dephosphorylation of tau protein characterize onset of the execution phase of apoptosis. J Cell Sci 111:625–636.

Muller R, Heinrich M, Heck S, Blohm D, Richter-Landsberg C. 1997. Expression of microtubule-associated proteins MAP2 and tau in cultured rat brain oligodendrocytes. Cell Tissue Res 288: 239–249.

Nuydens R, Heers C, Chadarevian A, De Jong M, Nuyens R, Cornelissen F, Geerts H. 1995. Sodium butyrate induces aberrant tau phosphorylation and programmed cell death in human neuroblastoma cells. Brain Res 688:86–94.

Nuydens R, Dispersyn G, De Jong M, Van Den Kieboom G, Borgers M, Geerts H. 1997. Aberrant phosphorylation and neurite retraction during NGF deprivation in PC12 cells. Biochem Biophys Res Commun 240:687–691.

Nuydens R, De Jong M, Van Den Kieboom G, Heers C, Dispersyn G, Cornelissen F, Nuyens R, Borgers M, Geerts H. 1998. Okadaic acid-induced apoptosis in neuronal cells: evidence for an abortive mitotic attempt. J Neurochem 70:1124–1133.

Otvos L, Feiner L, Lang E, Szendrei GI, Goedert M, Lee VM. 1994. Monoclonal antibody PHF-1 recognizes tau protein phosphorylated at serine residues 396–404. J Neurosci Res 39:669–673.

Patrick GN, Zukerberg L, Nikolic M, de la Monte S, Dikkes P, Tsai L-H. 1999. Conversion of p35 to p25 deregulates Cdk5 activity and promotes neurodegeneration. Nature 402:615–622.

Pellegri G, Rossier C, Magistretti PJ, Martin JL. 1996. Cloning, localization and induction of mouse brain glycogen synthase. Brain Res Mol Brain Res 38:191–199.

Privat A, Rataboul P. 1986. Fibrous and protoplasmic astrocytes. In: Fedoroff S, Vernadakis A, editors. Astrocytes. Orlando, FL: Academic Press, Inc. p 105–129.

Saito Y, Vandenheede JR, Cohen P. 1994. The mechanism by which epidermal growth factor inhibits glycogen synthase kinase 3 in A431 cells. Biochem J 303:27–31.

Sato-Harada R, Okabe S, Umeyama T, Kanai Y, Hirokawa N. 1996. Microtubule-associated proteins regulate microtubule function as the track for intracellular membrane organelle transports. Cell Struct Funct 21:283–295.

Schweers O, Schonbrunn-Hanebeck E, Marx A, Mandelkow E. 1994. Structural studies of tau protein and Alzheimer paired helical filaments show no evidence for β-structure. J Biol Chem 269: 24290–24297.

Scott CW, Spreen RC, Herman JL, Chow FP, Davison MD, Young J, Caputo CB. 1993. Phosphorylation of recombinant tau by cAMP-dependent protein kinase. Identification of phosphorylation sites and effect on microtubule assembly. J Biol Chem 68:1166–1173.

Sergeant N, David JP, Lefranc D, Vermersch P, Wattez A, Delacourte A. 1997. Different distribution of phosphorylated tau protein isoforms in Alzheimer's and Pick's diseases. FEBS Lett 412: 578–582.

Seubert P, Mawal-Dewan M, Barbour R, Jakes R, Goedert M, Johnson GVM, Litersky JM, Schenk D, Lieberburg I, Trojanowski JQ, Lee VMY. 1995. Detection of phosphorylated Ser262 in fetal tau, adult tau, and paired helical filament tau. J Biol Chem 270:18917–18922.

Shea TB, Cressman CM. 1998. A 26-30 kDa developmentally-regulated tau isoform localized within nuclei of mitotic human neuroblastoma cells. Int J Dev Neurosci 16:41–48.

SheaTB, Fischer I. 1996. Phosphatase inhibition in human neuroblastoma cells alters tau antigenicity and renders it incompetent to associate with exogenous microtubules. FEBS Lett 380:63–67.

Shirvan A, Ziv I, Zilkha-Falb R, Machlyn T, Barzilai A, Melamed E. 1998. Expression of cell cycle-related genes during neuronal apoptosis: is there a distinct pattern? Neurochem Res 23:767–777.

Tanaka T, Zhong J, Iqbal K, Trenkner E, Grundke-Iqbal I. 1998. The regulation of phosphorylation of tau in SY5Y neuroblastoma cells: the role of protein phosphatases. FEBS Lett 426:248–254.

van Weeren PC, de Bruyn KM, de Vries-Smits AM, van Lint J, Burgering BM. 1998. Essential role for protein kinase B (PKB) in insulin-induced glycogen synthase kinase 3 inactivation. Characterization of dominant-negative mutant of PKB. J Biol Chem 273:13150–13156.

Vincent I, Rosado M, Kim E, Davies P. 1994. Increased production of paired helical filament epitopes in a cell culture system reduces the turnover of tau. J Neurochem 62:715–723.

Vincent I, Rosado M, Davies P. 1996. Mitotic mechanisms in Alzheimer's disease? J Cell Biol 132:413–425.

Vincent I, Jicha G, Rosado M, Dickson DW. 1997. Aberrant expression of mitotic Cdc2/cyclin B1 kinase in degenerating neurons of Alzheimer's disease brain. J Neurosci 17:3588–3598.

Waterman-Storer CM, Salmon ED. 1998. Endoplasmic reticulum membrane tubules are distributed by microtubules in living cells using three distinct mechanisms. Curr Biol 8:798–806.

Welsh GI, Wilson C, Proud CG. 1996. GSK3: a SHAGGY frog story. Trends Cell Biol 6:274–279.

Wiesinger H, Hamprecht B, Dringen R. 1997. Metabolic pathways for glucose in astrocytes. [Review] GLIA 21:22–34.

Woodgett JR, Plyte SE, Pulverer BJ, Mitchell JA, Hughes K. 1993. Roles of glycogen synthase kinase-3 in signal transduction. [Review] Biochem Soc Trans 21:905–907.

Xie HQ, Litersky JM, Hartigan JA, Jope RS, Johnson GVW. 1998. The interrelationship between selective tau phosphorylation and microtubule association. Brain Res 798:173–183.

Yang LS, Gordon-Krajcer W, Ksiezak-Reding H. 1997. Tau released from paired helical filaments with formic acid or guanidine is susceptible to calpain-mediated proteolysis. J Neurochem 69: 1548–1558.

Zheng-Fischhofer Q, Biernat J, Mandelkow EM, Illenberger S, Godemann R, Mandelkow E. 1998. Sequential phosphorylation of Tau by glycogen synthase kinase-3beta and protein kinase A at Thr212 and Ser214 generates the Alzheimer-specific epitope of antibody AT100 and requires a paired-helical-filament-like conformation. Eur J Biochem 252:542–552.

Publikacja 6

ACTA NEUROBIOLOGIAE EXPERIMENTALIS

Acta Neurobiol Exp 2004, 64: 491-502

2-Deoxyglucose induces β-APP overexpression, tau hyperphosphorylation and expansion of the *trans*-part of the Golgi complex in rat cerebral cortex

Pawel Grieb[1], Wanda Gordon-Krajcer[2], Małgorzata Frontczak-Baniewicz[3], Michał Walski[3], Miroslaw S. Ryba[1], Tomasz Kryczka[1], Michal Fiedorowicz[1], Piotr Kulinowski[4], Zenon Sułek[4], Katarzyna Majcher[4] and **Andrzej Jasiński[4]**

[1]Laboratory of Experimental Pharmacology, [2]Department of Neurochemistry, [3]Laboratory of Cell Ultrastructure, M. Mossakowski Medical Research Centre, Polish Academy of Sciences, Warsaw, Poland; [4]Department of Magnetic Resonance, H. Niewodniczański Institute of Nuclear Physics, Polish Academy of Sciences, Krakow, Poland

Abstract. The effects of a single intraperitoneal injection of a non-metabolizable glucose analog 2-deoxyglucose (2-DG, 500 mg/kg) on the levels of β-APP expression, and phosphorylated and unphosphorylated tau protein in the rat cerebral cortex were investigated. The effects of 2-DG on the ultrastructure of cortical neurons with particular emphasis on the morphology of the Golgi apparatus, and on brain bioenergetics assessed by *in vivo* ^{31}P-MRS technique were also evaluated. Seven and a half hours after injection of 2-deoxyglucose a significant increase in brain cortex β-APP expression, increased tau phosphorylation, and a marked relative expansion of the *trans*- part of the Golgi intracellular secretory pathway in cortical neurons has been found. The changes of β-APP expression and tau phosphorylation appeared within 1 h after 2-DG application and continued for at least 24 h. However, brain ^{31}P resonance spectra remained unchanged for up to 7.5 h after 2-DG. It is suggested that the increase of β-APP expression represents a response of brain tissues to 2-DG-evoked biochemical stress, while tau hyperphosphorylation and the change in Golgi morphology may be secondary phenomena.

The correspondence should be addressed to P. Grieb, Email: pgrieb@cmdik.pan.pl

Key words: 2-deoxyglucose, beta-amyloid precursor protein, tau protein, Golgi apparatus, phosphorous magnetic resonance spectroscopy, brain cortex

INTRODUCTION

The "amyloid cascade" hypothesis of Alzheimer's disease (AD) assumes that formation of insoluble, neurotoxic amyloid deposits resulting from imbalance between amyloid beta peptide (Abeta) production and catabolism is the primary and central pathogenetic event. The other phenomena characteristic of the Alzheimer's brain such as formation of neurofibrillary tangles, cholinergic dysfunction, brain hypoperfusion, hypometabolism and oxidative stress, and finally neurodegeneration, are considered secondary to the amyloid neurotoxicity (Hardy and Higgins 1992, Hardy and Selkoe 2002). Although currently the most popular, the "amyloid cascade" hypothesis is not universally accepted. For example, Swaab and coauthors (2002) pointed out that neuropathological hallmarks of AD (amorphous and neuritic plaques, pretangles and neurofibrillary tangles, and neuronal death) cannot form a single pathogenetic cascade because they may occur independently.

One of the numerous alternative hypotheses of AD is the "insulin resistance" hypothesis (Hoyer 1998, 2002) which assumes that the primary and central pathogenetic event in the AD (sporadic type) is the desensitization of brain insulin receptors, i.e., AD is brain-specific analog of type 2 diabetes mellitus (IDDM). According to this concept, brain glucose metabolism is controlled by insulin receptors, and their desensitization results in progressive metabolic and functional failure. The other phenomena characteristic for the Alzheimer's brain, including formation of insoluble amyloid deposits, result from the cerebral hypometabolic state. This hypothesis is supported by experimental data showing that intracerebroventricular injections of a diabetogenic toxin streptozotocin are followed by a fall in brain glucose consumption (which is more pronounced than the concomitant fall in oxygen uptake), by a drop in the cellular energy pool, cholinergic deafferentation, learning and memory deficits and changes in membrane phospholipids. All these phenomena are similar to those which occur in sporadic AD (reviewed by Hoyer 2002). Streptozotocin, known to inhibit the phosphorylation of insulin receptor tyrosine kinase (Kadowaki et al. 1984), upon injection into the brain ventriculocisternal system is assumed to cause dysfunction of neuronal insulin receptors and impair insulin signal transduction across the brain. The "insulin resistance" hypothesis may explain some clinical, as well as experimental data, which does not fit well into the frame of the "amyloid cascade" hypothesis. These include, first of all, the early decrease of glucose metabolism in AD, which precedes not only the onset of dementia, but also the decrease of brain oxygen uptake (Fukuyama et al. 1994, Minoshima et al. 1997, Ogawa et al. 1996, Piert et al. 1996).

Abeta is a product of amyloidogenic proteolysis of beta-amyloid precursor protein (β-APP) (Mattson 1997). This protein, which has a relatively short half-life of 20-30 min (Weidemann et al. 1989), is translocated into the endoplasmic reticulum and posttranslationally modified within the Golgi system. Later it undergoes either nonamyloidogenic or amyloidogenic proteolysis which yields soluble nonamyloidogenic peptides or amyloidogenic Abeta, respectively. These peptides are released into the extracellular space. In normal conditions both proteolytic pathways are active and certain quantities of Abeta are released from cells (Selkoe 2001, see also the references cited therein). However, Abeta is effectively catabolized and no amyloid deposits are formed.

The equilibrium between Abeta formation and clearance may be disturbed when the production of β-APP is increased. Various patterns of β-APP overexpression in brain cells have been reported after several types of cerebral injury including focal and global ischemia, trauma, excitotoxicity (for references see Mattson 1997), hyperglycemic hypoxia (Pedersen et al. 1999), hypoglycemia (Shi et al. 1997) and simulated subarachnoid hemorrhage (Ryba et al. 1999). Altered expression and phosphorylation of β-APP have also been found in heat-shocked neuronal PC12 cells *in vitro* along with the induction of heat shock protein hsp72 (Johnson et al. 1993, Wallace et al. 1993). Interestingly, stimulation of the amyloidogenic pathway of β-APP processing following glucoprivation of cultured hippocampal cells by a combination of 2-deoxyglucose (2-DG) and sodium azide has been found by Gabuzda and coauthors (1994) who attributed this effect to the inhibition of cellular energy metabolism. 2-DG is a non-metabolizable glucose analog which enters the cells and is phosphorylated to 2-DG-6-phosphate (2-DG-6-P), but is not metabolized further and acts as the competitive inhibitor of glucose-6-phosphoisomerase (Wick et al. 1957). Several investigators have used 2-DG as a non-specific stressor and employed it, for example, to define stress effects on immune responses (Dreau et al. 2000).

In the experiments described herein we attempted to find out whether a biochemical stress evoked *in vivo* by a single systemic injection of 2-deoxyglucose involves changes in brain bioenergetics and whether it is followed by the β-APP overexpression, tau protein hyperphosphorylation and ultrastructural changes in the morphology of the Golgi apparatus resembling those characteristic for the Alzheimer's brain.

METHODS

The protocol of the study was approved by the First Ethical Committee of the City of Warsaw. Chemicals, antibodies and standards were purchased from Sigma (St Louis, MO, USA), unless stated otherwise. The experiments were performed on outbred male Wistar rats, 230-350 g body weight, bred in the Animal House of the Mossakowski MRCPAS. All experimental animals were injected intraperitoneally with 500 mg/kg 2-DG (prepared as 1g/ml solution in physiological saline). Control animals received solvent injection.

For Western blotting of β-APP- and tau-related immunoreactivity the animals were sacrificed by decapitation at different times after 2-DG injection (0 and 7.5 h in the first, and 0, 1, 2, 3, 6, 12 and 24 h in the second series of the experiments, 4-8 animals per each time point). The brains were immediately snap-frozen in liquid nitrogen and stored at -70°C until further processed. The cortex (grey matter) from each hemisphere was dissected out on a coated glass surface and homogenized (1:10, w/v) in 20 mM MES/Na buffer pH 6.8 containing 5 mM EGTA, 1 mM $MgCl_2$, 1 mM PMSF, 50 μg/ml leupeptin, 25 μg/ml pepstatin A and 0.1 mg/ml aprotinin. For β-APP the following antibodies raised against synthetic peptides corresponding to the amino acid residues of (697 aa) isoform were used: mAb which reacts with the near-end N-terminal domain of β-APP (46-60 aa) (1:1 000); mAb 6E10 recognizing 1-17 aa residues of Abeta corresponding to 597-613 aa of β-APP, further referred to as the M-domain (1:1 000); pAb RAS57 against the C-terminal domain of β-APP (672-695 aa) (a gift from Prof. Henry Wiśniewski, IBR, Staten Island, NY, USA, 1:1 000). For phosphorylated and unphosphorylated forms of tau protein mAb AT-8 (from Innogenetics, Ghent, Belgium, 1:10) and mAb Tau-1 (from Boehringer Mannhein Germany, 1:200) were used, respectively. Tau-1 recognizes a non-phosphorylated and AT-8 a phosphorylated epitope of tau.

Aliquots of brain tissue homogenates containing 40 μg protein for β-APP and 0.5-5 μg protein for tau were electrophoresed on linear SDS-PAGE 10% polyacrylamide gels (Laemmli 1970), and on trycine–SDS-polyacrylamide gels (Schagger and von Jagow 1987) using 4% T 3% C stacking gel 10%, using II-Protean Gel Apparatus and Mini Trans-Blot Electrophoretic Transfer Cell (Bio-Rad, USA), respectively. The separated proteins were electrotransferred onto nitrocellulose membranes (Towbin et al. 1979). Non-specific binding sites were blocked with 5% skim milk in TBS for 2 h at 25°C. The membranes were incubated with primary antibodies for 4 h and the complexes were exhibited to appropriate secondary antibodies and visualized with an ECL Western Blotting Detection Reagent Kit (Amersham, UK), or an Alkaline Phosphatase Conjugate Substrate Kit (Bio-Rad, USA).

The intensity of immunoreactivity was quantified on nitrocellulose membranes, or ECL X-ray films by densitometric scanning using Gel Expert Software and Analysis System Apparatus Nucleo Vision 920 (NucleoTech Corporation, USA). To cover the range of isoforms detected by the antibodies, scanning was performed within 112-116 kD and 63-68 kD limits (according to the high MW standard), for uncleaved β-APP and tau, respectively. Quantitative data are presented in the figures as means ± SD. Statistical significance was tested with *t*-test for independent data, or one-way ANOVA followed by *post-hoc* Sheffe's test, as appropriate.

To assess the effects of 2-DG on brain energy metabolism ^{31}P MR localized spectra were acquired *in vivo* from rat cortex using a research MRI/MRS system (located at the H. Niewodniczański INPPAS), equipped with a 4.7T/31 cm horizontal bore superconducting magnet (Bruker Germany), actively shielded gradient coil (Magnex Scientific, UK) and a digital console MARAN-DRX (Resonance Instuments, UK). A home-made dedicated probe with a double tuned surface coil (^1H at 200.121 MHz, ^{31}P at 81 MHz) placed over the skull was used to acquire MR signals from the brain cortex. The rats, anesthetized with a 2% halothane in oxygen/air 40/60 mixture and maintained with 1-1.5% halothane in the same mixture, were placed in the magnet. Before each experiment RF pulses were optimized to obtain maximum S/N ratio from the cortex. B_0 homogeneity was corrected by manually protons over the whole brain to obtain final linewidth of 0.3 ppm. ^{31}P spectra were acquired using the excitation-acquisition

method just prior to, and then every 6 minutes after 2-DG injection, up to 7.5 h (or prior to death). A glass pellet of 3 mm inner diameter containing 0.5 mM PPA water solution, placed on the skull surface in the centre of the surface coil, served as an external standard. The MRUI graphical user interface package and the VARPRO non-linear fitting algorithm were used to process the acquired FID signals.

Brain tissue sampling for electron microscopy was performed under ketamine (70 mg/kg) and xylazine (20 mg/ml) anesthesia 7.5 h after injection of 2-DG or vehicle. The animals (4 2-DG treated and 3 vehicle-treated) were perfused *via* the left heart ventricle with a mixture of 2% paraformaldehyde and 2.5% glutaraldehyde in 0.1 M cacodylate buffer, pH 7.4 at 20°C. Tissues sampled from the fronto-parietal lobe of cerebral cortex were fixed in the same solution for 20 h, postfixed in a mixture of 1% OsO_4 and 0.8% $K_4[Fe(CN)_6]$, and processed for transmission electron microscopy. After dehydration in series of ethanol and propylene oxide, tissue specimens were embedded in Spurr resin. Serial ultrathin (50 nm) sections were examined with a JEM 1200EX electron microscope. In representative populations of neuronal cells, the average area of the whole Golgi apparatus as well as its *-cis* (proximal) and *-trans* (distal) parts was also determined, as described in detail in the accompanying paper (Grieb et al. 2004). Significance of differences between morphometric data for neurons from control and 2-DG-treated animals were evaluated with the Mann-Whitney U-test.

RESULTS

Seven and a half hours following subcutaneous 2-DG injection immunoreactivity detected in cortical homogenates by each of the three antibodies directed toward different domains of uncleaved β-APP revealed marked increases (Fig. 1). Interestingly, however, the effects on the immunoreactivity detected by the three antibodies recognizing different epitopes on uncleaved β-APP molecules were of different magnitude: the C-terminal immunoreactivity was increased by 59%, whereas that of N-terminal by 108%, and that of the middle domain of β-APP chain by 84%.

Immunoreactivity detected by the antibody recognizing the nonphosphorylated tau molecules revealed a marked decrease, while the opposite effect was seen with immunoreactivity directed toward the phosphorylated tau (Fig. 2). The effects of 2-DG on non-phosphorylated and phosphorylated tau were of comparable magnitude, namely a decrease of 55% and an increase of 45%, respectively, was found.

Electron-microscopic evaluation of the fronto-parietal cortex sampled 7.5 h after 2-DG application revealed enlarged endoplasmatic reticulum and markedly

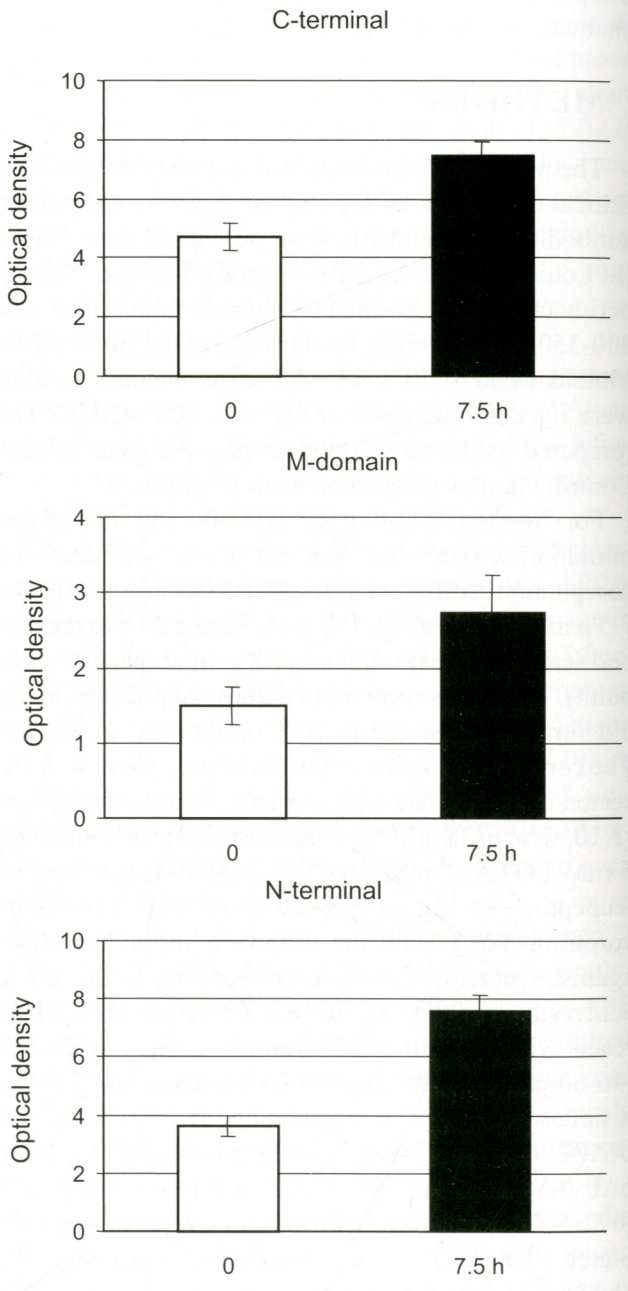

Fig. 1. The effects of 2-DG on β-APP-related immunoactivity detected by the three different antibodies. (0) homogenates of brain cortex of control animals; (7.5 h) homogenates of brain cortex of animals sampled 7.5 h after 2-DG injection. All differences are statistically significant ($P<0.01$).

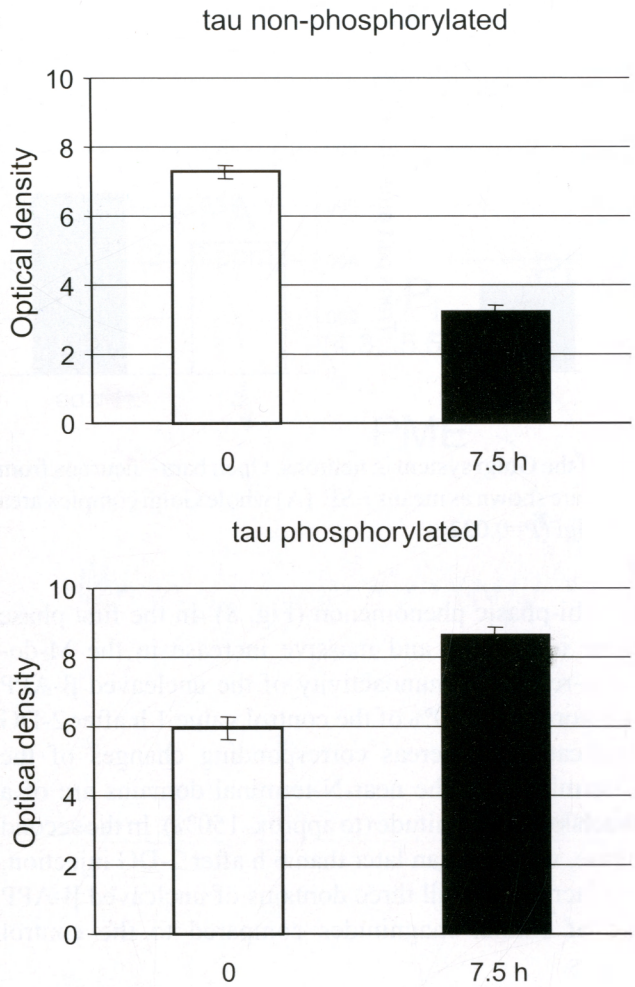

Fig. 2. The effects of 2-DG on nonphosphorylated (upper panel) and phosphorylated (lower panel) tau immunoreactivity. (0) homogenates of brain cortex of control animals, (7.5 h) homogenates of brain cortex of animals sampled 7.5 h after 2-DG injection. The differences are statistically significant ($P<0.01$).

expanded *trans*- part of the Golgi system in neuronal cells, while mitochondria were not affected (Fig. 3). For comparison, a micrograph of a cortical neuron from a vehicle-injected animal is also shown (Fig. 4). Quantitative morphometric analysis of the Golgi apparatus in neurons of control and 2-DG-treated animals showed that neither the average size of the whole Golgi complex, nor the average size of its *cis*- (i.e., proximal) part were significantly affected by the treatment (Fig. 5). However, in neurons from 2-DG-treated animals the size of the *trans*- (i.e., the distal) part of the Golgi was significantly increased (Fig. 5), and this resulted in markedly higher values of the *trans*/*cis* area ratio of the Golgi in most cells (Fig. 6).

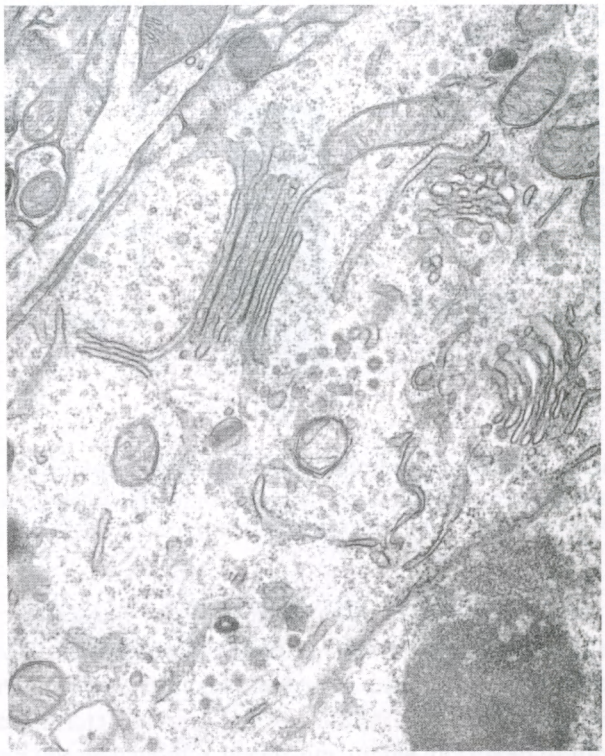

Fig. 3. Electron micrograph of a cortical neuron from a 2-DG-treated rat. Mitochondria are unaffected, but expanded *trans*-Golgi complex is clearly seen. Magnification, × 25 000.

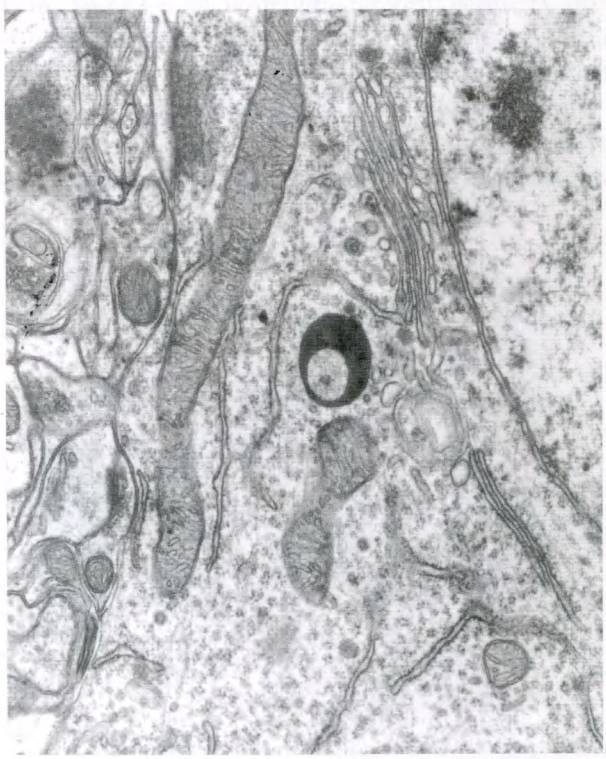

Fig. 4. Electron micrograph of a cortical neuron from a vehicle-treated rat. Magnification, × 20 000.

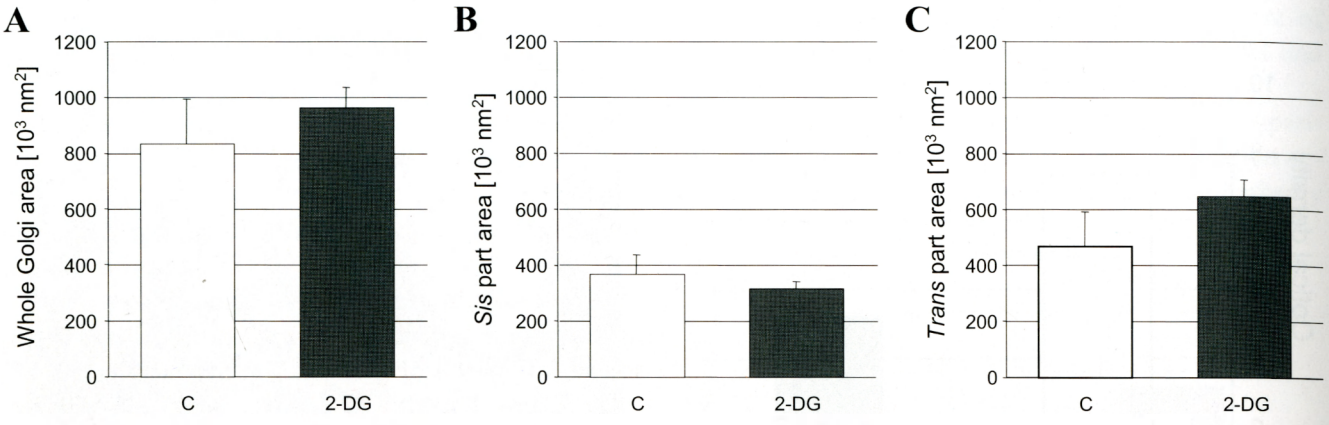

Fig. 5. Summary of the morphometric evaluation of the average size of the Golgi system in neurons. Open bars – neurons from control animals, filled bars – neurons from 2-DG-treated animals. Data are shown as means ± SE. (A) whole Golgi complex area (P>0.05); (B) *cis* part of the Golgi (P>0.05); (C) *trans* part of the Golgi (P=0.022).

MR spectroscopy evaluation of brain phosphorous compounds revealed no significant changes in the spectra for up to 7.5 h after subcutaneous injection of 2-DG (except when the condition of the animal deteriorated prior to death caused by anesthesia-related acidosis and hypotension). Following 2-DG application all spectral lines remained unchanged, except a transient increase of the phosphomonoesters (PME) signal at approx. 7 ppm (Fig. 7), reflecting accumulation of 2-DG-6P in the brain. According to Deuel and coauthors (1985) the chemical shift of 2-DG-6-P is 7.11 ppm.

The results of further immunoblotting experiments revealed that changes of all three β-APP-related immunoreactivities are highly significant and appear to be a bi-phasic phenomenon (Fig. 8). In the first phase there is a quick and massive increase in the M-domain-related immunoactivity of the uncleaved β-APP (to more than 250% of the control value 1 h after 2-DG application), whereas corresponding changes of the C-terminal and the near-N-terminal domains are of a much lower magnitude (to approx. 150%). In the second phase, which began later than 6 h after 2-DG injection, the increases in all three domains of uncleaved β-APP are of similar magnitudes compared to the control values.

The changes of unphosphorylated tau with time (Fig. 9, upper panel) were also highly significant, but did not show a bi-phasic characteristic. Instead, unphosphry-

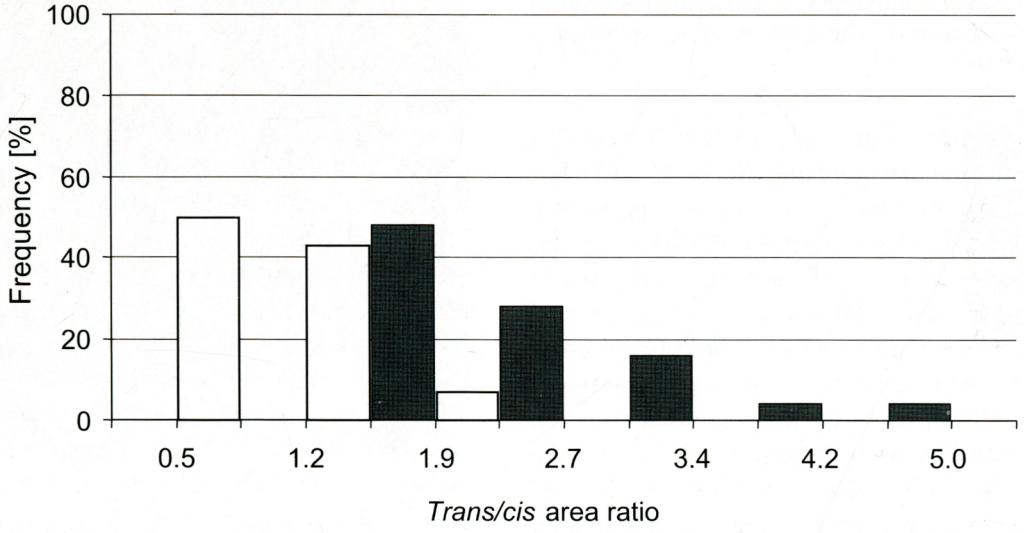

Fig. 6. Frequency distribution of the *Trans*/*Cis* ratio values in neurons from control (open bars) and from 2-DG-treated animals (filled bars)

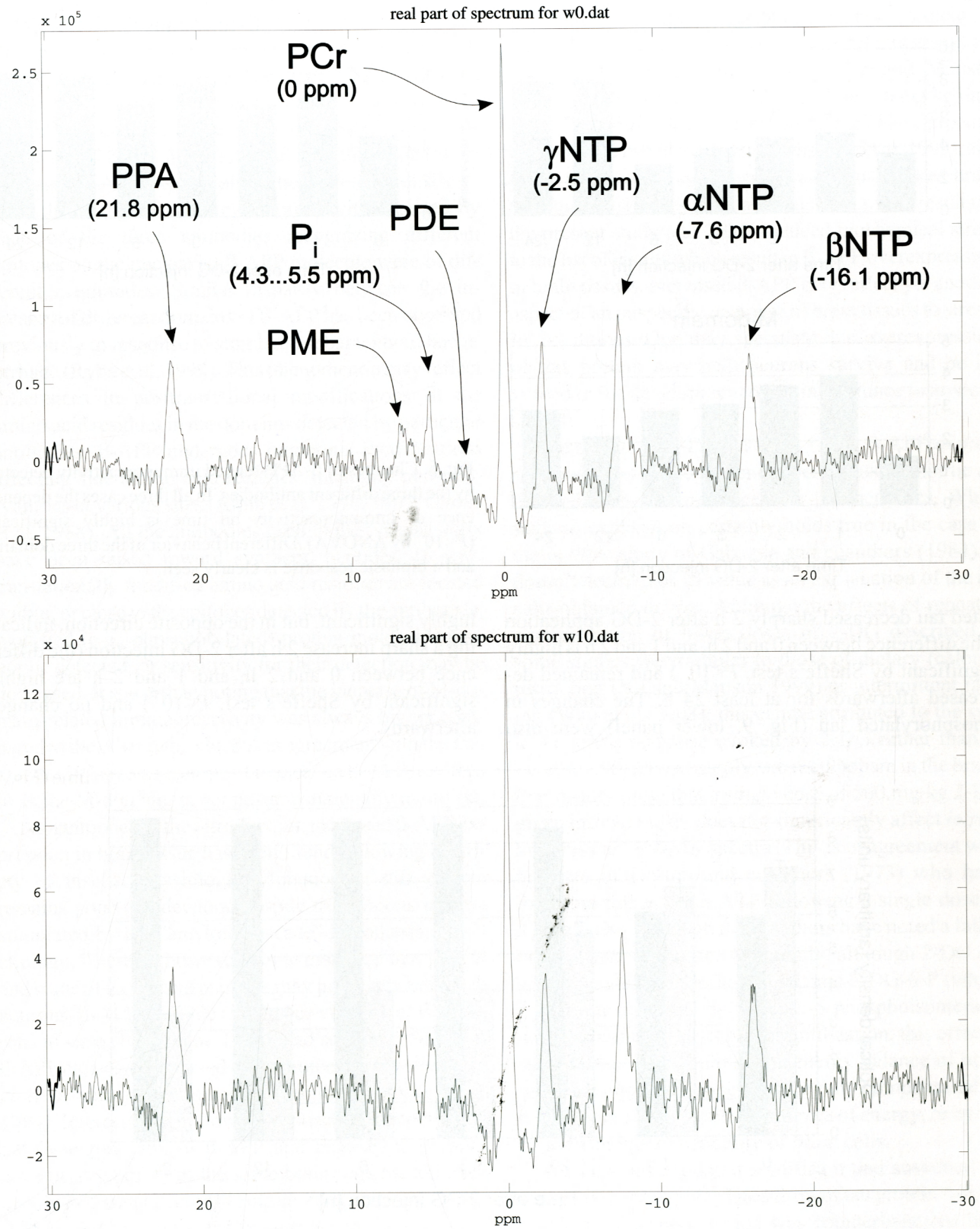

Fig. 7. Brain ^{31}P spectra acquired just prior to (upper panel) and approximately 2 h after the injection of 2-DG (lower panel). (PME) phosphomonoesters; (Pi) inorganic phosphates; (PDE) phosphodiesters; (PCr) phosphocreatine; (NTP) nucleoside triphosphates.

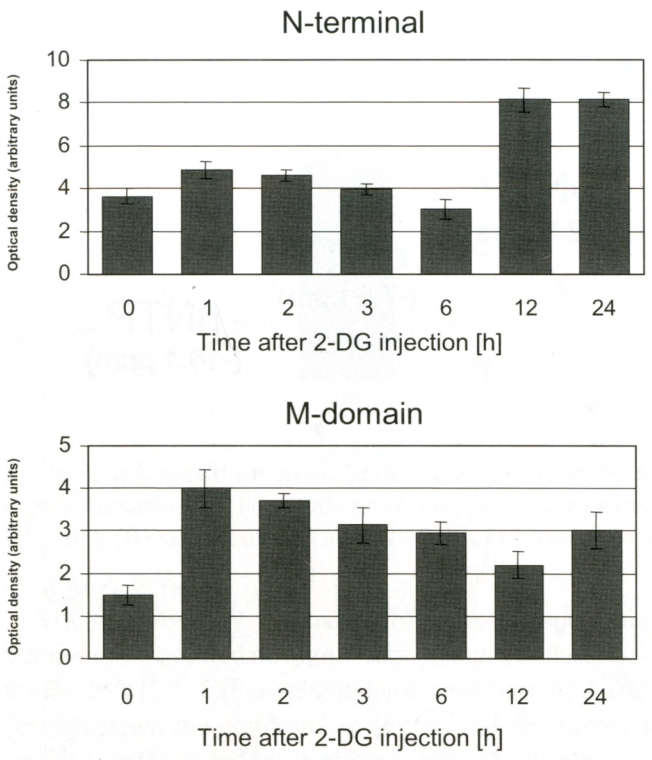

Fig. 8. Changes of β-APP-related immunoreactivity detected by the three different antibodies. In all three cases the dependence of immunoreactivity on time is highly significant ($P<10^{-5}$ by ANOVA). Different behavior of the three domains and a biphasic response is clearly seen.

lated tau decreased sharply 2 h after 2-DG application (the difference between 0 and 2 h, and 1 and 2 h is highly significant by Sheffe's test, $P<10^{-5}$) and remained decreased afterwards for at least 24 h. The changes in phosphorylated tau (Fig. 9, lower panel) were also highly significant, but in the opposite direction, indicating a sharp increase 2 h after 2-DG injection (the difference between 0 and 2 h, and 1 and 2 h are highly significant by Sheffe's test, $P<10^{-5}$) and no changes afterwards.

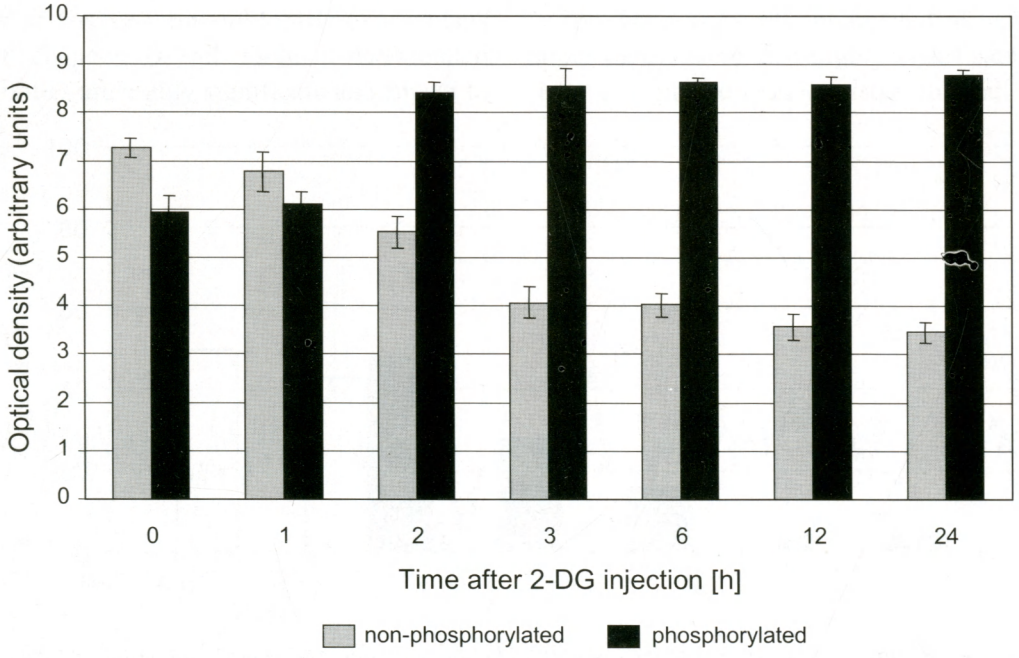

Fig. 9. Changes of non-phosphorylated (grey bars) and phosphorylated (black bars) tau immunoreactivity following 2-DG injection. In both cases the dependence of immunoreactivity on time is highly significant ($P<10^{-5}$ by ANOVA).

DISCUSSION

The results of the present study indicate that systemic application of 2-DG produces a quick and significant increase in the uncleaved β-APP-related immunoreactivities which may be interpreted as the evidence for increased β-APP expression at the protein level. However, the changes of the immunoreactivity detected by each of the three antibodies recognizing different epitopes on the uncleaved β-APP molecule were of different magnitudes. Similar disparity between the increases of different domains of β-APP has been observed previously in response to simulated subarachnoid haemorrhage (Ryba et al. 1999). This phenomenon may reflect differences in posttranslational modifications of the amino acid residues in the domains detected by particular antibodies. β-APP undergoes numerous modifications affecting side amino acid residues, including phosphorylations at various sites (Alpin et al. 1996, 1997, Gandy et al. 1988). All the antibodies used in the present study have been raised toward synthetic peptides. If posttranslationally modified amino acid residues are located within, or close to the epitopes detected by the antibodies, modified (e.g., phosphorylated) protein molecules may not be detected, or sensitivity for their detection may be decreased. It is worth to noting that the increase of M-domain-related immunoreactivity was always higher compared to the other two, which is in agreement with the fact that the 597-613 aa epitope of uncleaved β-APP, referred to as the M-domain, is not posttranslationally modified.

As mentioned in the introduction, increased β-APP expression in brain tissue has been found following a variety of insults. Physiological function of this protein remains poorly understood despite tremendous interest stimulated by the "amyloid cascade" hypothesis of AD etiology. There is, however, some evidence that β-APP and some of its nascent peptides may positively influence neurons. β-APP was able to enhance viability of the neurons *in vitro* (Perez et al. 1997), and soluble products of β-APP cleavage displayed neuroprotective activity in the *in vivo* brain ischemia model (Smith-Swintosky et al. 1994). Interestingly, following postischemic reperfusion the overexpression of β-APP and heat-shock proteins have been reported in the same brain regions, although mostly in distinct neurons (Tomimoto et al. 1994). In that study β-APP accumulated in neurons on the margin of the regions destined to die, but the majority of these neurons seemed to survive after ischemic insult (Tomimoto et al. 1994). On the other hand, 2-DG induced an increase in the level of the stress protein heat-shock protein 70 (HSP 70) in striatal cells *in vivo*, and 2-DG treatment induced HSP70 in cultured neurons (Yu and Mattson 1999). Repeated injections of 2-DG (dose 100 mg/kg/day) induced increased levels of the stress-responsive proteins GRP78 and HSP70 in brain neurons (Lee et al. 1999), and (dose 150 mg/kg/day) enhanced ischemia-evoked brain tolerance to seizures (Rejdak et al. 2001). The results of the present study add 2-DG-induced biochemical stress to the list of insults which result in β-APP overexpression in brain tissues. Increased β-APP may reflect yet another aspect of an unspecific response of brain tissues to stressful conditions. One may speculate that overexpression of this protein may help neurons survive and be involved in the development of brain tolerance to noxious stimuli.

The effects of 2-DG on brain tissue β-APP expression observed in the present experiments cannot be attributed to the failure of cellular bioenergetics. While such an explanation certainly holds true in the case of the *in vitro* study of Gabuzda and coauthors (1984), it doesn't seem to be of value as an explanation of the results obtained *in vivo*. Although the effects of repeated administration of lower doses of 2-DG described in some studies were similar to those of dietary (caloric) restriction (Yu and Mattson 1999) or intermittent fasting (Wan et al. 2003), this can be attributed to the systemic stress response evoked by 2-DG rather than to insufficient glucose supply and metabolism in the brain. Our results show that a single dose of 500 mg/kg 2-DG given intravenously does not significantly affect *in vivo* brain tissue ^{31}P NMR spectra. This is in agreement with the data of Horton and coauthors (1973) who have found no fall in brain ATP following a single dose of 3 g/kg 2-DG, although these authors have noted a fall in brain phosphocreatine. Apparently, although 2-DG enters brain and is phosphorylated, and 2-DG-6-P (which is not metabolized by glucose-6-phosphoisomerase) may transiently restrict glucose utilization, this effect is short lasting and, as far as the energy balance of brain tissue is concerned, appears to be fully compensated either by some other available sources of energy, or by decreased energy expenditure of brain cells.

We have also found a significant and sustained increase of the phosphorylated form of tau protein following 2-DG injection, which was counterbalanced by a decrease of unphosphorylated tau. The link between β-APP overexpression and tau phosphorylation may be provided by glycogen synthase kinase 3beta

(GSK3beta), the enzyme implicated in a variety of intracellular receptor-mediated processes including transduction of insulin signaling (Grimes and Jope 2001). GSK3beta activity has been implicated in virtually all aspects of Alzheimer's pathology, including pro-amyloidogenic phosphorylation of the carboxy-domain of β-APP (Alpin et al. 1996), tau hyperphosphorylation (Lee et al. 2003, Lovestone et al. 1994) and disassembly of neuronal Golgi apparatus (Elyaman et al. 2002). Its unique feature is that it is constitutively active in resting conditions. One may consider the possibility that 2-DG produces hypoinsulinemia which activates GSK3beta and hyperphosphorylates tau. Indeed, prolonged treatment of rats with lower doses of 2-DG has been recently found to cause a marked decrease in plasma insulin (Wan et al. 2003). However, Pascoe and coauthors (1989), using an experimental design identical to that of the present study, found that i.v. infusion of 500 mg/kg 2-DG to male Wistar rats resulted in the approximately 3-fold increase in plasma insulin level.

A recent finding that Abeta is a direct competitive inhibitor of insulin binding to its receptor binding and insulin receptor autophosphorylation (Xie et al. 2002) may link overexpression of β-APP directly to the activation of GSK3beta. One may speculate that overexpression of β-APP, which is a primary brain cellular response to 2-DG-evoked stress, shifts the balance between Abeta production and removal toward the increase of Abeta concentration outside brain cells. The next step would be the competition of Abeta with insulin at the insulin receptors, impaired transduction of the insulin signaling and the activation of GSK3beta, to create a vicious cycle.

The changes in Golgi morphology which we have found following 2-DG injection may also be driven by the same mechanism. It is worth noting that a similar morphological picture (i.e., the apparent relative expansion of the *trans*- part of the Golgi complex) has been previously found in our lab in brain neurons of rats subjected to acute insulin-induced hypoglycemia (Wierzba-Bobrowicz 1980, 1984 – unpublished doctoral thesis). These observations are in agreement with findings of the others. Agardh and coauthors (1981) have noted that the pathogenesis of cell damage in hypoglycemia is different from that in hypoxia-ischemia and indicated that other mechanisms than energy failure must contribute to neuronal cell damage in the brain. Also, according to Simon and coauthors (1986), the neuropathology of rat hippocampal neurons at the EM level following hypoglycemia was markedly different from that seen following status epilepticus and ischemia, the main difference being that microvacuoles were rarely seen and, when present, their ultrastructural correlate was swollen Golgi apparatus, not dilated mitochondria.

Neither the changes in Golgi morphology produced by intravenous injection of 2-DG, nor similar changes reported previously following hypoglycemia, seem to have a direct relation to brain tissues energy failure. It is also unlikely that they are related to hyperinsulinemia which would rather be expected to dephosphorylate tau protein in the brain. It is well known that starvation decreases insulin in blood, and Yanagisawa and coauthors (1999) have shown that starving induces tau hyperphosphorylation in the mouse brain. On the other hand, similar but even more pronounced enlargement of the *trans* compartment of the Golgi has been found following intracerebroventricular injections of streptozotocin, a toxin which desensitizes brain insulin receptors (Grieb et al. 2004). It is tempting to speculate that all these functional and ultrastructural effects may be related either to stimulation of β-APP synthesis and Abeta formation, modulation of GSK3beta activity, or an interplay between these two mechanisms at the level of brain insulin receptors.

CONCLUSION

A single dose of 2-deoxyglucose (500 mg/kg i.p.) induces in brain cortex of rats a bi-phasic β-APP overexpression, a hyperphosphorylation of tau protein, and a marked expansion of the *trans* part of the neuronal Golgi apparatus, but does not appreciably influence brain energy compounds.

ACKNOWLEDGEMENT

The study was supported by the State Committee for Scientific Research (KBN) project No. 4P05A 041 17 granted to the late professor Miroslaw J. Mossakowski, to whom the authors are indebted for his creativity and expertise in the early stage of the work.

REFERENCES

Agardh CD, Kalimo H, Olsson Y, Siesjo BK (1981) Hypoglycemic brain injury: metabolic and structural findings in rat cerebellar cortex during profound insulin-induced hypoglycemia and in the recovery period following

glucose administration. J Cereb Blood Flow Metab 1: 71-84.

Alpin AE, Gibb GM, Jacobsen JS, Gallo J-M, Anderton BH (1996) In vitro phosphorylation of cytoplasmic domain of the amyloid precursor protein by glycogen synthase kinase-3β. J Neurochem 67: 699-707.

Aplin AE, Jacobsen JS, Anderton BH, Gallo JM (1997) Effect of increased glycogen synthase kinase-3 activity upon the maturation of the amyloid precursor protein in transfected cells. Neuroreport 8: 639-643.

Deuel RK, Yue GM, Sherman WR, Schickner DJ, Ackerman JJH (1985) Monitoring the time course of cerebral deoxyglucose metabolism by ^{31}P nuclear magnetic spectroscopy. Science 228: 1329-1331.

Dreau D, Foster M, Morton DS, Fowler N, Kinney K, Sonnenfeld G (2000) Immune alterations in three mouse strains following 2-deoxy-D-glucose administration. Physiol Behav 70: 513-520.

Elyaman W, Yardin C, Hugon J (2002) Involvement of glycogen synthase kinase-3β and tau phosphorylation in neuronal Golgi disassembly. J Neurochem 81: 870-880.

Fukuyama H, Ogawa M, Yamauchi H, Yamaguchi S, Kimura J, Yonekura Y, Konishi J (1994) Altered cerebral energy metabolism in Alzheimer's disease: a PET study. J Nucl Med 35: 1-6.

Gabuzda D, Busciglio J, Chen L, Matsudaira P, Yankner B (1994) Inhibition of energy metabolism alters the processing of amyloid precursor protein and induces a potentially amyloidogenic derivative. J Biol Chem. 269: 13623-13628.

Gandy S, Czernik A, Greengard P (1988) Phosphorylation of Alzheimer disease amyloid precursor peptide by protein kinase C and Ca^{2+}/calmodulin-dependent protein kinase II. Proc Natl Acad Sci U S A 85: 6218-6221.

Grieb P, Kryczka T, Fiedorowicz M, Frontczak-Baniewicz M, Walski M (2004) Expansion of the Golgi apparatus in rat cerebral cortex following intracerebroventricular injections of streptozotocin. Acta Neurobiol Exp (Wars) 64: 481-489.

Grimes CA, Jope RS (2001) The multifaceted roles of glycogen synthase kinase 3β in cellular signalling. Prog Neurobiol 65: 391-426.

Hardy J, Higgins GA (1992) Alzheimer's disease: The amyloid hypothesis. Science 256: 1124-1125.

Hardy J, Selkoe DJ (2002) The amyloid hypothesis of Alzheimer's disease: progress and problems on the road to therapeutics. Science 297: 353-356.

Horton RW, Meldrum BS, Bachelard HS (1973) Enzymic and cerebral metabolic effects of 2-deoxy-D-glucose. J Neurochem 21: 507-520.

Hoyer S (1998) Is sporadic Alzheimer disease the brain type of non-insulin dependent diabetes mellitus. A challenging hypothesis. J Neural Transm 105: 415-422.

Hoyer S (2002) The brain insulin signal transduction system and sporadic (type II) Alzheimer disease: an update. J Neural Transm 109: 341-360.

Johnson G, Refolo LM, Merril CR, Wallace W (1993) Altered expression and phosphorylation of amyloid precursor protein in heat shocked neuronal PC12 cells. Brain Res Mol Brain Res 19: 140-148.

Kadowaki T, Kasaga M, Akamuma Y, Ezaki O, Takaku F (1984) Decreased autophosphorylation of the insulin receptor-kinase in streptozotocin diabetic rats. J Biol Chem 259: 14208-14216.

Laemmli UK (1970) Cleavage of structural proteins during the assembly of the head of bacteriophage T4. Nature 227: 680-685.

Lee CW, Lau KF, Miller CC, Shaw PC (2003) Glycogen synthase kinase-3 beta-mediated tau phosphorylation in cultured cell lines. Neuroreport 14: 257-560.

Lee J, Bruce-Keller AJ, Kruman Y, Chan SL, Mattson MP (1999) 2-Deoxy-D-glucose protects hippocampal neurons against excitotoxic and oxidative injury: evidence for the involvement of stress proteins. J Neurosci Res 57: 48-61.

Lovestone S, Reynolds CH, Latimer D, Davis DR, Anderton BH, Gallo JM, Hanger D, Mulot S, Marquardt B, Stabel S, et al (1994) Alzheimer's disease-like phosphorylation of the microtubule-associated protein tau by glycogen synthase kinase-3 in transfected mammalian cells. Curr Biol 4: 1077-1086.

Mattson MP (1997) Cellular actions of β-Amyloid Precursor Protein and its soluble and fibrillogenic derivatives. Physiol Rev 77: 1081-1132.

Minoshima S, Giordani B, Berent S, Frey KA, Foster NL, Kuhl DE (1997) Metabolic reduction in the posterior cingulate cortex in very early Alzheimer's disease. Ann Neurol 42: 85-94.

Ogawa M, Fukuyama H, Ouchi Y, Yamauchi H, Kimura J (1996) Altered energy metabolism in Alzheimer's disease. J Neurol Sci 139: 78-82.

Pascoe WS, Smythe GA, Storlie LH (1989) 2-Deoxy-D-glucose-induced hyperglycemia: role for direct sympathetic nervous system activation of liver glucose output. Brain Res 505: 23-28.

Pedersen WA, Culmsee C, Ziegler D, Herman JP, Mattson MP (1999) Aberrant stress response associated with severe hypoglycemia in a transgenic mouse model of Alzheimer's disease. J Mol Neurosci 13: 159-165.

Perez RG, Zheng H, Van der Ploeg LH, Koo EH (1997) The beta-amyloid precursor protein of Alzheimer's disease enhances neuron viability and modulates neuronal polarity. J Neurosci 17: 9407-9414.

Piert M, Koeppe RA, Giordani B, Berent S, Kuhl DE (1996) Diminished glucose transport and phosphorylation in Alzheimer's disease determined by dynamic FDG-PET. J Nucl Med 37: 201-208.

Rejdak K, Rejdak R, Sieklucka-Dziuba M, Stelmasiak Z, Grieb P (2001) 2-Deoxyglucose enhances hypoxic tolerance evoked by transient incomplete brain ischemia. Epilepsy Res 43: 271-278.

Ryba MS, Gordon-Krajcer W, Walski M, Chalimoniuk M, Chrapusta SJ (1999) Hydroxylamine attenuates the effects of simulated subarachnoid hemorrhage in the rat brain and improves neurological outcome. Brain Res 850: 225-233.

Schagger H, von Jagow G (1987) Tricine-sodium dodecyl sulphate polyacrylamide gel electrophoresis for the separation of protein in the range from 1 to 100 kDa. Anal Biochem 166: 638-661.

Selkoe DJ (2001) Alzheimer's disease: genes, proteins, and therapy. Physiol Rev 81: 741-766.

Shi J, Xiang Y, Simpkins JW (1997) Hypoglycemia enhances the expression of mRNA encoding beta-amyloid precursor protein in rat primary cortical astroglial cells. Brain Res 772: 247-251.

Simon RP, Schmidley JW, Swan JH, Meldrum BS (1986) Neuronal alterations in hippocampus following severe hypoglycaemia: a light microscopic and ultrastructural study in the rat. Neuropathol Appl Neurobiol 12: 11-26.

Smith-Swintosky VL, Pettigrew LC, Craddock SD, Culwell AR, Rydel RE, Mattson MP (1994) Secreted forms of beta-amyloid precursor protein protect against ischemic brain injury. J Neurochem 63: 781-784.

Swaab DF, Dubelaar EJ, Hofman MA, Scherder EJ, van Someren EJ, Verwer RW (2002) Brain aging and Alzheimer's disease: use it or lose it. Prog Brain Res 138:343-373.

Tomimoto H, Wakita H, Akiguchi I, Nakamura S, Kimura J (1994) Temporal profiles of accumulation of amyloid beta/A4 protein precursor in the gerbil after graded ischemic stress. J Cereb Blood Flow Metab 14: 565-573.

Towbin H, Staehelin T, Gordon J (1979) Electrophoretic transfer of proteins from polyacrylamide gels to nitrocellulose sheets: procedure and some applications. Proc Natl Acad Sci U S A 76: 4350-4354.

Wallace W, Johnson G, Sugar J, Merril CR, Refolo LM (1993) Reversible phosphorylation of tau to form A68 in heat-shocked neuronal PC12 cells. Brain Res Mol Brain Res 19: 149-155.

Wan R, Camandola S, Mattson MP (2003) Intermittent fasting and dietary supplementation with 2-deoxy-D-glucose improve functional and metabolic cardiovascular risk factors in rats. FASEB J 17:1133-1134.

Weidemann A, Konig G, Bunke D, Fischer P, Salbaum JM, Masters CL, Beyeruther K (1989) Identification, biogenesis and localization of precursors of Alzheimer's disease A4 amyloid protein. Cell 57: 115-126.

Wick AN, Drury DR, Nakada HI, Wolfe JB (1957) Localization of the primary metabolic block produced by 2-deoxyglucose. J Biol Chem 224: 963-969.

Wierzba-Bobrowicz T (1980) Electron-microscopic picture of rat brain in acute experimental hypoglycemia (in Polish). Neuropatol Pol 18: 289-300.

Xie L., Helmerhorst E, Taddei K, Plewright B, Van Bronswijk W, Martins R (2002) Alzheimer's beta-amyloid peptides compete for insulin binding to the insulin receptor. J Neurosci 22: RC221.

Yanagisawa M, Planel E, Ishiguro K, Fujita SC (1999) Starvation induces tau hyperphosphorylation in mouse brain: implications for Alzheimer's disease. FEBS Lett 461: 329-333.

Yu ZF, Mattson MP (1999) Dietary restriction and 2-deoxyglucose administration reduce focal ischemic brain damage and improve behavioral outcome: evidence for a preconditioning mechanism. J Neurosci Res 57: 830-839.

Received 10 August 2003, accepted 6 September 2004